University of Bath

UNIVERSITY OF BATH

PHD

Novel synthesis of highly cytotoxic cyclopropabenzindoles for incorporation into a prodrug system targeting prostate tumours

Kenny, Michael

Award date:
2019

Awarding institution:
University of Bath

[Link to publication](#)

Alternative formats

If you require this document in an alternative format, please contact:
openaccess@bath.ac.uk

Publication date:
2018

Link to publication

University of Bath

NOVEL SYNTHESIS OF HIGHLY CYTOTOXIC CYCLOPROPABENZINDOLES FOR INCORPORATION INTO A PRODRUG SYSTEM TARGETING PROSTATE TUMOURS

Michael Brendon Corrin Kenny

A thesis submitted for the degree of Doctor of Philosophy

University of Bath

Department of Pharmacy and Pharmacology

2018

COPYRIGHT

Acknowledgements

Abstract

Prostate cancer will affect one in eight men during their lifetime and is the fifth leading cause of cancer related deaths in men. Conventional treatments for prostate cancer include androgen-deprivation therapy, however, most men treated with androgen-deprivation therapy progress to hormone-refractory prostate cancer. There are currently no curative treatments for hormone-refractory prostate cancer. Cyclopropabenzindoles (CBI) are more biologically potent and synthetically accessible analogues of the cyclopropapyrroloindole (CPI) anti-tumour antibiotics, such as duocarmycin-SA and CC1065. *Seco*-amino-CBIs can be incorporated into a polymeric prodrug system that will release the *seco*-amino-CBIs at the site of tumour selectively. The polymeric prodrug system consists of linear polyethyleneglycol (20 KDa) bound to a PSA-cleavable linker peptide to which the *seco*-amino-CBI is attached. The prodrug has two modes of selectivity: activation by PSA and the EPR effect. The synthesis of a range of *seco*-amino-CBI compounds was performed in order to investigate the structure-activity relationship surrounding the non-alkylating DNA minor-groove binding subunit. A novel synthetic route was developed to bypass issues surrounding the required orthogonal protection of two amine groups. This route provided access to a range of *seco*-nitro-CBIs that were further investigated as hypoxia-activated prodrugs. Biological evaluation of the *seco*-nitro-CBIs and *seco*-amino-CBIs was investigated through DNA-melting assays which confirmed the ability of the *seco*-amino-CBIs to bind covalently to DNA. MTS-assays were carried out to evaluate the relative cytotoxicity's of the range of *seco*-nitro-CBIs and *seco*-amino-CBIs. Novel compound (5-amino-1-(chloromethyl)-1,2-dihydro-3H-benzo[e]indol-3-yl)(5-hydroxy-1H-indol-2-yl)methanone showed exquisite potency, with a determined IC_{50} value of 1.5 nM against PC3 cells. MTS-assays performed under hypoxic conditions allowed the investigation into the suitability of the *seco*-nitro-CBIs as hypoxia-activated prodrugs. (1-(chloromethyl)-5-nitro-1,2-dihydro-3H-benzo[e]indol-3-yl)(5-hydroxy-1H-indol-2-yl)methanone exhibited a hypoxia-cytotoxicity ratio of 2.34.

Contents

Abbreviations

AcOH	Acetic acid
ADEPT	Antibody-directed enzyme prodrug therapy
An.	Anhydrous
Aq	Aqueous
AR	Androgen receptors
Bn	Benzyl
Boc	*tert*-Butoxycarbonyl
Boc$_2$O	Di-*tert*-butyl dicarbonate
BPH	Benign prostatic hyperplasia
^{t}BuO$^-$K$^+$	Potassium *tert*-butoxide
^{t}Bu	*tert*-Butyl
CbBI	1,2,10,11-Tetrahydro-9*H*-cyclobuta[*c*]benzo[*e*]indol-4-one
CBI	1,2,9,9a-Tetrahydrocyclopropa[*c*]benz[*e*]indole-4-one
CBIn	1,2,9,9a-Tetrahydro-1*H*-cyclopropa[*c*]benz[*e*]inden-4-one
CBQ	5-Oxo-1,2,10,10a- tetrahydrobenzo[*f*]cyclopropa[*d*]quinoline-3(5*H*)-carboxylate
Cbz	Carboxybenzyl
CCBI	7-Cyano-1,2,9,9a-tetrahydrocyclopropa[*c*]benz[*e*]indol-4-one
CI	1,2,7,7a-Tetrahydrocyclopropa[1,2-c]indol-4-one
CNA	6-Oxo-2,3,11,11a-tetrahydro-1*H*-cyclopropa[*c*]naphtho[2,1-b]azepine-4(6*H*)-carboxylate
CPI	Cyclopropapyrroloindole
DA	duocarmycin A
DSA	duocarmycin SA
DCC	N,N'-Dicyclohexylcarbodiimide
DMA	Dimethylacetamide
DMAP	4-Dimethylaminopyridine
DMF	Dimethylformamide
DMP	2,2-Dimethoxypropane

DKP	Diketopiperazines
Dmo	5,5-Dimethyl-4-oxaproline
DMSO	Dimethylsulfoxide
Dmt	5,5-Dimethyl-4-thiaproline
DRE	Digital rectal examination
dThd	Thymidine
EAU	European Association of Urology
EBRT	External beam radiotherapy
EDA	Ethylenediamine
EDC	1-Ethyl-3-(3-dimethylaminopropyl)carbodiimide
EDTa	Ethylenediaminetetraacetic acid
EPR	Enhanced permeability and retention effect
ERG v-ets	avian erythroblastosis virus E26 oncogene homolog
Et_2O	Diethylether
EtOAc	Ethylacetate
EtOH	Ethanol
FBS	Foetal bovine serum
Fmoc	9-Fluorenylmethoxycarbonyl
fPSA	Free prostate-specific antigen
FSH	Follicle stimulating hormone
GDEPT	Gene directed enzyme prodrug therapy
Gln	Glutamine
HiFU	High-frequency ultrasound
HOBt	Hydroxybenzotriazole
HPLC	High performance liquid chromatography
HPMA	N-(2-hydroxypropyl)methacrylamide
IC_{50}	Concentration required for 50% inhibition of activity IR Infrared
J	Coupling constant
Leu	Leucine
LH	Luteinizing hormone
LHRH	Luteinizing hormone-releasing hormone
Lit	Literature

Lys	Lysine
MeOH	Methanol
Mp	Melting point
Ms	Methanesulfonyl
MTS	3-(4,5-Dimethylthiazol-2-yl)-5-(3-carboxymethoxyphenyl)-2-(4-sulfophenyl)-2*H*-tetrazolium, inner salt
m/z	Mass to charge ratio (mass spectrometry)
NEt$_3$	Triethylamine
NIS	N-Iodosuccinimide
PBS	Phosphate buffered saline
PCa	Prostate cancer
PEG	Poly(ethylene glycol)
PMT	Prodrug monotherapy
PSA	Prostate-specific antigen
Rf	Retention factor
Ser	Serine
TEMPO	(2,2,6,6-Tetramethylpiperidin-1-yl)oxyl
TFA	Trifluoroacetic acid
THF	Tetrahydrofuran
TLC	Thin layer chromatography
T_m	Transition-melting temperature
TMI	Trimethoxyindole
TNM	Tumour, lymph nodes and metastasis
TMPRSS2	Transmembrane protease serine 2
TRUS	Trans-rectal ultrasound
TsOH	*para*-Toluenesulfonic acid
UHP	Urea hydrogen peroxide
UV	Ultraviolet
VIS	Visible

1.0 Introduction

The prostate gland is a male organ that surrounds the urethra, sitting just beneath the bladder. Roughly the size of a walnut, the prostate plays a key role in the liquefaction of semen and is the site of the two most commonly encountered medical issues in elderly men; benign prostate hyperplasia (BPH) and prostate cancer (PCa).

1.1 Overview of the eukaryotic cell cycle

It is estimated that, during the course of a human life, 10^{16} cell divisions take place.[1] Two consecutive processes make up cell division, Interphase and Mitosis. Interphase involves the replication of DNA and can be separated further into three key stages, G_1, S and G_2. Mitosis (M phase) is then the process of segregation of the replicated chromosomes into two separate cells and can be broken down into prophase, prometaphase, metaphase, anaphase and telophase.[2] This whole process can be visualised below in Figure 1. In G_1, the cell begins initial preparations for mitosis by making more organelles, such as mitochondria and Golgi bodies. G_1 then progresses to the S phase, within which DNA is replicated, and this then leads onto G_2 where the cell continues to grow in size in preparation for imminent mitosis.[3] Mitosis begins with Prophase, within which the replicated chromosomes condense and the mitotic spindles begin to assemble. This leads on to prometaphase during which the chromosomes attach to the spindle microtubules, at which point metaphase can then occur where chromosomes align at the equator of the spindles.[4] Metaphase leads into anaphase whereby the chromosomes separate and are pulled along the spindles resulting in two sets of daughter chromosomes. Once the daughter chromosomes have arrived at the poles of the spindles, they decondense and a new nuclear envelope assembles around each set, in a stage known as telophase, signalling the end of mitosis.[4] Finally, the cytoplasm divides into two new daughter cells, in a process known as cytokinesis.
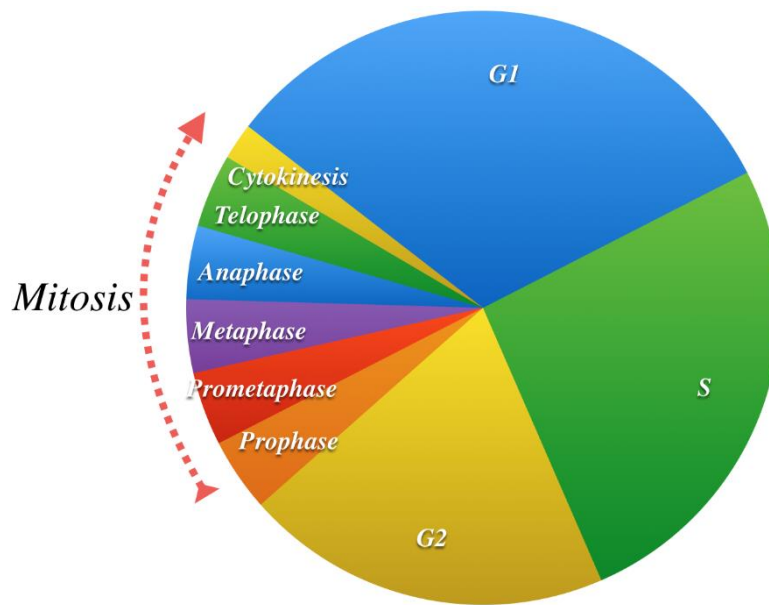
Figure 1: Overview of the cell cycle.

1.2 Regulation of the cell cycle

The cell cycle is tightly regulated to ensure that cells are copied without error and that they do not divide uncontrollably. One way that this is achieved is through apoptosis, or programmed cell death, which eliminates 'unnecessary' cells, controlling excessive proliferation.[5] The phosphatidylinositol 3-kinase (PI3K) pathway is of particular importance to cell cycle regulation and deregulation resulting in cancer.[5,6] With regard to cancer, deregulation of the PI3K pathway has been found in 42% of primary and 100% of metastatic cancers.[6] PI3K, or phosphatidylinositol 3-kinase, is directly responsible for the production of phosphatidylinositol (3,4,5)-triphosphate (PIP_3) through phosphorylation of phosphatidylinositol (4,5)-triphosphate (PIP_2) at the D3 position, shown in Figure 2. PIP_3 acts as a secondary messenger to activate downstream pathways and specifically the AKT pathway. PIP_3 is regulated by PTEN, a lipid phosphatase, which dephosphorylates at D3 to re-form PIP_2.[7] PIP_3, located in the plasma membrane, recruits AKT to the membrane through direct interaction with its PH domain. AKT is then activated by phosphorylation at Thr308 and Ser473 by PDK1 and PDK2.[8,9] Activation of AKT then has several biological effects that result in cell survival, proliferation and cell growth. Importantly, for cell survival, AKT inhibits BAD

and FKHR, which are key promoters of apoptosis as well as promoting NF-κB and MDM2 which both act to inhibit apoptotic processes.[10-13]
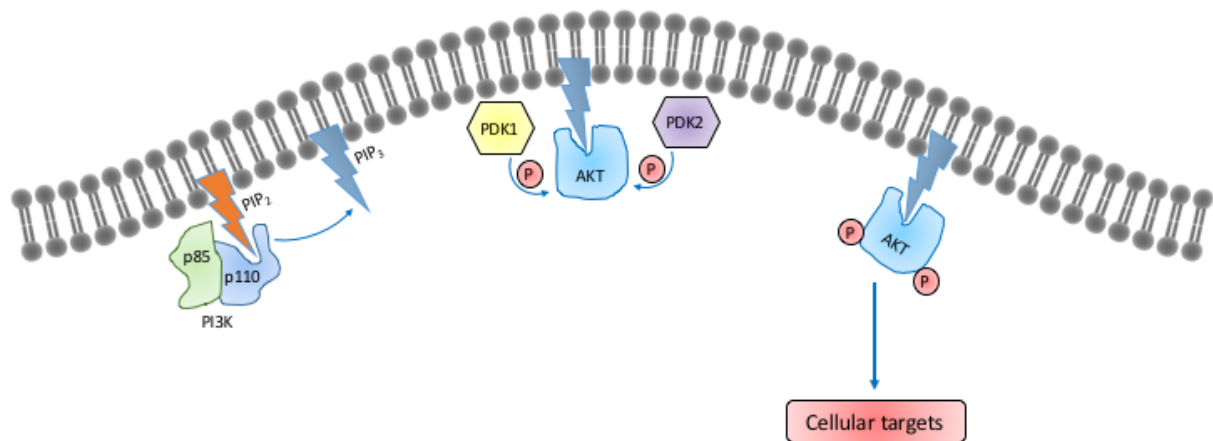
Figure 2: Overview of the AKT pathway.

1.3 Cancer as a result of the deregulation of the cell cycle

Cancer is a disease that fundamentally involves dynamic changes to the genome.[14] In 2000, Weinberg and Hanahan[14] introduced six 'hallmarks' of cancer, outlined in Figure 3, which are described as follows. Firstly, cancer cells can replicate without the need for external growth signals and, secondly, are resistant to growth prevention signals. Cancer cells can also continue to replicate, despite the presence of genetic damage (avoiding regulatory checkpoints) and can evade apoptosis. Cancer cells have the ability to induce angiogenesis to support increased tumour growth and, finally, also have increased motility, which allows for cancer to metastasise.[14] The combined effect of these properties enables the formation of tumours that have the ability to grow independently and indefinitely, producing their own blood supply to provide access to nutrients and metastasising around the body.

In order for a cell to become oncogenic, it must undergo a genetic change that results in either a deletion, amplification or mutation of a gene.[15] In oncogenesis, it is often the case that genes relating to regulatory checkpoints are mutated, rendering the regulation ineffective.[15,16] Inadequate regulation then allows for uncontrolled growth to occur, resulting in the growth of a tumour.
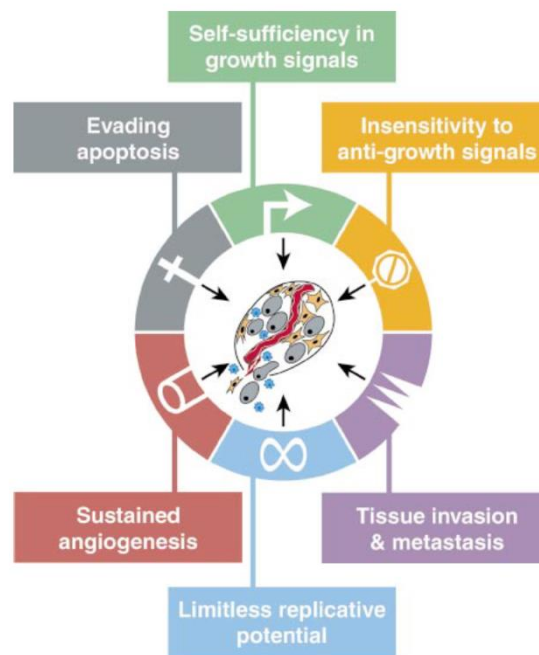
Figure 3: Acquired capabilities of cancer.[14]

1.4 Stages of cancer

Staging a cancer is a way of describing the size and spread of a tumour. Staging a cancer allows for a more well-informed treatment decision. There are two main staging systems that are most commonly used; the TNM system and the number system.

1.4.1 TNM staging

TNM stands for Tumour, Node, Metastases. A numerical value is determined for each category to provide a detailed insight into the state of the tumour. For the T value, a range of between one and four is used to describe the size of the tumour, with one signifying a small tumour and four signifying a large tumour. For the N value, the range is between zero and three and describes whether cancer cells are present within the lymph nodes. In this case, zero means that no cancer cells are detected within the lymph nodes and three means that

many cancer cells are within the lymph nodes. Finally, the M value describes whether the tumour has metastasized to other areas of the body or not and is simply given a value of zero (for no sign of metastases) or one (metastases has occurred).

Additionally, letters may also be used alongside the TNM numerical values to provide further detail into the stage of a tumour. A letter p preceding T, N or M indicates that the staging has been determined through a laboratory examination of cancer cells after surgery to remove the cancer. A letter c preceding T, N or M stands for clinical stage and indicates that the staging has been carried out prior to surgery, using test results and other clinical information.[17]

1.4.2 Number staging

Number staging is a system that takes a TNM stage and categorises it into one of four stages, described as I, II, III and IV. Stage I describes a small cancer contained within an organ whereas stage IV describes an advanced cancer that has metastasised to other parts of the body.

1.5 The prostate

The prostate gland is located underneath the bladder and is roughly the size of a walnut. The gland is a male sexual organ responsible for the production of seminal fluid and liquefaction of the semen.[18] There are three main conditions related to the prostate: prostatitis, benign prostatic hyperplasia and prostate cancer.

1.5.1 Prostate development

The development of the prostate in humans begins at around ten weeks of foetal-development.[19] Androgens stimulate urogenital sinus mesenchyme (UGM) which induces epithelial budding, proliferation, and differentiation to form ductal structures.[20] At the same time, UGM proliferates and differentiates into prostatic smooth muscle and interfascicular fibroblasts.[19] Interestingly, foetal genetic sex does not determine prostate development rather it is determined by androgen stimulation at the appropriate developmental period.[19,21] During puberty, the human prostate undergoes significant growth by around ten-fold, corresponding to the rise in concentration of testosterone in the serum. After puberty,

prostatic weight then remains fairly constant until around forty years old when it begins to rise slowly.[22]

1.5.2 Prostate function

The primary functions of the prostate relate to production of the seminal fluid and to gelation, coagulation and liquefaction of the semen.[23] This is achieved through the secretion of semenogelin (I and II), fibronectin and lactoferrin. Semenogelin is the predominant protein in seminal fluid.[24] Semenogelin I and II, and fibronectin are involved in the postejaculatory coagulation of semen.[25–27] Semenogelin I and II interact non-covalently and *via* disulfide bridges, resulting in the instant formation of a coagulum upon ejaculation. In humans, the prostate also secretes Prostate-Specific Antigen (PSA), a widespread marker of prostate disease pathology.[19] PSA acts on the ejaculate coagulum by cleaving semenogelin I and II, resulting on a liquefaction of the semen and increased motility of the sperm.[25–27] The prostate also contains Δ^4-3-ketosteroid-5α-reductase, an enzyme that takes testosterone produced in the testes and reduces it to the much more biologically active androgen 5α-dihydrotestosterone (DHT).[19]

1.5.3 Prostate-Specific Antigen

Prostate-specific antigen (PSA) is a serine protease with chymotrypsin-like specificity and is one of the three most abundant prostatic-secreted proteins in human semen.[28] PSA is also known as human kallikrein 3 (hK3) with extensive similarities compared to that of the Arg-restricted glandular kallikrein-like proteinases.[28] PSA is a 33KDa single-chain glycoprotein, first isolated by Wang *et al.*[29], secreted from the prostate epithelium of both healthy and malignant cells. PSA exhibits chymotrypsin-like substrate specificity in contrast to the Arg-restricted substrate specificity common to all previously characterised kallikrein-like proteinases.[30,31] Investigation has also shown detectable activity against certain substrates containing a carboxy-terminal Arg residue, a feature common to the trypsin-like kallikreins.[31] PSA-levels are elevated in PCa and PSA is also more proteolytically active in prostate tumours compared to normal prostate tissues which lack detectable PSA enzyme activity.[32] PSA levels correlate with the presence of prostate tumours, increasing with advanced stage and tumour size.[33] PSA selectively cleaves semenogelin I and II, resulting on a liquefaction of the semen and increased motility of the sperm.[25–27] Isolation of the digestive fragments of PSA-cleaved

semenogelin have allowed for the identification of the PSA cleavage sites. It was observed that the peptide bond between Gln and Ser at positions 349 and 350 in semenogelin I was the most readily cleaved bond. Mhaka *et al.*[34] showed that the peptide His-Ser-Ser-Lys-Leu-Gln-OH (HSSKLQ) is also a PSA-specific peptide substrate that is efficiently and selectively cleaved by the enzymatic activity of PSA.[34] With this knowledge, one can design a peptide prodrug that is activated by PSA within the prostate to achieve selective delivery of drug to prostate tumour.

1.6 Diseases of the prostate

There are three main medical conditions involving the prostate: benign prostatic hyperplasia (BPH), prostatitis and prostate cancer (PCa).

1.6.1 Benign prostatic hyperplasia (BPH)

BPH represents the fourth most common health-related disease in older men. It is defined as an increased number of parenchymal cells and develops within the transition zone of the prostate. The current consensus is that BPH is mediated by DHT.[35] Symptoms of BPH include weakened urinary flow due to increased pressure on the bladder and urethra as a result of the enlargement of the prostate.

1.6.2 Prostatitis

Prostatitis is the inflammation of prostate gland tissues. Unlike BPH and PCa, prostatitis is not an age-related disease and can develop at any age. Prostatitis primarily affects men aged between thirty and fifty years old.[36] There are two main types of prostatitis; chronic and acute. Chronic prostatitis is the most common form of prostatitis, with the main symptoms relating to urinary issues and pain around the penis, testes, lower abdomen and lower back. Acute prostatitis is caused by an infection, usually due to *E. coli*. Acute prostatitis usually has a rapid onset of symptoms, unlike chronic prostatitis where symptoms can present sporadically over a period of months.[37] The underlying cause of chronic prostatitis is often unknown as signs of infection within the prostate gland can't usually be found, making it difficult to identify the cause of the symptoms. Medications such as antibiotics are used to treat prostatitis.[36]

1.6.3 Prostate cancer

According to Prostate Cancer UK, one in eight men in the UK will develop prostate cancer during their lives.[38] In 2008, prostate cancer was the second most frequently diagnosed cancer in developed countries.[39] Afro-Caribbean men are twice as likely to get prostate cancer, with one in four Afro-Caribbean men in the UK estimated to get prostate cancer during their lives.[38]

1.6.3.1 Incidence

PCa is the second most common cancer in men and fifth leading cause of death from cancer in men globally.[40] In 2012, an estimated 1.1 million people were diagnosed with PCa and 307,000 deaths resulted from PCa with around 70% of these cases presenting in developed regions as can be seen in Figure 4.[40] In the UK, 47,000 new cases of PCa where recorded in 2015 accounting for 13% of the total UK cancer cases that year. UK incidence rates have increased by around 44% since the early 1990s.[41]
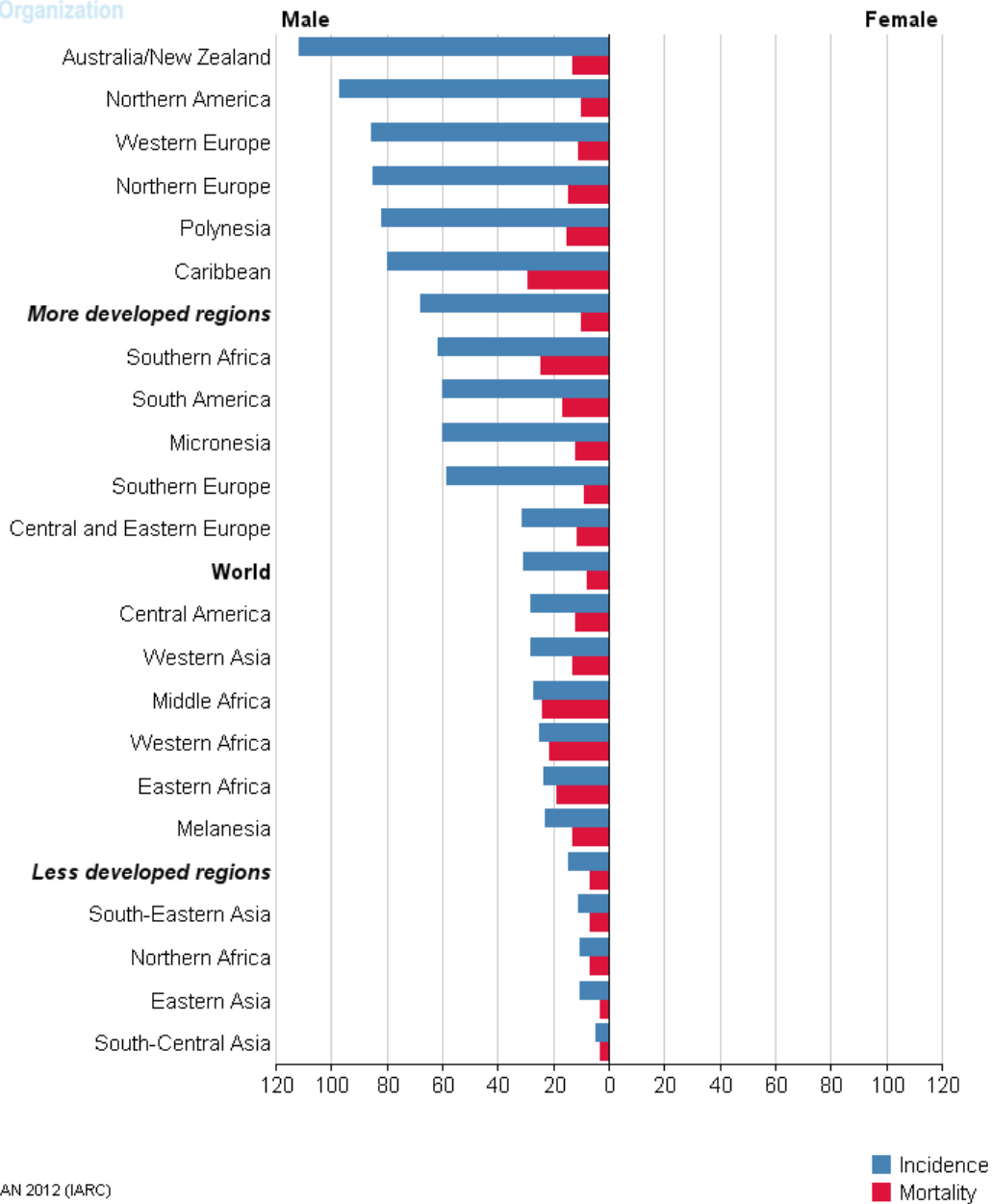
Figure 4: WHO data on PCa incidence and mortality by region for 2012.[31]

9

1.6.3.2 Mortality

Due to the introduction of PSA-testing in developed countries leading to an increase of PCa presentation at localised stage in these areas, mortality rates have much less variation than incidence rates, as can be seen in Figure 4. Mortality rates are higher in areas where there are a large proportion of men from African descent such as Africa and the Caribbean and lowest across Asia.[40] In the UK, there were 11,000 deaths from PCa in 2014, accounting for 13% of all male cancer deaths. Age-standardised PCa mortality rates in the UK have fallen by 13% over the last decade.[41]

1.7 Risk factors associated with PCa

Prostate cancer is the most common solid neoplasm in males in Europe, with an incidence rate of 214 cases per 1000 men.[42] Three well-established risk factors have been established with regards to PCa: age, heredity and ethnicity.[42] There is a 40% lifetime risk of developing PCa for a male born in the Western world.[43,44] Prostate cancer is an age-associated disease, with >70% of PCa diagnoses in the USA involving men >65 years old.[45] The risk of PCa is very low in men <40-years old, with the incidence increasing exponentially with age.

1.7.1 Ethnicity

African-Americans have the highest incidence of PCa in the world (275.3 per 100,000 men).[45] The ethnicity with the lowest associated risk of PCa is Asians/Pacific islanders, with an incidence of 107.2 per 100,000 men. The mortality rate of African-Americans from PCa is five times that for Asians/Pacific islanders, with African-Americans more likely to present with metastatic disease.[45] One in four black men will develop PCa, as opposed to one in eight men overall. The reason for this variation is currently unknown.

1.7.2 Family history

Like with many cancers, one's risk of PCa increases if a first-line relative has the disease. If one first-line relative has PCa, the risk doubles and if multiple first-line relatives have the disease then the risk increases by between five and eleven-fold. True hereditary PCa is a category of PCa whereby the patients have three or more relatives affected by PCa or two relatives

affected by PCa under the age of 55. True hereditary PCa currently accounts for about 9% of the total incidence of PCa.[42]

1.7.3 Exogenous factors

Exogenous factors such as diet, exercise, exposure to UV radiation and pattern of sexual behaviour may also be involved in the incidence of PCa. To date, however, no randomised trials performed have produced level-1 evidence to justify recommendations of change of lifestyle according to the European Association of Urology (EAU) guidelines on PCa.[42]

1.7.4 Occupation

Interestingly, agricultural workers, such as farmers, have been found to have an increased risk of PCa of between 7-12%. Male workers in other industries, such as rubber manufacturing and newspaper printing, may also have an increased risk. Whilst not yet proven, the current hypothesis to account for this deviation from the mean is that exposure to certain chemicals is encountered in these industries, such as herbicides and pesticides in the case of farmers.[46]

1.8 Stages of PCa

There are three major stages of prostate cancer; clinically localised prostate cancer, locally advanced prostate cancer and metastatic prostate cancer. At present, diagnosis of an individual's PCa stage is evidenced by histopathological or cytological specimens taken from the prostate, usually obtained through transrectal core biopsies. The biopsy material is then graded on a Gleason score that ranges from 2-10, with 2 being the least aggressive form of the disease and 10 being the most aggressive.[39] The Gleason score system is further expanded in part 1.10.

1.8.1 Clinically localised PCa

Localised prostate cancer is the stage that is most commonly presented at diagnosis. At this stage, the disease is confined to the prostate and is potentially curable; however, it may also follow a non-impacting course, meaning no negative symptoms are experienced by the patient, in the absence of any treatment. Therefore, several factors determine which treatment is given, of which there are choices such as radical prostatectomy or radiotherapy,

or whether treatment is given at all and the disease is simply monitored. It is recommended that men with a life expectancy of fewer than ten years from other potential causes of death should be actively monitored as their first treatment.[39]

1.8.2 Locally advanced PCa

At this stage of the disease, the tumour spreads through the whole of the prostate and can have an extracapsular extension that may be invading the bladder or rectum. Some patients can still be offered treatment with curative intent (radiotherapy); however, the most mainstay treatment of this stage of the disease is hormonal therapy.[39,47] Hormonal therapy aims to decrease androgen signalling and can be described as a sort of chemical castration. Normal prostate cells are androgen-sensitive. Androgens, such as 5α-dihydrotestosterone **1** (Figure 5), act on androgen receptors on the surface of prostate cells and signal growth.
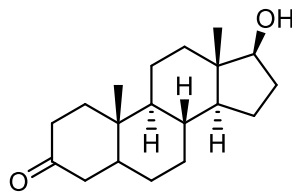
Figure 5: Structure of 5-α-dihydrotestosterone **1**.

Early prostate tumours are also androgen-sensitive and hence depleting androgen levels within the body will prevent further growth of a prostate tumour.[48] On its own, hormonal therapy will not rid the body of prostate cancer but it can manage the disease for several years before further treatment is needed or it can be used in addition to radiotherapy in a curative approach.[49] After a period of time, however, further mutation within prostate tumours often results in the tumour cells progressing to an androgen-insensitive state. At this point, hormonal therapy will no longer have a positive effect.[50]

1.8.2.1 Androgen signalling within the prostate

Androgens, such as 5α-DHT, bind to androgen receptors located in the cytoplasm, resulting in a conformational alteration in the receptor, which, in turn, causes the complex to translocate from the cytosol into the cell nucleus, where it signals for cell proliferation as outlined in Figure 6.[19,51]
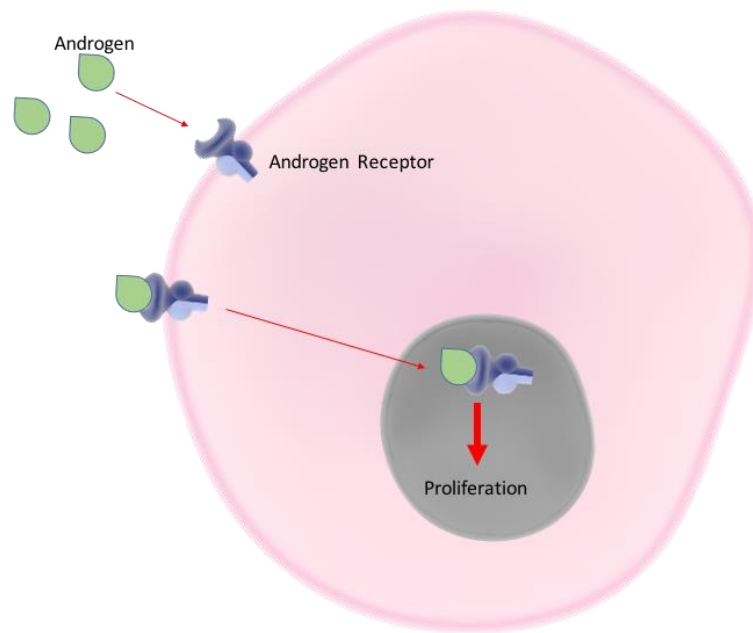
Figure 6: Androgen pathway.

1.8.3 Hormone-refractory PCa

According to Wang *et al.*, "The evolution of prostate cancer from an androgen-dependent state to one that is androgen-independent marks its lethal progression."[52] Once the cancer has become androgen-independent, hormonal therapy is rendered ineffective. At this stage of the disease, chemotherapy is introduced into the line of treatment; however, few effective chemotherapeutic drugs exist, and their effectiveness is limited. Docetaxel is the recommended drug in the UK, as advised by NICE.[47] The median survival length from start of chemotherapy at this stage of the disease is just under two years.[53]

1.8.4 Cell cycle mis-regulation in PCa

Deletion of the PTEN tumour-suppressor gene and fusion of TMPRSS2:ERG are the most commonly known genetic alterations that result in prostate cancer.[33,54,55] Fusion of TMPRSS2:ERG is thought to occur *via* interstitial deletion and translocation. ERG is an oestrogen-regulated gene and functions as a transcriptional regulator, losing its function if it is fused to TMPRSS2 through chromosomal translocation. In about 60% of prostate cancers, deletion of PTEN is observed.[33] PTEN acts as a tumour-suppressor through the negative regulation of the Akt/PKB signalling pathway as previously outlined in Figure 2.[56]

1.9 Diagnosis

Whilst there is no single, definitive test for prostate cancer diagnosis, there are several established methods including digital rectal examination (DRE), PSA blood test, TRUS biopsy and, more recently, multi-parametric MRI that are used to assess the likelihood of prostate cancer in a patient. According to the American Cancer Society (ACS), most prostate cancers are first diagnosed through DRE or a PSA blood test.[57]

1.9.1 Digital rectal examination (DRE)

A digital rectal examination involves the physical examination of the prostate to detect for any signs of tumour growth. By inserting a digit into the rectum, a doctor can detect a tumour growth. A tumour volume of 0.2 mL or more may be detected by DRE. If tumour growth is suspected, a DRE allows a doctor to identify whether the growth is on one side, both sides or is likely to have spread to surrounding areas.

1.9.2 PSA test

The introduction of PSA testing has dramatically reduced the amount of men presenting with metastatic PCa.[47] PSA is produced in the prostatic epithelial cells and secreted into the ductal lumina, from where it is removed by ejaculation. In a normal environment, PSA does not cross through the epithelial membrane and thus is not typically found in the bloodstream.[19] In diseases of the prostate such as PCa, the prostatic architecture is disrupted to a level where PSA can leak back into the prostatic stroma and into the bloodstream.[19] This finding led to the development of the PSA blood test where a rise of PSA-serum levels indicates disease (although not necessarily PCa). The normal range of PSA concentration within serum for a 60-69 year old male is between 0 and 4.5 ng/mL.[58] The PSA test is mainly used to determine whether further investigation is required and not as a definitive PCa diagnosis tool.

1.9.3 TRUS

Trans-Rectal Ultrasound, or TRUS, is an imaging tool that allows one to detect abnormal features such as hypo-echoic areas, loss of differentiation zones, capsular distortion and asymmetry. With regard to PCa, TRUS is primarily used to guide transrectal core biopsies that

allow for further investigation into the histopathological and cytological nature of prostate specimens.[39]

1.9.4 Biopsy

A prostate biopsy involves extracting a small sample of prostate tissue using thin needles. This prostate samples can then be examined to determine the aggressiveness of PCa and the chance of metastases occurring. This type of grading of PCa is known as a Gleason score. There are two types of biopsy commonly used in the clinic; Trans-Rectal Ultrasound (TRUS) guided biopsy and template biopsy. TRUS biopsy uses the aforementioned imaging tool to guide where to obtain biopsy samples and is the most common biopsy type in the UK. Template biopsy involves taking multiple tissue samples from various areas of the prostate by passing a needle through the perineum and is often used in cases where TRUS-guided biopsy cannot be used, due to health problems for example.[59]

1.9.5 mpMRI

mpMRI, or multi-parametric Magnetic Resonance Imaging, is a novel type of MRI involving taking multiple MRI scans and combining them to assemble a much clearer image of the prostate. mpMRI overcomes the issue of missing PCa that can occur *via* TRUS biopsy due to samples taken from across the prostate that don't represent the entirety of the prostate. mpMRI creates an image of the entire prostate, making missing PCa much less likely. mpMRI is non-invasive and non-painful, resulting in it developing into a promising alternative to biopsy.[60]

1.10 Grading PCa – Gleason score system

The Gleason score is the grading system used to determine the aggressiveness of PCa (Table 1). As can be seen in Figure 7, examination of biopsy samples taken from the prostate can provide an insight into the stage of the cancer and a grade between one and five can be obtained. According to the Prostate Conditions Education Council (PCEC), most cancers score a grade of three or greater. To obtain a Gleason score, traditionally two grades are determined; one for the cells that take up the largest are and one for the cells that take up the next largest area. These two grades are added together to give an overall Gleason score. The higher the Gleason score, the more aggressive the cancer, with typical scores ranging between six and ten.[61]
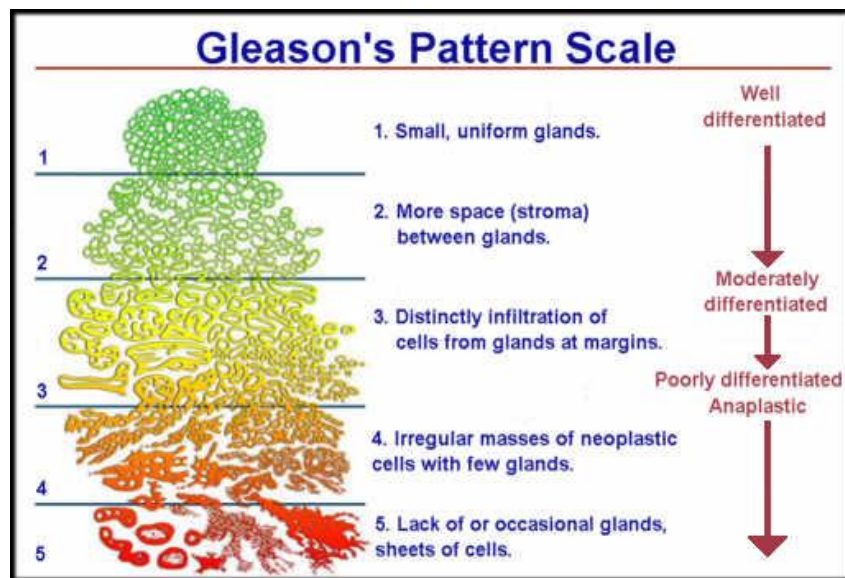
Figure 7: Overview of the Gleason score grading system.[54]

A new Gleason score system has been developed to simplify this scoring and provide more accurate grading stratification, shown in Table 1. Using this system, the cancer is categorised into one of five grades depending on its pathological characteristics.

Table 1: New Gleason grading system.

Traditional Gleason Score	New Grading System
GLEASON 3 + 3 = 6 Only individual discrete well-formed glands.	**GRADE 1**
GLEASON 3 + 4 = 7 Predominantly well-formed glands with a lesser component of poorly-formed/fused/cribiform glands.	**GRADE 2**
GLEASON 4 + 3 = 7 Predominantly poorly-formed/fused/cribiform glands with a lesser component of well-formed glands.	**GRADE 3**
GLEASON 4 + 4 = 8 Only poorly-formed/fused/cribiform glands. Predominantly lacking glands with a lesser component of well-formed glands.	**GRADE 4**
GLEASON 9 – 10 Lacks gland formation (or with necrosis). With or without poorly-formed/fused/cribiform gland.	**GRADE 5**

1.11 Current treatment by stage

Due to the slow-progressing nature of the disease, if detected early enough, many men will not necessarily require immediate treatment as often the side effects, such as loss of bladder control and sexual impotence outweigh the PCa risk to quality of life.

1.11.1 Localised PCa

Localised PCa refers to tumours that have not yet spread out of the prostate gland. Men with this stage of the disease are placed into a risk category determined by the results of a PSA test and Gleason score in order to decide the best treatment course.

1.11.1.1 Active surveillance

Replacing traditional 'watchful waiting', active surveillance involves no treatment until disease progression is observed. The patient undergoes regular PSA testing to monitor PSA levels over a time course. Escalation of treatment will occur at the point of progression.

1.11.1.2 Radical prostatectomy

Radical prostatectomy involves the surgical removal of the prostate, the seminal vesicles and potentially the pelvic lymph nodes. In the case of localised PCa, if the cancer is fully contained within the prostate then radical prostatectomy can be curative and so is seen as the best treatment option for men in this position. The procedure can be performed *via* robot-assisted keyhole surgery. It is possible to spare the nerves required for erectile function in a surgery known as nerve-sparing radical prostatectomy if no sign of PCa is detected in those regions. Side effects of this treatment most commonly experienced are the inability to have children naturally (unless sperm storage has been carried out prior to the operation), impotence and urinary problems.[62]

1.11.1.3 Radiotherapy

There are two main forms of radiotherapy used in the treatment of PCa; external beam radiotherapy (EBRT) and brachytherapy. EBRT involves delivery of external radiation to the tumour over a course of 4-8 weeks. Radiation toxicity to the bowel and bladder is common due to their proximity to the prostate. Damage to the neurovascular system can also result in erectile dysfunction. Vessel-sparing radiotherapy, analogous to nerve-sparing radical prostatectomy, has been successfully developed in order to preserve erectile function.[63] Brachytherapy involves either the permanent implantation of low dose radioactive seeds or high dose radioactive wires directly into the prostate, with analogous side-effects to EBRT.[44]

1.11.2 Advanced PCa

At this stage of the disease, the disease is no longer localised to the prostate and has spread to other areas of the body, with the most common areas being the bones and the lymph nodes. There is no current curative treatment for advanced PCa however, treatment can keep the disease under control for several years.[64]

1.11.2.1 Hormone therapy

Hormone therapy is the main treatment for advanced PCa and involves ridding the body of androgens due to the cancer cells requiring androgen for growth. Figure 8 outlines the main areas targeted by hormone therapy. Luteinizing hormone-releasing hormone (LHRH) agonists

and antagonists can both be used to achieve androgen deprivation. In the pituitary gland, LHRH agonists act by overstimulating LHRH receptors which in turn leads to downregulation of luteinizing hormone (LH). LHRH antagonists block LHRH receptors, leading to a rapid decrease in LH levels. LH acts on the testes to stimulate testosterone production and so without LH, the amount of testosterone produced falls to castration levels (< 50 ng/dL).[65] Anti-androgen drugs act on the androgen receptor to block androgen stimulation and are often used in combination with LHRH agonists or antagonists to enhance androgen deprivation over a period of time.
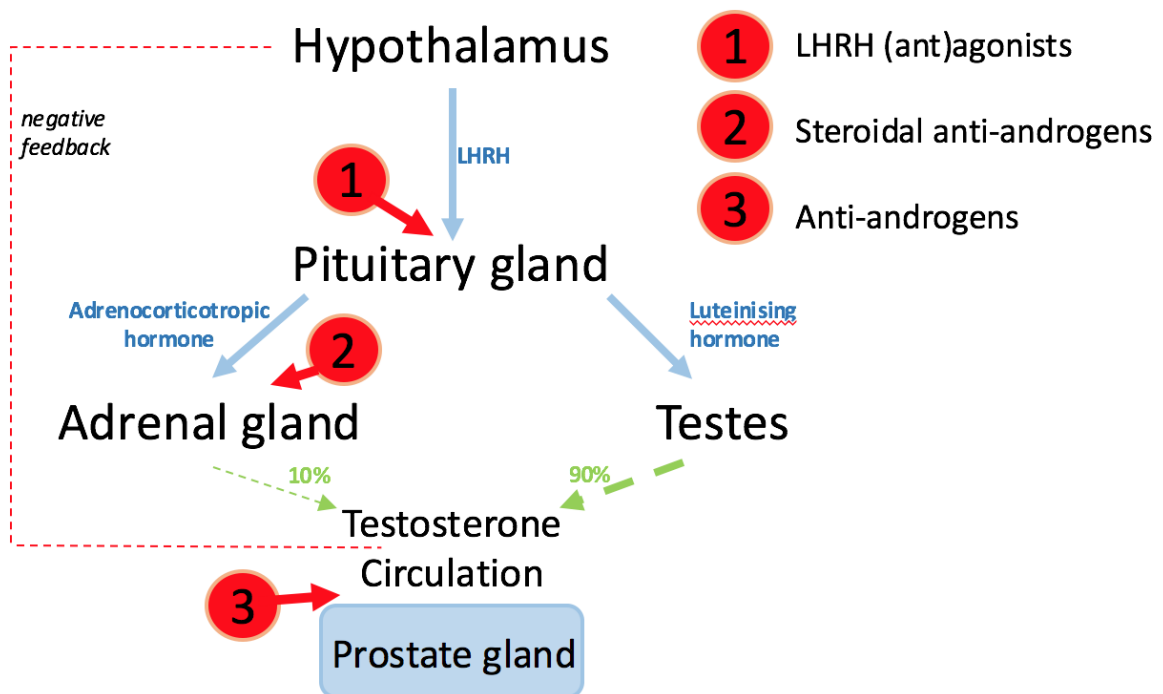
Figure 8: Overview of hormonal therapy targets.

1.11.2.1.1 Luteinising hormone releasing hormone (LHRH) agonists

LHRH agonists are the most common type of treatment for patients with advanced PCa. By overstimulating LHRH receptors, LHRH agonists such as Leuprolide, cause the pituitary gland to stop releasing luteinising hormone *via* the negative feedback loop outlined in Figure 8. Over the long term, this results in down-regulation of LHRH receptors and leads to castration levels of testosterone (< 50 ng/DL) within 2-4 weeks in 90% of patients. In the short term however,

symptoms such as bone pain may flare up due to an initial rapid increase in testosterone levels.[65]

1.11.2.1.2 LHRH antagonists

Testosterone suppression may also be achieved using LHRH antagonists and research has shown that they are also associated with improved disease control compared to LHRH agonists.[65]

1.11.2.1.3 Steroidal anti-androgens (SAA)

A steroidal anti-androgen is simply an androgen with a steroidal chemical structure. Cyproterone acetate (CPA) **2** (Figure 9) is the major SAA used in the treatment of PCa and acts as a competitive androgen receptor weak partial agonist, blocking DHT activation of the AR receptor.[66]

2
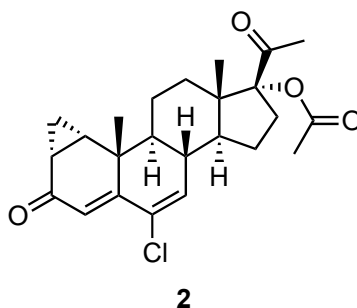
Figure 9: Structure of cyproterone acetate **2**.

1.11.2.1.4 Anti-androgens

Non-steroidal anti-androgens, such as Enzalutamide® **3** and Bicalutamide® **4** (Figure 10), act in a similar way to SAA compounds however do not share their chemical structures with steroidal compounds. Bicalutamide® is a first generation anti-androgen that is typically used alongside a gonadotropin-releasing hormone (GnRH) analogue or after orchidectomy.[67] Enzalutamide® is a second generation anti-androgen also commonly prescribed alongside castration. Enzalutamide® and Bicalutamide® both work as selective silent antagonists of the androgen receptor. Interestingly, work by Chang *et al.*[68] has found that androgen deprivation therapies combined with anti-androgens such as Enzalutamide® and Bicalutamide® can in fact lead to promotion of PCa metastasis. Hu *et al.*[69] found that Enzalutamide® increased

expression of AR3, an androgen receptor lacking an AR binding domain, which may then enhance cell cycle-related genes to promote PCa progression.
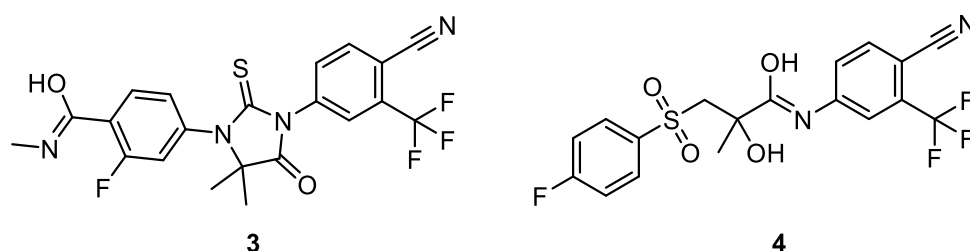
Figure 10: From left to right; structures of Enzalutamide® **3** and Bicalutamide® **4**.

1.11.2.2 Orchidectomy

Alternatively, surgical removal of the testes (orchidectomy) can be performed which will result in castration levels of testosterone. Unlike with chemical hormonal therapy, common side effects such as loss of libido and impotence are irreversible due to the permanent nature of the surgery.

1.11.3 Hormone-refractory PCa

Patients with advanced PCa will most likely progress to hormone refractory PCa where the cancer becomes androgen-independent and thus no longer responds to hormonal therapy. Treatment of PCa at this stage of the disease is symptomatic and aims to improve QOL.

1.11.3.1 Chemotherapy

There are several drugs in the clinic that are commonly used to treat advanced PCa including; docetaxel **5**, cabazitaxel **6** and mitoxantrone **7** (Figure 11). In the UK, docetaxel is the most commonly prescribed first line chemotherapeutic treatment for advanced PCa on the NHS. Docetaxel, sold under the brand name Taxotere®, was first approved for medical use in 1995.
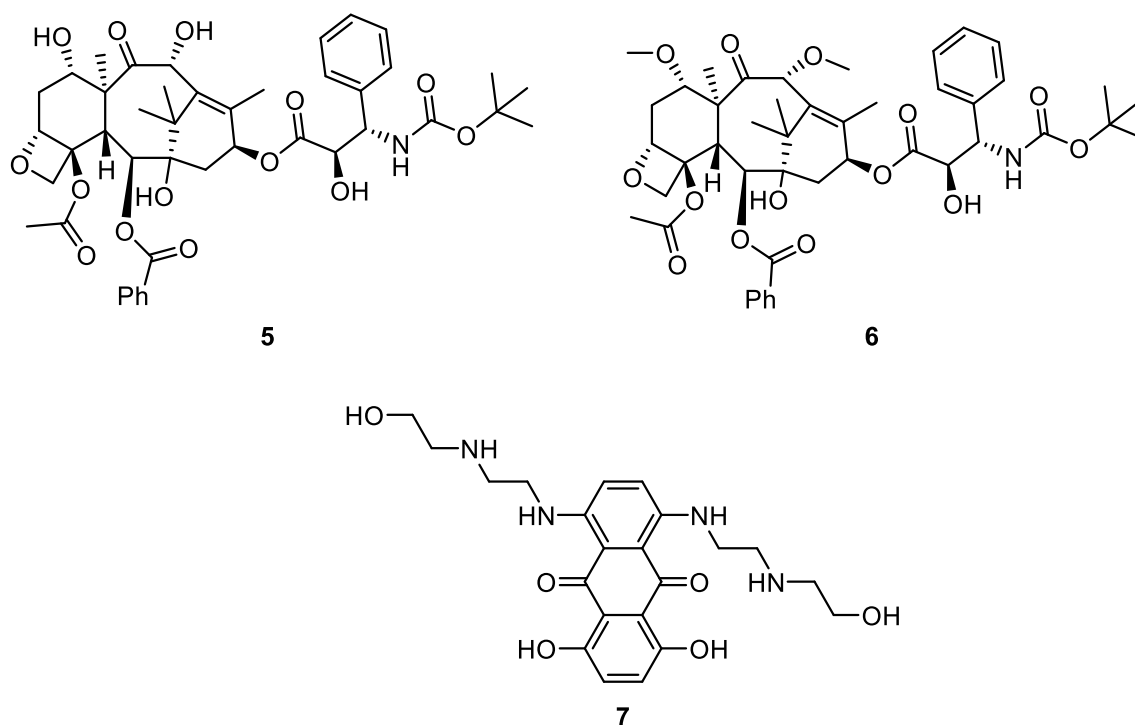
Figure 11: Structures of docetaxel **5**, cabazitaxel **6** and mitoxantrone **7**.

Docetaxel 5 and cabazitaxel **6** promote and stabilise microtubule formation, resulting in a significant decrease in free tubulin dimers, which in turn limits mitotic cell division. The accumulation of stabilised microtubules inside the cell initiates apoptosis.[70] Taxane therapy is non-selective and affects all highly proliferating cells, such as those of the bone marrow and intestinal epithelium. Common side effects of taxanes include immunosuppression and gastrointestinal disorders. According to NICE, after a docetaxel treatment regime, patients with advanced PCa may undergo further chemotherapy with either Enzalutamide® or abiraterone. Patients who cannot tolerate docetaxel are usually treated with a combination of mitoxantrone and prednisolone. Mitoxantrone **7** is a type ii topoisomerase inhibitor, disrupting DNA synthesis and repair by intercalating between DNA base pairs.[71]

1.11.3.2 Second-line hormonal therapy

Many patients with hormone-sensitive PCa go on to experience recurrence or progression despite first-line androgen deprivation therapy. At this stage, second-line hormonal therapies can be implemented to attempt to control the growth of the tumour. Abiraterone **8** (Figure 12) is a selective inhibitor of androgen biosynthesis, which acts by irreversibly blocking CYP17A1, an enzyme involved in the synthesis of testosterone. Until 2016, abiraterone **8** was

only available through the NHS in England to patients who had previously had chemotherapies such as docetaxel **5**. Since 2016, however, abiraterone **8** is now available on the NHS to men with prostate cancer whether they have had chemotherapy or not. In the recently completed STAMPEDE clinical trial, the effect of abiraterone **8** in combination with first-line hormonal therapies was investigated. Half the men in the study were treated with hormone therapy while the other half received hormone therapy and abiraterone **8**. In men who were given abiraterone **8**, there was a 70% reduction in disease progression.[72]
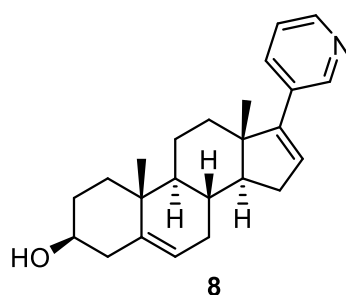
Figure 12: Structure of abiraterone **8**.

1.11.3.3 Novel therapies

The lack of curative treatment for advanced PCa and severe side-effects of existing treatments has led to research focusing on alternative therapies. One promising avenue of research is the development of novel drugs that are based on a class of naturally occurring cyclopropapyrroloindole (CPI) compounds known as anti-tumour antibiotics.

1.12 CPI alkylating agents
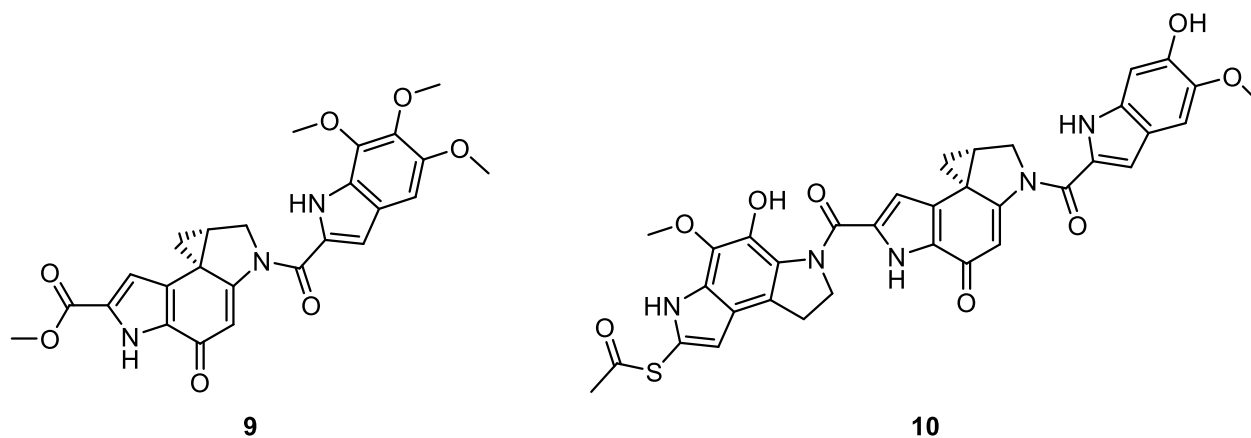
Figure 13: Structures of duocarmycin SA **9** and yatakemycin **10**.

Isolation of (+)duocarmycin SA **9** and (+)-yatakemycin **10** (Figure 13), two highly potent anti-tumour antibiotics, from fermentation cultures of *Streptomyces* sp, opened up a new class of naturally derived DNA-alkylating agents known as cyclopropapyrroloindoles (CPIs), such as the highly potent CC-1065 **11** (Figure 14).[73,74] Studies on alkylation of DNA show that CPI compounds alkylate sequence-selectively adenine-N^3 at AT-rich sites ($\geq$ 90%) in a reversible manner and are extremely potent cytotoxic compounds with IC_{50} values in the picomolar range.[75] Severe toxic side-effects, such as delayed death (after 50-90 d) in healthy mice from hepatotoxicity resulting from a single dose of CC-1065 **11**, have precluded these CPI compounds from clinical development. Mice treated with high doses of CC-1065 died within 12 days with hepatic necrosis, whereas the delayed death phenomenon occurred at lower doses and was associated with changes in hepatic mitochondrial morphology, most likely due to binding of mitochondrial DNA to CC-1065 **11**.[76] It has been postulated that this delayed death toxicity is associated with large DNA interaction parameters through formation of stable drug-DNA adducts and significant non-covalent binding of CPI compounds to minor-groove of DNA; however, compounds with decreased non-covalent drug-DNA binding do not exhibit this delayed death toxicity whilst remaining biologically active.[77] This phenomenon appears to be connected with the ethano-bridges in the non-covalent binding subunits. Due to the intense potency of this class of compounds, efforts have been made to develop analogous compounds that retain biological activity whilst limiting toxicity.
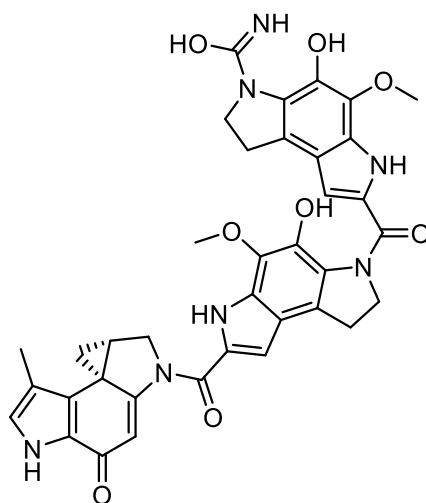
11

Figure 14: Structure of CC-1065 **11**.

1.12.1 Mechanism of action

The structure of CPI compounds can be split into two distinct parts; firstly non-covalent association with the minor-groove of DNA occurs, followed by sequence-selective alkylation at adenine-N^3, which then leads to a cellular cascade of events resulting in apoptosis.[74,78] These two steps are associated with two distinct subunits of the CPI; a minor groove-binding subunit and an alkylating subunit. Initial binding to the minor-groove of DNA occurs through van der Waals forces and hydrophobic interactions to AT-rich regions of the minor groove. This interaction brings the highly strained electrophilic cyclopropyl ring into a close spatial proximity with adenine-N^3. Nucleophilic attack of adenine to the least sterically hindered cyclopropyl carbon and subsequent electron cascade to the C5-carbonyl results in the formation of covalently-bound drug-DNA adduct (Scheme 1).
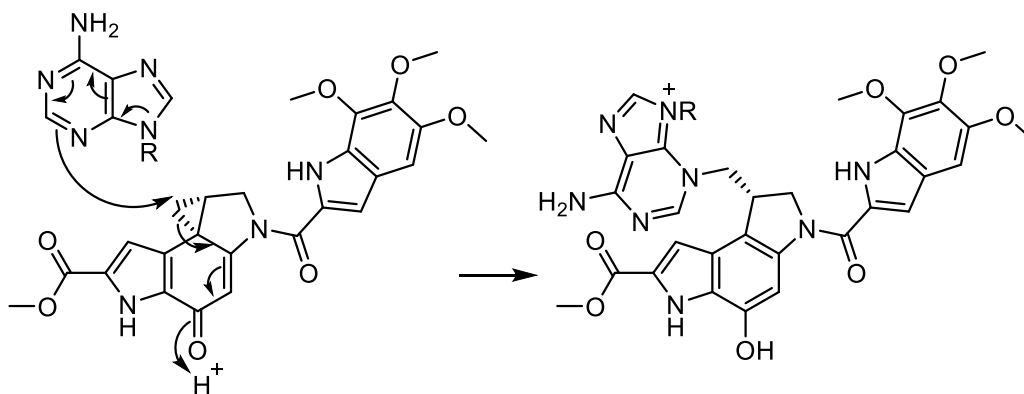
Scheme 1: Mechanism of DNA alkylation of duocarmycin SA **9**.

1.12.2 DNA alkylation of duocarmycin SA and CC-1065

Site-selectivity of DNA alkylation can be determined through several methods. One such method is through thermally induced depurination and strand cleavage whereby labelled DNA is exposed to the alkylating agent in question to induce alkylation. Thermally induced depurination and strand cleavage is then carried out to allow for the identification as to the site of alkylation. The site-selectivity of alkylation by (+) duocarmycin SA **9** and CC-1065 **11** was determined *via* this method. (+) duocarmycin SA **9** and CC-1065 **11** both exhibited preference towards an alkylation site preceded by 5' A or T bases, with the order identified as 5'-AA<u>A</u> > 5'-TT<u>A</u> > 5' TA<u>A</u> > 5' AT<u>A</u>.[75,77–83] A smaller amount of alkylation at guanine-N^3 has been detected.[73] Calf Thymus DNA (CT-DNA) melting assays showed that the thermal melting parameter of CT-DNA (ΔT_m) when exposed to CC-1065 **11** was increased by ≥ 30 °C (the detectable limit of the machine was 30 °C).[77]

12
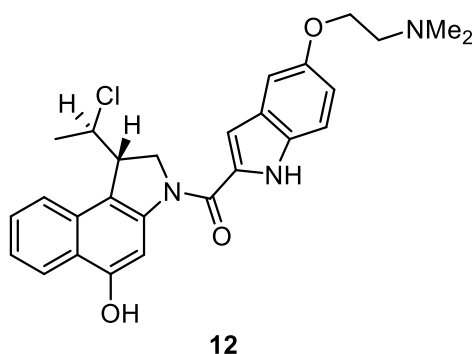
Figure 15: Structure of *seco*-hydroxy-CBI analogue **12**.

More recently, Tietze *et al.*[84] investigated the DNA alkylation selectivity of an analogous *seco*-hydroxy-CBI compound **12** (Figure 15) through High-Resolution Mass Spectrometry. Electrospray ionization Fourier transform ion cyclotron resonance mass spectrometry (ESI-FTICRMS) measurements were carried out directly with the reaction solution (diluted with methanol), without chromatographic purification and enrichment of the alkylated DNA common to similar MS investigations. The simultaneous detection of substrates, intermediates, and alkylated oligonucleotide products allows for direct conclusions concerning the efficiency and the selectivity of the alkylation as well as the nature and amount of the compounds present in the reaction solution. Fragmentation of the adducts in the region of the alkylation site can also be induced by variation of the measurement conditions to allow precise localization of the binding site.[84] Compound **12** exhibited alkylation selectivity towards TT<u>A</u> and TA<u>A</u> sites (5' -> 3'), complementing the selectivity of duocarmycin **9** and CC-1065 **11**.[84]

1.12.3 Mechanism of cell death

There are several mechanisms by which cell death can occur, such as apoptosis, oncosis, nepoptosis, autophagic cell death and pyroptosis.[85,86] Apoptosis is by far the most well understood mechanism of cell death, having been extensively studied.[86] Figure 16[87] outlines the pathways towards apoptosis. Activation of the execution pathway led by caspase 3 is performed by either by extrinsic or intrinsic pathways. The execution pathway results in characteristic cytomorphological features including cell shrinkage, chromatin condensation, formation of cytoplasmic blebs and apoptotic bodies and finally phagocytosis of the apoptotic bodies by adjacent parenchymal cells, neoplastic cells or macrophages.[87] Wrasidlo *et al.*[75] identified apoptosis as the primary cell death route resulting from cell exposure to CPIs, through conducting microscopic examination of Molt-4 leukaemia cells after several hours of CPI incubation. The cells were found to have undergone shrinkage and blebbing characteristic cytomorphological features of apoptosis without the occurrence of lysis, a phenomenon characteristic of necrosis. Investigation also showed that, if cells were exposed to

duocarmycin SA **9** for 20 min followed by removal of drug, cell death was observed, indicating rapid uptake of duocarmycin SA **9** into cells that led to immediate initiation of cell death.[75]
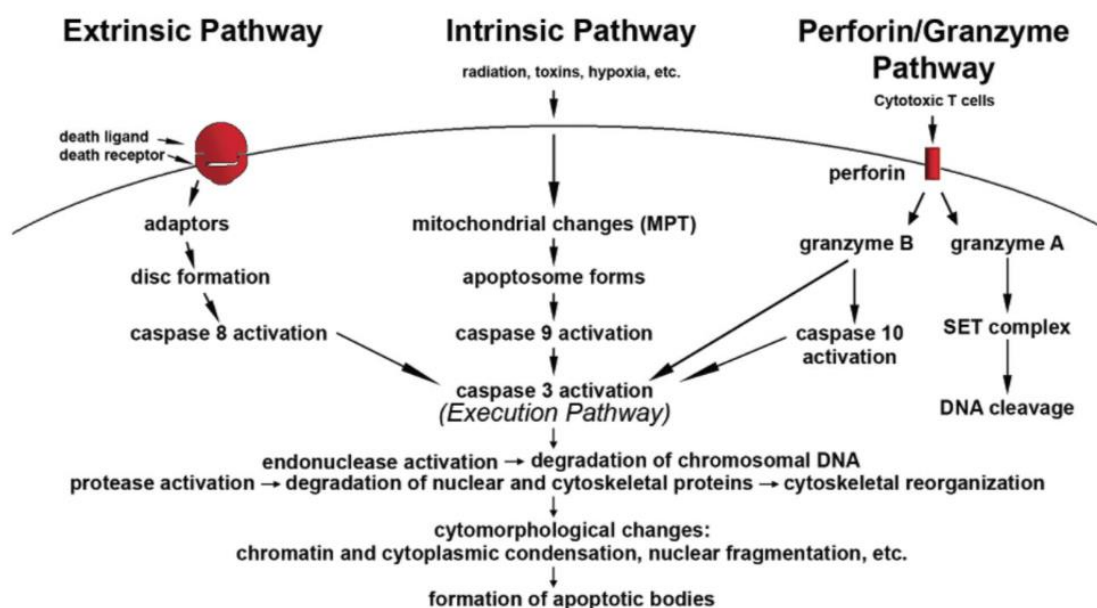
Figure 16: Overview of the apoptosis pathway.[81]

1.12.4 SAR exploration towards novel analogues of CPIs

As previously stated, extensive effort has led to the development of compounds analogous to the CPIs that retain their exquisite potency whilst removing the extreme systemic toxicity that has prevented these compounds from progressing clinically. SAR of duocarmycin SA **9** was carried out, identifying four areas for investigation, as outlined in Figure 17, namely; modification of the A-ring, modification of the 5-C group, modification of the C-ring and linking amide, and modification of the minor-groove binding subunit.
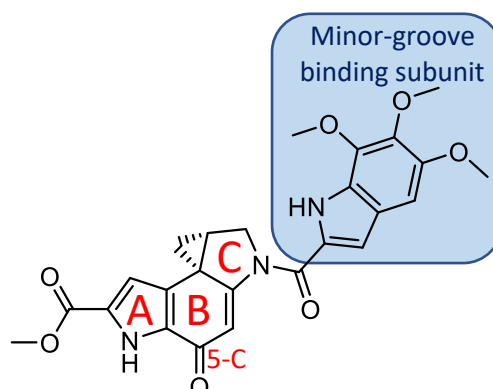
Figure 17: An overview of the areas of duocarmycin SA **9** investigated through SAR; the ring system A-B-C and the minor-groove binding subunit are highlighted.

1.12.4.1 Exploration of the C-ring and linking amide

SAR investigations around the C-ring explored two main areas; importance of a 5-membered ring, and importance of a cyclopropane. It was found that the stereo-electronically controlled ring-opening of the cyclopropane (solvolysis) was influenced by the difference in alignment of the cyclopropane bond from the quaternary carbon to the secondary and tertiary carbons as shown in Figure 19.
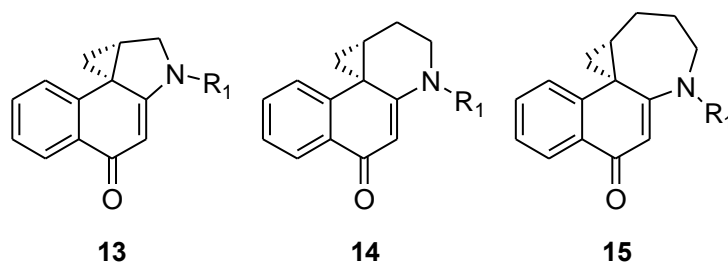
Figure 18: Exploration of the C-ring. From left to right; structures of N-Boc-CBI **13**, N-Boc-CBQ **14** and N-Boc-CNA **15**.

The rate of solvolysis of two analogues of N-Boc-CBI **13** with differing sizes of C-ring (Figure 18) were investigated. In the case of N-Boc-CBQ **14**, with a 6-membered C-ring, solvolysis of the cyclopropane occurred much more rapidly (63-fold) compared to N-Boc-CBI **13** yet cytotoxicity diminished by 50-fold.[88] When compared to N-Boc-CBI **13**, the steric constraints of the fused five-membered ring results in placing the cyclopropane ring at 20° away from the plane of cyclohexadienone (Figure 19). This causes non-ideal alignment and non-ideal conjugation of the cyclopropane ring. It is this difference that results in a parabolic relationship between compound stability and cytotoxicity which went directly against the prior hypothesis that a greater reactivity of the electrophilic cyclopropane would result in greater cytotoxicity due to increased rate of alkylation at adenine-N^3.[88]
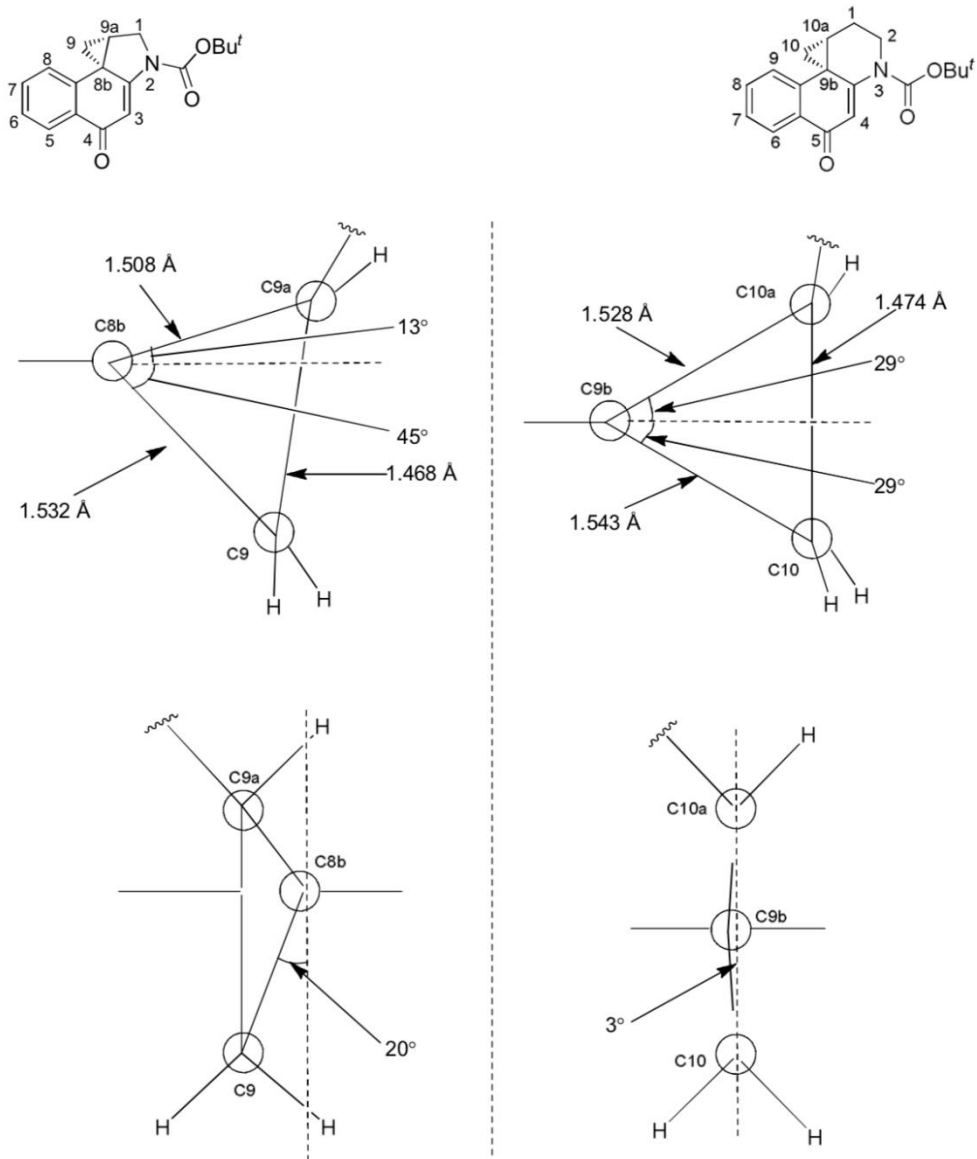
Figure 19: Side and 90° rotation view of cyclopropane ring of CBI **13** and CBQ **14**.[82]

N-Boc-CNA **15**, with a 7-membered C-ring, was shown to undergo much faster solvolysis under acidic conditions, with a half-life at pH 3 of just 0.03 h compared to 133 h for N-Boc-CBI **13**. X-ray crystallography showed that the cyclopropane ring of this compound is nonideally conjugated with the π-system and rises above the plane of the cyclohexadienone resulting in a better steroelectronic alignment of the more substituted carbon for nucleophilic attack. This results in a reversal of solvolysis regioselectivity with nucleophilic addition to the cyclopropane ring occurring exclusively at the tertiary cyclopropane carbon, rather than the least substituted carbon, and the sole formation of the ring-expansion product (Figure 20).[89]
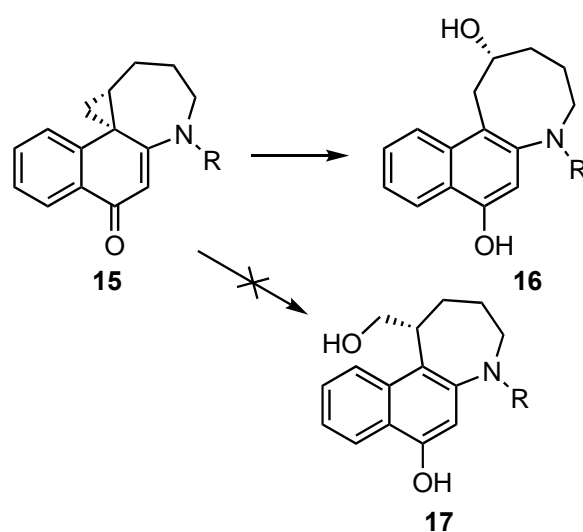
Figure 20: Solvolysis of N-Boc-CNA **15** to yield ring expansion product **16**.

Synthesis of the methylene analogue CBI-CH$_2$-TMI **19** allowed for investigation into the importance of rigidity about the N^2. Amide bonds restrict rotation about the N^2 bond through mesomerically induced SP$_2$ character. By removing the carbonyl, and therefore the SP$_2$ character, rotation about N^2 is increased. Acid solvolysis studies showed a great increase in the solvolysis stability, i.e. resistance of ring opening under acid conditions, of CBI-CH$_2$-TMI **19** compared to CBI-TMI **18** with half-lives at pH 3 of 3.6 y and 230 h respectively. In stark contrast to the previously evidenced conclusion that greater solvolysis stability equated to greater cytotoxicity, CBI-CH$_2$-TMI **19** showed a relative decrease in cytotoxicity of > 10^5-fold.[90] Given that the linking amide decreases the electrophilicity of the C4-carbonyl through mesomeric effects, one would expect a more basic C^4-carbonyl in CBI-CH$_2$-TMI **19** and therefore, increased acid solvolysis. This effect, however, is outweighed by the alteration in conformation (specifically the dihedral angle χ$_1$) caused by a lack of vinylogous amide

stabilisation for DNA binding-induced conformational change activating the compound for nucleophilic attack with $K_{A2} > K_{A1}$ and $K_{B1} >> K_{B2}$ as shown in Figure 21.
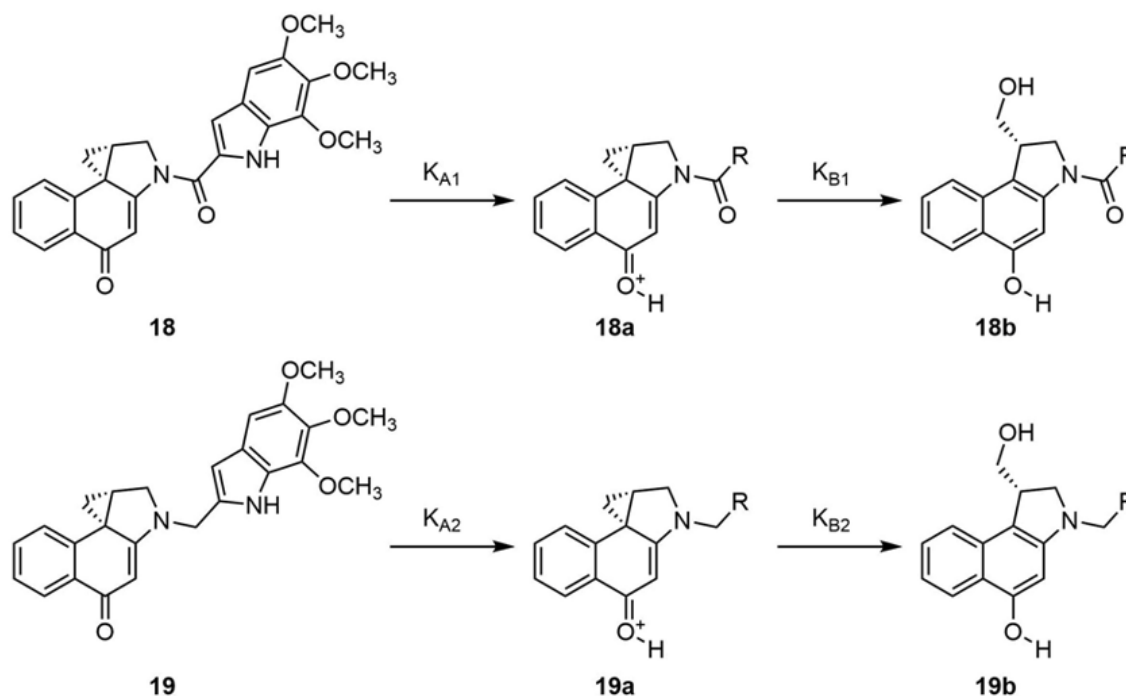
Figure 21: Importance of the linking amide. Comparison of the rate of solvolysis of **18** and **19**. R = 5,6,7-trimethoxyindole.

1.12.4.2 Exploration of the A-ring; CI and CBI analogues of the CPIs

Duocarmycin SA **9**, yatakemycin **10** and CC-1065 **11** all contain a pyrrole-like A ring. Exploration as to the importance of this A-ring was carried out firstly by synthesis and biological evaluation of cyclopropaindol-4-one (CI) compounds shown in Figure 22.[91] This structure was found to be the minimum potent pharmacophore. CI compounds were identified as a precursor to CC-1065 and thus were more facile to synthesise, while maintaining exceptional electrophilicity required for alkylation of DNA.[78,91,92] CI compounds were found to maintain the selectivity of alkylation exhibited by their CPI counterparts, although with a much lower cytotoxic potency.
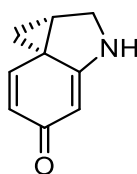
Figure 22: Core structure of CI compounds.

1.12.4.3 Exploration of minor-groove binding subunits

The cytotoxicities of analogues of the anti-tumour antibiotics has been found to depend heavily on the presence of a non-alkylating subunit. Analogues that lack this subunit tend to have reduced cytotoxicity, suggesting an important role for the non-alkylating subunit in terms of enhancing the rate of alkylation and potency of the compounds. Several investigations have been carried out in order to gain a deeper understanding of the structure activity relationship regarding the subunit whilst also developing compounds with better solubilities and lower toxicities.[80,83,93] Increasing cytotoxicity has been observed with increase in size and length of the non-alkylating subunit.[94] 5,6,7-Trimethoxyindole (TMI) has been identified as a potent subunit and studies into the effect of the three methoxy groups have indicated that the C5 substituent is of heightened importance, with the analogous 5-methoxyindole compound shown to be fully active (Figure 23).[95] Parrish *et al*,.[96] observed that a variety of substituents in this position had different effects on potency. A hydroxy-substituent at C5 resulted in a 4-fold reduction in potency and an ethoxy group resulted in a 5-fold increase in cytotoxicity.[96] Milbank *et al*,.[97] investigated the use of dimethylaminoethoxyindol-2-carboxylic acid (DMAI) (Figure 23) as a non-alkylating subunit as a way to increase the aqueous solubility through incorporation of a basic dimethylaminoethyl group whilst retaining a C5 alkoxy group for enhanced cytotoxicity. Biological and solubility assays showed that the DMAI-containing analogue exhibited greater efficacy across a range of cell lines compared to the C5-OMe analogue, with solubility also considerably increased.[97]
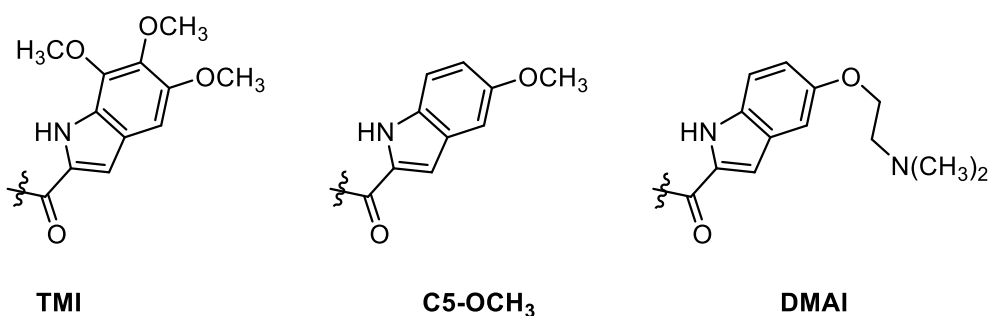
Figure 23: Structures of minor-groove binding subunits, from left to right; TMI, C5-OMe, DMAI.

1.13 CBI alkylating agents

More chemically stable and synthetically accessible than their CPI analogues, cyclopropabenzindoles (CBIs) have been the focus of a great effort of research aimed at developing anti-cancer therapy utilising the exquisite potency associated with these compounds.

1.13.1 *Seco*-CBI and Winstein cyclisation
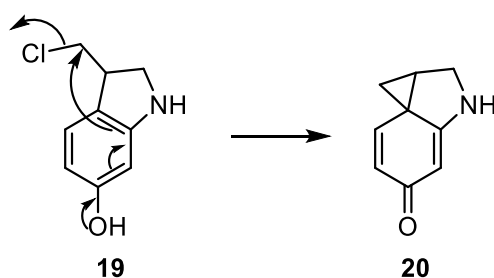
Scheme 2: Mechanism of the Winstein cyclisation with *seco*-hydroxy-CI **20** to yield cyclised CI **21**.

Seco (non-cyclised) analogues generate the reactive cyclopropane ring *in situ via* Winstein-cyclisation before reacting with DNA. Winstein demonstrated that substituted phenols undergo intramolecular cyclisation with participation of the phenoxide ion group to form dienones.[98] Various works have concluded that this reaction occurs through an intramolecular S_N2 reaction and therefore, reactivity depends on the nucleophilicity of the phenoxide or amine, the nature of the leaving group and the reactivity of the electrophilic centre.[99] Several

reports in the literature have demonstrated that the phenoxide group can be replaced by an amine group without being deleterious to the Winstein cyclisation.[100–102]

1.14 Reported synthetic approaches to the CBI 'warhead'

Various synthetic approaches have been developed to CBIs. The CBI 'warhead' can be split into two distinct parts, the alkylating subunit and the non-alkylating minor-groove-binding subunit. Synthesis of the alkylating subunit has proven to be much more challenging and can further be broken down into two stages; synthesis of a pre-cyclisation '*seco*' key intermediate followed by Winstein cyclisation. Most previous investigations have focused on 5-hydroxy-*seco*-CBI analogues, with much fewer focused on 5-amino-*seco*-CBI analogues. Below is a review of some of the synthetic approaches adopted in the synthesis of 5-hydroxy- and 5-amino-CBI 'warhead', split into pre- and post-cyclisation.

1.14.1 Reported synthesis of key intermediate of 5-hydroxy-*seco*-CBI derivatives
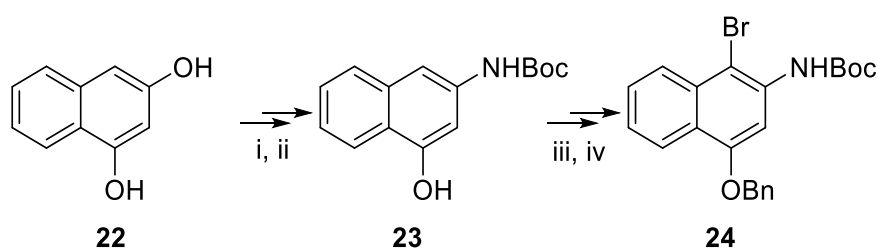
Scheme 3: Synthesis of *tert*-butyl (4-(benzyloxy)-1-bromonaphthalen-2-yl)carbamate **24**. Reagents and conditions: i. liquid NH_3, 130°C; ii. Boc_2O, dioxane; iii. BnBr, K_2CO_3, n-Bu_4NI; iv. NBS, conc. H_2SO_4.

Boger *et al.* developed a synthetic route to pre-cyclisation key intermediate **24** (Scheme 3).[103] Starting from commercially available 1,3-dihydroxynaphthalene **22**, reaction with ammonia under forcing conditions yielded 1-hydroxy-3-naphthylamine. Boc-protection of the amine

gave **23** followed by benzyl protection at the hydroxy group. Finally, reaction with N-bromosuccinimide gave key intermediate **24** *via* electrophilic bromination.[103]

1.14.2 Reported cyclisation of enantiopure 5-hydroxy-CBI derivatives
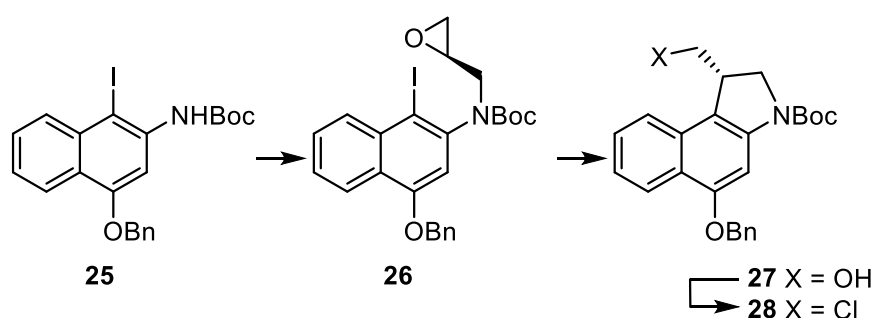
Scheme 4: Synthesis of the benzyl-protected *seco*-CBI precursor **28**. Reagents and conditions: i. NaH, DMF, *R*-glycidyl nosylate; ii. ZnCl$_2$, MeLi, THF, TMS-NCS; iii. PPh$_3$, CCl$_4$, CH$_2$Cl$_2$.

Tietze *et al.*[104] developed a synthetic route to access enantiomerically pure *seco*-OBn-CBI **28** (Scheme 4). Starting with Boc-protected **25**, reaction with *R*-glycidyl nosylate (4-nitrobenzenesulfonate) ensured sole formation of **26**. The importance of having the nosylate leaving group is that it makes the exocyclic CH$_2$ of the epoxide a more powerful electrophile than the CH$_2$ of the oxirane. This ensures that nucleophilic attack will take place solely at the exocyclic CH$_2$, with concerted S$_N$2 displacement of the nosylate, retaining the stereochemical configuration at the oxirane. Weaker leaving groups, such as chloride, result in nucleophilic attack at the oxirane CH$_2$, opening the oxirane. The alkoxide formed then attacks the exocyclic CH$_2$, leading to introduction of a CH$_2$-oxirane unit but with inversion of configuration. Intermediate-strength leaving groups, such as tosylate, proceed by both mechanisms, leading to loss of stereochemical integrity. Halogen-metal exchange at the C-I bond was then carried out, followed by metal-mediated cyclisation.

There are two possible sites of attack on the epoxide to form either the 5-*exo*-trig and/or the 6-*endo*-trig products; however, Tietze *et al.* observed only the 5-*exo*-trig product, yielding

enantiomerically pure *seco*-CBI **27**. The hydroxy group can then be replaced with chlorine by an Appel reaction (Scheme 5), whereby activation of triphenylphosphine by reaction with the tetrahalomethane is followed by attack of the hydroxy oxygen at phosphorus to generate an oxyphosphonium intermediate. S_N2 displacement by halide then takes place, proceeding with inversion of configuration if the carbon is asymmetric. Removal of Boc then allows coupling of **28** to a range of minor-groove-binding subunits. This synthetic route offers the prospect of enantiopure synthesis, which is of particular importance as one enantiomer is significantly more active than the other, as discussed previously.[104]
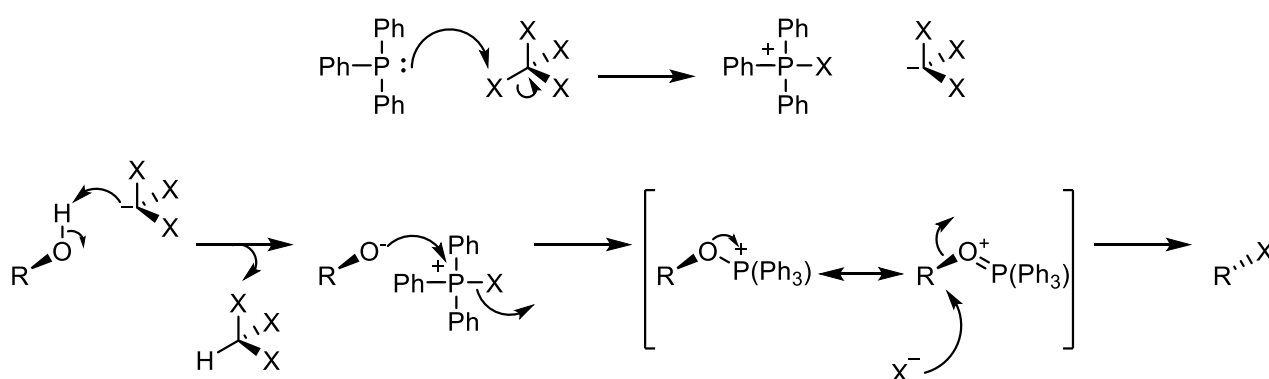
Scheme 5: Mechanism of the Appel reaction and activation of triphenylphosphine.

1.14.3 Reported synthesis of the key pre-cyclisation intermediate of the 5-nitro-CBI derivatives
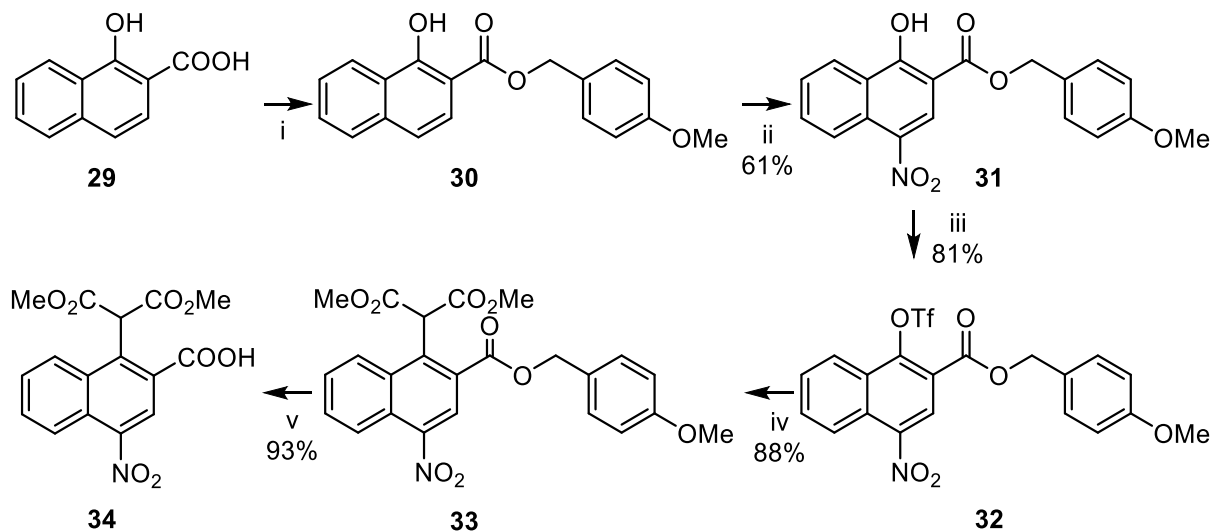
Scheme 6: Synthesis of **34**; *Reagents*: i. NaHCO$_3$, 4-methoxybenzyl chloride; ii. HNO$_3$, AcOH; iii. (Tf)$_2$O, Et$_3$N; iv. CH$_2$(CO$_2$CH$_3$)$_2$, K$_2$CO$_3$; v. TFA, PhOCH$_3$.

Early work into the synthesis of amino-CBI compounds was carried out by Denny *et al.*,[105] who developed a route to access racemic *seco*-amino-CBIs *via* pre-cyclisation key intermediate **34**, the synthesis of which is outlined in Scheme 6. Starting with 1-hydroxy-2-hydroxynaphthalene-2-carboxylic acid **29**, Williamson ester synthesis with 4-methoxybenzyl (PMB) chloride yielded the 4-methoxybenzyl ester **30**.[106] As shown in Scheme 7, deprotonation of carboxylic acid **29** in the presence of 4-methoxybenzyl chloride results in S$_N$2 attack from the negatively charged oxygen toward the δ-positive carbon, displacing the chloride to yield the PMB ester **30**.
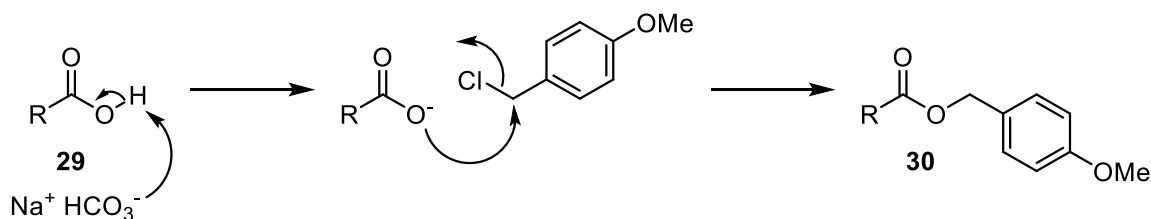
Scheme 7: Mechanism outlining the formation of PMB ester **30** from carboxylic acid **29**. R = C$_{10}$H$_8$OH.

PMB was chosen as the protecting group as, when the removal of a PMB ester is desired in the presence of other esters, many methods may be employed to induce cleavage.[107] In this case, orthogonal deprotection of the PMB ester can be carried out in the presence of the two methyl esters. Nitration at the C-4 position, followed by triflation of the hydroxy group, yielded triflate **32**, which was then treated with the anion of dimethyl malonate to yield **33**. Finally, selective removal of PMB in the presence of the methyl esters was achieved through reaction with anhydrous TFA (Scheme 8) to yield key intermediate **34**. Under these conditions, protonation of the oxygen and subsequent formation of the stabilised 4-methoxybenzyl carbocation which is then trapped with a sacrificial nucleophile such as *para*-methoxyphenol.
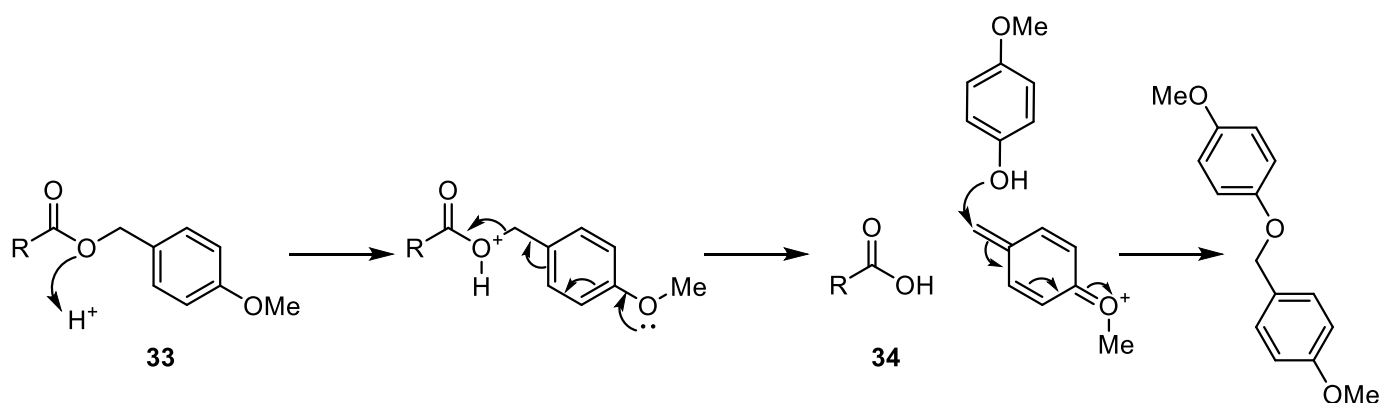
Scheme 8: Mechanism of PMB deprotection of **33** with TFA and *para*-methoxyphenol to yield carboxylic acid **34**. R = $C_{10}H_8OH$.

1.14.4 Reported synthesis of 5-nitro-CBI derivatives
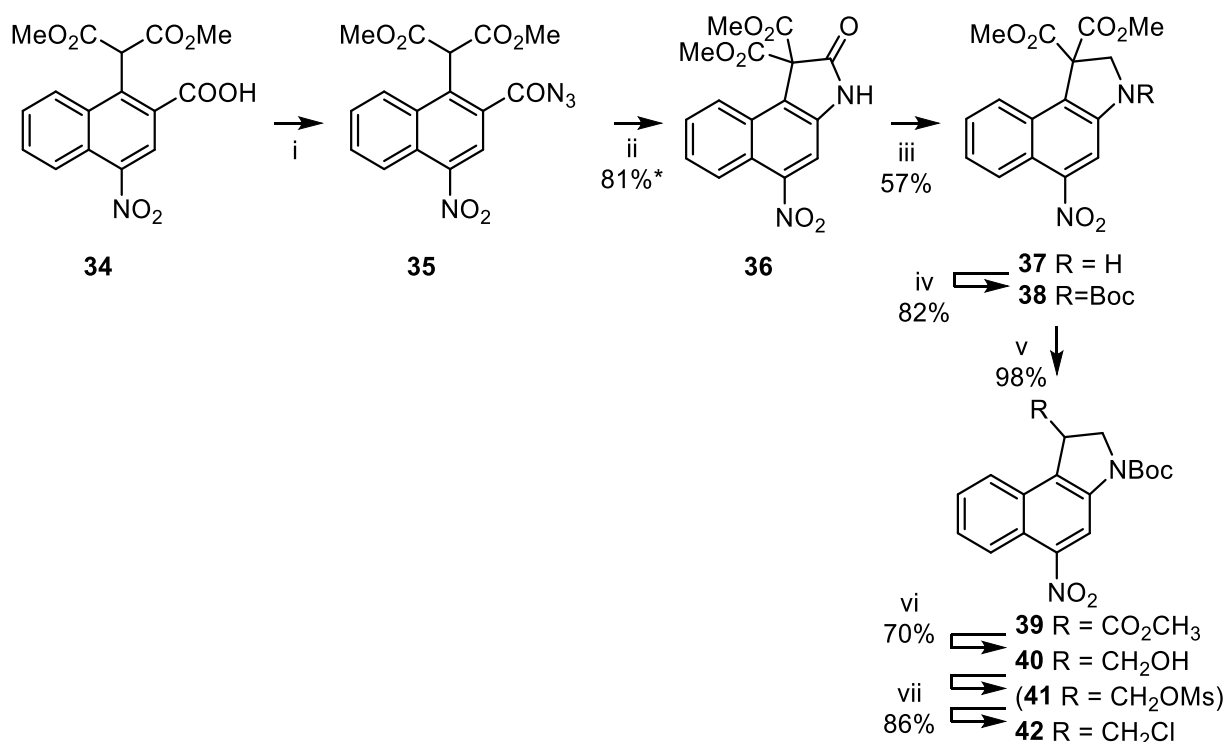
Scheme 9: Cyclisation and functionalisation of **34** to yield *seco*-nitro-CBI **42**. Reagents and conditions: i. a) pyridine, SOCl$_2$, DMF, b) NaN$_3$; ii. PhMe, heat; iii. BH$_3$·Me$_2$S; iv. (Boc)$_2$O; v. a) NaOMe, MeOH, THF b) TFA; vi. DIBALH; vii. MsCl. *Yield for steps i and ii combined.

At this point, cyclisation to yield **36** could then be achieved through a Curtius rearrangement of the carboxylic acid followed by subsequent cyclisation of the isocyanate outlined in Scheme 9. Formation of acid azide **35** with NaN$_3$, followed by heating in toluene, yielded cyclised compound **36**. Selective reduction of the amide carbonyl in the presence of the two methyl esters was achieved with BH$_3$·Me$_2$S. The Lewis acidity of the boron results in the formation of a complex between the boron and the nitrogen of the lactam in order to achieve selective reduction (Figure 24).
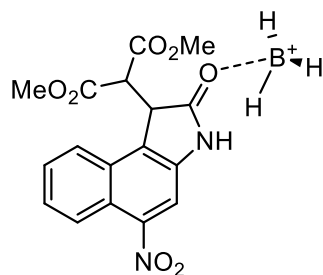
Figure 24: Lewis acid complex with **36**.

Boc protection of the resulting secondary amine yielded compound **38**. Reaction of diester **38** and anhydrous base (NaOMe/MeOH/THF), followed by quenching with TFA, yielded the monoester **39** (Scheme 10). This reaction can be achieved under mild conditions due to the capacity of the stabilised anion intermediate to act as a leaving group.
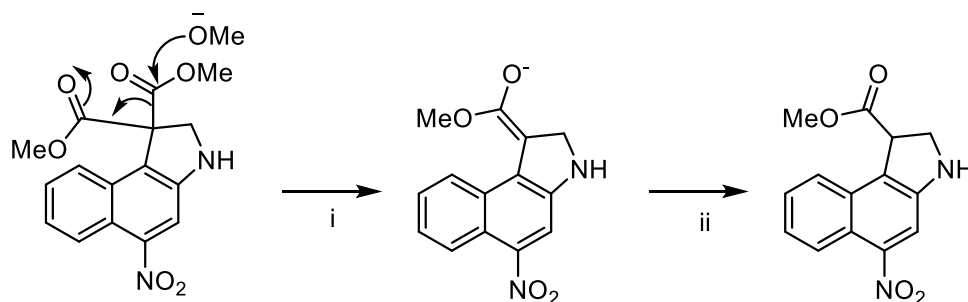
Scheme 10: Treatment of **38** with NaOMe followed by TFA to yield monoester **39**. *Reagents and Conditions:* i. NaOMe, MeOH, THF; ii. TFA.

Reduction of the monoester **39** with two equivalents of DIBAL-H gave the primary alcohol **40** (Scheme 11). The increased Lewis basicity of the carbonyl, compared to the nitro group, allowed for chemoselective reduction to take place solely at the carbonyl. Finally, **40** was converted *via* the mesylate **41** to the chloromethyl compound **42**.
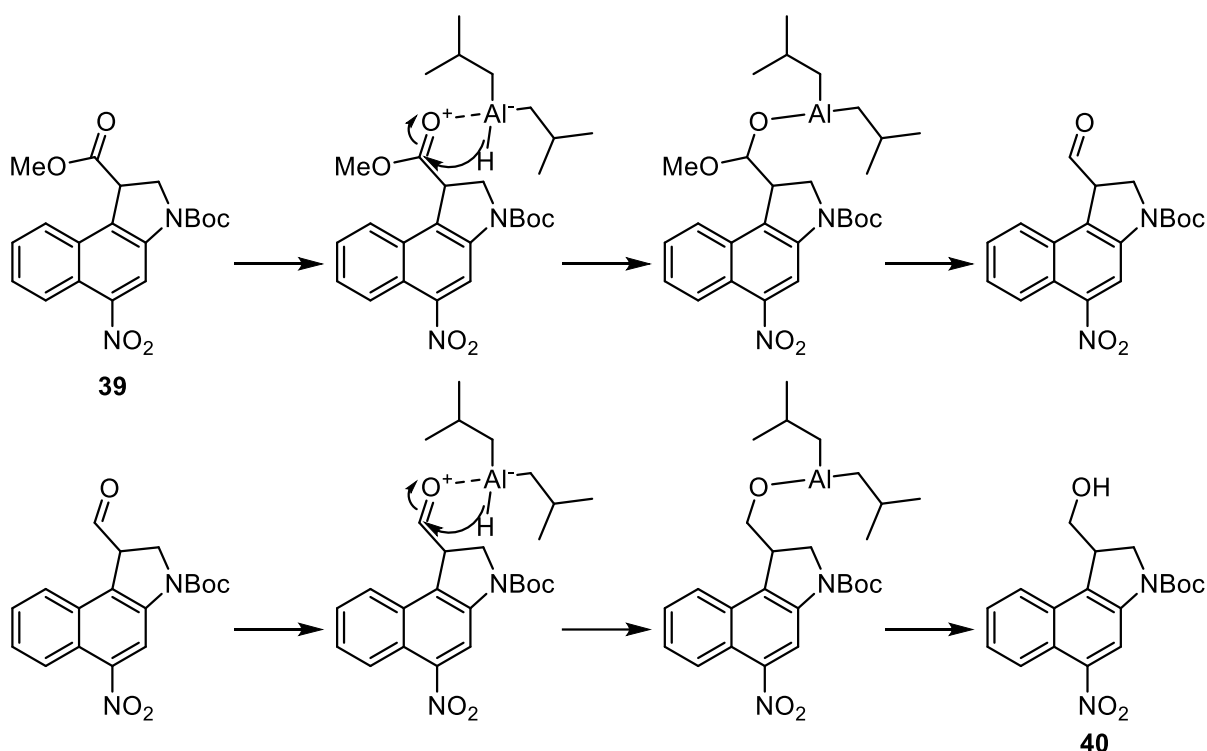
Scheme 11: Mechanism of the reduction of ester **39** with two equivalents of DIBAL-H to yield primary alcohol **40**.

1.14.5 Reported synthesis of pre-cyclisation key intermediates of *seco*-amino-CBI derivatives

Substantial previous work by the Threadgill group has explored synthesis towards enantiomerically pure *seco*-amino-CBIs.[100] Orthogonally protected **49** was identified as a key pre-cyclisation intermediate, the synthesis of which is outlined in Scheme 12. Starting with the commercially available dye Martius Yellow (2,4-dinitronaphthalen-1-ol **43**), the phenolic OH was triflated and S_NAr reaction with iodide yielded **45**. At this stage, reduction of the nitro groups resulted in concurrent hydrogenolysis of the C—I bond, affording naphthalene-1,3-diamine **46**. Formation of the trifluoroacetamide occurred selectively at the more sterically accessible 3-NH_2 to yield **47**; however, this reaction occurred in a low yield (15%) and a significant amount of the diamide **50** was also formed. This indicated that the reactivity of mono-TFA protected **47** was greater than that of starting material **46**. Orthogonal Boc-protection at the 1-NH_2 with Boc_2O was then followed by electrophilic re-insertion of iodine with NIS to yield the key intermediate **49**.
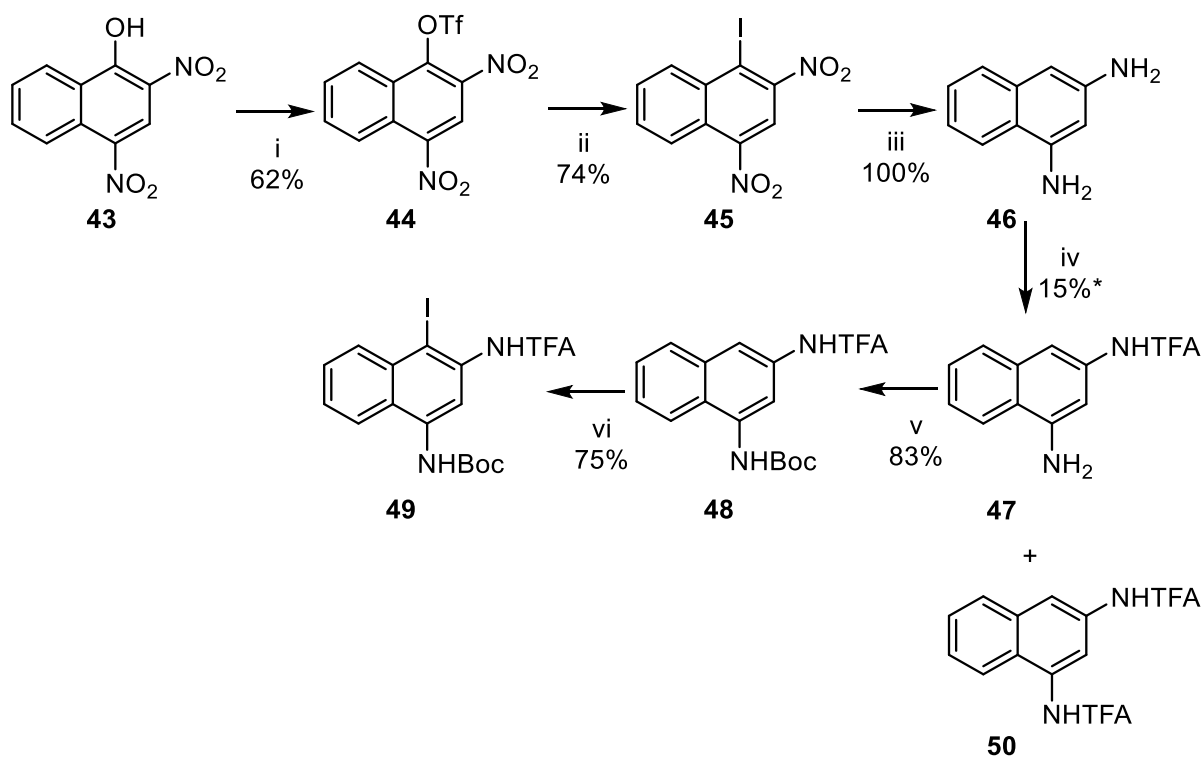
Scheme 12: Route established by Twum *et al.* to intermediate **49** starting with commercially available Martius Yellow **43**. *Reagents and conditions:* i. (Tf)₂O; ii. NaI, Me₂CO; iii. SnCl₂·2H₂O; iv. (F₃CCO)₂O, Pr^{i}₂NEt; v. Boc₂O; vi. NIS, TsOH. *15% yield of desired compound **47**.

1.14.6 Reported cyclisation of key intermediate 49

At this point, two routes to yield cyclised material were explored; a metal-mediated cyclisation that would yield enantiopure material and a free-radical cyclisation to yield racemic material.

1.14.6.1 Attempted metal-mediated cyclisation by Twum *et al*
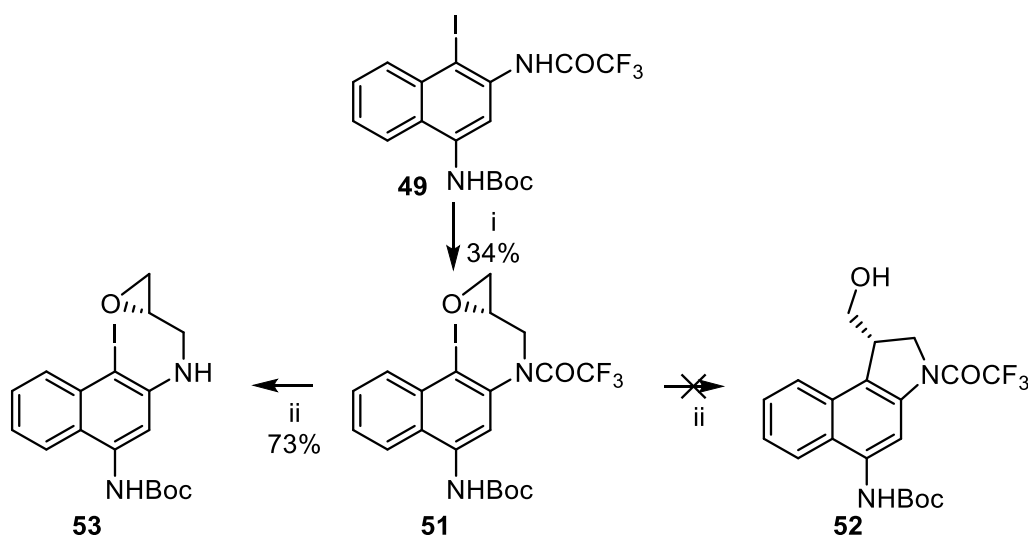
Scheme 13: Attempted metal-mediated cyclisation of **51** resulting in loss of trifluoroacetyl group. *Reagents and conditions*: i. *R*-glycidyl nosylate, K_2CO_3 ii. MeLi, CuCN, Et_2O, THF, N_2, -78°C.

Twum *et al*.[100] attempted metal-mediated cyclisation of key intermediate **49** to yield enantiomerically pure compound **52** through the method carried out on the analogous OBn compound **26**, reported by Tietze *et al*. previously.[100,108] **49** was reacted with *R*-glycidyl nosylate to yield **51**. Metal-mediated cyclisation of **51** was attempted with MeLi and CuCN. However, the sole product was **53**, the result of loss of the trifluoroacetyl group (Scheme 13), attributed to the highly nucleophilic cyanide ion carrying out nucleophilic attack toward the trifluoroacetyl carbonyl. It has been reported that electron-rich naphthalenes tend to undergo slow metal-halogen exchange and the more electron-deficient aromatic iodides are, the faster that metal-halogen exchange proceeds.[109–111] This is due to the inductive substituent effect that is responsible for the activation of the metal-halogen exchange.[109–111]

An electron-rich naphthalene may then result in the reaction conditions favouring the competing nucleophilic attack from the cyanide anion toward the trifluoroacetyl carbonyl carbon that results in loss of the trifluoroacetyl group (Scheme 14).[112]
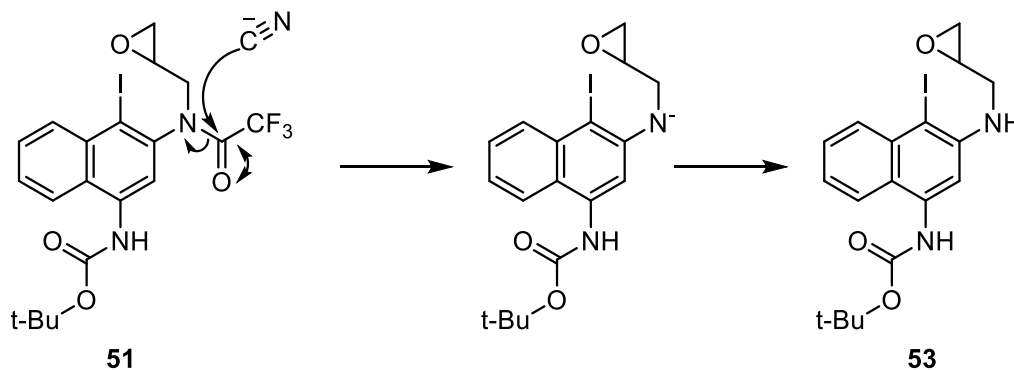
Scheme 14: Mechanism outlining nucleophilic attack from cyanide anion, resulting in loss of trifluoroacetyl group.

1.14.6.2 Reported free-radical cyclisation by Twum *et al*
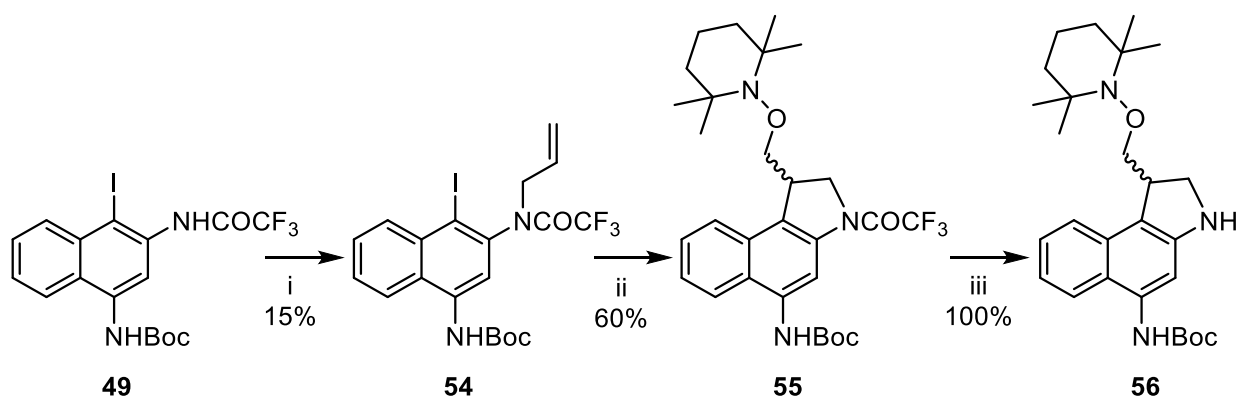
Scheme 15: Free-radical cyclisation of **55** to yield racemic cyclised compound 56. *Reagents and conditions*: i. allyl bromide, KO^{t}Bu, THF; ii. TEMPO, Bu$_3$SnH, benzene, 60°C; iii. NaOH, H$_2$O, THF.

Due to a failure to cyclise **51** under the conditions described by Tietze *et al.*,[104] the focus of Twum *et al*. turned to a free-radical based approach to yield racemic *seco*-amino-CBI **56** (Scheme 15). The trifluoroacetamide of **49** is more acidic than the BocNH, so deprotonation with KO^{t}Bu and alkylation of the anion with allyl bromide resulted in selective alkylation at the N^2-amide to yield **54**. Free radical cyclisation was then performed with Bu$_3$SnH and TEMPO

to form the racemic 5-*exo*-trig cyclisation product **55.** At this stage, chemoselective base-catalysed hydrolysis of the trifluoroacetamide group with sodium hydroxide gave **56**. Competing reductive cleavage of the TEMPO group was not observed as the strong electron-withdrawing fluorines of the trifluoroacetamide resulted in activation of the highly δ+ carbonyl group, making it much more reactive toward base-hydrolysis versus the competing reductive cleavage of the O-N bond of the TEMPO.

1.15 Prodrugs

Docetaxel **5** has an established side-effect profile with effects ranging from neutropenia and sensory neuropathy to alopecia and dysgeusia.[113] The reason that such off-target effects occur with many chemotherapeutics is because such drugs are untargeted and simply attack all cells within the body. The trait that cancer cells are dividing more rapidly than normal cells allows for these drugs to affect cancer cells more than normal cells but also explains common side effects of chemotherapy, such as alopecia. The extreme systemic toxicity of duocarmycin SA **9** and *seco*-amino-CBIs prevents their use as chemotherapeutic drugs in their current state. A prodrug is a compound that, once in the body, will undergo metabolism to produce the active drug and, through converting drugs into prodrugs, their ADME profiles can be altered greatly. By altering highly efficacious compounds, such as CBIs, into prodrugs, the hope is that one would retain the potency of the drugs but that their cytotoxicity could be more controlled. There are several examples in the literature of prodrugs based on duocarmycin analogues.[114–116]

1.15.1 Prodrug monotherapy (PMT)

Prodrug monotherapy exploits a common trait associated with tumour cells, that they often up-regulate an intrinsic enzyme. This enzyme can be used as a mechanism to selectively activate a prodrug which will therefore enhance drug targeting towards tumour cells.[117] Endo-proteases are often up-regulated in cancers as a consequence of, or necessity for, tumour expansion. One such enzyme is PSA, making it a potential target for PMT. Peptide-conjugated prodrugs can therefore be designed to be activated by PSA to achieve selectivity.

1.15.2 Antibody directed enzyme prodrug therapy (ADEPT)

ADEPT has emerged as a promising approach to selectively delivery prodrugs to tumours. It involves the administration of an enzyme-antibody conjugate, with the antibody being tumour-specific to locate the enzyme to the tumour site. Administration of an enzyme activated prodrug then results in selective release of the active drug at the tumour site. Allowing for a period of time to pass between administration of the enzyme-antibody conjugate and administration of prodrug, permits the enzyme-antibody conjugate to clear from normal tissue, preventing off-target activation of prodrug.[118–120]

Work by Chen *et al.*[114] in 2013 shows a glucuronide prodrug **57** (Scheme 16) based on a *seco-*CBI that is metabolised by β-glucuronidase to form a *seco*-drug which then undergoes Winstein cyclisation to yield the active drug.[114] This prodrug is tumour-selective as there are increased concentrations of β-glucuronidase in solid tumours and the charged glucuronide moiety improves aqueous solubility.[114]
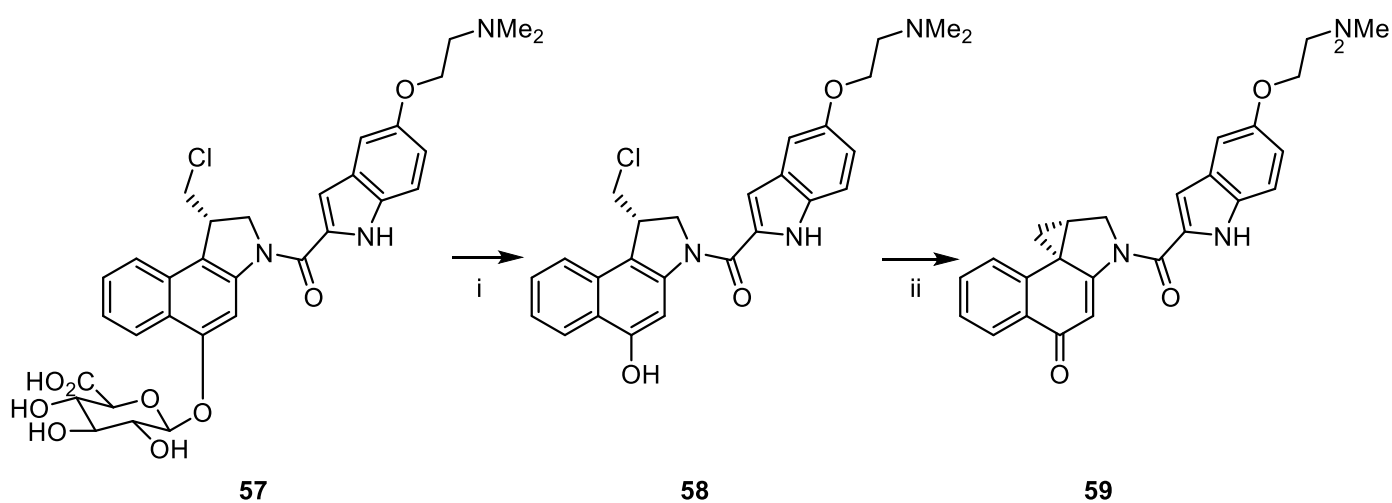
Scheme 16: Mechanism of activation of glucuronidase prodrug **57**. *Reagents and conditions*: i. β-glucuronidase; ii. Winstein cyclisation.

1.15.3 PSA-cleavable prodrugs

Investigation into the development of PSA-cleavable prodrugs incorporating the SSKLQ sequence described by Mhaka et al.[34] has been carried out with some success. DiPaola et al.[121] and DeFeo-Jones et al.[122] investigated the novel PSA-activated peptide-doxorubicin conjugate, L-377,202 **60** (Figure 25). In the presence of PSA-secreting prostate cells, the prodrug was hydrolysed to release Leu-doxorubicin and, subsequently, doxorubicin, both of which are cytotoxic to tumour cells. L-377,202 **60** was around 15-fold more effective than
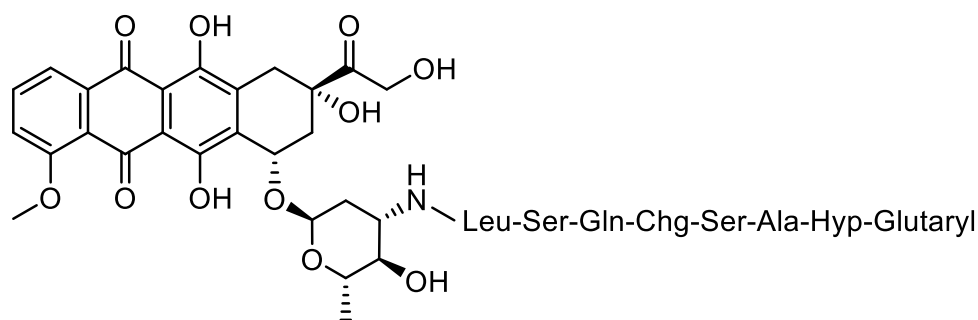
Figure 25: Structure of L-377,702 **60**.

doxorubicin at inhibiting the growth of human prostate cancer tumours in mice when both drugs were used at their maximally tolerated doses. L-377,202 **60** was also much less cytotoxic than doxorubicin to non PSA-expressing cells, with EC_{50} values of greater than 100 mM against DuPRO-1 and PC3 prostate tumour cells, Hct116 human colon tumour cells and NHME normal mammary epithelial cells.[122] DeFeo-Jones et al.[122] reported that mice treated with L-377,202 **60** at its most efficacious dose lost an average of 6% body weight compared to an average loss of 25% body weight by mice treated with doxorubicin. This improved tolerance of L-377,202 **60** was further shown in humans in the phase 1 clinical study by DiPaola et al.[121].

1.15.4 Bio-reductively activated prodrugs

Most solid tumours contain regions with either acute or chronic hypoxia due to the primitive state of the tumour vasculature.[123,124] Hypoxia is a reductive dysfunction of cells and in the case of tumour cells, is considered to be an important factor in resistance to therapy.[125,126] Various efforts have attempted to exploit this physiological difference in concentration of O_2 between normal (normoxic) and hypoxic cells to achieve selective therapeutic targeting of

tumour cells.[127–129] Bio-reductive prodrugs have been developed that are activated by enzymatic reduction in hypoxic tissue.[126] Two such examples are tirapazamine **61**, which is activated under moderate hypoxia, and PR-104 **62**, which is activated under severe hypoxia (Figure 26).
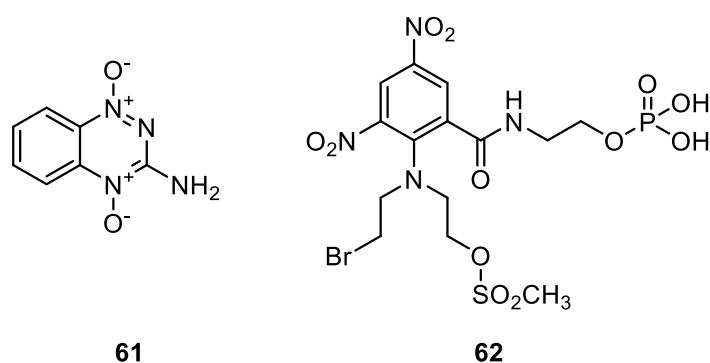
Figure 26: Structures of tirapazamine **61** and PR-104 **62**.

Work by Parveen *et al*,.[127] reported the potential of the 2-nitroimidazol-5-methyl unit **63** as a bio-reductively cleaved masking group for incorporation into PARP inhibitors as outlined in Scheme 17.
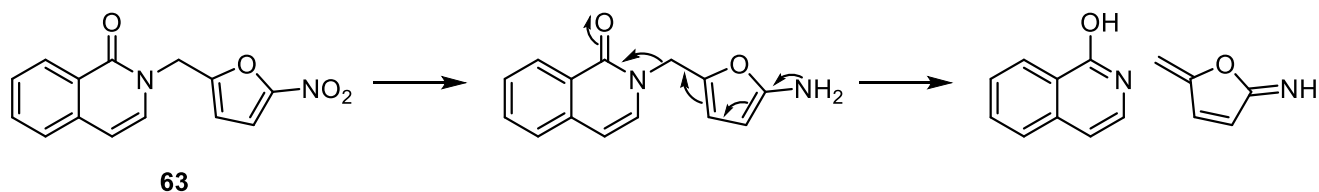
Scheme 17: Bio-reductively activated prodrug system developed by Parveen *et al*.

1.16 Molecular clip

PSA is an endopeptidase and, as such, will cleave between two amino-acids and not at the end of a peptide sequence. Therefore, as was observed by DiPaola *et al.*[121] when they attached doxorubicin to a PSA cleavable peptide, it was not the free drug doxorubicin that was released, but rather it was Leu-doxorubicin.[130] Leu-doxorubicin exhibited desired cytotoxicity however, it is possible that in some cases, a pendant amino acid may be deleterious to the activity of a drug. In the case of a *seco*-amino-CBI, if a peptide remained

attached to 4-N then this would hinder the necessary Winstein cyclisation. Previous work by the Threadgill group has examined the use of a molecular clip between an active drug and a PSA-cleavable peptide as a solution to this issue.[131,132] This self-immolative molecular clip is a peptide-like linker that will undergo intramolecular lactamisation to release the drug once PSA-induced cleavage has occurred. The Threadgill group has designed a specific molecular clip with the motif L-Leu-D-Dmt (Scheme 18).
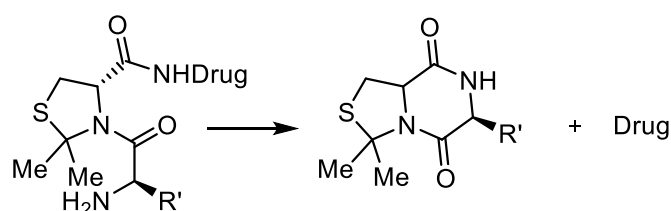
Scheme 18: Lactamisation of L-Leu-D-Dmt clip to release free drug. R = isobutyl.

1.17 Enhanced permeability and retention (EPR) effect

The EPR effect is a property observed in most tumours whereby certain sizes of molecules tend to accumulate in solid tumours much more than in normal cell tissue. This phenomenon has been attributed to two key characteristics of tumours. Firstly, tumours have greater vasculature permeability. Permeability-enhancing factors, such as bradykinin nitric oxide and VEGF, have been shown to be present in elevated levels in tumour tissue.[133] This increase in permeability then allows for extravasation of macromolecules and lipid particles into the interstitial space. Secondly, tumour tissue is known to lack effective lymphatic drainage, which results in a failure to drain macromolecules from the tumour site.[133]

This effect has been manipulated to deliver drugs to tumour sites. It has been reported that in order for the EPR effect to be optimal with regard to the size of PEG, the average molecular weight of PEG should be around 20 KDa.[134] Reports in the literature indicate that the polymer hydrodynamic radius is the major parameter that affects the ability of a polymer to exploit the EPR effect.[133,135–137]

1.18 Polymer-drug conjugates

Many anticancer agents currently in use are of low molecular weight, exhibiting short plasma half-lives and high overall clearance. The small size of these molecules means they diffuse quickly into both normal tissues and tumour tissues. This result in relatively small amounts of drug reaching the tumour site calling for a higher dose to be administered which in turn results in increased side-effects. Exploitation of the EPR effect through the conjugation of polymer to drugs with low molecular weight will alleviate these issues. Various polymers such as polyethylene glycol (PEG) (Figure 27) have been used as carriers of anti-cancer drugs, such as doxorubicin.
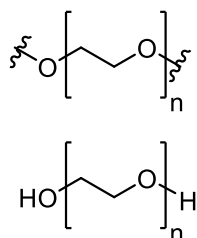
Figure 27: General Structures for PEG.

An optimal polymeric drug carrier system would ideally be water-soluble, biocompatible and non-toxic. The use of polymeric carrier systems not only improves water solubility but also improves bio-distribution and plasma clearance of the drug.[138] For example, Yin, *et al*. have demonstrated how a poly(ethylene glycol) (PEG) – paclitaxel prodrug conjugate **64** (Figure 28) accumulates at a tumour site and has much reduced systemic cytotoxicity compared to just paclitaxel, owing to enhanced tumour specificity.[139]
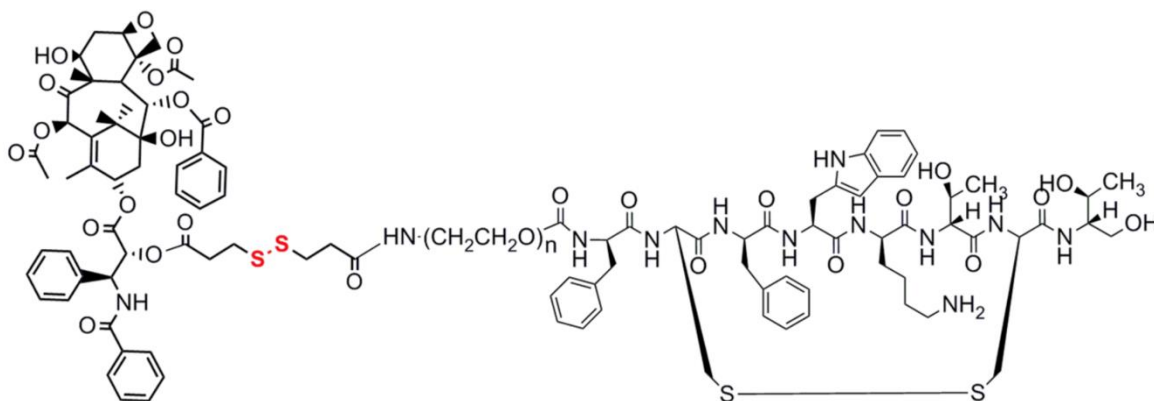
Figure 28: poly(ethylene glycol) (PEG) – paclitaxel prodrug **64**.

An investigation into the biodistribution of N-(2-hydroxypropyl)methacrylamide (HPMA) co-polymer-conjugated doxorubicin, by Seymour *et al.*,[140] observed that the doxorubicin **9** showed a preferential localisation to tumour tissues 10-15 times more than that achieved using free doxorubicin **9** administered at equal doses (5 mg of doxorubicin per Kg).
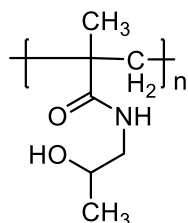
Figure 29: General structure for HPMA.

Toxicity relating to the polymer-conjugated doxorubicin was much lower than that of free doxorubicin and allowed for elevated doses (18 mg of doxorubicin per Kg) to be administered which achieved levels of drug in the tumour, 45-fold higher than that resulting from the standard dose of free doxorubicin **9** (5 mg/Kg). The polymeric doxorubicin also showed a lower volume of distribution and longer plasma half-life than free doxorubicin **9**.[140]
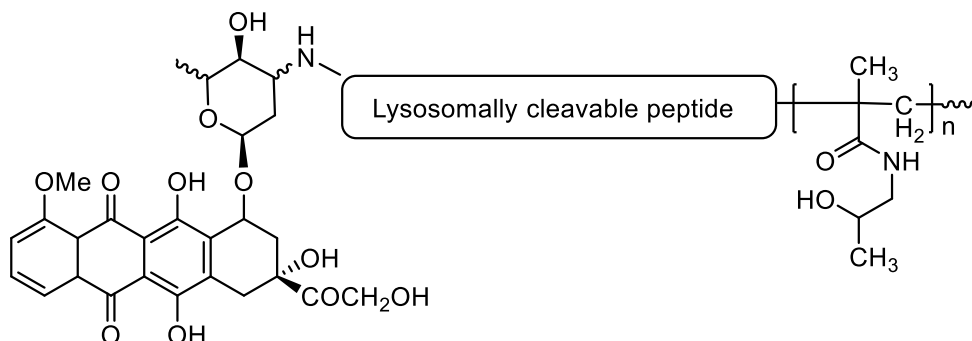
Figure 30: Structure of PK1 **65**.

Vasey *et al.*[141] undertook a phase 1 clinical and pharmacokinetic study on PK1 **65**; doxorubicin bound to N-(2-hydroxypropyl)methacrylamide (HPMA) copolymer through a lysosomally cleavable peptide linker (Figure 30). Despite the administration of higher doses, typical toxicities observed with anthracycline-like compounds were decreased. For instance, with prophylactic 5HT3 antiemetic administration, nausea and vomiting was found not to pose any problem. Additionally, just 8% of patients (3 out of 36) experienced grade 2 alopecia and there were no incidences of congestive cardiac failure.[141]

A polymeric-peptide-prodrug system will allow for selective delivery to prostate tumour through exploitation of the EPR effect to passively locate and retain the drug at the tumour site coupled with protease activation to release free drug. Activation of the prodrug by PSA will occur in the extracellular fluid at the tumour location. The prodrug is therefore not required to pass through the cell membrane before being activated. The presence of free drug within the extracellular fluid then allows for the bystander cytotoxic effect to target both PSA-secreting and non-PSA-secreting cells.

2.0 Aims and objectives

2.1 Aims

CBIs react in the DNA minor groove in a two-step process. Firstly, the non-covalent minor-groove binding subunit locates the molecule in the minor groove through hydrogen-bonding and hydrophobic interactions. This non-covalent binding anchors the amino-CBI in the minor groove with its complementary curve, allowing the amino-CBI to slide along the groove until the electrophilic spirocyclopropane is located close to a nucleophilic site. At this stage, covalent alkylation of the amino-CBI to an adenine residue occurs. Both steps are essential for potent cytotoxicity. A range of minor groove-binding subunits will be investigated in order to investigate the structure-activity relationship and optimise the potency of the amino-CBI compound that is to be incorporated into a prodrug system. The overall aim of the project is the development and refinement of a polymeric prodrug system that will deliver a highly potent 'warhead' selectively to prostate tumours. Two forms of targeting toward the tumour will be incorporated into the system; active targeting and passive targeting. Passive targeting will be achieved through exploitation of the enhanced permeability and retention effect (EPR). Two units of the 'warhead' will be joined to either end of water-soluble PEG (20 KDa, linear) which will then satisfy the necessary requirements for successful passive accumulation within solid tumours by EPR.[133] Active targeting toward prostate tumour cells will be achieved through the use of a PSA-cleavable peptide (SSKLQ) positioned between drug and polymer.[121,130] Prostate-Specific Antigen (PSA) has been shown to exhibit catalytic activity only within the prostate and so will act to cleave the prodrug at the peptide-drug interface, resulting in release of drug within the prostate. Within the peptide-drug interface, a self-immolative *pseudo*-peptide molecular clip will ensure that the no residual amino-acids remain attached to the drug post PSA-cleavage as observed in the previously described L-377202 prodrug **60** that yielded Leu-doxorubicin upon PSA-cleavage as opposed to release of free doxorubicin.[122,130] In order to compensate for the high M.W. loading that will be required of the prodrug and to counter incomplete active and passive targeting, a highly potent range of CBIs will take on the role of the 'warhead' with literature IC_{50} values in the low nanomolar range.[101] A range of analogues of amino-*seco*-CBI compounds will be synthesised to develop

an understanding of the SAR regarding the minor-groove binding subunit. The project will investigate and build upon an alternate hypoxia-directed prodrug approach previously explored by Tercel *et al.*[129] A range of nitro-*seco*-CBI analogues will be synthesised and biologically investigated to evaluate the effectiveness of a hypoxia-based approach to selective prostate tumour targeting.
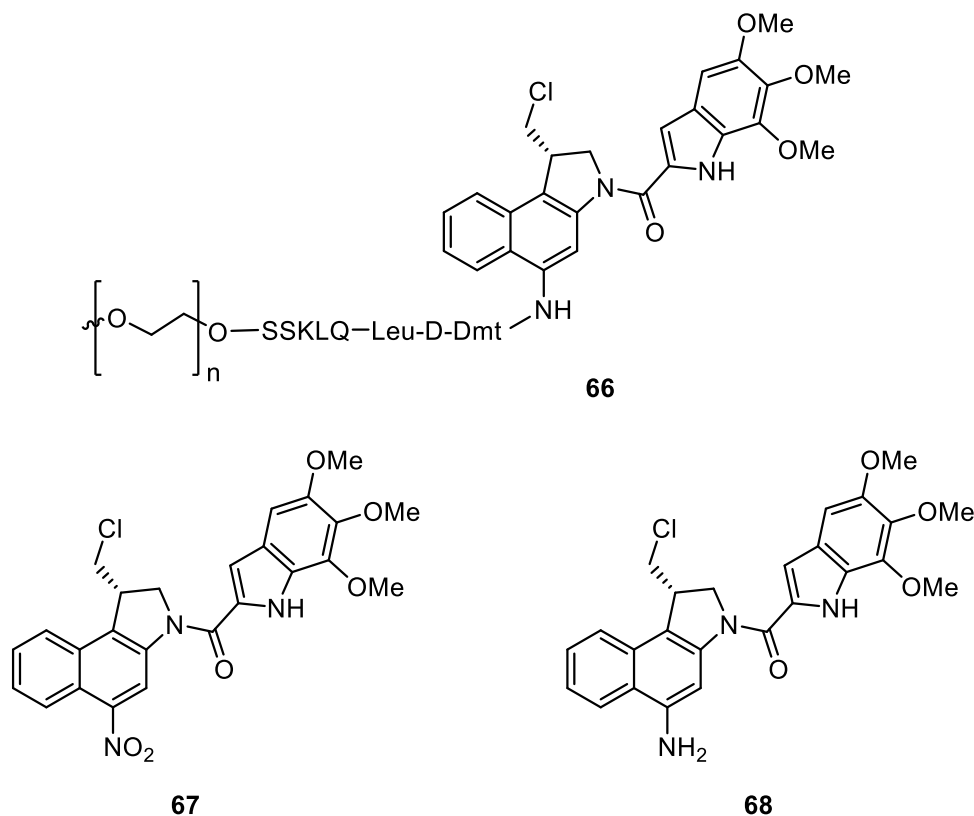
Figure 31: Proposed *seco*-amino-CBI **68** and corresponding *seco*-nitro-CBI **67** and polymeric-*seco*-CBI prodrugs **66**.

2.2 Objectives

The project can be split into three stages:

- Design and optimisation of a chemical synthesis toward stereochemically pure alkylating *seco*-nitro-CBI and *seco*-amino-CBI subunits.
- Coupling the alkylating subunits with a range of non-covalent minor-groove binding subunits.
- *In vitro* evaluation of the range of *seco*-nitro-CBIs and *seco*-amino-CBIs synthesised.

55

The proposed amino-CBI drug comprises of a CBI alkylating subunit and a minor groove-binding subunit. CBIs have been extensively studied as previously discussed however, while synthesis of stereochemically pure 5-hydroxy CBI derivatives has been reported, asymmetric synthesis of 5-amino CBI derivatives has not.[116] The first stage of the project involved optimisation of the current synthesis (Scheme 19) toward nitro-CBI and amino-CBI derivatives to achieve stereochemically pure CBIs.
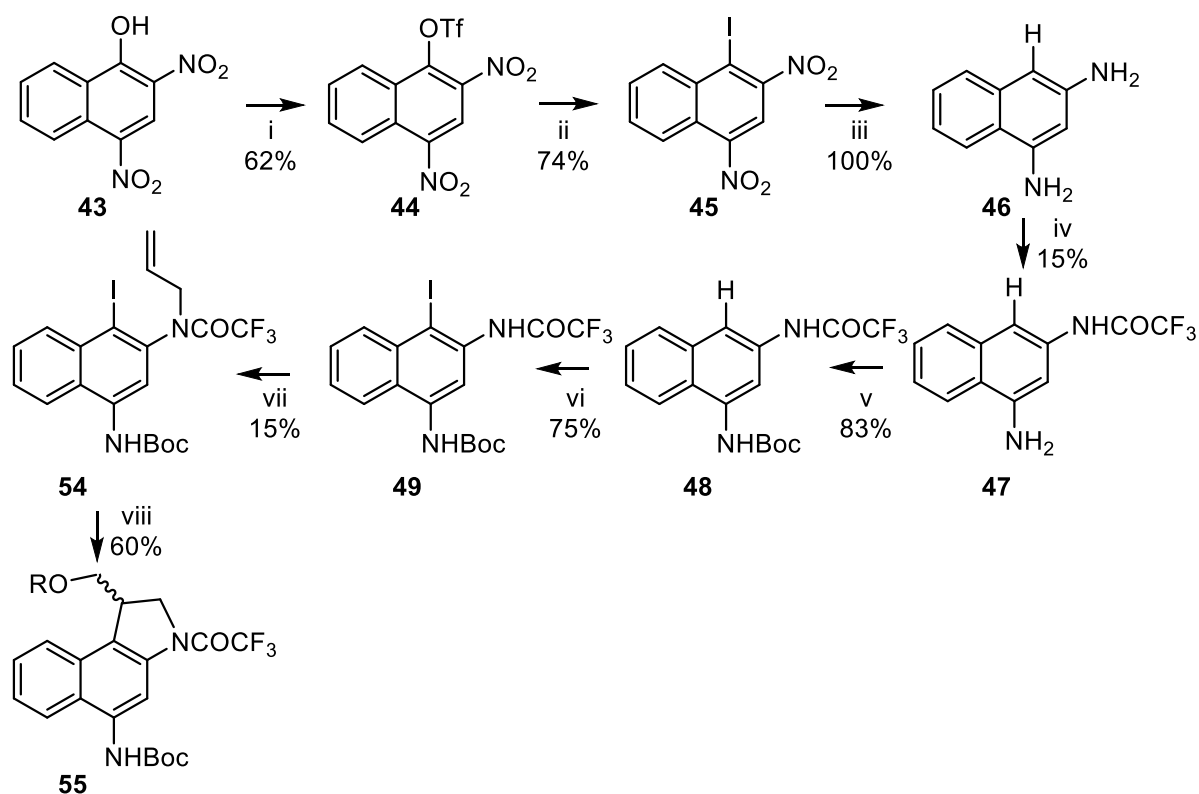
Scheme 19: Current synthetic route toward racemic *seco*-amino-CBIs. R = 2,2,6,6-dimethylpiperidinyl. *Reagents*: i. Tf$_2$O; ii. NaI, acetone; iii. SnCl$_2$, HCl; iv. (CF$_3$CO)$_2$O; v. Boc$_2$O; vi. NIS; vii. allyl bromide; viii. TEMPO, Bu$_3$SnH.

The current synthetic route requires eight steps to achieve cyclised racemic material.[100] Reduction of the dinitro compound **45** results in non-desired loss of iodine. The resulting diamino **46** has proven difficult to selectively react at the 3-N. The proposed route outlined in Scheme 20 was investigated to achieve cyclised enantiopure nitro-CBI in just six steps. Starting with commercially-available 1-hydroxy-2-naphthoic acid **29**, nitration at the 4-position masked the required amine at that position. Insertion of iodine was achieved *via* a triflate intermediate as in the previous synthetic route. At this stage, reaction of the carboxylic acid

71 through Curtius rearrangement to yield the isocyanate followed by subsequent reaction of the isocyanate with ^{t}BuOH yielded a Boc-protected amine at the 2-position. This then enabled selective alkylation of **72** at the *ortho*-amino group with *2R,3S*-3-methyl-2-(4-nosyloxymethyl)oxirane. A metal-mediated cyclisation of **73** would then form the pyrrolidine ring of **74** with inversion of stereochemistry. Reduction of the nitro-group will then provide access to *seco*-amino-CBI.

A range of non-alkylating subunits **75-81** were then utilised to yield a short library of amino-
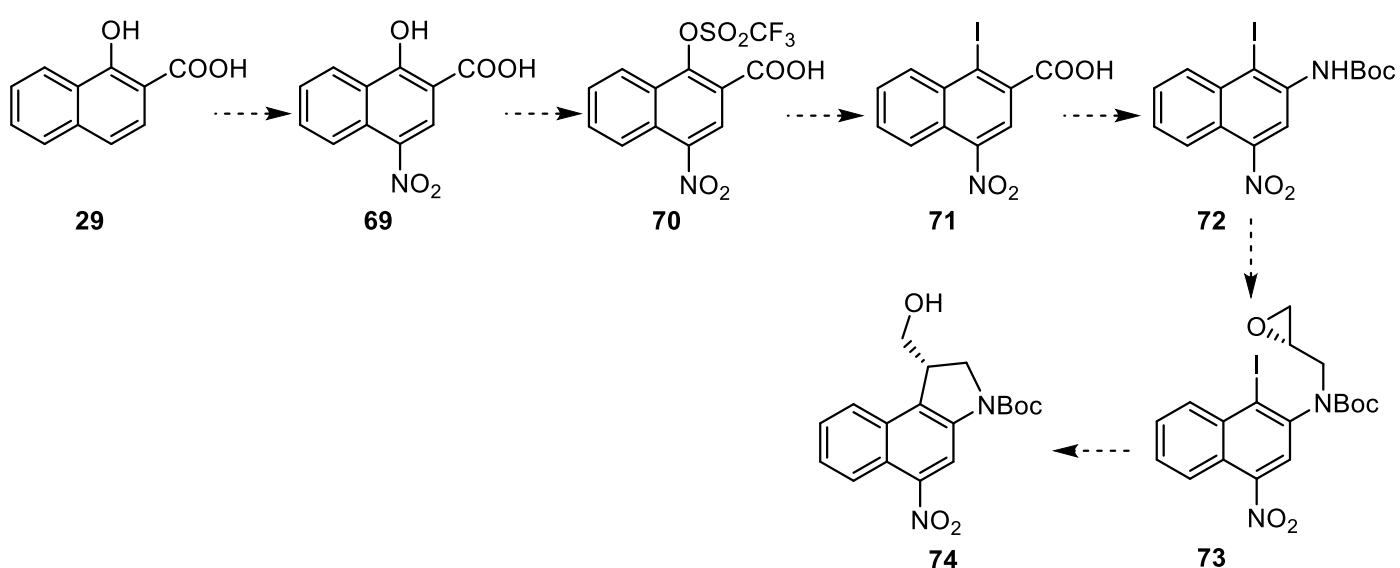
Scheme 20: Proposed route toward stereochemically pure nitro-CBI **74**.

CBIs to investigate their structure-activity relationship (Figure 32). The importance of an indole motif was investigated through incorporation of a benzofuran subunit. Reports in the literature have indicated the importance of a 5-methoxy group.[96] Tolerance of a 5-hydroxy group was investigated. *Seco*-amino-CBI derivative **68** is known in the literature and has been shown to exhibit substantial potency. Compound **68** was therefore synthesised to provide a benchmark comparison.
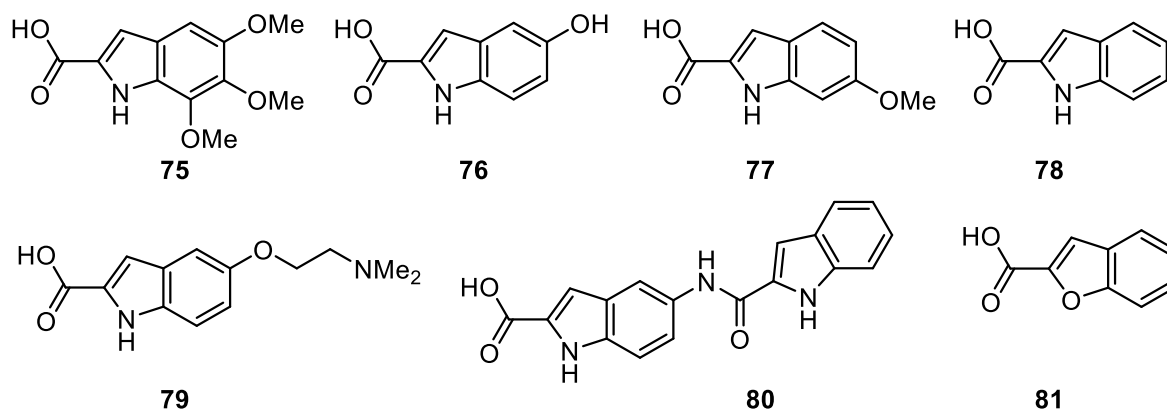
Figure 32: Structures of the non-alkylating subunits **75-81** to be investigated, shown in the carboxylic acid form prior to amide coupling to the alkylating subunit.

In the final stage, DNA alkylation studies were carried out on the library of synthesised *seco*-nitro-CBIs and *seco*-amino-CBIs to ascertain the effect on the melting temperature on calf-thymus DNA. This will allow direct comparison of the binding affinity to the minor-groove of DNA between the range of non-alkylating subunits. The degree of shift in the DNA-melting temperature of calf-thymus DNA will provide an insight into the relative potencies of the compounds. An MTS cytotoxicity assay was also carried out on prostate cancer cell lines to investigate further the structure-activity relationship of the various non-alkylating subunits. Cytotoxicity tests on the range of *seco*-nitro-CBIs will help predict the effect of conjugating the *seco*-amino-CBIs to the polymeric prodrug system.

3.0 Results and discussion

A major drawback to many chemotherapeutic treatments for all cancers, including PCa, is a lack of intrinsic selectivity. There is, therefore, a need to develop novel chemotherapeutics that target tumour tissue selectively over healthy tissue. The duocarmycin class of compounds have shown high cytotoxicity to various tumours, including PCa cell lines; however, they are unsuitable for clinical use due to toxic side effects such as myelosuppression.[78,142]
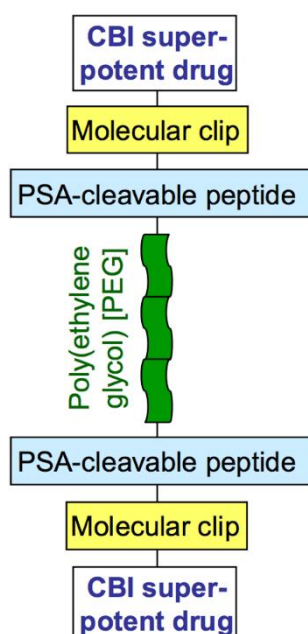
Figure 33: Cartoon outline of the polymeric prodrug system.

Previous work by the Threadgill group[100] has looked at the development of *seco*-amino-CBIs to be used in a polymeric prodrug system to deliver an activated amino-CBI alkylating agent selectively to prostate tumours. The proposed polymeric prodrug system (Figure 33) consists of a *seco*-amino-CBI attached to the PSA-cleavable peptide sequence SSKLQ through a self-immolative molecular clip. PSA has previously been shown to cleave aromatic amines from the C-termini.[130] L-377202 **60** for example, is a doxorubicin-peptide conjugate that has been shown to release active Leu-doxorubicin through PSA-mediated hydrolysis of the peptide.[122] Leu-doxorubicin is 10-fold less cytotoxic than doxorubicin.[122] To avoid situations where pendant amino-acid(s) attached to drugs can have a negative impact on the activity of the

drug, such as in the case of L-377202 **60**, incorporation of a self-immolative molecular clip will be introduced between the CBI and PSA-cleavable peptide. This will cause enzymatic cleavage between the peptide sequence and the self-immolative clip, which will then undergo intramolecular lactamisation to release the active drug with no pendant amino-acids as previously outlined. Release of *seco*-amino-CBI without any pendant amino-acid(s) is vital, as the subsequent Winstein-cyclisation to form the active CBI compound depends on electron-density from the Ar-NH$_2$ feeding into the aromatic ring. A pendant amino-acid would mask the Ar-NH$_2$ as an amide, which reduces the electron-density and thus prevents the Winstein cyclisation. Linear PEG (20 KDa) is bound to two units of [SSKLQ]-[Clip]-[*seco*-amino-CBI] (Figure 31) to enhance solubility and allow the prodrug to exploit the previously explained EPR effect, which will cause the prodrug to persist at the tumour site.[133]

3.1 Novel synthesis of the alkylating subunit

The following work describes the approaches taken to access enantiopure material. As with the previously described work, the approach taken can be split into two parts; synthesis of the alkylating subunit and synthesis of the minor-groove binding subunit.

3.1.1 Synthesis of the alkylating subunit pre-cyclisation key intermediate 72

Synthesis of the alkylating subunit has been explored previously by the Threadgill group;[100] however, the current synthetic route to key intermediate **49** (Scheme 12) is plagued by a reduction of the two nitro groups, where a C-I bond is also cleaved reductively. It has been reported that carbon-halogen bonds can be reduced under basic conditions and Twum found that dehalogenation occurred alongside reduction of the nitro group even under acidic conditions.[143–146] This is followed by a low-yielding selective mono-TFA protection of the resulting 1,3-diaminonaphthalene **46**. It is vital to achieve mono-protection with TFA to allow for the synthesis of an orthogonally-protected diamine compound. Orthogonal protection is vital as it then allows chemoselective transformations to be performed at each amine. Initial work was focused on addressing these issues through development of a novel synthetic route to the alternate key intermediate *tert*-butyl (4-nitro-1-iodonaphthalen-2-yl)carbamate **72**,

where the two nitrogens are orthogonally masked. The retrosynthetic analysis outlined in Scheme 21 resulted in the proposed synthetic route shown in Scheme 22.
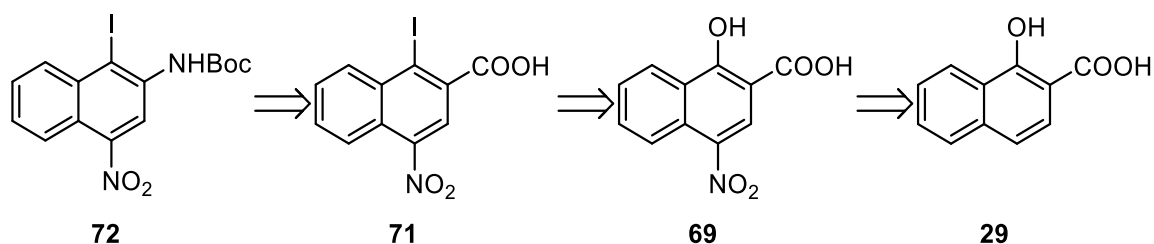
Scheme 21: Retrosynthetic analysis from key intermediate **46**.
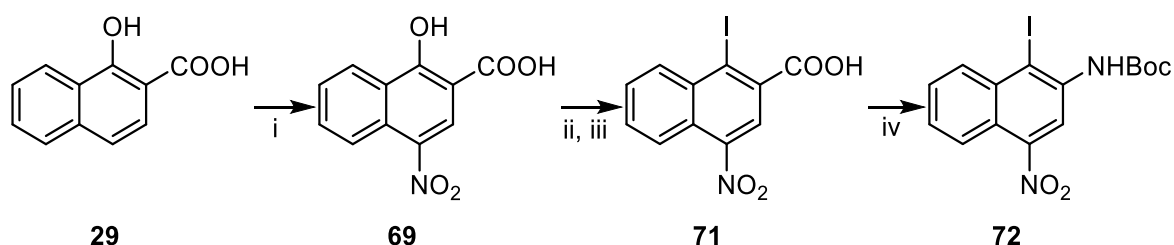
Scheme 22: Proposed synthetic route to key intermediate **46**. Reagents and conditions: i, HNO$_3$, AcOH ii, Tf$_2$O iii, NaI, acetone iv, a) SOCl$_2$, DMF, b) TMSN$_3$ c) heat, d) ^{t}BuOH, NEt$_3$.

The rationale behind this novel synthetic route to orthogonally masked amines at positions-2 and -4 is that it does not require chemoselectivity between the two free amines at any stage in the synthesis, the major drawback to the previous route. This is achieved through a Curtius rearrangement of the 2-carboxylic acid **71** to yield a Boc-protected amine whilst also masking the amine at the 4-position as a readily reducible nitro group. The lack of a need to carry out a nitro-reduction until late on in the synthesis also offered the possibility of avoiding the loss of iodine exhibited in the previous route with the possibility of keeping the 4-nitro until after metal-mediated or radical cyclisation had been carried out. Additionally, the desired key intermediate could be reached in only four steps, as opposed to the six steps in the Twum route.

3.1.2 Nitration of 1-hydroxynaphthalene-2-carboxylic acid 29

Nitration of 1-hydroxynaphthalene-2-carboxylic acid **29** by Electrophilic Aromatic Substitution (outlined in Scheme 23) was predicted to occur solely at the desired 4-position due to the strongly *para*-directing hydroxy group and *meta*-directing carboxylic acid group. Nitro substituents are strongly deactivating, due to being powerful electron withdrawing groups; therefore, one would not expect multiple substitutions to occur. Nitration at the 4-position occurred successfully in a 95% yield.
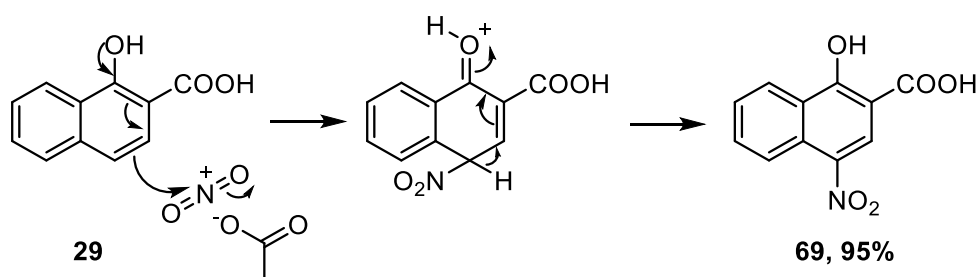
Scheme 23: Nitration mechanism for the reaction of compound **29** with HNO_3 and AcOH.

3.1.3 Synthesis of 1-iodo-4-nitronaphthalene-2-carboxylic acid 71
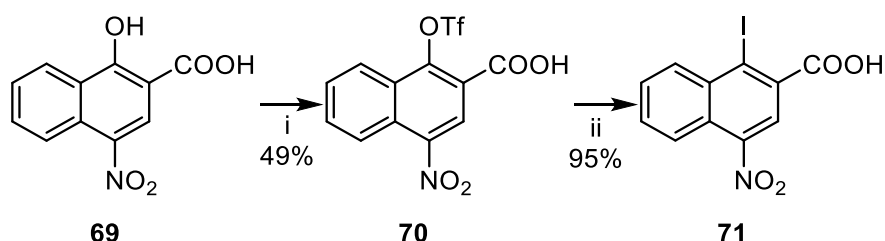
Scheme 24: Synthesis of 1-iodo-4-nitronaphthalene-2-carboxylic acid **71**. *Reagents and yields*: i. NEt_3, Tf_2O, CH_2Cl_2, **49%**; ii. NaI, $(CH_3)_2CO$, reflux, **95%**.

From 1-hydroxy-4-nitronaphthalene-2-carboxylic acid **69**, the next steps involved displacing the hydroxy group at the 1-position with an iodine *via* triflate intermediate **70** to yield **71** prior to Curtius rearrangement of an acyl azide to an isocyanate. Treatment of the isocyanate with ^{t}BuOH would then yield the desired Boc-protected amine. In order to insert iodide *via* an S_NAr reaction, the hydroxy group of **69** was first treated with trifluoromethanesulfonic anhydride

to yield the corresponding triflate **70** in 49% yield. At this point, reaction with NaI in acetone gave the desired 1-iodo-4-nitronaphthalene-2-carboxylic **71** acid in a 95% yield.

Over the course of a few weeks, decomposition of **71** was observed by NMR, with a plethora of new signals observed in the aromatic region. This was highly problematic, especially whilst issues regarding the Curtius rearrangement were being investigated. In order to mitigate the instability issue regarding 1-iodo-4-nitronaphthalene-2-carboxylic acid **71**, the synthetic route was altered, as shown in Scheme 25, to protect the carboxylic acid as an ester. Hydrolysis of the ester could then be carried out immediately prior to the Curtius rearrangement to limit the need to handle 1-iodo-4-nitronaphthalene-2-carboxylic **71** for any length of time.
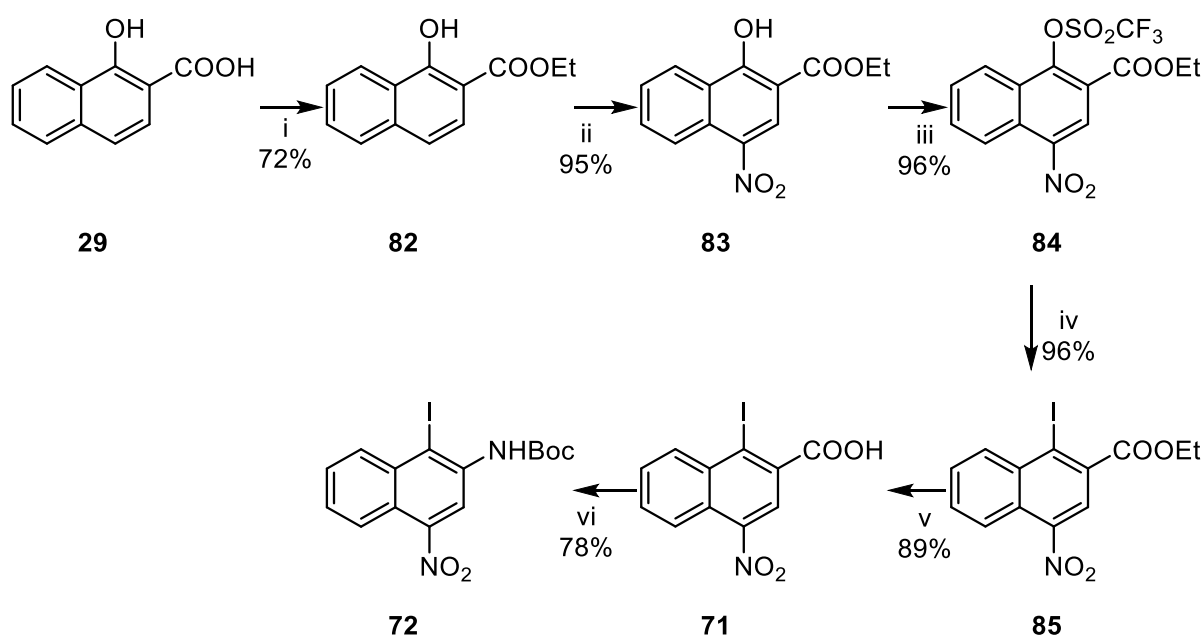
Scheme 25: Updated synthesis to key intermediate **46**. *Reagents and yields*: i. EtOH, H_2SO_4, **72%**; ii. HNO_3, AcOH, **95%**; iii. Tf_2O, CH_2Cl_2, **96%**; iv. NaI, $(CH_3)_2CO$, **96%**; v. NaOH, **89%**; vi. a) $SOCl_2$, DMF; b) $TMSN_3$; c) heat, d) ^tBuOH, NEt_3, **78%**.

3.1.4 Esterification of 1-hydroxynaphthalene-2-carboxylic acid 29
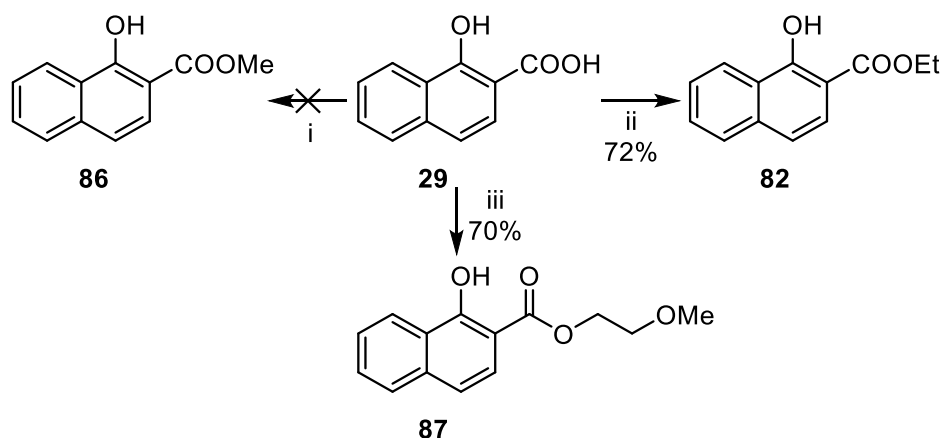
Scheme 26: Fischer esterification of 1-hydroxynaphthalene-2-carboxylic acid **29**. *Reagents and conditions*: i. MeOH, H_2SO_4, heat, **0%**; ii. EtOH, H_2SO_4, heat, **72%**; iii. 2-methoxyethanol, H_2SO_4, heat, **70%**.

Initially, synthesis of the methyl ester **86** was attempted *via* a Fischer-esterification. This approach was, however, unsuccessful, as the reaction mixture contained starting material after 14 d (Scheme 26). It was hypothesised that the reaction failure was due to the low boiling point of methanol (bp 64.7°C) preventing the reaction from reaching the required activation energy. In order to achieve the required higher reflux temperature, methanol was substituted with either 2-methoxyethanol (bp 124°C) or ethanol (bp 78.4°C) to yield the corresponding 2-methoxyethyl and ethyl esters **87** and **82**.

3.1.5 Synthesis of 71 *via* ethyl 1-iodo-4-nitronaphthalene-2-carboxylate 85

After formation of the ethyl ester, the remaining steps towards ethyl 1-iodo-4-nitronaphthalene-2-carboxylate **71** proceeded as expected. Nitration of **82** at the 4-position, again directed *para* to the 1-OH, occurred in a 95% yield to yield **83**. Triflation of the 1-OH to yield **84** followed by substitution with iodide to yield **85** occurred in 92% overall yield. Base-catalysed hydrolysis of the ethyl ester to 1-iodo-4-nitro-2-naphthoic acid **71** was then carried out in an 89% yield. Interestingly, the vastly improved yield of the triflation step for the ethyl ester compared to the carboxylic acid (96% compared to 49%) resulted in an improvement to the overall yield, despite increasing the number of steps to include esterification and

hydrolysis of the ester. This is due to the competing reaction between the carboxylic acid of **69** and Tf$_2$O to yield non-desired **88** outlined in Scheme 27.
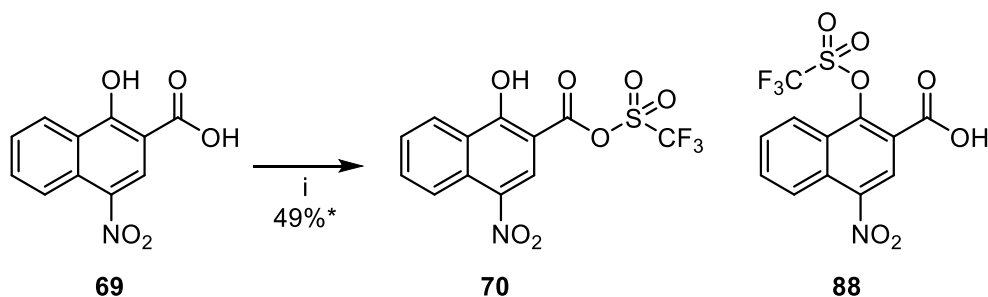
Scheme 27: Reaction of carboxylic acid **69** with Tf$_2$O to yield desired **70** and non-desired **88**. *Reagents and yields*: i. Tf$_2$O, NEt$_3$, CH$_2$Cl$_2$, **49%*** yield of desired **70**.

3.1.6 Synthesis of Boc-protected 72

The final step towards formation of key intermediate **72** involved synthesis of the Boc-protected amine through transformation of the 2-carboxylic acid of **71**. There a several well-established methods in the literature that allow the transformation of carbonyl compounds such as carboxylic acids and amides to amines including the Hofmann, Schmidt and Curtius reactions.[147,148]

The Hofmann rearrangement involves the transformation of a primary amide to a primary amine with one fewer carbon atom, through reaction with molecular bromine and alkali such as sodium hydroxide.[149] As shown in Scheme 28, deprotonation of the amide N-H of **89** by hydroxide followed by nucleophilic attack towards bromine to form an N-bromoamide **90** is followed by deprotonation of the amide N-H. The resulting intermediate rearranges to an isocyanate **91**, releasing bromide. The isocyanate carbon is π-bonded to two strongly electronegative atoms, which makes the carbon an excellent electrophile. Nucleophilic addition of water towards this carbon followed by proton transfer results in the formation of the zwitterionic intermediate **93** which finally undergoes decarboxylation to yield the primary amine **94**.[147–150]
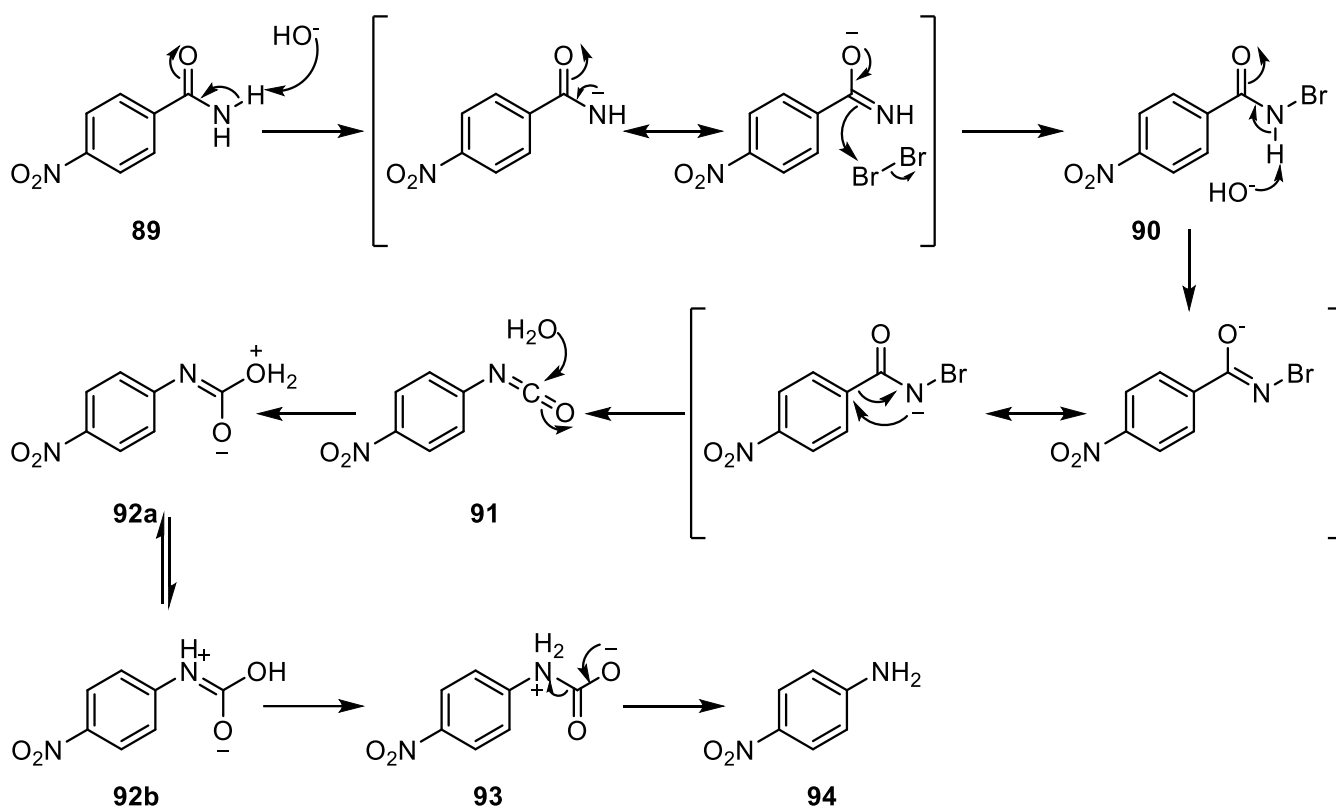
Scheme 28: Mechanism of the Hofmann rearrangement.

Hall and Stockel[151] showed that 4-nitrobenzoic acid **89** could be converted to *para*-nitroaniline **94** at room temperature in a 48% yield through reaction with polyphosphoric acid and excess sodium azide by a Schmidt reaction as outlined in Scheme 29.
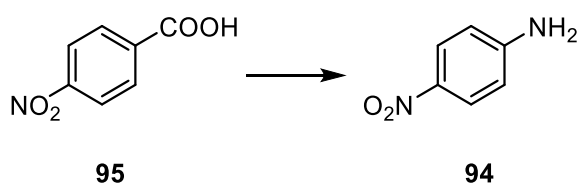
Scheme 29: Schmidt reaction to form *para*-nitroaniline **94** from *para*-nitrobenzoic acid **95**. *Reagents and conditions*: i. PPA, NaN$_3$, 25°C.

As can be seen in Scheme 30, the Schmidt reaction begins with the formation of an acylium ion through protonation and loss of water. Reaction of **95** with hydrazoic acid, formed from the reaction of sodium azide and acid, yields the protonated azido-ketone **96**, which then undergoes a rearrangement to release nitrogen and form a protonated isocyanate intermediate. Nucleophilic attack of water toward the isocyanate carbon forms carbamate **97** which finally undergoes deprotonation and decarboxylation to yield the amine **94**.
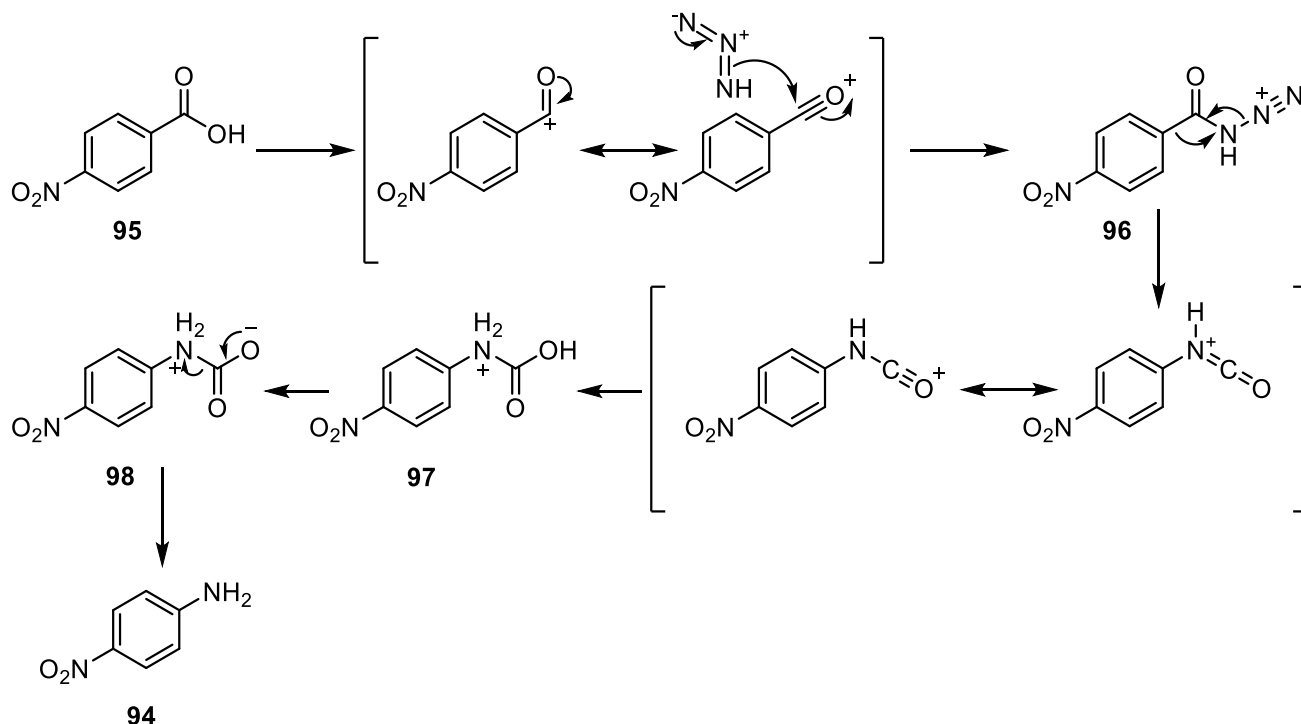
Scheme 30: Mechanism of the Schmidt Reaction.

Similar to both the Schmidt and Hofmann reactions, the Curtius rearrangement is the formation of an isocyanate intermediate from an acyl azide. Formation of the acyl azide **100** is carried out through reaction of the acid chloride **99** with an azide compound such as sodium azide or trimethylsilyl azide (TMSN₃). Alternatively, diphenylphosphorylazide (DPPA) will yield the acyl azide **100** straight from the carboxylic acid **98**. Thermal decomposition of the azide, releasing nitrogen with migration of the R-group to form a highly reactive nitrene that then
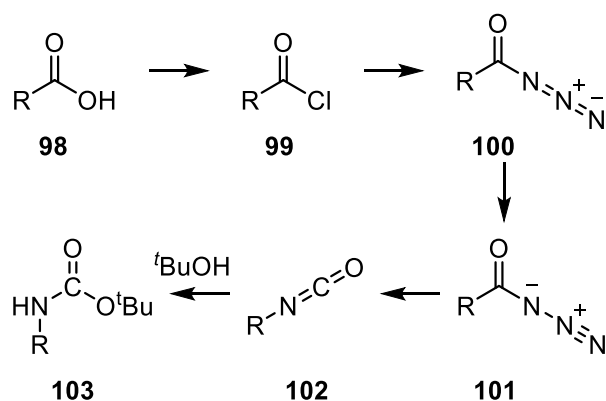
Scheme 31: Overview of the intermediates involved in the Curtius rearrangement. R = allyl, alkyl, aryl.

undergoes a rearrangement to yield the isocyanate **102** (Scheme 31). This step occurs through loss of N_2 to yield the isocyanate. After the Curtius rearrangement, reaction of the isocyanate with an alcohol such as *tert*-butanol yields the corresponding carbamate **103**. In the case of *tert*-butanol, formation of the Boc-protected amine is observed, which can easily be deprotected under acidic conditions to yield the primary amine. Through the formation of the acyl azide from either the carboxylic acid or acyl chloride and subsequent Curtius rearrangement to synthesise the isocyanate, one can then yield a protected amine. This will then allow for the reduction of the 4-nitro group without resulting in two amines being 'unmasked' at the same time as encountered by Twum *et al*,.[100] making it an ideal way to yield **72** from 1-iodo-4-nitronaphthalene-2-carboxylic acid **71**.
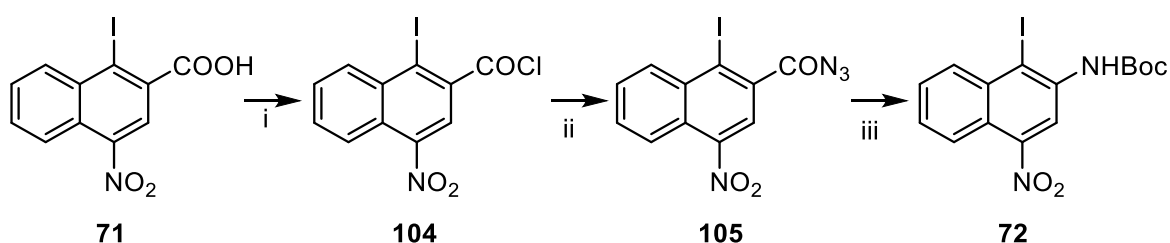
Scheme 32: Curtius rearrangement of **71** to yield Boc-protected **72**. *Reagents and Conditions:* i. $SOCl_2$, DMF; ii. $TMSN_3$; iii. a) heat, b) ^{t}BuOH, NEt_3. *Overall yield:* 78%.

Acyl halides are one of the most electrophilically reactive of acid derivatives and so, in order to promote formation of the acyl azide, the acyl chloride **104** was prepared from the carboxylic acid **71**.[152] Formation of acyl chloride **104** was performed through reaction with $SOCl_2$ and catalytic DMF. DMF catalyses the reaction through formation of the Vilsmeier-Haack reagent **106** (Scheme 33).[153,154]
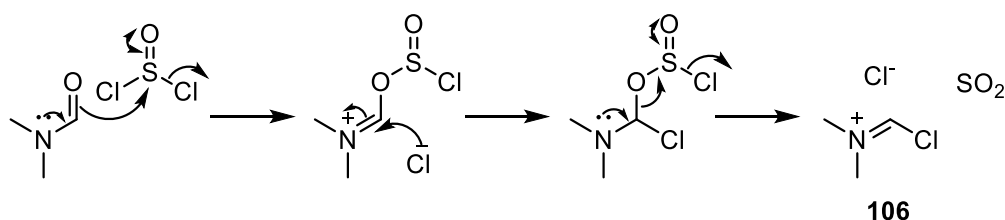
Scheme 33: Formation of the Vilsmeier-Haack reagent **106**.

The Vilsmeier-Haack reagent **106** contains an iminium cation with a strongly electrophilic carbon that is subject to nucleophilic attack by the carboxylic acid of **71**, as outlined in Scheme 34. The intermediate formed is extremely electrophilic and first reacts to re-form the iminium cation through expulsion of chloride. The chloride then performs nucleophilic addition-elimination towards the carbonyl to form the acyl chloride **104** with release of DMF.
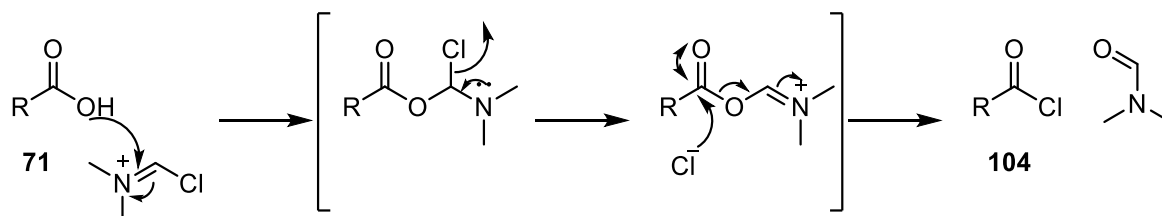
Scheme 34: Mechanism outlining the formation of an acyl chloride from a carboxylic acid. R = $C_{10}H_5INO_2$.

Formation of the acyl chloride **104** was then followed by reaction with trimethylsilylazide (TMS-N$_3$) to form the acid azide **105** through a concerted nucleophilic substitution to displace chloride which in turn attacks at Si to form the acid azide **105** and TMS-Cl by-product. There are two potential nucleophiles within TMSN$_3$, the terminal N: and the Si-N$^-$. Kaye *et al.*[155] showed, through ^{1}H NMR experiments, that the Si-N acts as the nucleophile as opposed to the terminal N.
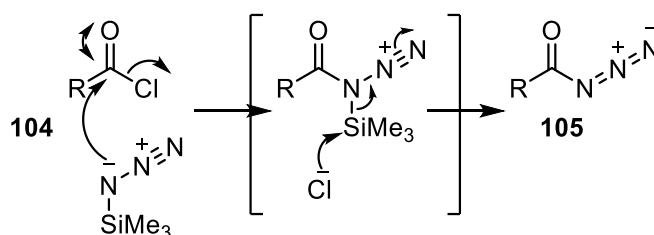
Scheme 35: Mechanism outlining the formation of acyl azide **105** from acyl chloride **104**. R = $C_{10}H_5INO_2$.

At this stage, heating the azide intermediate **105** results in decomposition and release of nitrogen, forming a highly electrophilic nitrene intermediate **107**. The nitrene nitrogen has only one bonded pair and two lone pairs of electrons, totalling six electrons in all, making it a species analogous to a carbene. At this point, A Wolff-style migration then occurs, whereby the R substituent migrates from the carbonyl carbon to the electron-deficient nitrogen atom of the nitrene to form isocyanate **108** as shown in Scheme 36.
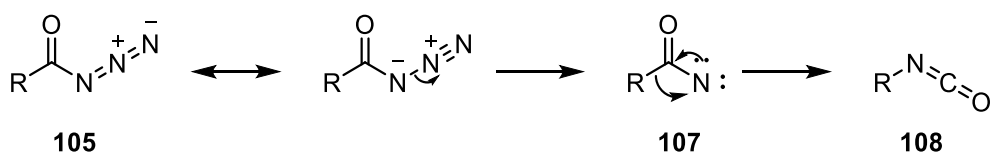
Scheme 36: Mechanism outlining the formation of isocyanate **108** from acid azide **105**. R = $C_{10}H_5INO_2$.

Isocyanates are prone to hydrolysis, with attack by water on the carbonyl group producing a carbamic acid which then decomposes to an amine. In order to yield the Boc-protected amine, the reaction was performed under anhydrous conditions. This then allows the isocyanate **108** to be treated with an alcohol, such as *tert*-butanol, to yield the corresponding carbamate **72** as outlined in Scheme 37.
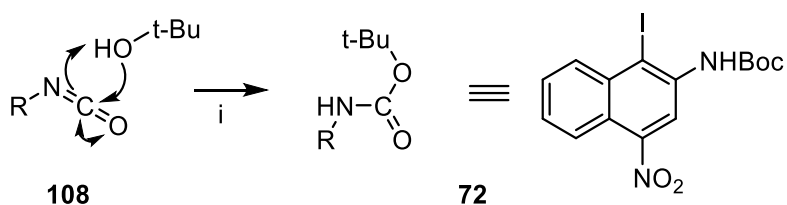
Scheme 37: Mechanism outlining the formation of carbamate **72** from an isocyanate **108**. R = $C_{10}H_5INO_2$. *Reagents and conditions*: i. ^{t}BuOH, NEt₃, anhydrous.

Interestingly, under the reaction conditions described above, the side products produced through a one-pot synthesis of Boc-protected amine **72**, starting with carboxylic acid **71**, are all either gaseous (SO_2, N_2), highly volatile (TMS chloride) or water-soluble (excess ^{t}BuOH). It was therefore observed that pure **72** could be recovered simply through dilution of the reaction mixture with CH_2Cl_2 and washing this crude mixture with sat. aq. $NaHCO_3$, without the need for further purification through column chromatography.
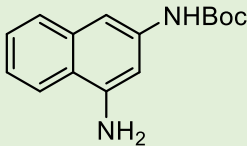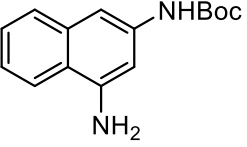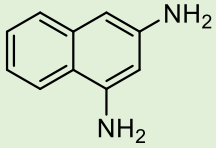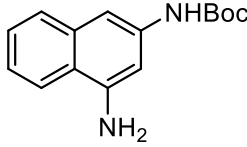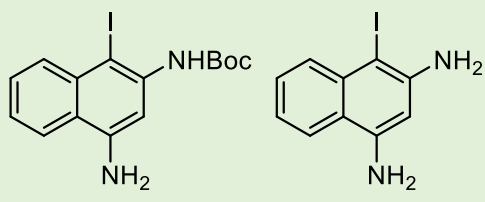
3.1.7 Attempted selective reduction of compound 72

A key issue with previous routes within the literature involves the tendency of the C-I bond to break in the presence of reducing agents such as $SnCl_2 \cdot 2H_2O$. The possibility of selective reduction of the nitro group in compound **72** whilst retaining the iodine at the 1-position was investigated as outlined in Table 2. Successful reduction of **72** to yield **109** without loss of iodine was achieved using $HSiCl_3$ as a reducing agent, albeit in low yield.
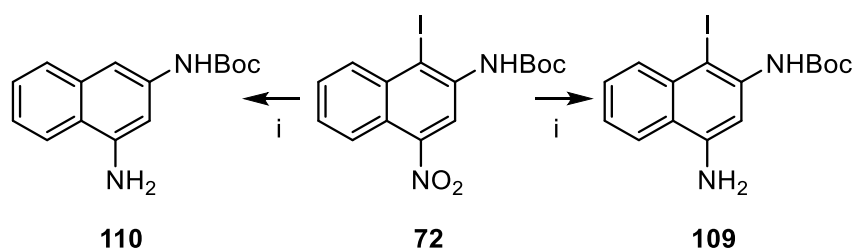
Scheme 38: Selective reduction of compound **72**. *Reagents:* multiple reagents as summarised in Table 2.

Table 2: Overview of attempts to reduce **72** selectively

Entry	Reagents	Product
1	Pd–C, H$_2$, MeOH	**110**
2	SnCl$_2$·2H$_2$O, EtOAc	**110**
3	FeCl$_3$, AcOH, EtOH	**46**
4	HSiCl$_3$, DIPEA, CH$_2$Cl$_2$	**110**
5	HSiCl$_3$, DIPEA, MeCN	Desired **109** Non-desired **111**

HSiCl$_3$ has been reported in the literature as a mild and metal-free way to reduce both aromatic and aliphatic nitro groups whilst exhibiting a wide tolerance of functional groups.[156] Reaction of HSiCl$_3$ with an organic base such as DIPEA generates SiCl$_2$ *in situ*.[157] Orlandi *et al*.[156] have proposed a mechanism as to how reduction of the nitro group occurs as shown in Scheme 39.
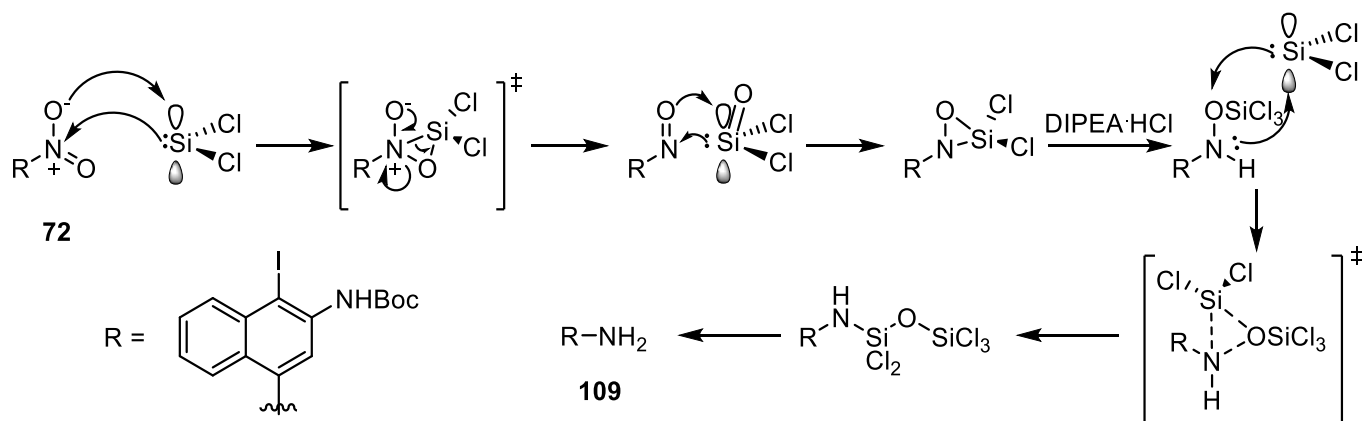
Scheme 39: Proposed mechanism for the HSiCl$_3$-mediated nitro reduction of **72** to **109**.

Due to time constraints and the low yield of this reaction, attention focused on the possibility of enantioselective metal-mediated cyclisation with a nitro at the 4-position. Future work would investigate optimisation of this reaction.

3.2.1 Attempted metal-mediated cyclisation to yield enantiopure *seco*-nitro-CBI derivative 74
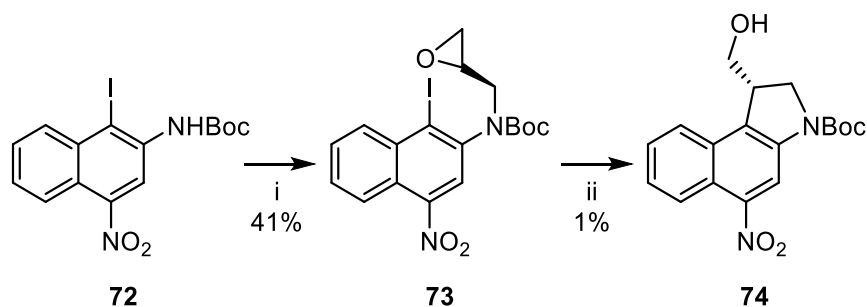
Scheme 40: Attempted metal-mediated cyclisation to yield **74**. *Reagents and yields:* i. *R*-glycidyl nosylate, NaH; ii. a) Pr^{i}MgBr·LiCl or b) Li$_2$Zn(SCN)Me$_3$.

Building on the work of both Twum *et al.*[100] and Tietze *et al.*,[108] it was hypothesised that metal-mediated cyclisation to yield enantiopure **74** would be achievable without the drawbacks experienced by Twum with regard to the acidic 4-NHX proton through masking the 4-amine as a 4-nitro group. Knochel *et al.* found that adding LiCl to organozinc reagents such as ZnR$_2$ could improve their reactivity.[158] This was subsequently found to be as a result of the formation of *X*-zincates (X = Cl or Br).[159,160] SCN$^-$ acts as a *pseudo*-halogen in the case of Li$_2$Zn(SCN)Me$_3$, known as a *pseudo*-halogen-zincate. For this reason, the use of two metal reagents, Pr^{i}MgBr·LiCl and Li$_2$Zn(SCN)Me$_3$, was investigated. Formation of **73** from **72** was achieved through deprotonation of NH with NaH followed by reaction with *R*-glycidyl nosylate.

3.2.1.1 Metal-mediated cyclisation with Pr^{i}MgBr·LiCl

Pr^{i}MgBr·LiCl is a readily available reagent that requires no preparation prior to use, making it an ideal choice to use in the attempted metal-mediated cyclisation. Tietze showed that cyclisation of the analogous OBn compound **26** was possible with Pr^{i}MgBr·LiCl.[104] Attempts to cyclise **73** in any significant yield proved unfruitful, with only trace amounts of desired **74** being detected by MS. Investigation into the formation of side-products indicated that the starting material had decomposed during the course of the reaction, with no naphthalene-containing side-products being identified. In Tietze's example (Scheme 48), use of Li$_2$Zn(SCN)Me$_3$ gave the desired compound in 72% yield, with no loss of enantiomeric

selectivity. In contrast, Pr^{i}MgBr·LiCl gave similar enantiomeric selectivity but in a 38% yield.[108] Therefore, attention was turned to focus on the use of Li$_2$Zn(SCN)Me$_3$.

3.2.1.2 Metal-mediated cyclisation with Li$_2$Zn(SCN)Me$_3$
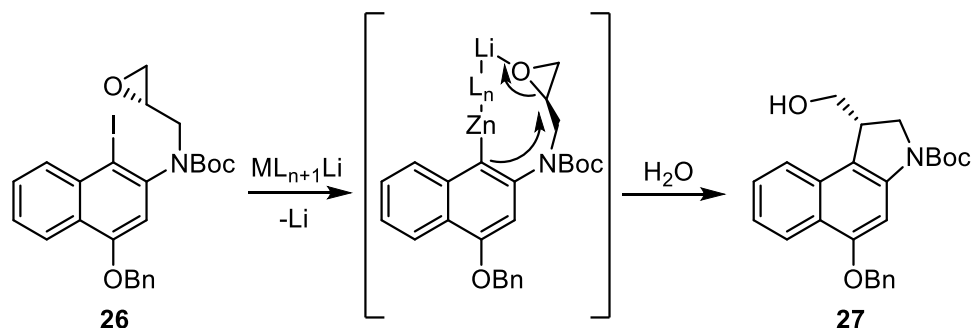
Scheme 41: Tietze *et al*. mechanism for the metal mediated cyclisation of **26** to yield **68**.[104]

Scheme 41 outlines the mechanism for the metal-mediated cyclisation of **26**, as carried out by Tietze *et al*.[104] This procedure was applied to the cyclisation of compound **73** with limited success. Desired compound **74** was isolated in a very poor yield (1%), proving that enantiopure *seco*-amino-CBI was accessible without the need to prepare and separate racemic material; however, attempts to optimise the reaction proved challenging. A large amount of starting material **73** was recovered (40%) indicating that Zn insertion into the C-I bond was hindered. The presence of a strongly electron-withdrawing *para*-nitro group was expected to improve the reactivity of metal-halogen exchange, as the more electron-deficient aromatic iodides are, the faster metal-halogen exchange reaction proceeds.[109–111] The major identified side-product was the de-iodinated compound **112** (15%), which also lacked the Boc group (Scheme 42).
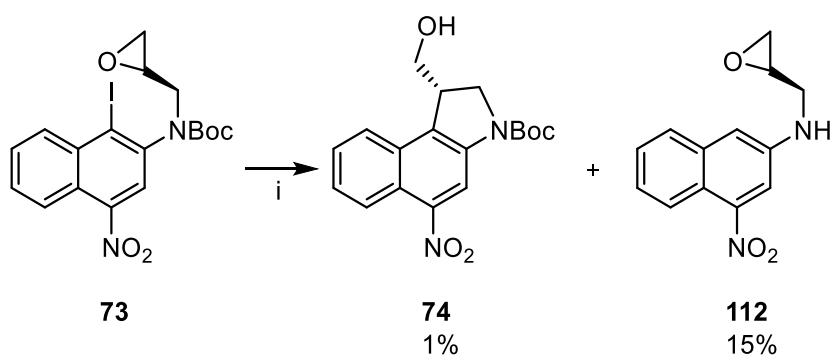
Scheme 42: Formation of de-iodinated **112** and desired enantiopure **73**. *Reagents*: i. Li$_2$Zn(SCN)Me$_3$.

This indicates that, in these molecules, insertion of the metal had taken place but that the resulting organometallic was not sufficiently nucleophilic to attack the epoxide. This may be due to the nitro group withdrawing electron density from the aromatic ring. The Boc group may have been cleaved while complexed with the Lewis-acidic metal in the metallated intermediate as outlined in Scheme 43.
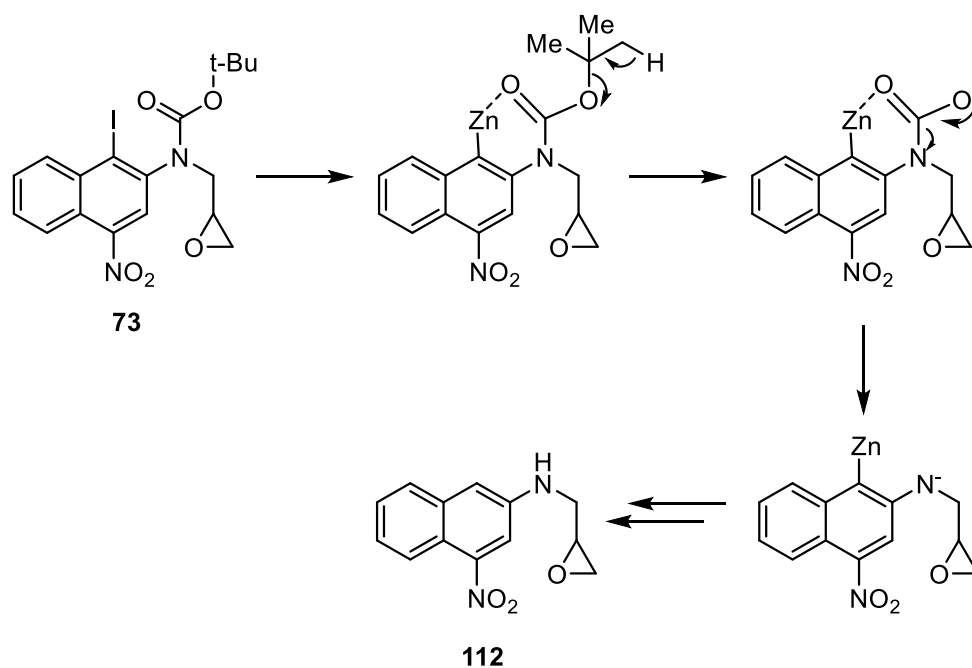
Scheme 43: Proposed mechanism for the formation of de-iodinated **112**.

3.2.2 Synthesis of 5-H *seco*-CBI derivatives
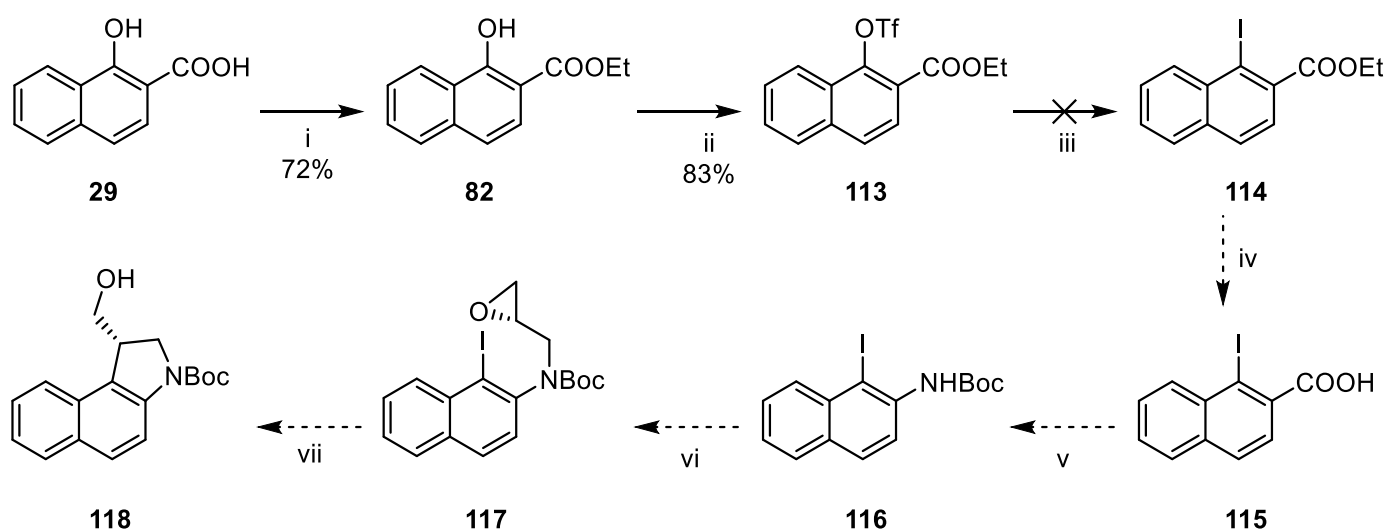
Scheme 44: Proposed synthetic pathway towards 5-H *seco*-CBI derivatives. *Reagents and conditions*: i. EtOH, cat. H_2SO_4, ii. Triflic anhydride, NEt_3, CH_2Cl_2; iii: NaI, acetone; iv. NaOH, EtOH; v. a) $SOCl_2$, DMF (cat.), b) $TMS-N_3$, toluene, c) Δ, d) ^tBuOH, NEt_3; vi. R-glycidyl nosylate; vii. $Li_2Zn(SCN)Me_3$.

The synthetic pathway toward 5-H *seco*-CBI derivatives outlined in was proposed as a potential route to mask the amines orthogonally, overcoming the selectivity issues experienced by Twum *et al.*[100] and alleviating the issues previously mentioned with regard to the strong electron-withdrawing effects of a nitro group in the 4-position preventing metal-mediated cyclisation. A 5-NH_2 group is required for Winstein cyclisation to occur. Therefore, it was hypothesised that nitration of **118** in order to insert a nitrogen at the 5-position, followed by reduction of the nitro group would yield the desired amino compound. This method has been described by Tercel *et al.* for analogous compounds.[129]

3.2.2.1 Triflation of ethyl 1-hydroxynaphthalene-2-carboxylate 89 and attempted SNAr reaction with NaI to yield 125
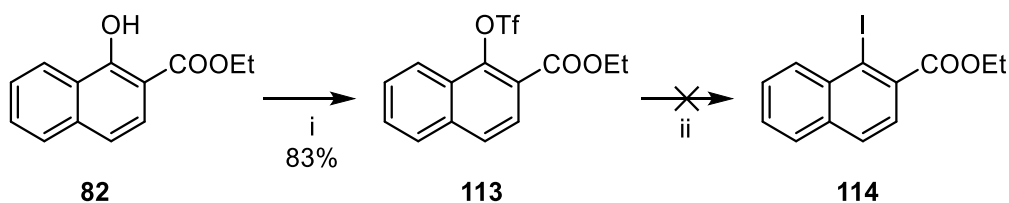
Scheme 45: Triflation of ethyl 1-hydroxy-2-naphthoate **82** followed by attempted S$_N$Ar reaction with NaI. *Reagents and conditions*: i. Tf$_2$O, NEt$_3$, CH$_2$Cl$_2$, rt, 72 h; ii. NaI, acetone, reflux, 17 h, no reaction, or NaI, DMF, reflux, 5 d, no reaction.

Triflation of the 1-hydroxy group in **82** was carried out under standard triflation conditions in high yield. However, displacement of the triflate with iodide by an S$_N$Ar reaction failed to occur, even under reflux at 153°C in DMF for 5 d. Recovery of triflate starting material **113** was confirmed by ^{1}H and ^{19}F NMR. Displacement of triflate by iodide is only possible when the aromatic ring is very electron-deficient, failure to displace the triflate in **113** indicated that the *ortho*-ester was not sufficiently electron-withdrawing and confirmed the requirement for a strong electron-withdrawing group such as a nitro group, *ortho* or *para* to the triflate in order to make the 1-position sufficiently electrophilic for nucleophilic attack by the iodide ion.

3.2.3 Improved synthesis toward 5-H *seco*-CBI derivatives
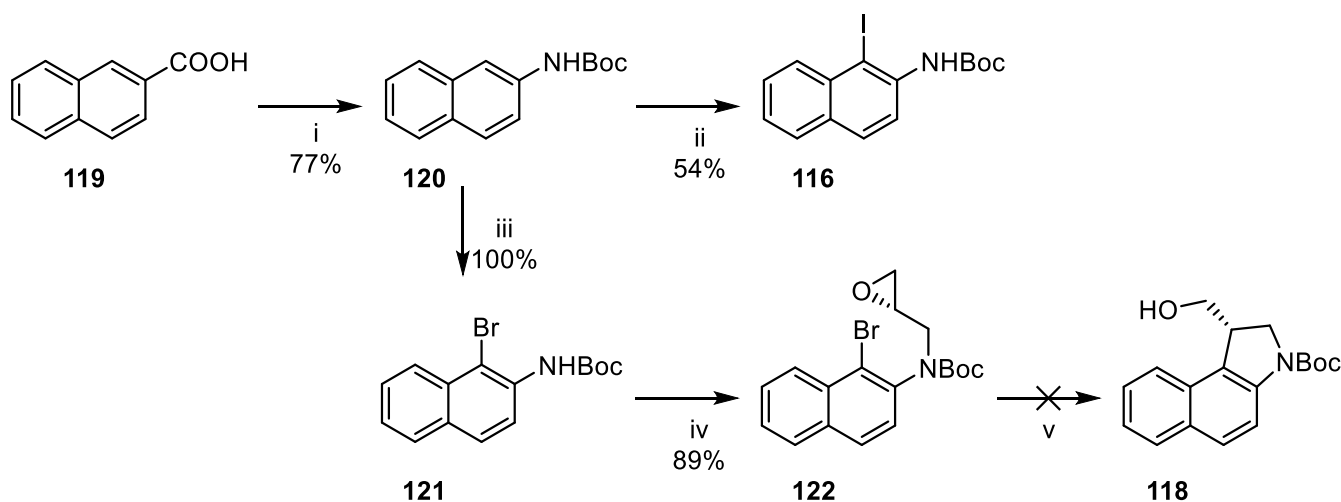
Scheme 46: Overview of optimised 4-H pathway. *Reagents and yields*: i. ^tBuOH, DPPA, NEt_3; ii. NIS; iii. NBS, CH_2Cl_2; iv. R-glycidyl nosylate; v. $Li_2Zn(SCN)Me_3$.

Given the inability to displace the triflate of **113** with iodide, a new approach was investigated, starting from naphthalene-2-carboxylic acid **119**, as outlined in

Scheme 46. Starting with commercially available naphthalene-2-carboxylic acid **119**, a Curtius rearrangement would yield the Boc-protected amine **120** in one step. Insertion of iodine could then be achieved by electrophilic addition through reaction with NIS to yield **116** . This would bypass the issues encountered previously with regard to displacement of triflate with iodide. Alternatively, the bromo analogue **121** can be synthesised through reaction with NBS.

Reaction of **121** with *R*-glycidyl nosylate as described previously would then yield the pre-cyclisation key intermediate **122**. Metal-mediated cyclisation with $Li_2Zn(SCN)Me_3$ should then yield enantiopure material **118**. The lack of a *para*-nitro group will avoid the issue previously encountered of a lack of δ- at the 1-C during metal-mediated cyclisation due to the strong electron-withdrawing effects of the nitro group. This optimised route is particularly interesting given that it would yield enantiomerically pure cyclised **118** in just four steps, albeit without the required amine at the 4-position.

Reaction of carboxylic acid **119** with DPPA yielded the acyl azide without the need to go *via* an acyl chloride. The lack of a strong electron-withdrawing nitro group resulted in the carboxylic acid being reactive enough to perform nucleophilic attack towards the DPPA phosphorus to form the phosphoryl intermediate **123** as shown in Scheme 47.

119   **123**   **124**
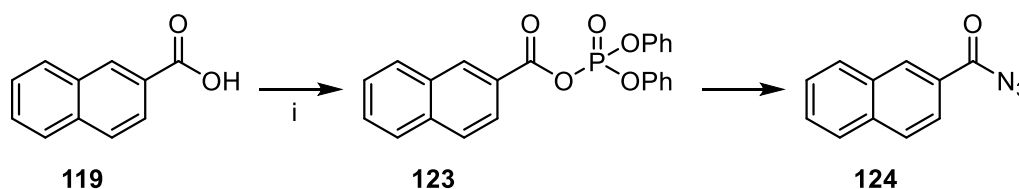
Scheme 47: Formation of acyl azide **124** from carboxylic acid **123**. Reagents: i. DPPA.

Formation of the isocyanate through a Curtius rearrangement followed by treatment with *tert*-butanol yielded *tert*-butyl N-(naphthalen-2-yl)carbamate **120** in 77% overall yield. At this stage, both iodo and bromo analogues **116** and **121** were synthesised through electrophilic addition with NIS and NBS, respectively. As previously mentioned, electrophilic insertion with NIS / NBS bypassed the requirement of an electron-deficient naphthalene when inserting a halide *via* a triflate intermediate. *Tert*-butyl 1-bromo-naphthalen-2-yl carbamate **121** was then alkylated with *R*-glycidyl nosylate to give key intermediate **122** in an 89% yield.

3.2.4 Attempted metal-mediated cyclisation of key intermediate 122

At this point, metal-mediated cyclisation was attempted on key intermediate **122** using Li$_2$Zn(SCN)Me$_3$, by a method developed by Tietze *et al.*[108] and applied successfully to the analogous compound **67** as shown in Scheme 48.

26   **27**
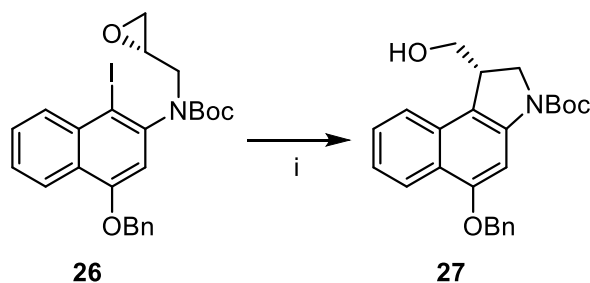
Scheme 48: Metal-mediated cyclisation of compound **26** to yield enantiomerically pure compound **27**, as published by Tietze *et al.*[108] *Reagent*: Li$_2$Zn(SCN)Me$_3$.

Unfortunately, this proved unsuccessful, with no formation of cyclised **118** being detected by MS and the formation of **125**, through ⁻NCS nucleophilic addition *via* epoxide attack and ring opening. Due to a lack of zinc-halogen exchange with key intermediate **122**, nucleophilic attack by 1-C did not occur, resulting in the competing nucleophilic attack by ⁻NCS to occur (Scheme 49).
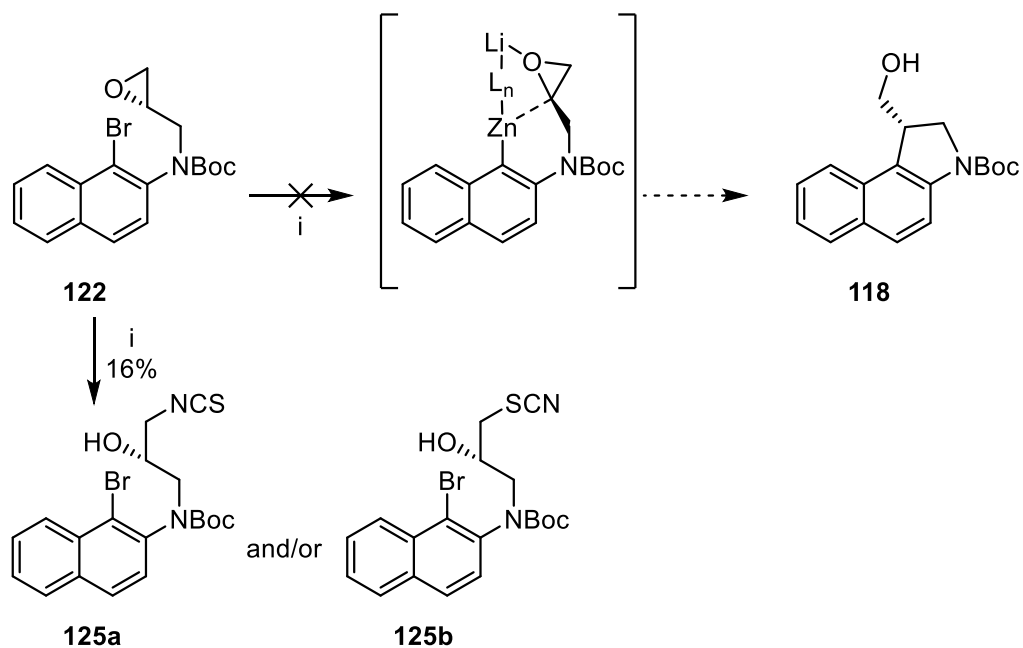
Scheme 49: Attempted metal-mediated cyclisation of key intermediate **133**. *Reagents and yields*: Li₂Zn(SCN)Me₃.

3.2.4.1 Proposed mechanism of attack by SCN⁻
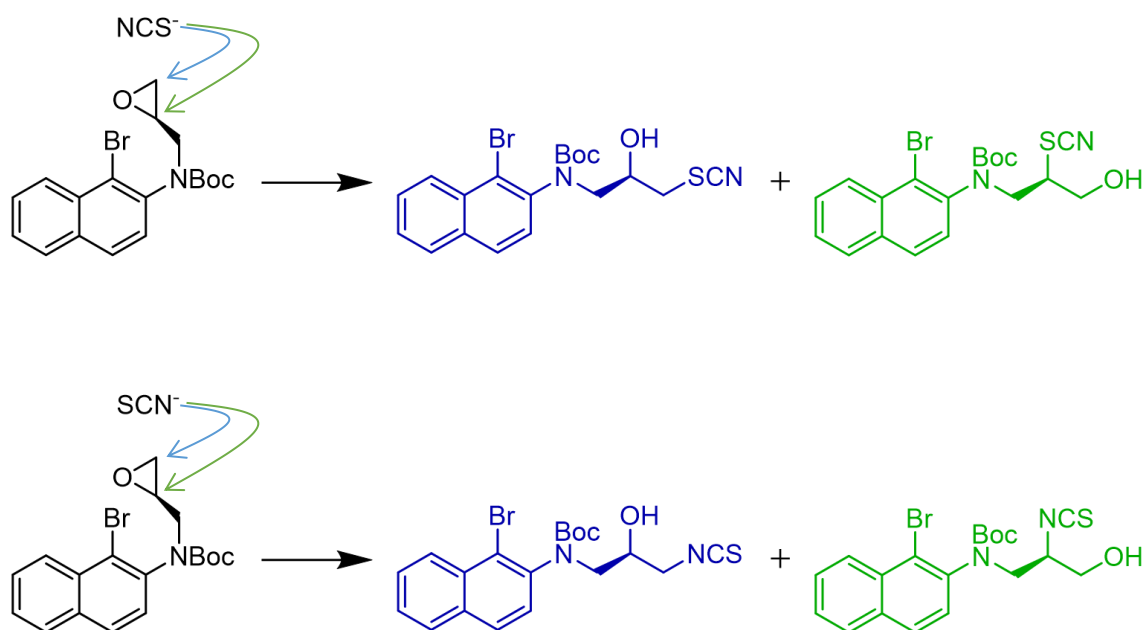
Scheme 50: Possible mechanisms of SCN attack towards key intermediate **122**.

Tietze et al.[108] postulated that metal-mediated cyclisation with $Li_2Zn(SCN)Me_3$ is initiated by metal-halogen exchange at the 1-position, resulting in the formation of a metal complex transition state outlined in Scheme 41 which is then followed by nucleophilic attack towards the epoxide from the δ^- 1-C. However, in the reaction of key intermediate **122**, metal-halogen exchange does not occur at the 1-position, preventing nucleophilic attack towards the epoxide from 1-C. At this stage, it is then possible for nucleophilic attack from the SCN⁻ nucleophile. Due to the ambident nature of SCN⁻, it is possible to form either the R-thiocyanate or R-isothiocyanate product. There are also two possible sites of attack at the epoxide, to yield either the primary or secondary alcohol product as outlined in Scheme 50.

3.2.4.2 Determination of the unknown side-product resulting from the metal-mediated cyclisation of 122.

High Resolution Mass Spectrometry in positive-ion electrospray mode indicated the presence of bromine, with two main peaks at m/z 436.0380 [M]$^+$ and 438.0360 [M]$^+$ for $C_{19}H_{21}{}^{79}BrN_2O_3S$ and $C_{19}H_{21}{}^{81}BrN_2O_3S$ respectively ($C_{19}H_{21}{}^{79}BrN_2O_3S$ requires 436.0456 and $C_{19}H_{21}{}^{79}BrN_2O_3S$ requires 438.0436) as shown in Figure 34. This gave a clear indication as to some form nucleophilic attack and opening of the oxirane by [SCN]$^-$.
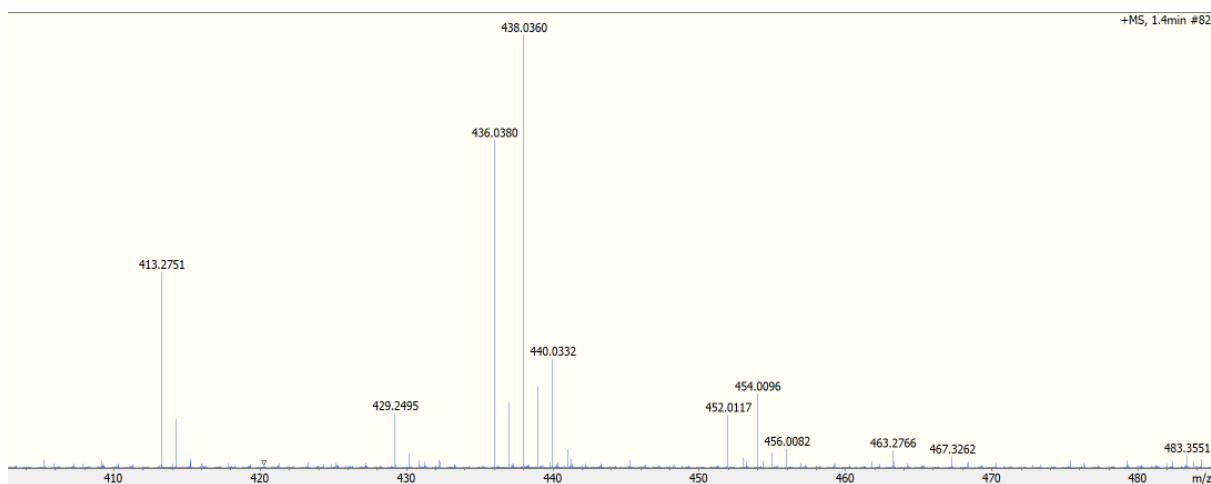
Figure 34: High Res MS (ES +) of compound **125**.

The ^{1}H NMR data showed two sets of signals, each containing six Ar-H, the 9 H singlet for the ^{t}Bu and five alkyl-H in a -CH$_2$CHXCH$_2$- arrangement. The five alkyl-H were downfield relative to the five alkyl-H of the starting material **122**, showing that the oxirane had been opened, relieving ring strain. These two sets are due to the presence of two diastereoisomers arising from the chiral centre in the -CH$_2$CHXCH$_2$- side-chain and epimeric atropisomers around the Ar-N bond shown in Figure 35.

Finally, in order to determine whether the thiocyanate had carried out nucleophilic attack at the primary or secondary carbon of the epoxide, attention was turned to the relative proton shifts within the -CH$_2$CHXCH$_2$- arrangement. The tertiary CH shift was found at δ 4.01 and 4.40 for each atropisomer respectively indicative of a H-C-O bond rather than H-C-N or H-C-S which tend to be more upfield, between δ 2.00 - 3.00. This indicated that nucleophilic attack had occurred at the least hindered terminal CH$_2$ as would be expected.
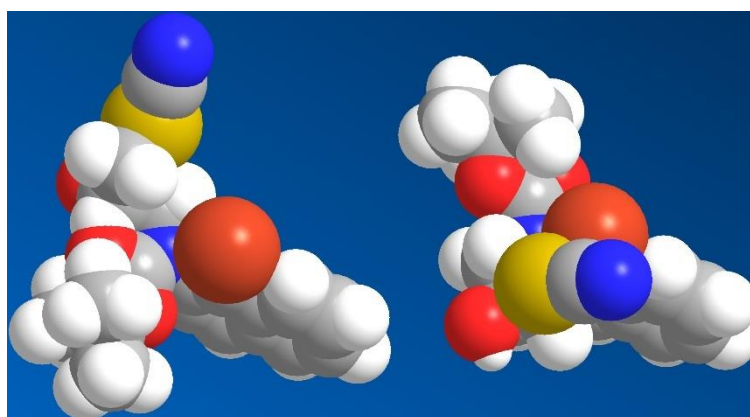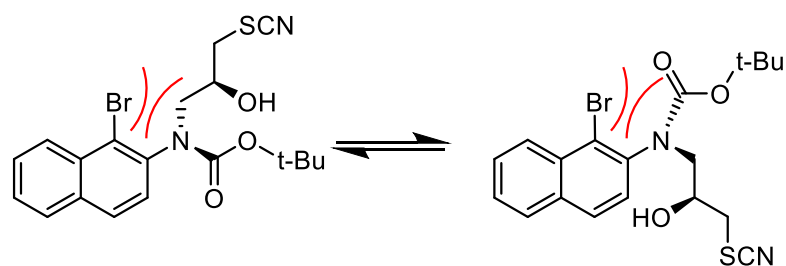
Figure 35: Steric hindrance around the Ar-N bond of **125** as a result of a bulky bromine group results in the formation of two epimeric atropisomers.

3.2.5 Synthesis of 4-bromo-*seco*-CBI derivatives
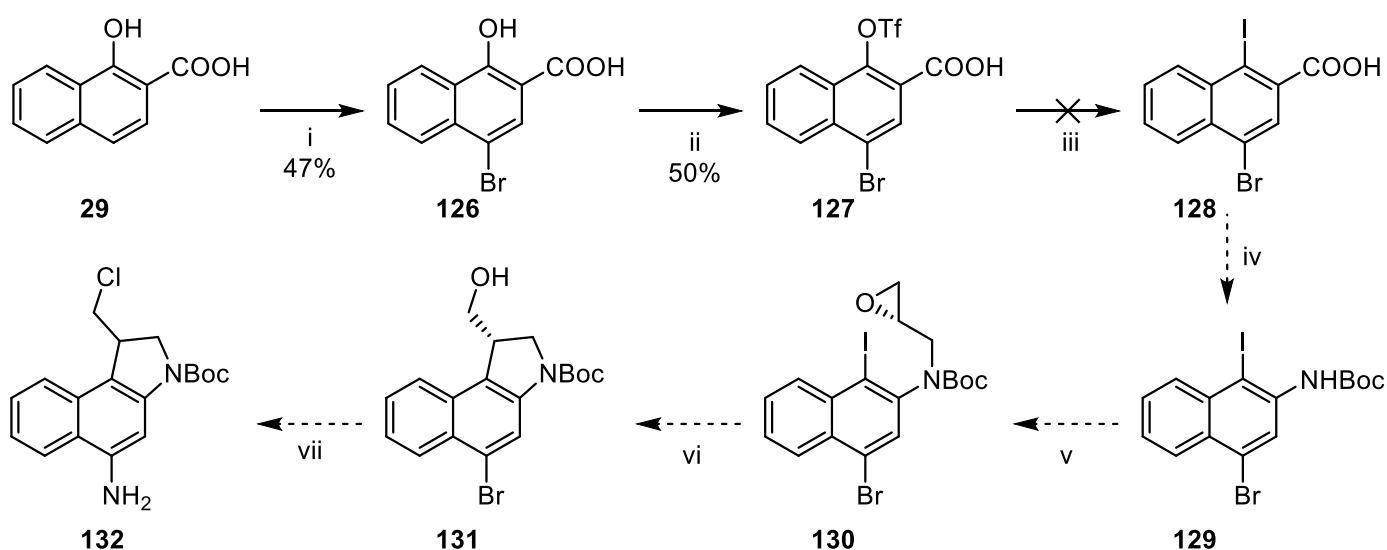
Scheme 51: Overview of the 4-bromo pathway. *Reagents and conditions*: i. NBS, CH$_2$Cl$_2$; ii. Triflic anhydride, NEt$_3$, CH$_2$Cl$_2$; iii: NaI, (CH$_3$)$_2$CO; iv. a. SOCl$_2$, DMF (cat.), b. TMSN$_3$, toluene, c. Δ, d. ^{t}BuOH, NEt$_3$; v. *R*-glycidyl nosylate; vi. Li$_2$Zn(SCN)Me$_3$; vii. *multiple steps*.

The 4-bromo pathway outlined in Scheme 51 was proposed as a potential route to avoid the issue experienced by Twum et al.[100] surrounding protecting the 2-N in the presence of the 4-N. The difficulty in selectively protecting one amine versus the other was a route-limiting step, with mono-protection achieved in a 15% yield. The 4-bromo pathway should also alleviate the issues previously mentioned with regard to the strong electron-withdrawing effects of a nitro group in the 4-position preventing metal-mediated cyclisation, whilst allowing access to the required amine at the 4-position through an aromatic amination reaction. Starting with 1-hydroxynaphthalene-2-carboxylic acid **29**, mono-bromination with NBS to yield 4-bromo-1-hydroxynaphthalene-2-carboxylic acid **126**, followed by conversion of the 1-hydroxy to iodine *via* triflate intermediate **127** would give 4-bromo-1-iodonaphthalene-2-carboxylic acid **128**. A Curtius rearrangement to yield key intermediate *tert*-butyl (4-bromo-1-iodonaphthalen-2-yl) carbamate **129** from the 2-carboxylic acid **128** followed by reaction with *R*-glycidyl nosylate to yield **130** would then allow exploration of metal-mediated cyclisation to yield enantiopure material **131** as well as free-radical cyclisation to yield racemic material. Once cyclisation of **130** has been achieved, aromatic amination can then convert the bromine at the 4-position to the required (protected) amine.
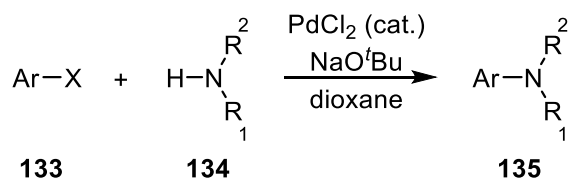
Scheme 52: Buchwald-Hartwig Cross Coupling Amination reaction.

Work by Buchwald[161] and Hartwig[162,163] has shown that Pd can be used to promote aromatic nucleophilic substitution at a C-Br to prepare an aromatic amine (Scheme 52). This process can be viewed as a catalytic cycle, outlined in Scheme 53. The cycle begins with oxidative addition of the aryl halide to a Pd(0) species followed by addition of the amine to the oxidative addition complex. Base-induced deprotonation of the complex is then followed by reductive elimination in which Ar-NRR' is eliminated from the complex.
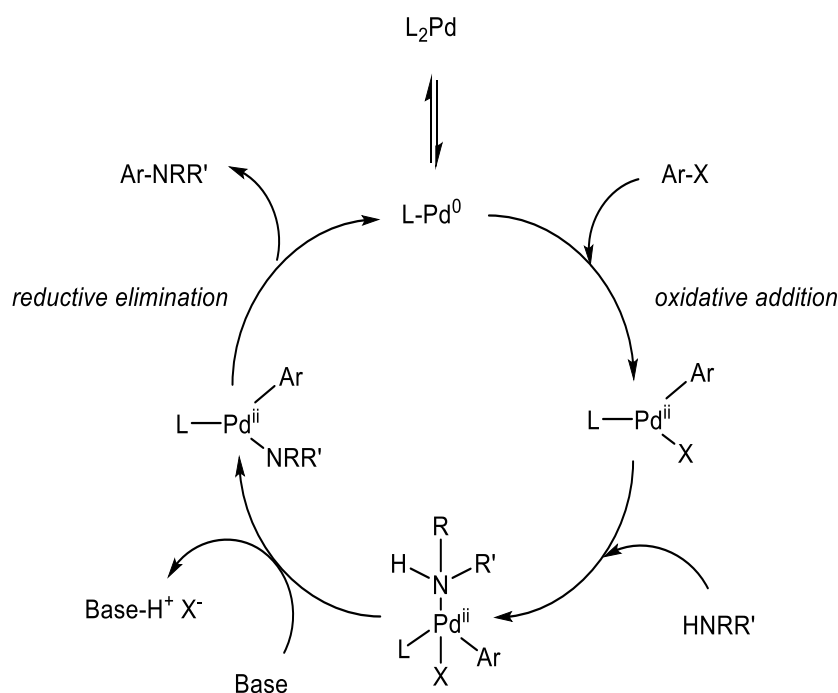
Scheme 53: Catalytic cycle outlining the Buchwald-Hartwig amination mechanism.

As the bromine in **126-131** effectively masks an amine, this eliminates the need to discriminate between two primary amines as in the previous route developed by Twum *et al.*[100] Furthermore, bromine is much weaker deactivating group than a nitro group, which should overcome the issues alluded to previously with regard to metal-mediated cyclisation being hindered by the presence of a strongly deactivating *para*-nitro group.

3.2.5.1 Mono-bromination of 1-hydroxynaphthalene-2-carboxylic acid 29
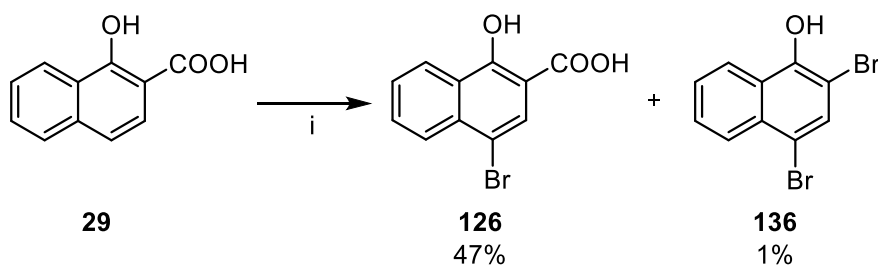
Scheme 54: Bromination of 1-hydroxynaphthalene-2-carboxylic acid **29**. *Reagents and conditions:* i. NBS, CH$_2$Cl$_2$, rt, 24 h.

An attempt was made to synthesise 4-bromo-1-hydroxynaphthalene-2-carboxylic acid **126** by monobromination of 1-hydroxynaphthalene-2-carboxylic acid **29** (Scheme 54). The expected bromination at the 4-position of **29** was based on the *ortho/para*-directing effect of the strongly activating mesomerically electron-donating hydroxy group coupled with the *meta*-directing effect of the moderately deactivating mesomerically electron-withdrawing carboxylic acid group. The weakly deactivating bromine at the 4-position, unlike the much stronger deactivating nitro group, allowed for the possibility of polybromination. Interestingly, 1-hydroxy-2,4-dibromonaphthalene **136** was detected as a minor side product by MS, *via* the decarboxylation mechanism outlined in Scheme 55.
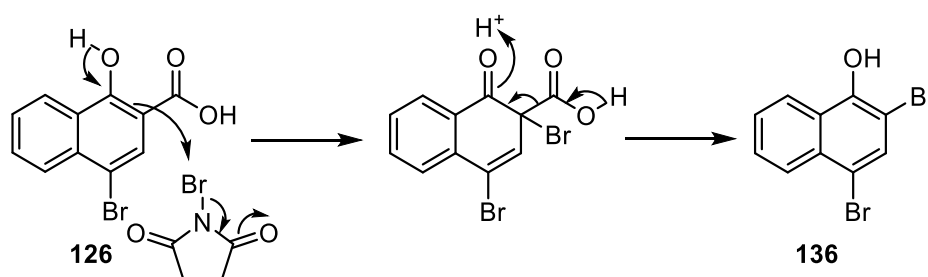
Scheme 55: Possible mechanism outlining the decarboxylation of 4-bromo-1-hydroxynaphthalene-2-carboxylic acid **126** to yield 1-hydroxy-2,4-dibromonaphthalene **136**.

As can be seen in Scheme 55, the activating *ortho*-hydroxy group in **126** induces nucleophilic attack by 2-C towards the electrophilic bromine in NBS. Decarboxylation then occurs in order to restore aromaticity of the naphthalene ring, yielding **136**.

3.2.5.2 Attempted nucleophilic displacement of triflate group with iodine in 4-bromo-1-(trifluoromethylsulfonyloxy)naphthalene-2-carboxylic acid 126
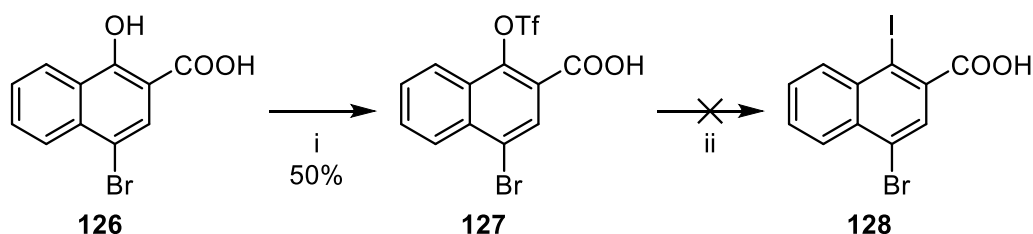
Scheme 56: Triflation of **126** followed by the attempted substitution of the triflate group in **127** with iodide. *Reagents and conditions*: i. Tf$_2$O, NEt$_3$, CH$_2$Cl$_2$, 0˚C, 17 h, 50%; ii: NaI, acetone, reflux, 72 h.

A literature search around the synthetic routes undertaken to analogous derivatives[100,164] suggested that triflation of the hydroxy group in **126** followed by S$_N$Ar displacement of the triflate with iodide would yield 4-bromo-1-iodonaphthalene-2-carboxylic acid **128**. At this stage, formation of the acyl azide from the carboxylic acid *via* an acyl chloride intermediate could then be followed by a Curtius rearrangement to yield the isocyanate. Reaction with ^{t}BuOH to give a Boc-protected amine at the 2-position would provide access to the key intermediate **129**. Triflation of the hydroxy group occurred readily and in moderate yield to yield **127**; however, attempted S$_N$Ar displacement of the triflate with iodide failed to yield the desired 4-bromo-1-iodonaphthalene-2-carboxylic acid **128**. ^{19}F NMR suggested that the triflyl group had been lost, due to a lack of a CF$_3$ peak. However, high resolution MS surprisingly indicated formation of a compound with the empirical formula C$_{10}$H$_7$BrO, suggesting formation of the decarboxylation product 1-hydroxy-4-bromonaphthalene **150** (Scheme 57). This compound has been reported in the literature and so formation was confirmed by comparison with reported NMR data.[165] It is likely that the lack of strong electron-withdrawing group *para* to the triflate in **127** results in the 1-position not being sufficiently electrophilic for nucleophilic attack by the iodide ion. In this case, the best remaining electrophile is the triflate sulfur and so an alternate reaction mechanism takes place outlined in Scheme 57 to yield 4-bromo-1-hydroxynaphthalene-2-carboxylic acid. Acid catalysed

decarboxylation can then occur to yield 4-bromo-1-hydroxynaphthalene **137**. This mechanism is aided by the *ortho*-hydroxy group that pushes electron density into the aromatic system mesomerically, helping to promote decarboxylation.
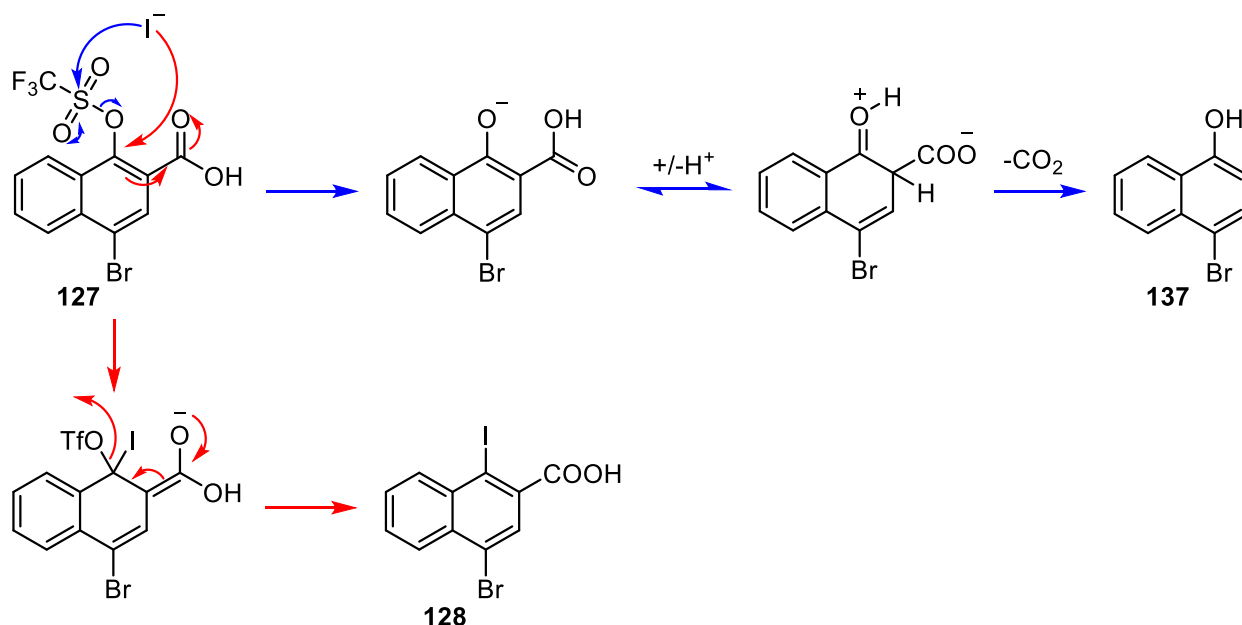
Scheme 57: The desired S_NAr reaction with NaI to yield **128** is outlined in red. The proposed mechanism of decarboxylation to yield **137** is outlined in blue.

3.2.5.3 Attempted esterification of 1-hydroxy-4-bromo-2-naphthoic acid 126
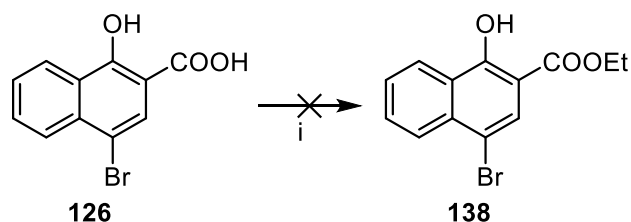
Scheme 58: Attempted esterification of 4-bromo-1-hydroxynaphthalene-2-carboxylic acid **126**. *Reagents and conditions*: i. EtOH, cat. H_2SO_4, reflux, 17 h.

As the carboxylic acid of **127** appeared to be prone to decarboxylation, esterification of 4-bromo-1-hydroxynaphthalene-2-carboxylic acid **126** was attempted to protect the carboxylic acid group. Fischer esterification was attempted by boiling **126** in EtOH in the presence of

catalytic H_2SO_4; however, after 17 h no reaction had taken place and starting material **126** was recovered. The presence of a hydroxy group *ortho* to the carboxylic acid will increase electron density at the carboxylic acid mesomerically. This makes the carbonyl carbon less δ^+ and therefore less susceptible to nucleophilic attack from the EtOH nucleophile, hindering esterification.

3.2.5.4 Mono-bromination of ethyl 1-hydroxy naphthalene-2-carboxylate 82
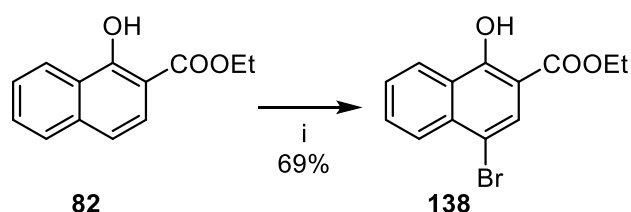
Scheme 59: Bromination of ethyl 1-hydroxynaphthalene-2-carboxylate **82**. *Reagents and conditions*: i. NBS, CH_2Cl_2, rt, 72 h.

With decarboxylation hindering progress towards the synthesis of key intermediate 4-bromo-1-iodonaphthalene-2-carboxylic acid **128** and the unsuccessful esterification attempt to yield ethyl 4-bromo-1-hydroxynaphthalene-2-carboxylate **138**, focus was turned to the mono-bromination of ethyl 1-hydroxynaphthalene-2-carboxylate **82**. This reaction proceeded in a respectable 69% yield with no formation of side products observed. At this point, good progress with the 4-nitronaphthalene synthetic pathway suspended further investigation of the 4-bromo pathway.

3.2.6 Synthesis of 5-NHR-*seco*-CBI derivative 142
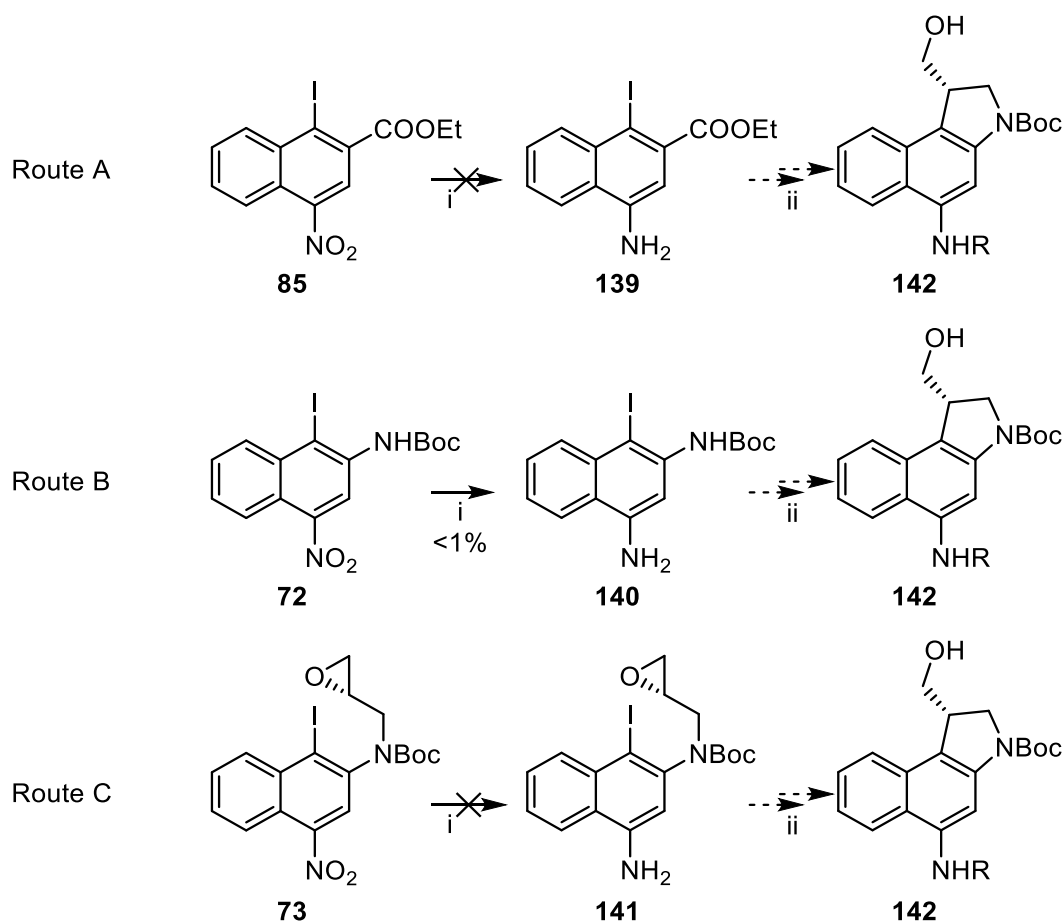
Scheme 60: Proposed synthetic routes towards 5-NHR-*seco*-amino-CBI derivative **142** showing possible stages to reduce the 4-NO$_2$; prior to the Curtius rearrangement, immediately post-Curtius rearrangement and prior to metal-mediated cyclisation. *Reagents*: i. HSiCl$_3$; ii. *multiple steps*.

As the strong electron-withdrawing effects of the nitro group *para* to the 1-position in **73** were hypothesised to be preventing metal-mediated cyclisation through hindering nucleophilic attack on the epoxide, attention was focused towards reducing the nitro group and protecting the subsequent amine. Unlike nitro groups, amino groups are electron donating towards aromatic systems and so should improve the nucleophilicity at the 1-position of an appropriate organometallic intermediate, improving the chance of nucleophilic attack toward the epoxide. Three points in the synthetic pathway were identified as potential stages to reduce the 4-NO$_2$, as outlined in Scheme 60. Reduction can either occur when there is an ester at the 2-position (**85**), and then the 4-amino group of **139** can be protected prior

formation of the Boc-protected amine at the 2-position (Route A). Alternatively, reduction of the 4-NO$_2$ can occur immediately after formation of the Boc-protected amine **72**. Finally, reduction of **73** immediately before metal-mediated cyclisation can occur, followed by protection of the resulting amine **141** prior to cyclisation. In all cases, the 4-amino group will be protected, this is important in order to ensure that there are no acidic N-Hs that would not be tolerated by the organometallic reagents.

3.2.6.1 Reductive de-iodination of ethyl 1-iodo-4-nitronaphthalene-2-carboxylate 85
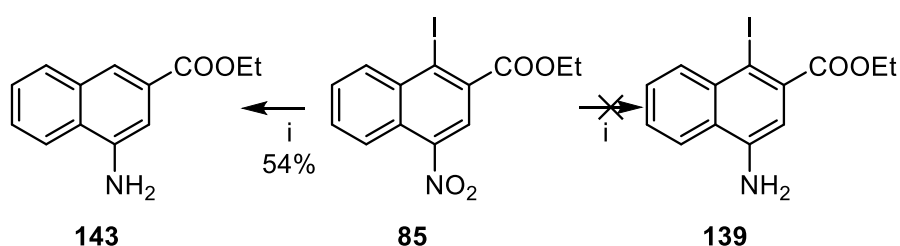
Scheme 61: Reduction of ethyl 1-iodo-4-nitronaphthalene-2-carboxylate **90**. *Reagents and yield*: i. Fe, AcOH; *or* Pd-C, H$_2$; *or* SnCl$_2$.

Reduction of ethyl 1-iodo-4-nitronaphthalene-2-carboxylate **85** was attempted many times to try to reduce the 4-NO$_2$ selectively whilst maintaining the iodine; however, attempts with Fe / AcOH, Pd-C / H$_2$ and SnCl$_2$ all yielded de-iodinated ethyl 4-amino-2-naphthoate **143**. Similar issues regarding reductive deiodination were experienced by Twum *et al*,.[100] with regard to reduction of 1-iodo-2,4-dinitronaphthalene. While non-ideal in terms of atom-efficiency, ethyl 1-aminonaphthalene-3-carboxylate **143** could potentially be taken forward to the key intermediate as shown in Scheme 62.
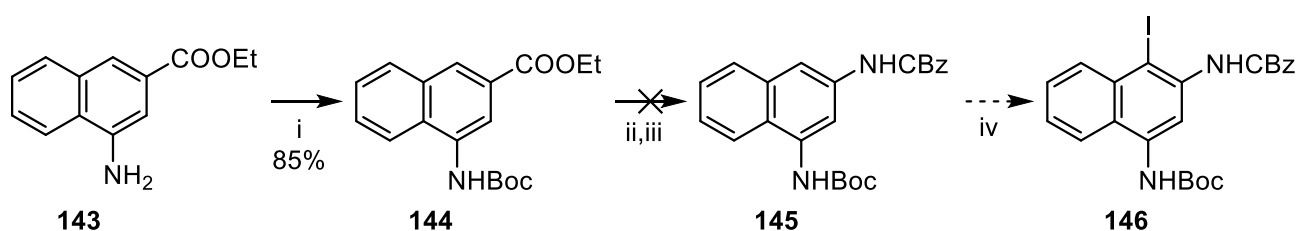
Scheme 62: Synthetic pathway from ethyl 1-aminonaphthalene-3-carboxylate **143** to pre-cyclisation key intermediate **146**. *Reagents and yield*: i. Boc$_2$O; ii. NaOH, EtOH; iii. a) DPPA, b) benzyl alcohol, NEt$_3$; iv. NIS.

3.2.6.2 Attempted synthesis of *tert*-butyl (4-iodo-3-((2-oxo-2-phenyl-1-ethyl)amino)naphthalen-1-yl)carbamate 146
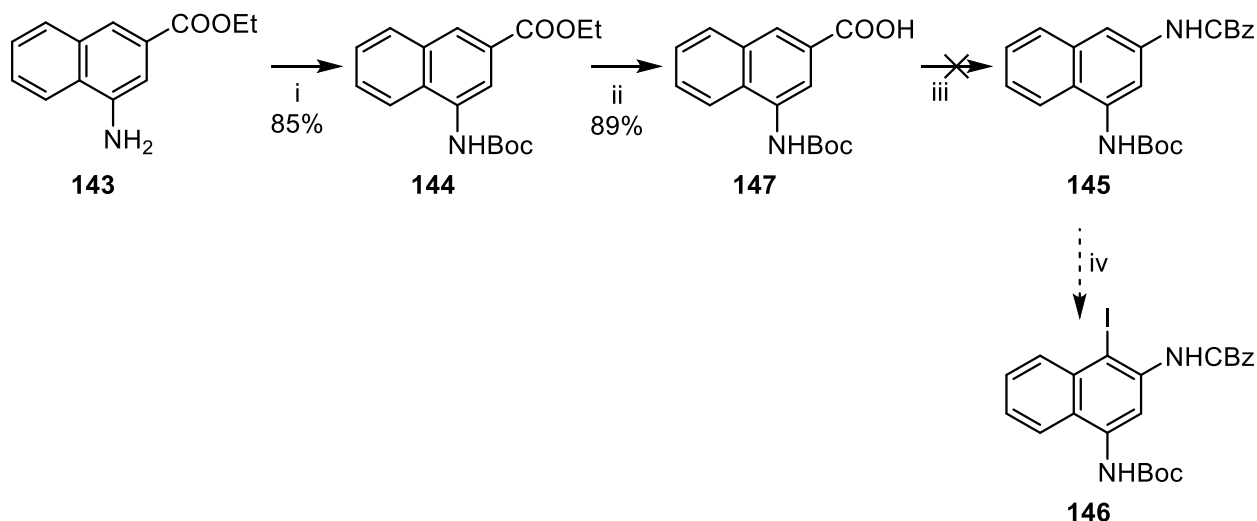
Scheme 63: Attempted synthesis of **146**. *Reagents:* i. Boc$_2$O; ii. NaOH, EtOH; iii. a) DPPA, b) benzyl alcohol, NEt$_3$.

Following the synthetic route shown in Scheme 63, ethyl 4-aminonaphthalene-2-carboxylate **143** was treated with Boc$_2$O to form ethyl 4-((*tert*-butoxycarbonyl)aminonaphthalene)-2-carboxylate **144** in 86% yield. Boc was chosen as a protecting group due to its stability under basic conditions. This allowed base-catalysed hydrolysis of the ethyl ester, yielding **147**, to occur without incident in an 89% yield. The next stage in the synthesis involved formation of an acyl azide with DPPA followed by a Curtius rearrangement to yield an isocyanate. Reaction with benzyl alcohol would then form a benzyl-protected amine at the 1-position, resulting in two amines that are orthogonally protected to each other as required. However, reaction with DPPA followed by benzyl alcohol and NEt$_3$ failed to yield desired **145**. Common side-products associated with Curtius rearrangements include the formation of carbamates due to the reaction of water with the isocyanate. For this reason, reaction conditions must be anhydrous. Recovery of starting material **147** was verified by high resolution mass spectrometry indicating that formation of the acyl azide did not occur rather than an undesired reaction of the acyl azide with water.

3.3 Free-radical cyclisation approach towards *seco*-amino-CBI derivatives
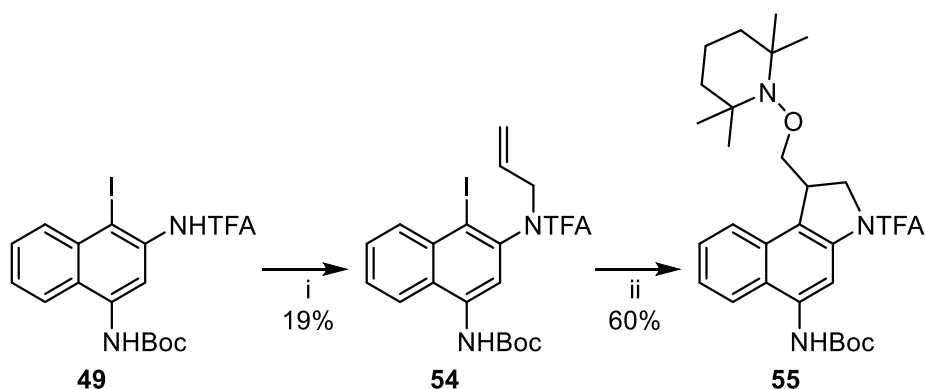
Scheme 64: Reported free-radical cyclisation approach to yield racemic **55**. *Reagents and yields*: i. 3-bromopropene, K_2CO_3; ii. Bu_3SnH, TEMPO.[100]

Despite synthesis of enantiopure *seco*-nitro-CBI **74**, albeit in low yield, a racemic synthesis of the pyrrolidine ring was pursued alongside attempted optimisation of the metal-mediated cyclisation. Work by Twum[100] reported that selective alkylation of the N2-amide of **49** with 3-bromopropene to yield **54** followed by free-radical cyclisation yielded racemic *seco*-amino-CBI **55** as shown in Scheme 64.
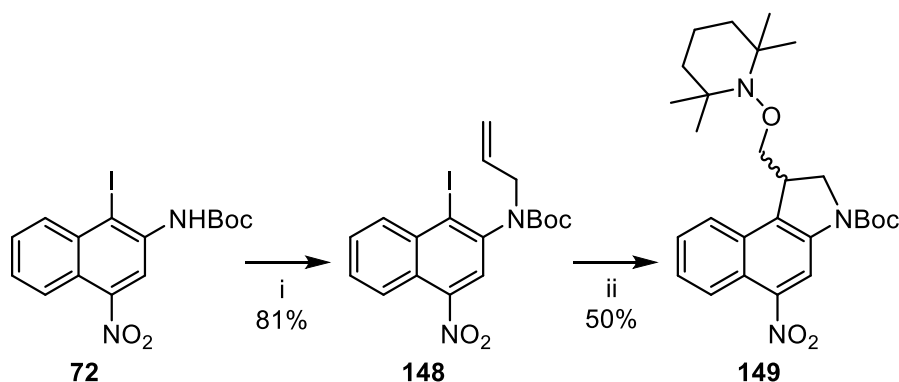
Scheme 65: Allylation of **72** followed by free-radical cyclisation of **148** to yield **149**. *Reagents and yields*: i. 3-bromopropene, K_2CO_3; ii. Bu_3SnH, TEMPO.

This approach was applied to the analogous compound **72**, as outlined in Scheme 65. Reaction of **72** with allyl bromide and K_2CO_3 yielded desired **148** as a pair of inseparable rotamers around the 2-C-N bond. The slow rotation about this bond is due to the bulkiness of the groups on N2 as well as a possible steric clash with the bulky iodine and the peri-5 hydrogen during rotation around the C—N bond. This means that the allyl groups can either be on the same side or the opposite side of the naphthalene ring, resulting in the observed rotamers shown in Scheme 66.
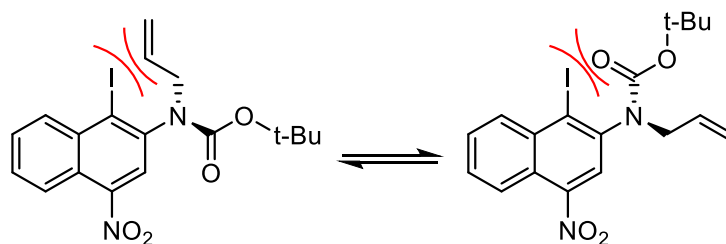
Scheme 66: Observed rotamers of **148** as a result of steric interactions between the bulky iodine and N2-substituents.

The N2-allyl compound **148** was treated with tributyltin hydride and 2,2,6,6-tetramethyl-piperidine-1-oxyl (TEMPO), which promoted a 5-*exo*-trig free radical cyclisation with *in situ* TEMPO trap of the intermediate cyclisation product radical to give racemic **149**. The TEMPO radical also acts as the free radical initiator to generate tributyltin radical as shown in Scheme 67.
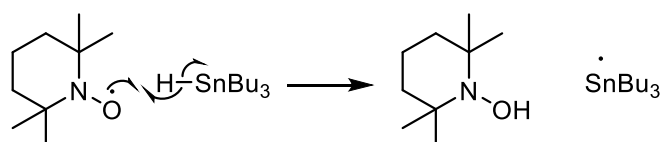
Scheme 67: Mechanism of the initiation step to form the $SnBu_3$ radical.

Abstraction of iodine by the tributyltin radical generates an aryl radical which then attacks the allyl double bond to generate the free radical cyclisation product. Entrapment by TEMPO generates the desired compound **149** in a 50% overall yield (Scheme 68).
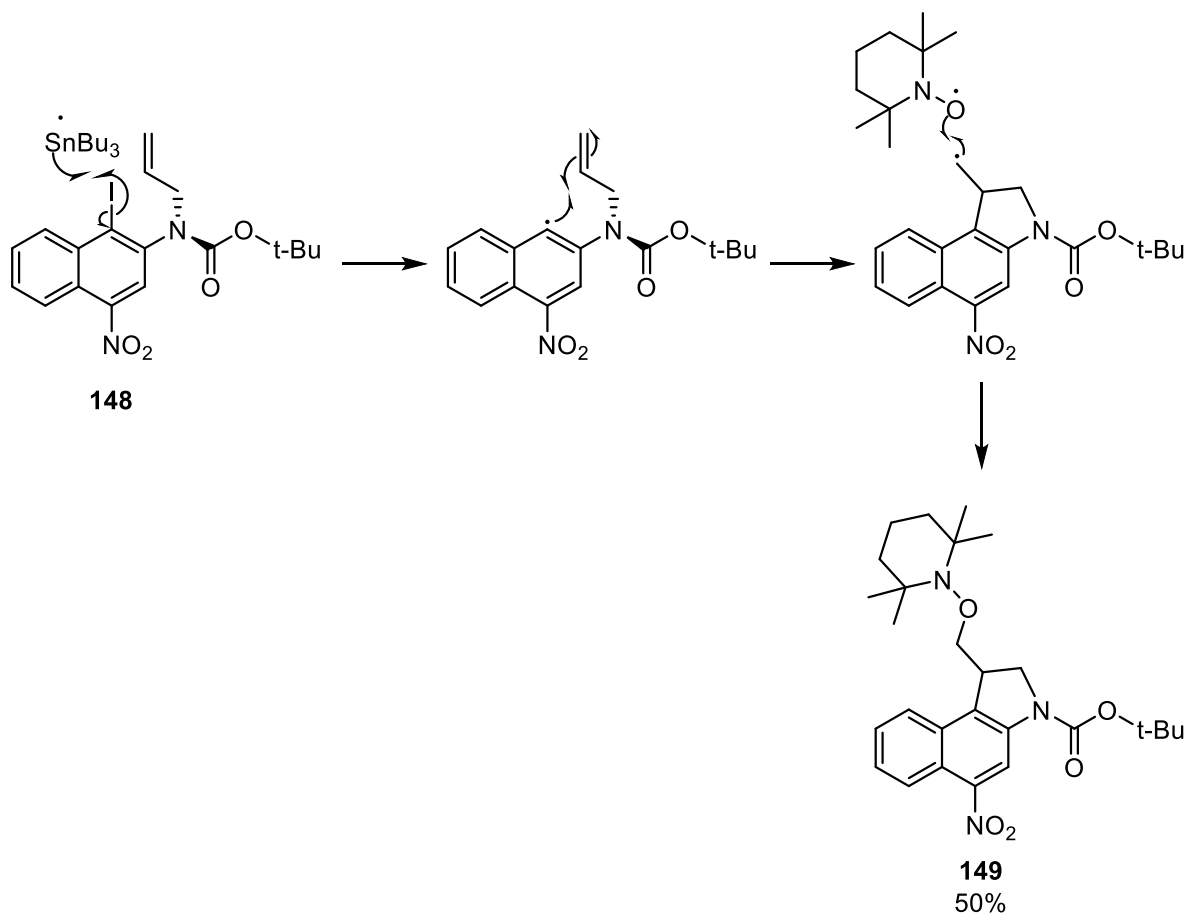
Scheme 68: Mechanism of the free-radical cyclisation to yield **149**.

Interestingly, this reaction does not go to completion unless excess reagents are used. This is likely to be due to the competing reaction between TEMPO and the generated tributyltin radical. This is especially true since the rate constant (k = ~8 × 108 $M^{-1}s^{-1}$ at 80°C) of tributyltin radical abstracting the iodine is similar to the rate constant (k = ~7.6 × 108 $M^{-1}s^{-1}$ at 25°C) for reaction between the TEMPO and tributyltin radical (Scheme 69).
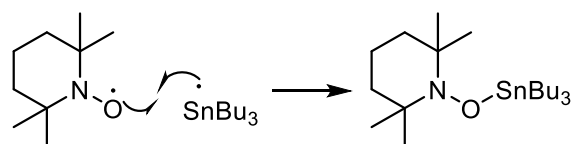
Scheme 69: Competing free-radical termination reaction between TEMPO and SnBu$_3$ radical

3.3.1 Investigation into the use of a chiral TEMPO auxiliary
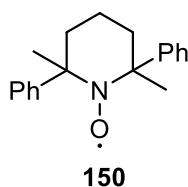
Figure 36: Structure of chiral TEMPO **150**.

The synthetic route in Scheme 70 was proposed whereby the reagent TEMPO is replaced with a single diastereomer of the chiral TEMPO **150** to yield cyclised diastereomer **151**. Unlike an enantiomeric compound, where each enantiomer is chemically identical, with identical physical properties, diastereoisomers have different physical and chemical properties, making it possible to isolate the desired diastereomer of **151** through standard techniques such as chromatography. The chiral TEMPO can then be cleaved reductively from **151** and then recycled by oxidation of the piperidine.
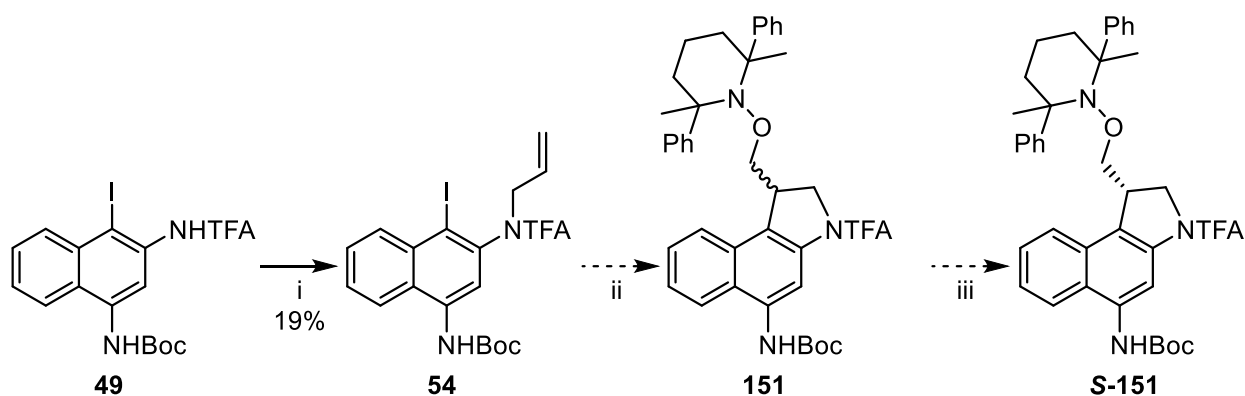
Scheme 70: Proposed synthesis of cyclised diastereomer **151** to then obtain enantiopure **151**. *Reagents and yields*: i. 3-bromopropene, K$_2$CO$_3$; ii. Bu$_3$SnH, 'chiral TEMPO' **150**; iii. chiral column chromatography.

3.3.2 Synthesis of chiral TEMPO 150

Synthesis of chiral TEMPO **150** began with a methyl-trioxorhenium-catalysed oxidation of 2,6-dimethylpiperidine **152** to yield nitrone **153**, using urea-hydrogen peroxide complex (UHP) as an oxidant, as reported by Goti.[166] The mechanism of oxidation has previously been reported by Herrmann.[167] Treatment of methyltrioxorhenium (MTO) **155** with UHP (2 eq) leads to the formation of the active species **152** shown in Scheme 71, which then goes on to oxidise **152** to the nitrone **153**. Treatment of **153** with PhMgBr then inserted a phenyl group at 2-C through a Grignard reaction.
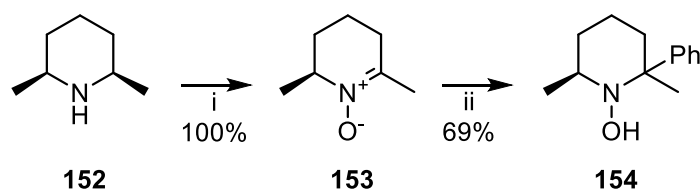
Scheme 72: Oxidation of **152** to yield **153** followed by Grignard reaction to yield **154**. Reagents: i. MTO, Urea hydrogen peroxide (UHP); ii. PhMgBr.
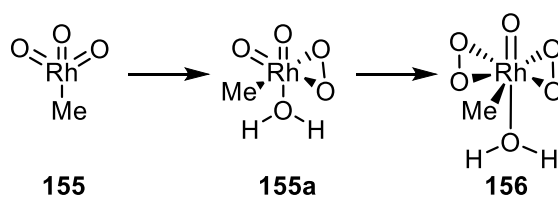
Scheme 71: Formation of the MTO active species **156**.

3.3.2.1 Synthesis of racemic 159
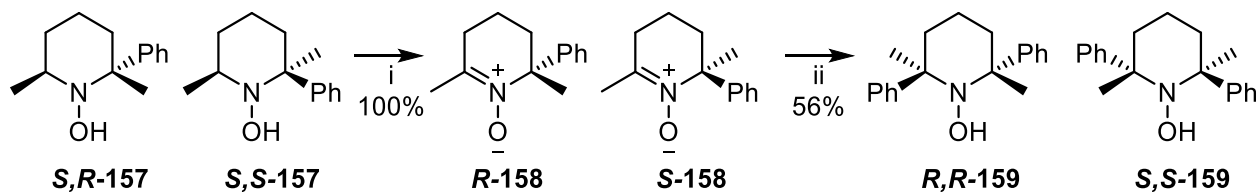
Scheme 73: Synthesis of racemic **159** from **157**. *Reagents*: i. MnO$_2$, **100%**; ii. PhMgBr, **56%**.

The next step involved oxidation of **157** to the corresponding nitrone **158**, followed by a second Grignard reaction with PhMgBr to yield racemic **159** as shown in Scheme 73. Oxidation of **157** with MnO$_2$ was confirmed by high resolution mass spectrometry and followed immediately by Grignard reaction with PhMgBr to yield **159** in a 56% yield. At this stage, it is now possible to have two pairs of enantiomers due to the chiral centres at the 2 and 6 positions. It has been reported in the literature[168] that this reaction only yields enantiomers R/R and S/S. This is due to the large steric interactions between the two phenyl groups, forcing them into a *trans* arrangement.

3.3.2.2 Reduction of 159 to yield 160
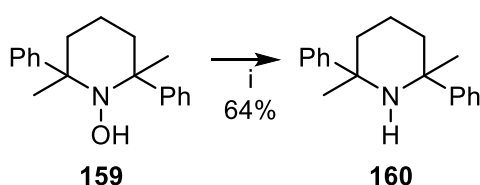
Scheme 74: Reduction of **159** to yield **160**. *Reagents and yield*: Zn, HCl.

Zinc reduction of **159** gave **160** in a 64% yield. However, due to time constraints this route was not investigated further in order to focus on metal-mediated cyclisation. At this stage, it should be possible to attempt separation of the two diastereoisomers through fractional crystallisation of their diastereomeric salts formed with mandelic acid as described by Einhorn *et al*,.[168] (Scheme 75). Once separation has been achieved, enantiopure **160** can be oxidised to the nitrone **161** using oxone® which can then be used in place of TEMPO in a free-radical cyclisation.
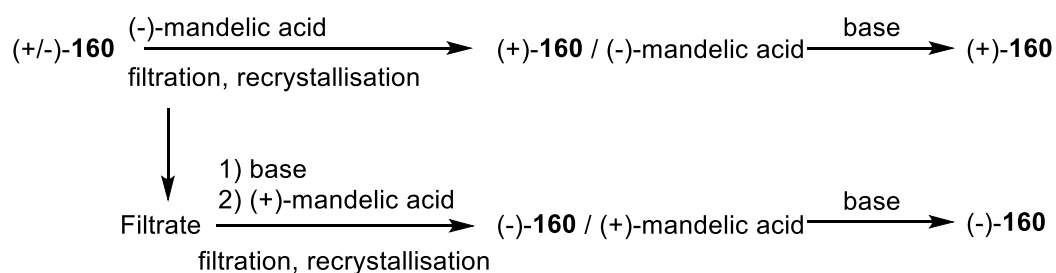
Scheme 75: Overview of the chiral resolution of **160**.

3.4 Deprotection of 149 2-N to allow for coupling to non-alkylating subunits
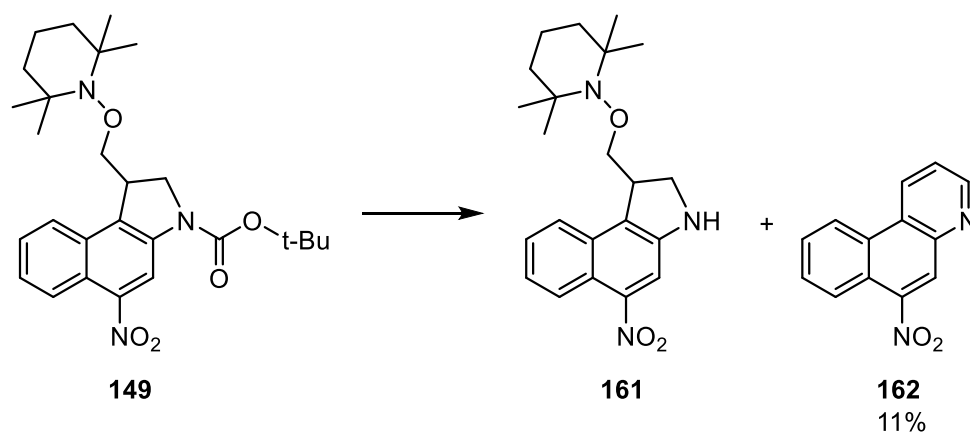
Scheme 76: Deprotection of **149** 2-N to yield desired **161** and unexpected **162**. *Reagents*: TFA.

One drawback to the free-radical cyclisation of **148** to yield *seco*-nitro-CBI **149** was the difficulty in removing residual Bu₃SnI and other tributyltin- derivatives due to their solubility in organic solvents. A common method for Boc-deprotection is to treat the Boc compound with TFA in CH₂Cl₂.[169] When **149** was treated with TFA in CH₂Cl₂, as well as the expected product **161**, unexpected compound **162** was also produced in 11% yield (Scheme 76). This unexpected compound is hypothesised to have been synthesised through an initial Winstein cyclisation and rearrangement, outlined in Scheme 77, to yield nitro CBI **163**.
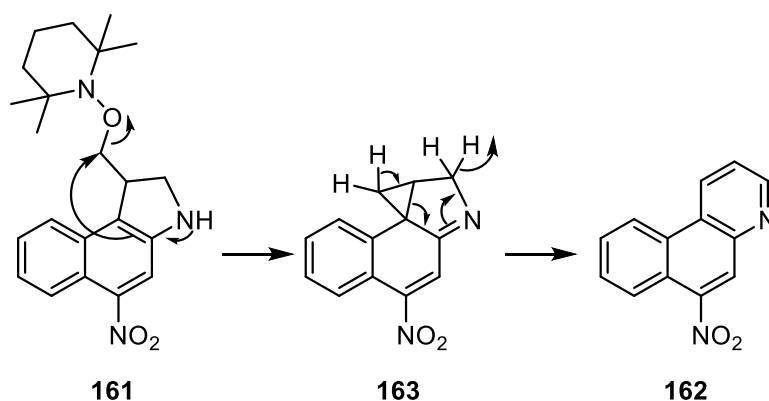
Scheme 77: Proposed mechanism of the rearrangement to yield **162** *via* a nitro-CBI intermediate **163**.

Formation of nitro-CBI **163** is immediately followed by an intramolecular rearrangement to form fully aromatic **162**. It is hypothesised that the process of gaining aromaticity is what drives this mechanism to occur. To overcome this issue, deprotection of **149** 2-N was achieved through bubbling HCl gas through a crude solution of **149** in Et₂O. The deprotected chloride salt, **161·HCl** precipitated from the solution. As the chloride salt, the positively charged secondary amine no longer has enough electron-density to carry out a Winstein cyclisation.

3.5 Optimisation of the free-radical approach to *seco*-amino-CBI derivatives
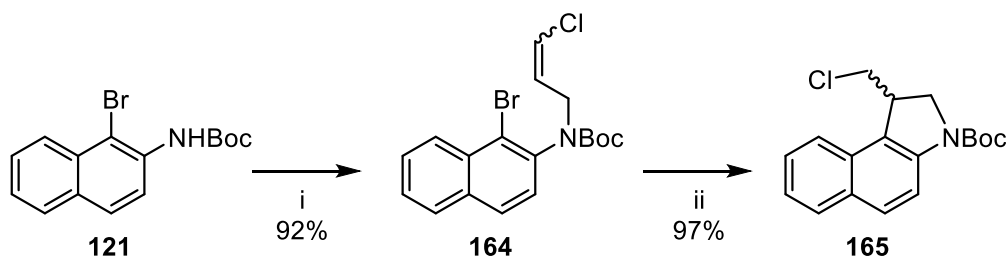
Scheme 78: Tercel synthesis of *seco*-CBI **165**. *Reagents*: i. 1,3-dichloropropene, NaH; ii. Bu₃SnH, AIBN.[129]

With the synthesis and purification of chiral TEMPO **150** proving challenging, attention turned to the optimisation of the free-radical approach towards racemic *seco*-amino-CBI derivatives. Tercel[129] reported that reaction of *tert*-butyl (1-bromonaphthalen-2-yl)carbamate **121** with 1,3-dichloropropene and NaH yielded chloroallyl **164** which could then be cyclised under free-radical conditions (Bu₃SnH, AIBN) to yield racemic *seco*-CBI **165** as outlined in Scheme 78. It

was hypothesised that this synthetic route could be applied to key intermediate **72** to yield *seco*-nitro-CBI **167**. Cyclisation to yield **167** with the chlorine already in place would also remove several steps compared to forming the TEMPO compound and then having to remove TEMPO and convert the hydroxy group to a chlorine through an Appel reaction.
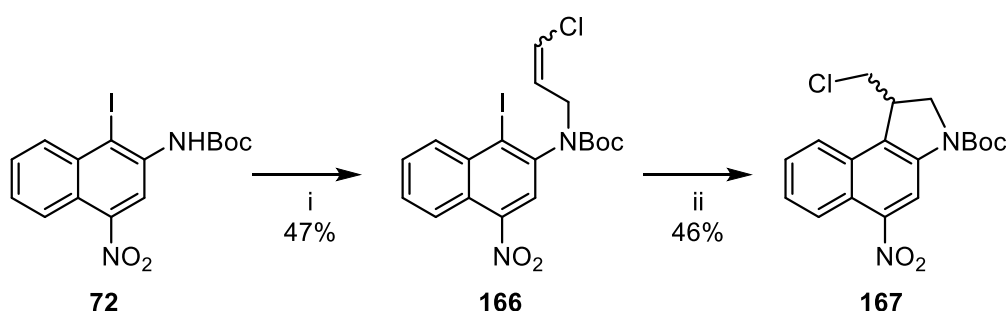
Scheme 79: Synthesis of *seco*-nitro-CBI derivative **167** from key intermediate **72**. *Reagents*: i. 1,3-dichloropropene, NaH; ii. Bu$_3$SnH, AIBN.

Deprotonation of the carbamate N-H of **72** was achieved with NaH. This was followed by nucleophilic attack from the N$^-$ toward the less sterically hindered sp^3 carbon, displacing chloride in a concerted S$_N$2 process to yield **166** as a pair of rotamers about the C-N bond. (Scheme 80). In addition to the pair of rotamers, the 1,3-dichloropropene was a mixture of both the *cis* and *trans* isomers and therefore, there were four possible isomers to distinguish between. In order to simplify NMR analysis, variable-temperature NMR (VT NMR) was used. NMR spectra of **166** were taken at temperatures between 25˚C and 105°C. At higher temperatures, rotation about the C-N bond increases to a point where the NMR records an average spectrum of the two rotamers of **166**, simplifying the spectrum greatly (Figure 37).
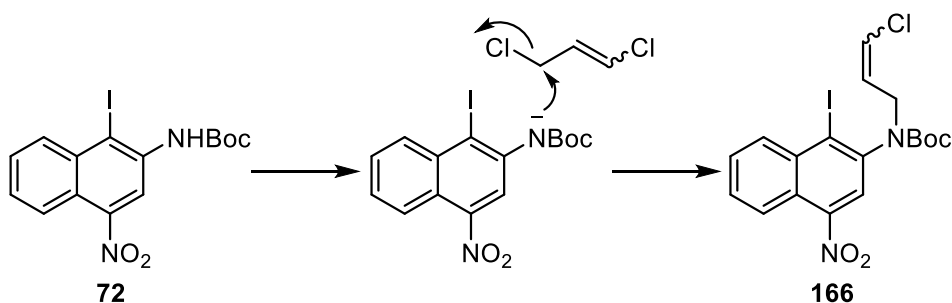
Scheme 80: Mechanism outlining the deprotonation of the carbamate NH of **72** followed by nucleophilic attack toward 1,3-dichloropropene to yield **166**.

At this stage, free-radical cyclisation with Bu₃SnH and AIBN yielded cyclised *seco*-nitro-CBI **167** in a 46% yield. In the previous free-radical cyclisation attempts with TEMPO, the Bu₃Sn· radical is formed by reaction of Bu₃SnH and TEMPO through the homolytic fission of the Sn-H bond. For this reason, in the free-radical cyclisation of **166**, AIBN is added to act as a free-radical initiator. AIBN decomposes to release N₂ and two 2-cyanoprop-2-yl radicals. These radicals then abstract hydrogen from Bu₃SnH to form the tributyl-tin radical that then goes on to abstract iodine from **166**. The resulting 1-C radical then attacks the sp2 2'-H on the allyl chain to yield the 5-*exo*-trig product as shown in Scheme 81.
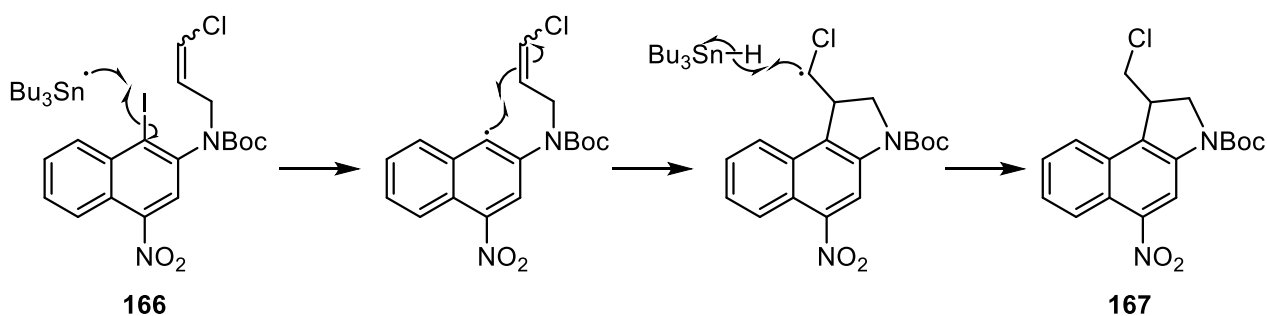
Scheme 81: Mechanism outlining the free-radical cyclisation reaction of **166** and tributyl tin radical to yield **167**.
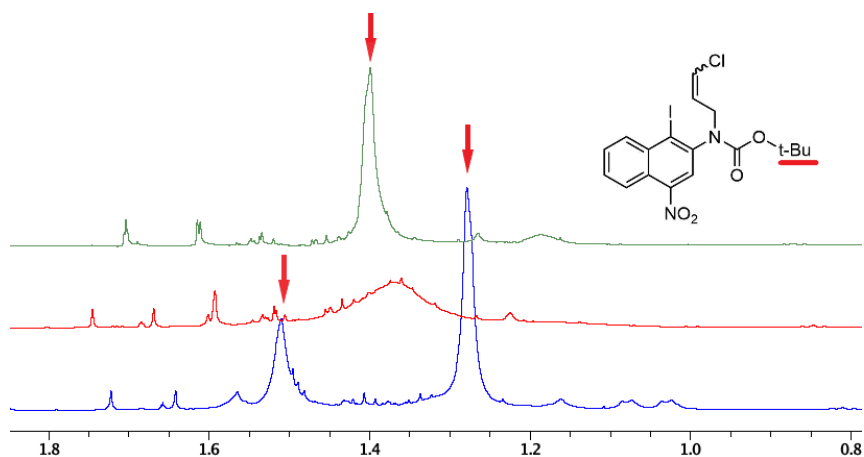
Figure 37: Variable temperature NMR showing the convergence of two rotamer *tert*-butyl peaks of **166**. The red arrows indicate the ᵗBu singlet.

3.6 Synthesis of the non-alkylating subunits

The non-alkylating subunit of CBI compounds plays a key role in determining their biological activity. It is the non-alkylating subunit that first binds to DNA at the minor groove through non-covalent interactions such as hydrogen bonding and Van der Waals forces. In the case of CC-1065, evidence within the literature suggests that its poor side effect profile, including delayed death, are attributed to the non-alkylating subunit-DNA interaction, and specifically the interaction with the ethylene group as discussed previously.[142,170] A range of non-alkylating subunits (**75**-**81**) shown in Figure 38 were chosen to develop a range of amino-CBI compounds and develop the structure-activity relationship surrounding the non-alkylating subunit. These subunits are devoid of the ethylene moiety responsible for the delayed death effect of CC-1065. These subunits were also chosen due to the ease of synthesis and ability to investigate SAR around the benzene ring as well as the importance of an indole-N. 5-Hydroxyindole-2-carboxylic acid **76**, 6-methoxyindole-2-carboxylic acid **77,** Indole-2-carboxylic acid **78** and benzofuran-2-carboxylic acid **81** were all commercially available. The synthesis of 5,6,7-trimethoxyindole-2-carboxylic acid **75**, 5-(2-dimethylaminoethoxy)indole-2-carboxylic acid **79** and 5-(indole-2-carboxamido)indole-2-carboxylic acid **80** are described below.
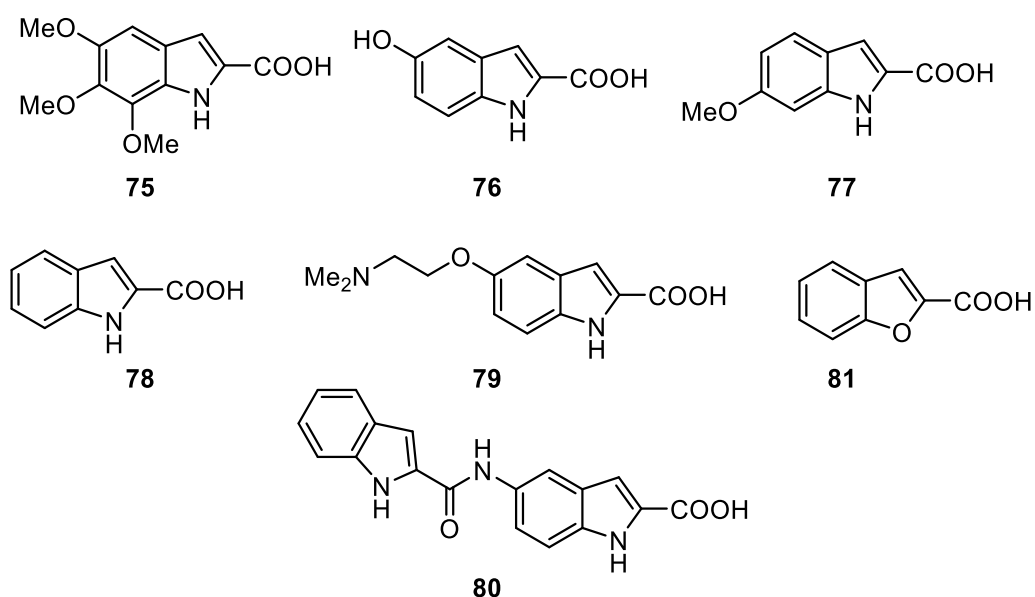
Figure 38: Structures of the non-alkylating subunits **75**-**81** chosen to be investigate structure-activity relationship.

3.6.1 Synthesis of 5-(2-(dimethylamino)ethoxy)-1H-indole-2-carboxylic acid 79
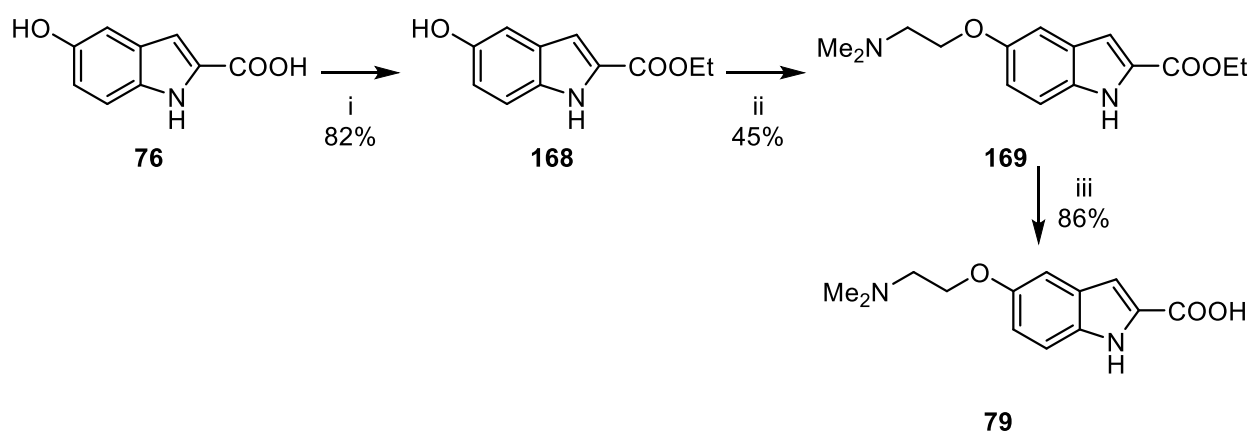
Scheme 82: Synthesis of DMAI **79**. *Reagents*: i. H_2SO_4, EtOH; ii. 2-chloro-*N,N*-dimethylamine HCl, K_2CO_3; iii. NaOH, EtOH.

Starting with commercially available 5-hydroxyindole-2-carboxylic acid **76**, synthesis of desired compound **79** can be achieved in just three steps; esterification of the carboxylic acid, a Williamson ether synthesis to alkylate the 5-OH and finally hydrolysis of the ester. The Williamson ether synthesis is a two-step process to yield an ether. First, the hydroxy group is

deprotonated with a base such as K_2CO_3, the resulting alkoxide then undergoes nucleophilic substitution with an alkyl halide to yield the alkyl ether (Scheme 83). It is vital to mask the carboxylic acid as an ester prior to the Williamson ether reaction as otherwise, deprotonation will occur at the more acidic carboxylic acid, and the ester will be yielded rather than the desired ether.
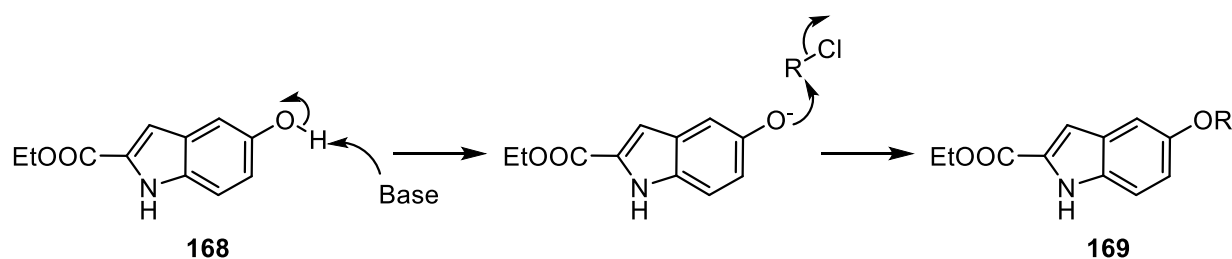
Scheme 83: Mechanism of the Williamson ether synthesis to yield **169**. R = $(CH_3)_2NCH_2CH_2$.

Fischer esterification of carboxylic acid **76** occurred with an 82% yield of the desired product. Now that the carboxylic acid was protected as the ester, the Williamson ether synthesis was then carried out by reaction of ester **168** with 2-chloro-*N,N*-dimethylamine HCl in the presence of K_2CO_3. Successful alkylation at the phenolic-OH occurred in a 45% yield. The final step involved hydrolysis of the ester **169** to yield the desired carboxylic acid **79**. Hydrolysis was achieved under basic conditions and **79** was isolated as the sodium salt. The pKa of the carboxylic acid is around 5 and the pKa of the corresponding conjugate acid of the tertiary amine is around 10. This provided a narrow pH range of between 7 and 8 to yield the neutral compound **79** based on the Henderson-Hasselbalch equation outlined below. For a particular functional group, when pH = pKa, 50% of the functional group in question is ionised and 50% unionised. At pH values ±2 units from the pKa, the functional groups are either fully unionised or fully ionised.

Equation 1:

$$pH = pKa + \log_{10}\left(\frac{[A^-]}{[HA]}\right) = pKa + \log_{10}\left(\frac{[ionised]}{[unionised]}\right)$$

3.6.2 Synthesis of 5,6,7-trimethoxyindole-2-carboxylic acid 75
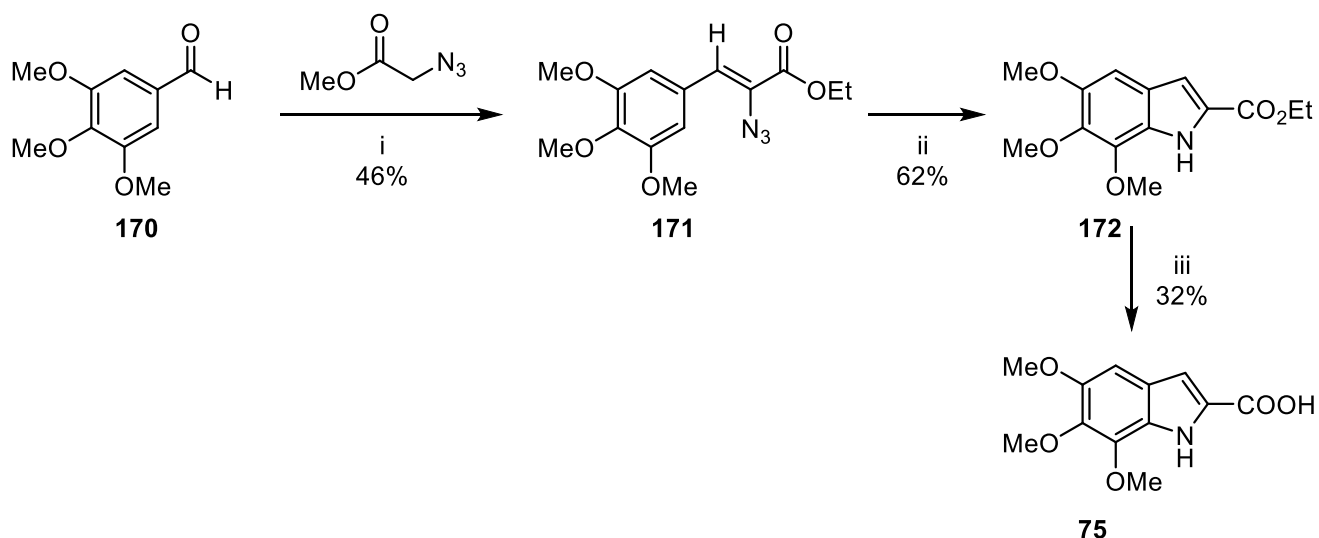
Scheme 84: Synthesis of **75**. *Reagents*: i. Methyl 2-azidoacetate, NaOEt; ii. heat; iii. NaOH, EtOH.

For the synthesis of **75**, a Knoevenagel-Hemetsberger reaction sequence (Scheme 84) was applied as opposed to a Fischer-indole synthesis due to its simpler method.[171] Treatment of 3,4,5-trimethoxybenzaldehyde **170** with methyl 2-azidoacetate and sodium ethoxide provided styryl azide **171** through a Knoevenagel condensation pathway in 46% yield. It has been reported that the Knoevenagel condensation occurs in a stereospecific way to yield solely the *Z*-isomer due to increased thermodynamic stability of the *Z*-isomer versus the *E*-isomer due to steric interactions between the phenyl and carboethoxy group.[171] Use of sodium ethoxide resulted in trans-esterification to the ethyl ester. Warming a solution of **171** in xylene initiated a Hemetsberger indole cyclisation to afford **172** in a respectable 62% yield. The mechanism is believed to proceed *via* the highly electrophilic azirine intermediate **173** which then inserts into the adjacent aromatic ring as outlined in Scheme 85.[172,173] Azirines have inherent ring-strain energy, which results in them being highly susceptible to nucleophilic addition. This highly strained system therefore allows for intramolecular nucleophilic addition to occur under reflux in xylene. The ethyl ester of **172** was subsequently hydrolysed under basic conditions to afford the desired 5,6,7-trimethoxyindole-2-carboxylic acid **75**.
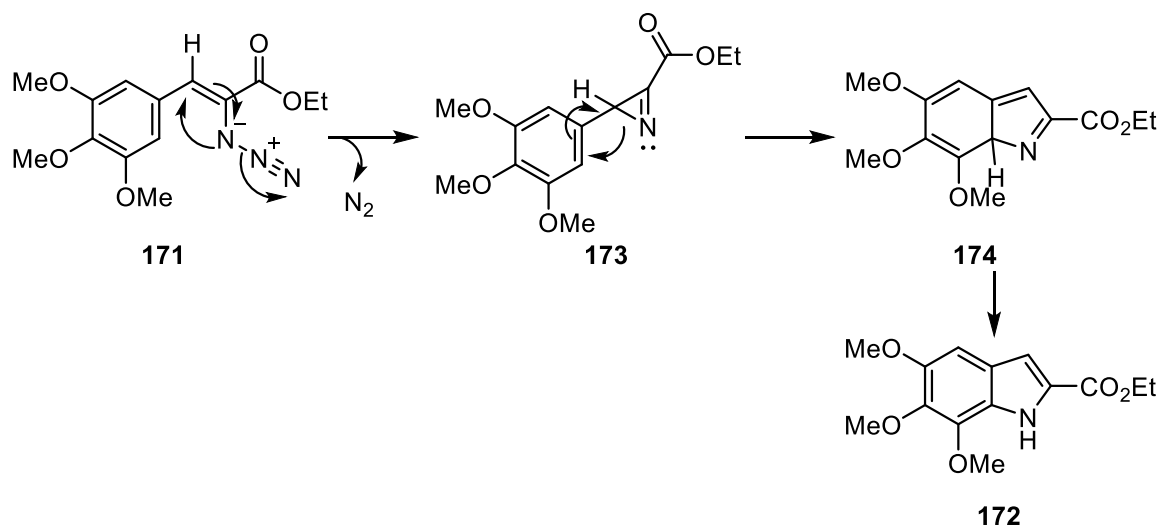
Scheme 85: Proposed Hemetsberger indole cyclisation mechanism of **171**.

3.6.3 Synthesis of ethyl 5-(indole-2-carboxamido)indole-2-carboxylate 80
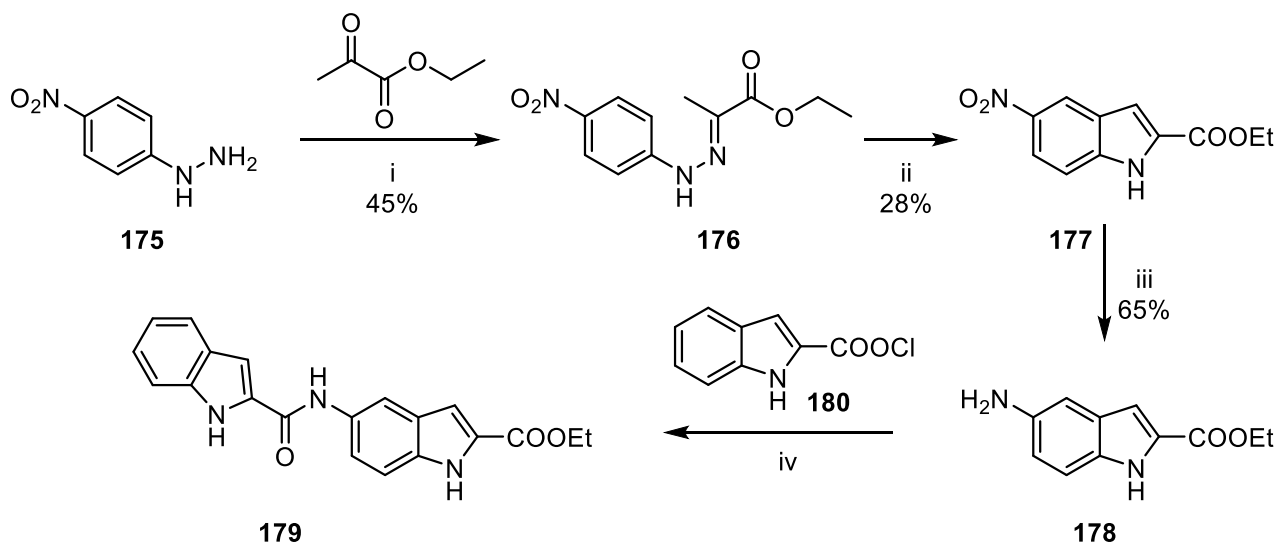
Scheme 86: Synthesis of **80**, *Reagents and conditions*: i. ethyl pyruvate; ii. polyphosphoric acid, xylene; iii. Pd-C, H$_2$; iv. acyl chloride **195**.[174]

Synthesis of **80** began with a Fischer-indole synthesis of nitro-indole **177**, prepared by Prateesh Chauhan. Prateesh Chauhan joined the Threadgill group for three months as part of an Erasmus placement and his research focused on synthesis of the non-alkylating subunits.[174] One-pot synthesis, whereby a reactant is subjected to successive chemical reactions in one reaction vessel in order to improve the efficiency of a chemical reaction, of **177** was attempted as described by Sudhakara *et al.*[175]; however, the reaction yielded only intermediate **176** with the required cyclic sigmatropic rearrangement and subsequent cyclisation failing to take place. Refluxing the phenylhydrazone intermediate **176** in xylene under acidic conditions resulted in formation of **177** in 28% yield. As shown in Scheme 87, the phenylhydrazone tautomerises to enamine **181**. An irreversible cyclic sigmatropic rearrangement then takes place to form diamine **182** which regains aromaticity *via* a 1,3-proton transfer to yield **183**. Cyclisation then occurs to yield **184** followed by β elimination to yield indole **177** with loss of ammonia. PPA is an extremely viscous liquid and as such, this hindered the work-up process, which was hypothesised to be a major factor contributing to the low isolated yield of the reaction. Palladium-catalysed hydrogenation of **177** yielded

amino-indole **178**, which was subsequently coupled with acyl chloride **180** through a nucleophilic addition-elimination mechanism to afford desired compound **179**.
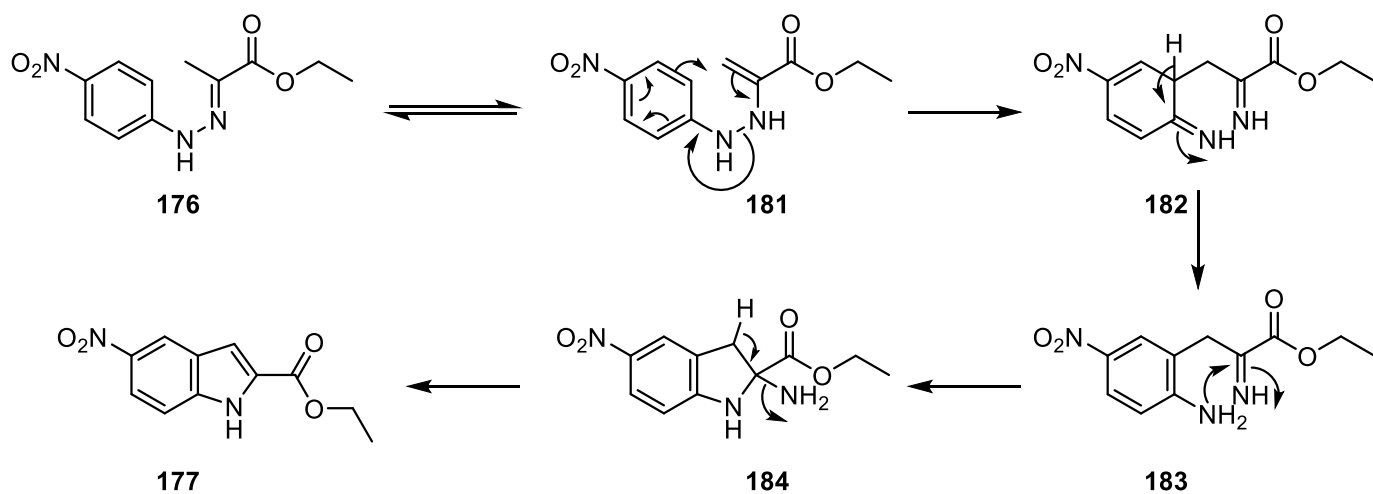
Scheme 87: Mechanism outlining the formation of indole **177** from phenylhydrazone intermediate **176**.

3.7 Synthesis of the molecular clip
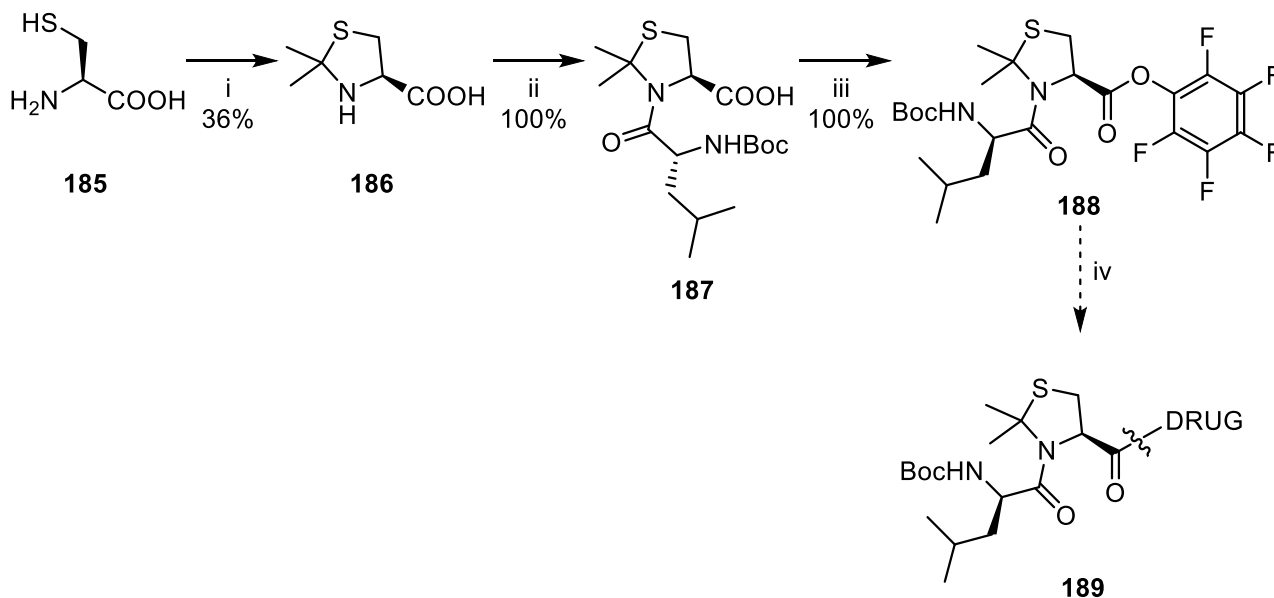
Scheme 88: Overview of the synthetic route toward molecular clip **188** and subsequent coupling to drug to yield **189**. *Reagents*: i. 2,2-dimethoxypropane, acetone; ii. Boc-L-Leu-OPFP, DCC; iii. PFP-OH, DCC; iv. *seco*-amino-CBI, DCC.

Previous work by the Threadgill group has investigated a wide range of molecular clips based on an L-Aaa-*S*-Dmt or L-Aaa-*S*-Dmo motif.[176,177] Suaifan *et al*,.[176,177] have previously shown that synthesis of peptides containing *S*-Dmt is difficult, owing to the rapid cyclisation of L-Aaa-*S*-Dmt amides and esters to form the corresponding diketopiperazines (DKP) as outlined in Scheme 89.[176]
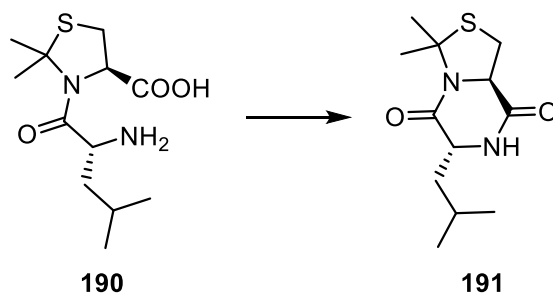
Scheme 89: Intramolecular lactamisation of **190** to yield diketopiperazine **191**.

Previous work has shown that L-Val-*S*-Dmt incorporated into the synthesis of PSA-cleavable peptide Ser-Ser-Lys-Leu-Gln-Val-Dmt, caused PSA to release Gln-Val-Dmt as opposed to desired Val-Dmt.[176] This meant rapid cyclisation to release drug attached to the C- terminal

was not possible. For this reason, L-Leu-*S*-Dmt **190** has been chosen the proposed dipeptide molecular clip because Leu-Dmt has been shown to be essential for cleavage by PSA at the appropriate site. A synthetic strategy to yield protected Boc-L-Leu-*S*-Dmt-PFP **188** has previously been developed as outlined in Scheme 88.[132,177]

3.7.1 Synthesis of *S*-Dmt 186
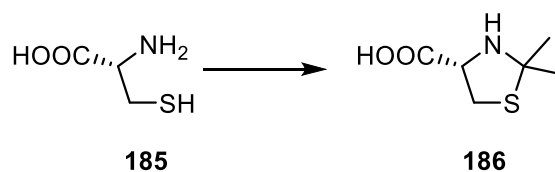
Scheme 90: Synthesis of *S*-Dmt **186**. *Reagents and conditions*: i. 2,2-dimethoxypropane, acetone, reflux, 17 h.

Formation of cyclised *S*-Dmt **186** was achieved by refluxing D-cysteine **185** in 2,2-dimethoxypropane and acetone through an acid-catalysed cyclo-condensation reaction as shown in Scheme 90.

3.7.2 Synthesis of Boc-L-Leu-*S*-Dmt 187
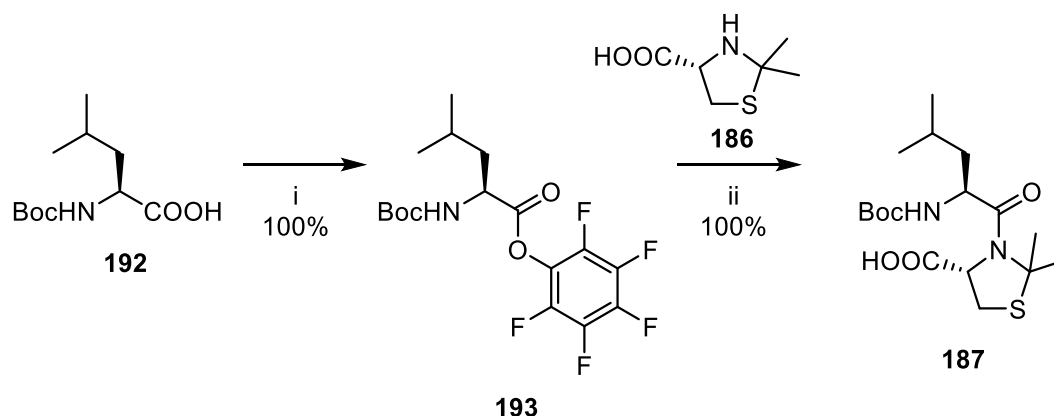
Scheme 91: Synthesis of **187**. *Reagents*: i. PFP-OH, DCC; ii. **186**, DCC.

Following a procedure developed by the Threadgill group,[176,177] activation of carboxylic acid **192** was achieved through formation of the pentafluorophenyl (PFP) ester **193** (Scheme 91). It has previously been shown that conversion of amino acids to their corresponding pentafluorophenyl (PFP) esters yields stable compounds that can be isolated or utilised *in situ* as activated intermediates for the preparation of amides.[178] PFP-esters are highly activated

due to having a highly electron-deficient benzene ring as a result of the five electron-withdrawing fluorine atoms. This highly electron-deficient aromatic system can therefore stabilise the pentafluorophenoxide displaced upon nucleophilic attack of **186** toward **193**. Amide coupling with **186** yielded the desired compound **187** in a quantitative yield.[132,177] Finally, activation of carboxylic acid of **187** was achieved through formation of the PFP ester, ready for coupling to the drug as outlined in Scheme 92.
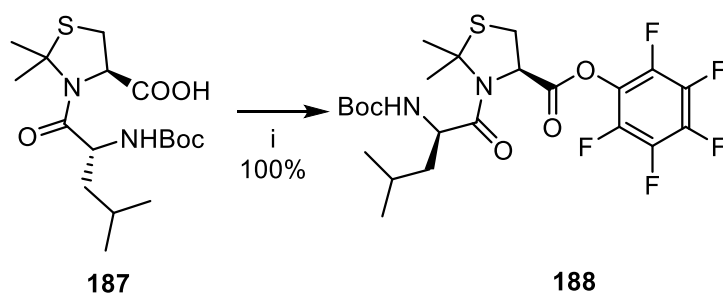
Scheme 92: Synthesis of **203**. *Reagents*: i. PFP-OH, DCC.

3.8 Coupling the alkylating and non-alkylating subunits

With the synthesis of the alkylating subunits **42** and **161** having been achieved, the next step in the synthetic process was coupling the secondary amine of **42** and **161** with the carboxylic acid of the non-alkylating subunits **75-81**. There are several reported ways in the literature to form an amide bond including coupling using carbodiimides,[179] benzotriazole reagents[180] and through acid halides.[181] Previous work by Twum[146] had coupled analogous compounds using diisopropylcarbodiimide in a satisfactory 64% yield. As can be seen in Scheme 93, reaction of carboxylic acid **195** and a carbodiimide such as DCC (**194**) forms activated carbonyl compound **196** that is then susceptible to nucleophilic attack from an amine.
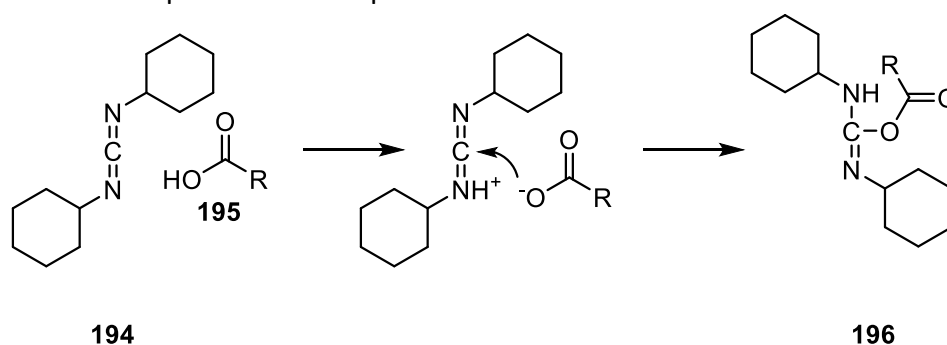
Scheme 93: Mechanism of activation of carboxylic acid **195** with DCC **194**.

3.8.1 Coupling of alkylating subunit 161 and non-alkylating subunits – synthesis of *seco*-nitro-CBI target compounds
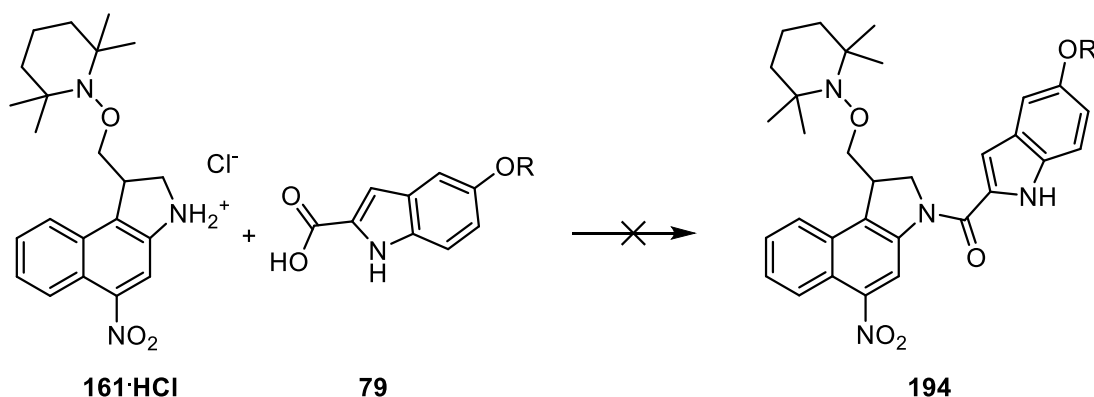
Scheme 94: Attempted coupling of **161·HCl** and **79**. R = $(CH_3)_2NCH_2CH_2$. *Reagents*: i. a) **79**, oxalyl chloride, DMF, CH_2Cl_2, b) **161·HCl**, DIPEA; or i. a) **79**, HOBt, b) **161·HCl**, DIPEA, DCC.

Initial efforts to synthesise **194** *via* the acid chloride of **79** failed, resulting with recovery of starting materials. The use of the coupling agent N,N'-Dicyclohexylcarbodimide (DCC) was tried but this attempt failed, despite initial reaction of **79** with HOBt to produce the activated ester. It was hypothesised that the zwitterionic nature of **79** could be complicating the reaction and so attention was turned to coupling **161·HCl** with trimethoxyindole (TMI) **75**.
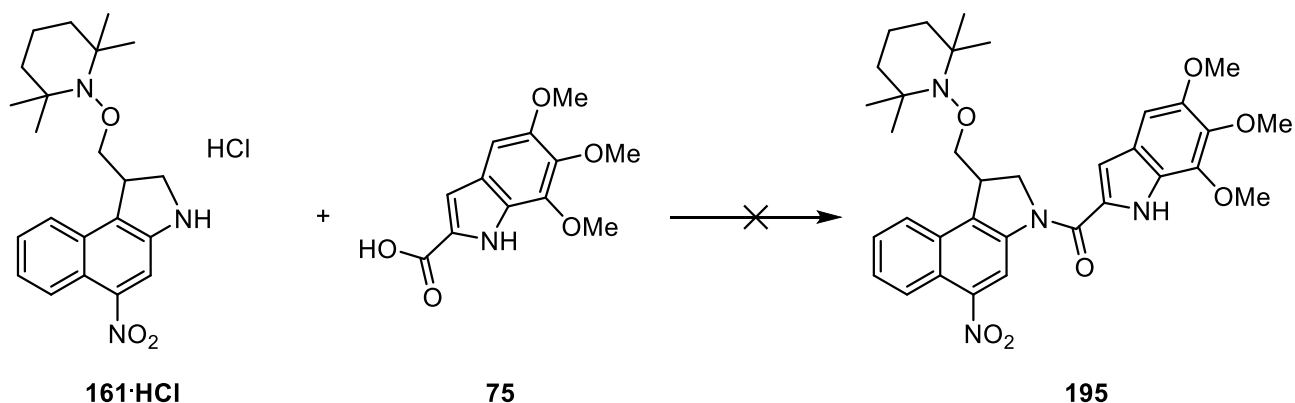
Scheme 95: Attempted coupling of **161·HCl** and TMI **75**. *Reagents*: i. DIC, DIPEA, THF; or DIC, DIPEA, DMF; or EDC·HCl, DIPEA, DMAP DMF; or EDC·HCl, DIPEA, DMAP, THF.

Several attempts were made to couple **161·HCl** with TMI **75** using the carbodiimide procedure. EDC·HCl was used in conjunction with the use of 4-dimethylaminopyridine (DMAP) as a catalyst. DMAP acts as a proton-transfer catalyst, deprotonating the carboxylic acid of **75**

which then performs nucleophilic attack toward EDC·HCl. Unfortunately, no attempt yielded the desired compound **195** and starting material was recovered. As continued failures were depleting stocks of both **161** and TMI **75**, attention turned to attempting to couple **161·HCl** with *meta*-methoxybenzoyl chloride **196** to investigate the coupling step (Scheme 96). However, this reaction failed to yield desired **197** even after extending the reaction time and using an excess of both **196** and NEt₃.
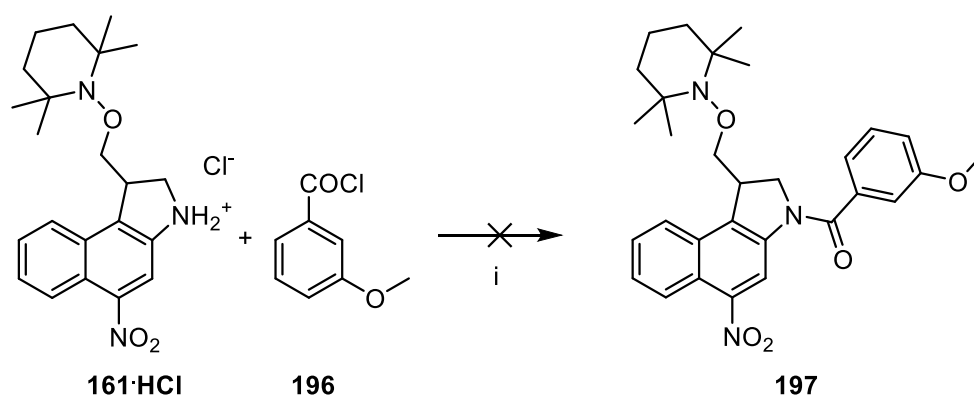
Scheme 96: Attempted coupling of **161·HCl** with *meta*-methoxybenzoyl chloride **196**. *Reagents*: i. NEt₃.

The failure to couple **161** with DMAI **79**, TMI **75** or **196** under a range of different conditions despite literature precedent with analogous compounds was perplexing.[100,129] For coupling to occur, the secondary amine of **161** must perform nucleophilic attack towards the carbonyl of the corresponding non-alkylating subunit. Twum[100] had shown that the presence of a TEMPO group did not hinder coupling and Tercel[129] had shown that presence of a 5-NO₂ did not deactivate the secondary amine enough to hinder its nucleophilicity. At this point, synthesis of chloro **42** meant that focus shifted to coupling **42** with the range of non-alkylating subunits.

3.8.2 Coupling of alkylating subunit 42 and non-alkylating subunits 75-81 – synthesis of *seco*-nitro-CBI target compounds 197-201
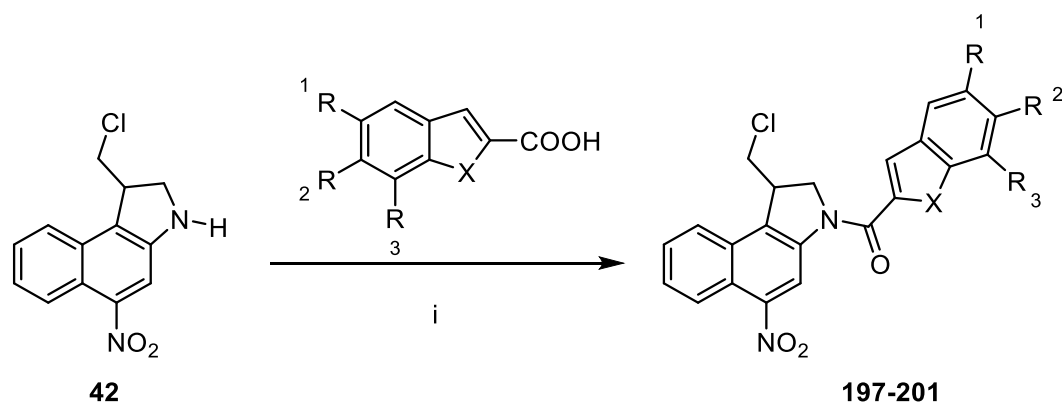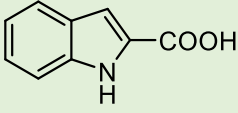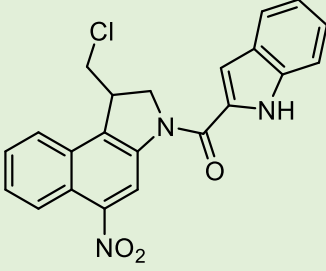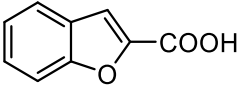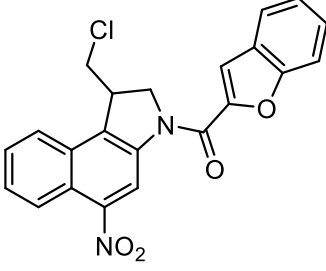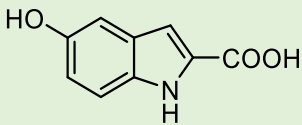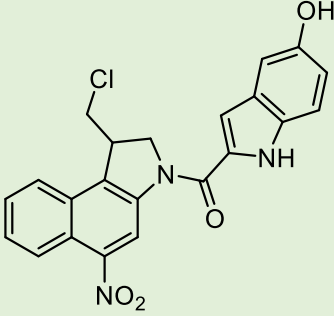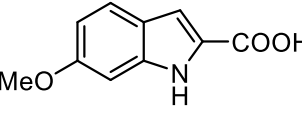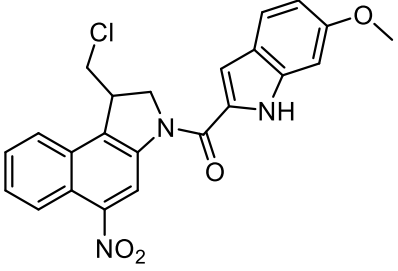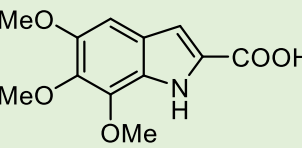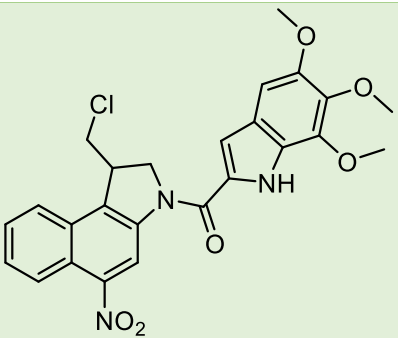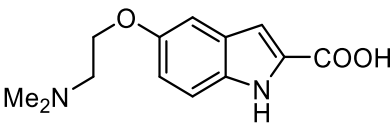
Scheme 97: Synthesis of *seco*-nitro-CBI compounds **197-201**. The X and R groups are summarised in Table 3. *Reagents*: i. EDC·HCl, DMA.

After cyclisation to afford the alkylating subunit **42**, the next step involved amide-coupling **82** to the range of previously described non-alkylating subunits **75-81** (Scheme 97). A carbodiimide approach was followed due to literature precedent in this area.[129]

Table 3 provides an overview of the conditions and yields for each non-alkylating subunit.

Table 3: Outline of coupling conditions and results

Entry	Non-alkylating subunit	Conditions	Product and Yield
1	**78**	EDC·HCl (2.5 Eq), DMA, Rt, 17 h	**197**, 42%
2	**81**	EDC·HCl (2.5 Eq), DMA, Rt, 17 h	**198**, 45%

3	**76**	EDC·HCl (2.5 Eq), DMA, Rt, 17 h	**199**, 75%
4	**77**	EDC·HCl (2.5 Eq), DMA, Rt, 17 h	**200**, 54%
5	**75**	EDC·HCl (2.5 Eq), DMA, Rt, 17 h	**201**, 32%
6	**79**	a. EDC·HCl (2.5 Eq), DMA, Rt, 17 h b. EDC·HCl (2.5 Eq), DMA, TsOH, Rt, 17 h c. EDC·HCl (2.5 Eq), DMA, DIPEA Rt, 17 h	Failed to react Failed to react Failed to react

Compounds **197-201** were all synthesised in satisfactory yields ranging from 32-75% however, reaction of **42** and DMAI **79** failed to occur. The pre-activation of carbodiimide coupling agents such as EDC·HCl relies on protonation of the carbodiimide by the carboxylic acid. The unhindered basic amino group present in **79** will be preferentially protonated compared to the carbodiimide and hence may interfere with this pre-activation step. To attempt to counteract this, coupling was attempted in the presence of TsOH, following a procedure by Tercel[129] however, in all cases, only starting material was recovered.

In evaluating amide bond formation there are two factors to investigate; the nucleophilicity of the amine and the electrophilicity of the carbonyl carbon. As the alkylating subunit **42** was the same for all the above reactions, the main factor that should determine amide-coupling is therefore the electrophilicity of the carbonyl carbon on the non-alkylating subunit. Formation of TMI *seco*-nitro-CBI **201** occurred in a disappointing 32% yield. One would expect this reaction to be the lowest yielding as TMI **75** is the most electron-rich subunit in the series, with three electron-donating methoxy groups leading to reduced carbonyl reactivity as shown in Scheme 98.
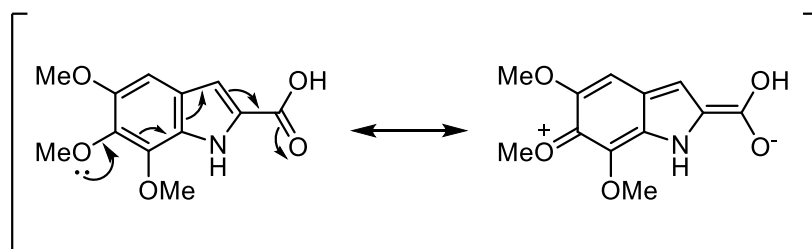
Scheme 98: Resonance effects exhibited by TMI **75** resulting in deactivation of the carbonyl toward nucleophilic attack.

6-OMe **77** exhibits similar resonance effects to TMI **75** and so this accounts for the low yield of 54%. In the case of 5-OH **76**, resonance to deactivate the carbonyl is not possible and therefore the 5-OH acts as an inductively electron withdrawing group, activating the carbonyl toward nucleophilic attack hence why this reaction is highest yielding. One would expect indole **78** and benzofuran **81** to have an isolated yield for the corresponding amide bonds that is lower than that of reaction with 5-OH **76** and greater than that of TMI **75** due to an absence of either electron withdrawing or donating groups. This was observed, with yields of 42% and 45% respectively.

3.8.3 Reduction of *seco*-nitro-CBI compounds 197-201 to yield *seco*-amino-CBIs 202-206
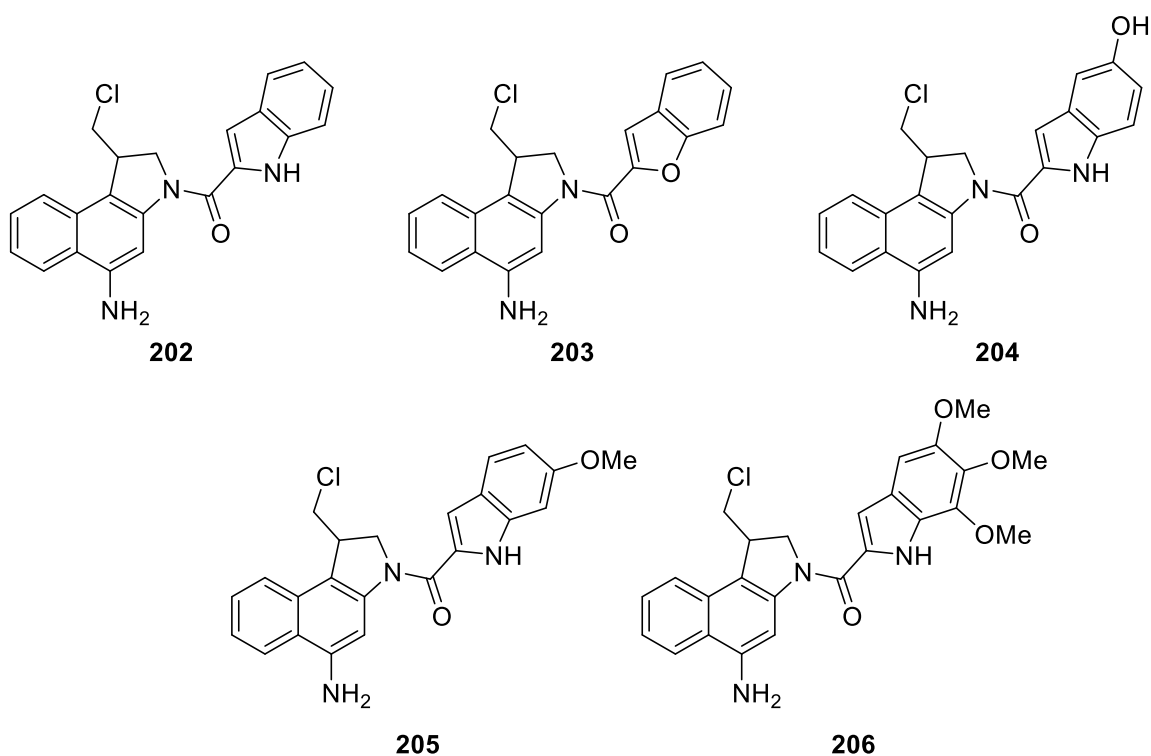
Scheme 99: Structures of the *seco*-amino-CBI compounds **202-206**.

With the synthesis of five *seco*-nitro-CBIs (**197-201**) completed, the final step in the synthesis toward *seco*-amino-CBIs **202-206** (Scheme 99) involved reduction of the 5-NO_2 group to yield the corresponding amino compounds. As reduction would potentially yield the free amine, there was the possibility that rapid Winstein cyclisation would occur post-reduction to yield the active amino-CBI compounds. After reduction, the compounds would also be evaluated biologically, carried out by Dr Amit Nathubhai, a Post-doctoral researcher in the Threadgill group, and so it was important to ensure that any residual metals from the reduction process were removed, so as not to interfere with the biological assay results.

3.8.3.1 NMR monitored SnCl₂ Reduction of the *seco*-nitro-CBIs 197-201

Due to the expected extreme cytotoxicity of these compounds, Reduction of each of the *seco*-nitro-CBI compounds **197-201** was carried out in $(CD_3)_2SO$ using $SnCl_2$ as the reducing agent. The reduction was monitored by ^1H NMR at regular time intervals to determine the relative rates of nitro reduction and to assess if Winstein cyclisation occurred immediately post-reduction. By carrying out a proton NMR experiment at regular time intervals, it is possible to determine the rate of a reaction through analysis of integral value of a peak corresponding to a proton in the starting material versus the integral value of a peak corresponding to a proton in the product. As can be seen from Figure 39, The indole NH peak of **200** decreases at the same rate as the indole NH peak of **205** appears. Furthermore, NMR analysis revealed that reduction to the amino compound **205** was not followed immediately by a Winstein cyclisation. One reason for this may be that because the compound was not isolated from the reaction mixture, the primary amine was complexed to the Lewis-acidic tin.
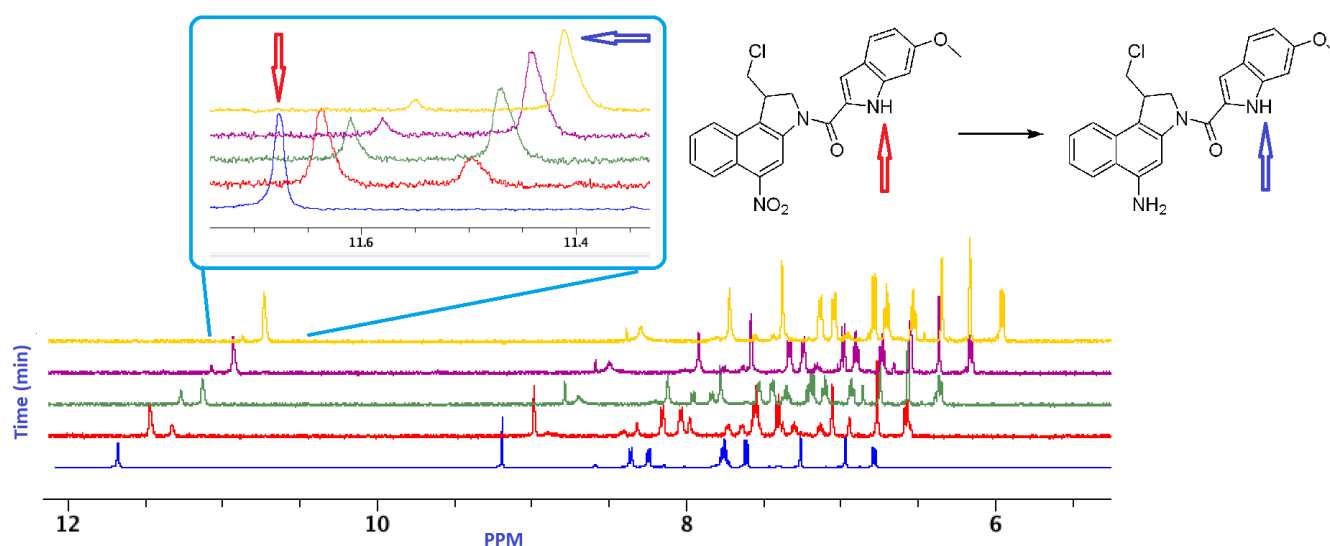
Figure 39: NMR timed experiment stacked spectra for the reduction of **200** focusing on the indole N-H peak. As time progresses, one can see the indole NH of **200** disappear and the indole NH of **205** appear.

Through knowing the time elapsed between each spectrum, one can calculate the rate of reaction through the following equation:

Equation 2:

$$Rate\ of\ reaction = k\ [A]$$

It can be assumed that the reaction proceeds in a pseudo first order fashion with respect to [A] as a large excess of $SnCl_2 \cdot 2H_2O$ was used. One can calculate k through plotting a graph of ln[A] vs time t where the gradient of the line will be equal to -k. Alternatively, as the relative concentrations of starting material A and product B will be determined through NMR integral values, one can calculate k through plotting a graph of ln[B] vs time t where the gradient will be equal to k. Table 4 summarises the determined rates of reaction for each compound **197-201**.

Table 4: Experimentally determined k values for the $SnCl_2$ reduction of *seco*-nitro-CBIs **197-201**.

Entry	Starting Material	k / s^{-1}	Relative rate of reaction
1	Indole-197	0.0321	2.6
2	Benzofuran-198	0.0124	1
3	5-OH-199	0.0147	1.2
4	6-OMe-200	0.0529	4.3
5	TMI-201	0.0152	1.2

To evaluate levels of hypoxia-activation of prodrugs, hypoxic cytotoxicity ratio (HCR) may be calculated.[182,183] The HCR is the ratio of drug concentrations under normoxic and hypoxic condition to produce the same cell kill.[182] As in the case of hypoxia-activated prodrugs the aim is to minimise cytotoxicity under normoxic conditions, a larger HCR equates to a more selective prodrug toward hypoxic cells. Using the data shown in Table 4, it was proposed that one could have a crude indication as to the relative rates of bio-reduction in normoxic and hypoxic tissue. *Seco*-nitro-CBI **200** (6-OMe) exhibited the fastest relative rate of reduction, indicating that reduction occurs most readily out of compounds **197-201**. From the data in

Table 4, one would therefore hypothesise that **200** (6-OMe) would exhibit the lowest HCR whilst benzofuran **198** would exhibit the greatest HCR.

3.8.3.2 Reduction of *seco*-nitro-CBIs immediately prior to biological testing
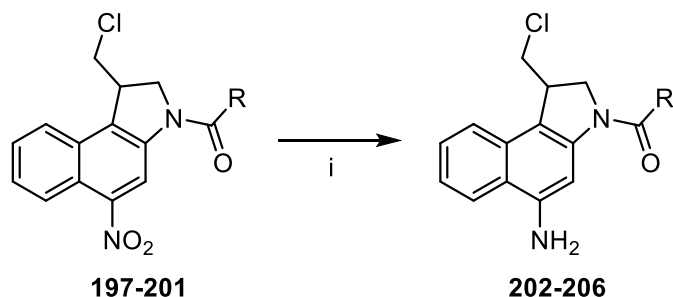
Scheme 100: Reduction of the *seco*-nitro-CBIs **197-201**. R = non-alkylating subunit. *Reagents*: i. Pd-C, H$_2$, CD$_3$OD.

Reduction had been shown to occur readily with SnCl$_2$ however, removal of residual tin post-reduction is not facile. Due to the expected cytotoxicity of the *seco*-amino-CBI compounds **202**-**206**, a method for reduction was required that would have a facile work-up to remove the reducing agent. Palladium on carbon was chosen as the reducing agent as reports in the literature have shown that >99.1% of residual palladium can be effectively removed by filtering through celite®.[184] In the pharmaceutical industry, there is a regulatory standard requiring less than 5–10 ppm of residual palladium in any active pharmaceutical ingredient (API).[185] Additionally, reduction of compounds **197-201** were carried out deuterated methanol-d4. This allowed for the reaction to be carried out, the resulting reaction mixture filtered through celite® to remove palladium followed by MgSO$_4$ to remove water and then analysed directly by NMR. This was done to increase safety when handling **202**-**206**. The concentrated samples of **202**-**206** were then assessed biologically through DNA-melting assays and MTS assays.

4.0 Biological Evaluation

With synthesis of a range of both *seco*-nitro-CBIs **197-201** and *seco*-amino-CBIs **202-206** complete, the next stage involved biological evaluation. In order to evaluate the efficacy of both the *seco*-nitro-CBIs **197-201** and *seco*-amino-CBIs **202-206**, a combination of calf-thymus DNA melting assays and MTS assays were carried out. Calf-thymus DNA melting assays would provide insight into the structure-activity relationships of the various minor-groove binding subunits. Comparison of the *seco*-nitro-CBI compounds **197-201** with the *seco*-amino-CBIs would also provide insight into the suitability of *seco*-nitro-CBIs as hypoxia-activated prodrugs as if **197-201** were found to be similarly biologically active toward calf-thymus DNA, then that would be indicative of a decrease in selectivity between hypoxic and normoxic cells. MTS assays would further evaluate the structure-activity relationship surrounding the minor-groove binding subunit in addition to validating the selectivity of *seco*-nitro-CBIs toward hypoxic cells through carrying out MTS assays under both normoxic and hypoxic conditions.

4.1 Calf-thymus DNA melting assay

Calf-thymus DNA melting assays were carried out in collaboration with fourth year undergraduate MPharm project students Aarash Ahmadi, Catia Alexandre, Rachel Lee and Khalid Seyed. Calf-thymus DNA melting assay is a useful tool in determining the strength of binding of drugs to DNA by observing changes in the temperature at which dsDNA denatures. Heating DNA causes it to denature as the duplex structure unwinds and unzips, the result of hydrogen bonds between DNA bases breaking and bases becoming unstacked. The transition-melting temperature (T_m) is the temperature at which 50% of DNA is denatured, shown in Figure 40. Changes in T_m as a result of drug-DNA interactions can provide insight into the mode of action of the drug in question. Agents such as doxorubicin increase the T_m by stabilising the DNA double helix. The extent as to which the T_m is altered (either through an increase or decrease) provides a way to correlate the strength of interaction between drugs and DNA. Small increases (around 2°C) in the T_m indicate non-covalent interactions between the drug and DNA whereas larger increases (around 8°C) indicate covalent interactions.
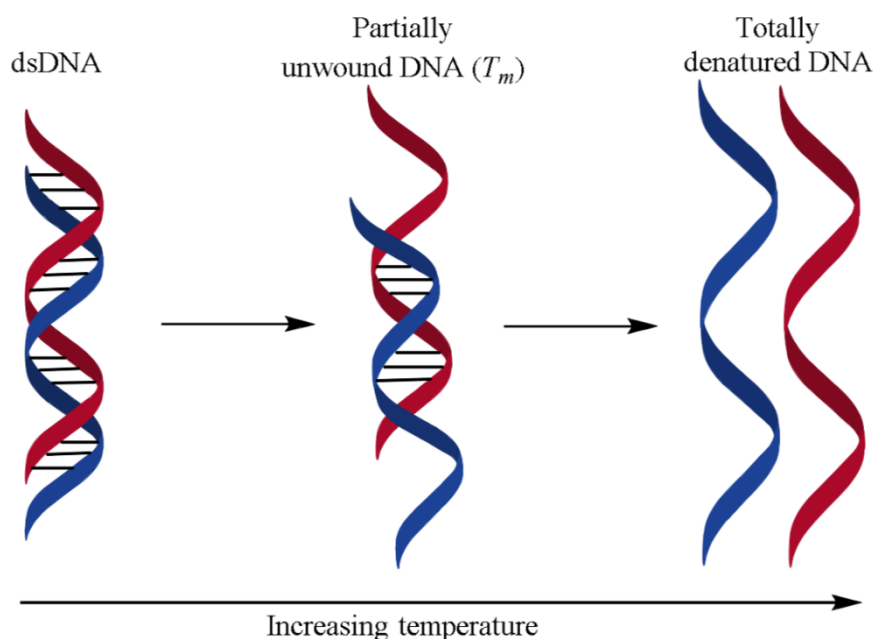
Figure 40: Overview of dsDNA denaturation process.

4.1.1 Calf-thymus DNA melting assay procedure

Melting temperature measurements using calf-thymus DNA were obtained for both the nitro-CBI and amino-CBI compounds. For each compound, calf-thymus DNA was treated with a range of concentrations (between 0.1 and 0.4 MEq) and allowed to incubate for 1 h at 40°C. The amount of drug required per molar equivalent to dsDNA was calculated using the following equation:

Equation 3

Volume of sample = Molar concentration of diluted DNA × Volume of diluted DNA × MW of drug sample × Molar equivalent required

The drug-DNA mixtures were heated at a rate of 1°C/minute and absorbance values (256 nm) obtained at deg C intervals between 60-90°C. For each compound, normalised absorbance was plotted *vs* temperature for each drug concentration measured. Normalised absorbance was calculated to provide a range between 0 and 1 using the following equation:

$$Normalised\ Abs = (Abs_n - Abs_{min.})\ /\ (Abs_{max} - Abs_{min})$$

4.1.2 DNA melting comparison between *seco*-nitro-CBI 197 and *seco*-amino-CBI 202

Plotting a graph of normalised absorbance against temperature gives a sigmoidal curve. As can be seen in Figure 41, the rightward shifts of the sigmoidal curves on increasing the concentration of **197** and **202** respectively shows an increasing T_m. This confirms that both *seco*-nitro-CBI **197** and *seco*-amino-CBI **202** bind to double-stranded DNA and that the effect of this binding is to stabilise the dsDNA as a greater temperature is required to melt the dsDNA. Initially at low temperatures the absorbance rises slowly as the majority of DNA is in the duplex form and so is tightly held together through hydrogen bonding between base pairs. The sudden rise in absorbance then signifies the melting of dsDNA into single strands. Once all the dsDNA has melted, the absorbance becomes constant. The midway point of the sigmoidal curve represents T_m which can be more easily visualised through plotting a graph of the first derivative curves of the normalised absorbance curves.
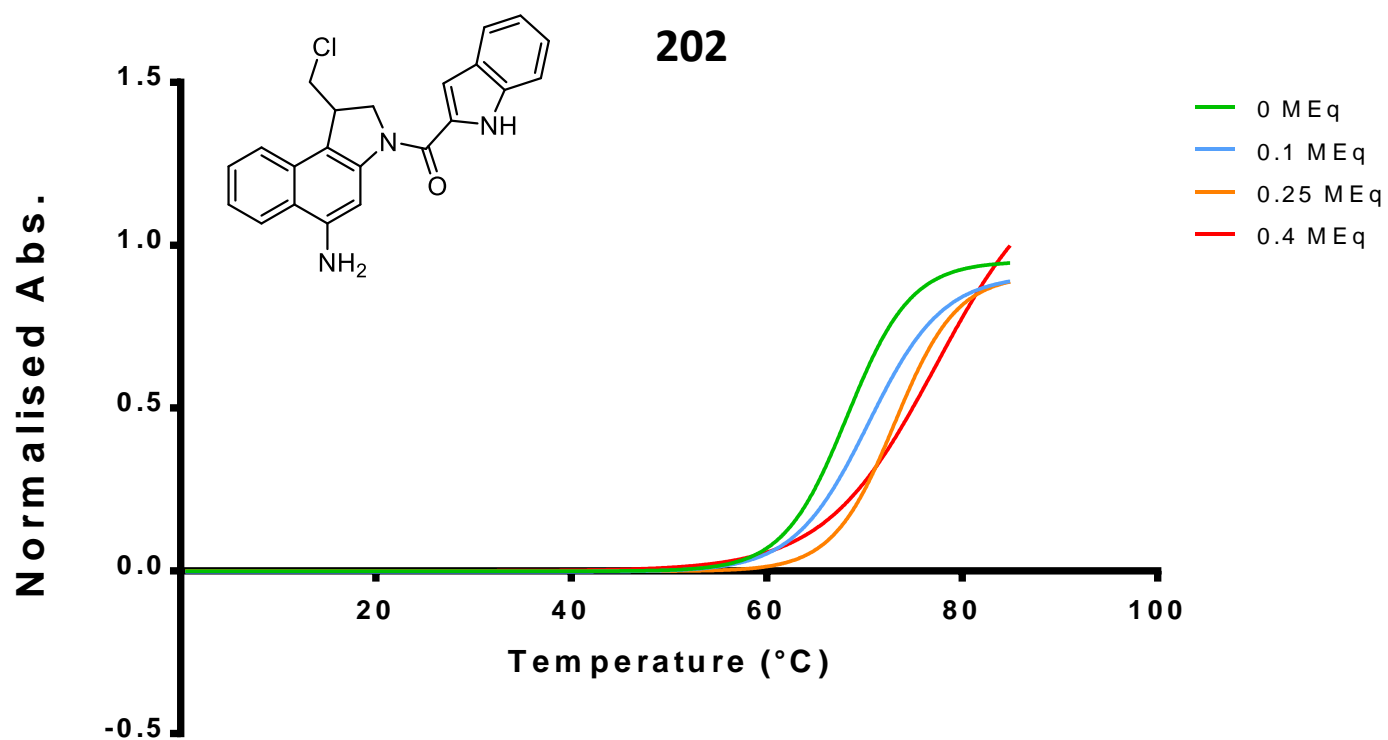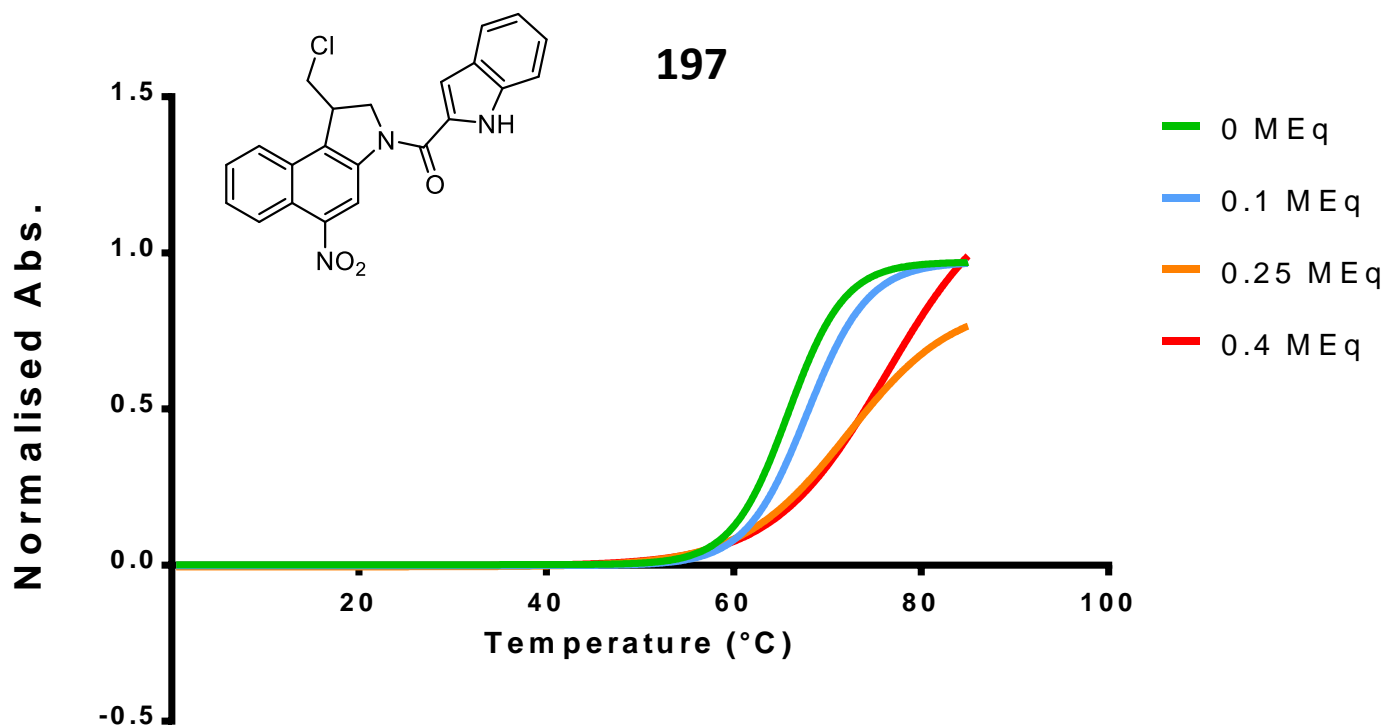
Figure 41: Normalised melting curves for **197** (top) and **202** (bottom) at different molar equivalents. As the concentration of drug is increased, the T_m increases.

The first derivative of the melting curves shown in Figure 41 was obtained by plotting the change in absorbance / change in temperature against temperature (Figure 42). This gives a bell-shaped curve, the peak (midpoint) of it being the T_m for the concentration of drug. There is a general increase (rightward shift) of the peak of the curves which corresponds to an increase in T_m with concentration. At 0.25 MEq, *seco*-nitro-CBI **197** increased the T_m by 0.6^{o}C whereas *seco*-amino-CBI **202** increased the T_m by 4.8^{o}C at the same concentration. This is to be expected as *seco*-nitro-CBI **197** is unable to undergo Winstein cyclisation and therefore can only bind to the dsDNA minor-groove non-covalently through interactions with the non-alkylating subunit. *Seco*-amino-CBI **202** is able to undergo Winstein cyclisation and hence the resulting amino-CBI is able to covalently bind to the dsDNA, stabilising it and much more than just non-covalent binding interactions alone. Therefore, the T_m is much greater with treatment of **202** compared to **197**.
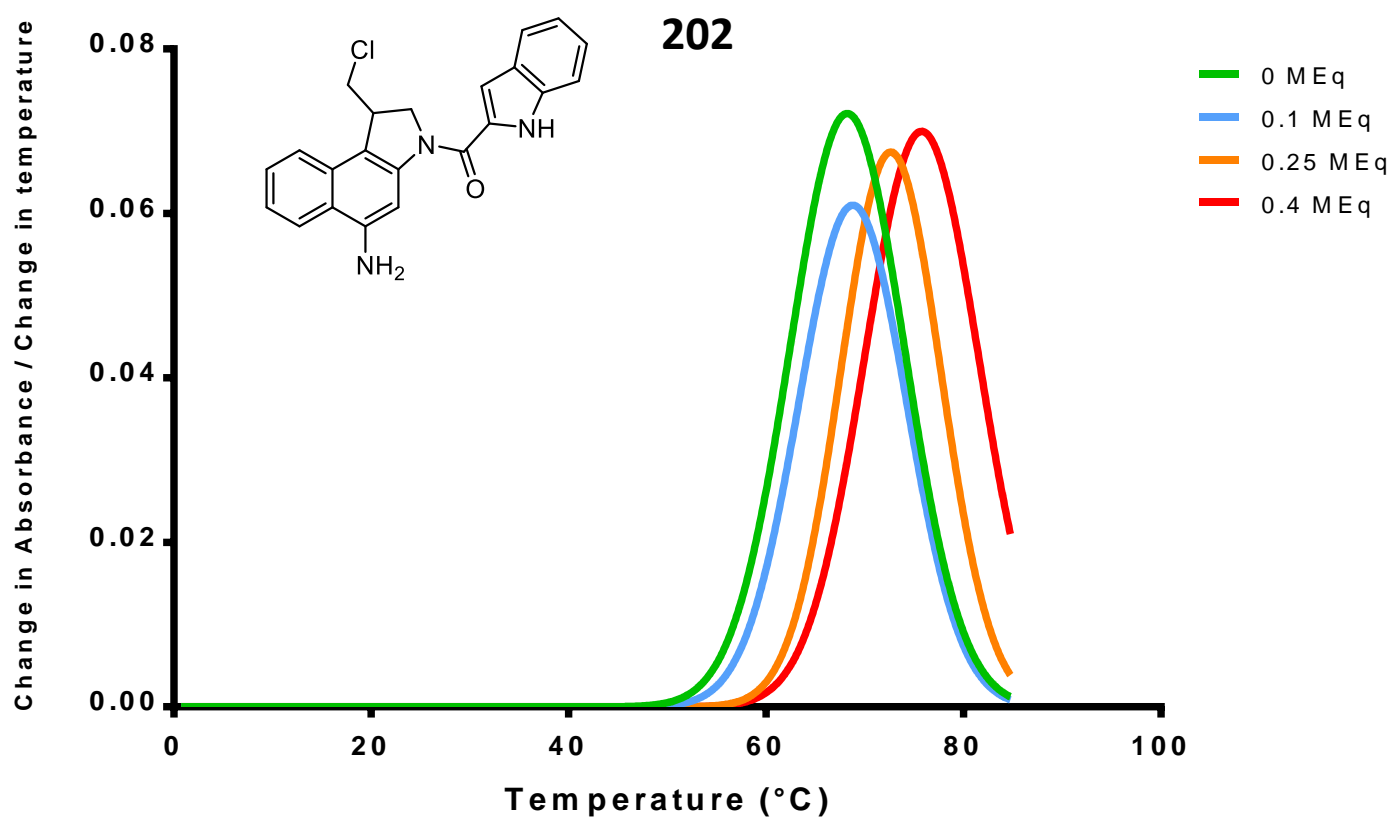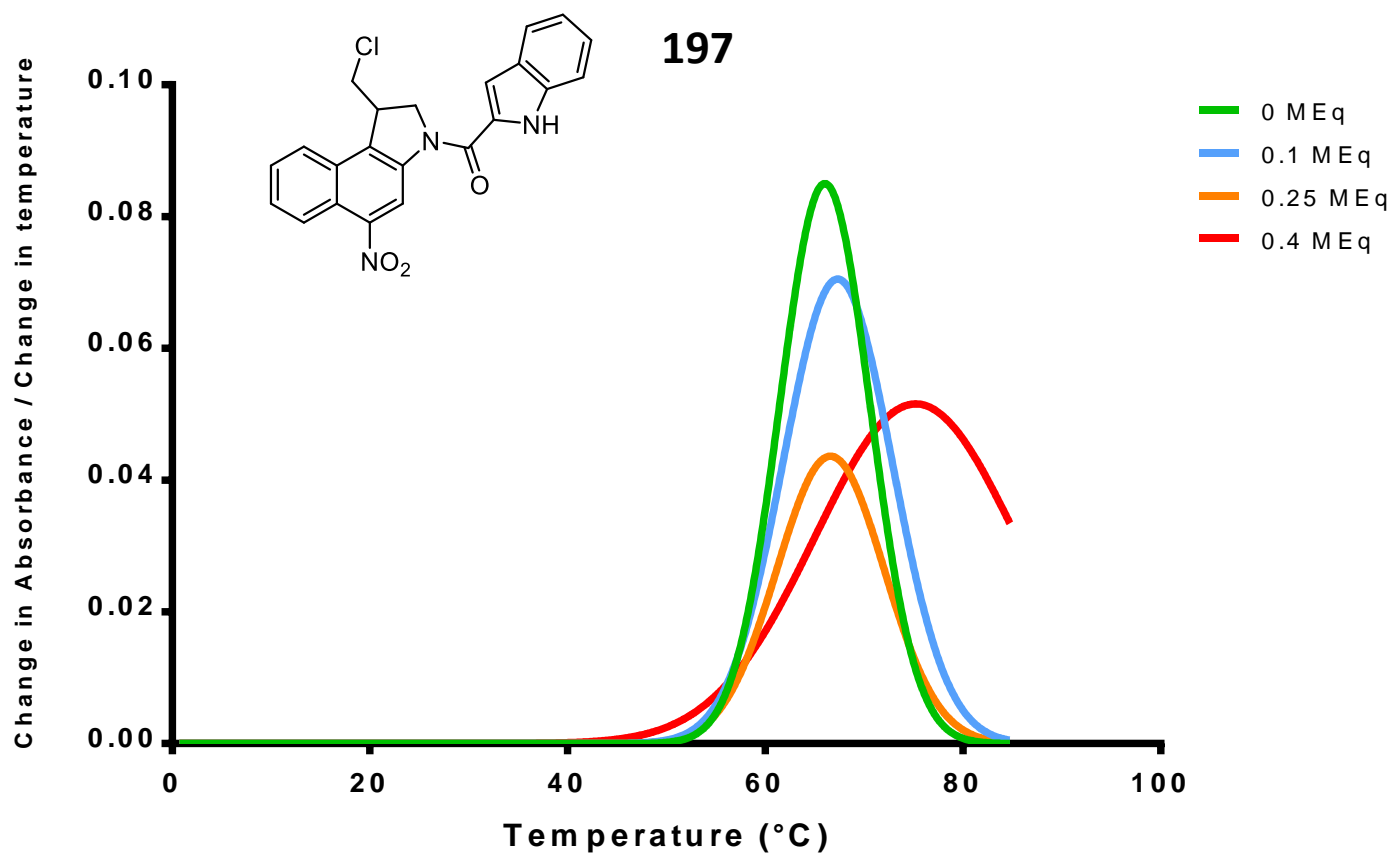
Figure 42: First derivative melting curves for **197** (top) and **202** (bottom) at varying molar equivalents (MEq).

4.1.3 DNA melting comparison between *seco*-nitro-CBIs 197-200 and *seco*-amino-CBIs 202, 203 and 205

The analysis described in 4.1.2 was carried out on *seco*-nitro-CBI compounds **197**-**200** and *seco*-amino-CBI compounds **202**, **203** and **205**. The results have been summarised in Table 5 to show the Δ *Tm* values obtained at two different concentrations. At a concentration as low as 0.1 MEq, a significant difference can be observed between the *seco*-nitro-CBIs and *seco*-amino-CBIs. As expected, the *seco*-nitro-CBIs have much lower *Tm* values, ranging from 0.2-2.5˚C. These results show that the *seco*-nitro-CBIs are not capable of covalently binding to the DNA and can only bind through non-covalent interactions. On the other hand, the *seco*-amino-CBIs have greater Δ *Tm* values ranging from 1.6-5.5˚C at 0.1 MEq and 4.8-14.6˚C at 0.25 MEq. These results show that the *seco*-amino-CBIs are capable of covalently binding to the DNA. Previous work by Twum[146] reported a Δ *Tm* of 13.0˚C at a drug concentration of 0.6 MEq for the analogous *seco*-amino-CBI **207**.

207
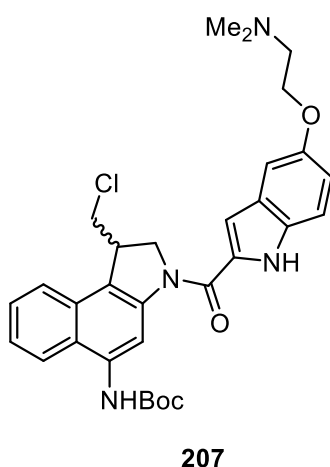
Figure 43: Structure of **207**.

Compound **203** shows a Δ *Tm* of 14.6˚C at just 0.25 MEq showing that **203** binds more strongly to DNA than **207** and at a lower concentration. The pharmacological effect of the CBI drug is brought about by its ability to stabilise DNA. The stabilised DNA will then be unable to be transcribed and translated and hence several cellular processes will be inhibited, leading to cell death. A control containing $SnCl_2$ was tested to ensure that residual tin by-products from the reduction of the *seco*-nitro-CBIs to their *seco*-amino-CBIs did not interfere with the assay. As can be seen in Table 5, no increase in *Tm* was observed at 0.25 MEq of $SnCl_2$.

Table 5: Δ Tm values obtained for *seco*-amino-CBIs **197**-**200** and *seco*-nitro-CBIs **202**,**203** and **205**.

Concentration (MEq)	*Seco*-nitro-CBIs Δ T_m (˚C)				*Seco*-amino-CBIs Δ T_m (˚C)			Control Δ T_m (˚C)
	197 Indole	**200** 6-OMe	**199** 5-OH	**198** benzofuran	**202** indole	**205** 6-OMe	**203** benzofuran	SnCl$_2$
0.1	0.2	1.0	2.5	-	1.6	5.1	2.4	-
0.25	0.6	1.9	2.3	2.4	4.8	12.1	14.6	0

The data from Table 5 also provides an insight into the SAR of the various minor-groove binding subunits. With regard to the *seco*-nitro-CBIs, 5-hydroxy-**199** binds much more strongly to DNA at lower concentrations compared to indole-**197** and 6-methoxy-**200**. This is in agreement with the reports in the literature that a group at the 5-position results in greater activity of drug as previously discussed.[186] With regard to the *seco*-amino-CBI **203**, it is clear that a benzofuran group is well tolerated in place of the indole group of the non-alkylating subunit and in fact binds much more strongly to DNA at higher concentrations of drug. At 0.25 MEq, there was a large difference between indole-**202** and 6-methoxy-**205** with Δ T_m values of 4.8˚C and 12.1˚C respectively. This result goes against the work by Boger *et al*,.[186] that methoxy substituents in the 6-position contribute little or nothing to its properties as a non-alkylating subunit. Even at 0.1 MEq, there was a significant difference between the Δ T_m values for **202** and **205** of 3˚C. It is important to note that the DNA-melting studies reported here are preliminary results and will be further scrutinised in comparison with the MTS-assay data reported in section 4.2.

4.2 Cell viability assay

A microculture tetrazolium colorimetric assay was identified as a viable way to obtain preliminary data as to the SAR surrounding the different minor-groove binding subunits as well as to compare the efficacy of nitro-*seco*-CBIs compared to amino-*seco*-CBIs. In this category there are three main assays, namely the MTT, XTT and MTS assays. These are all chromogenic assays to test cell viability. All three assays are based upon the bio-reduction of a tetrazolium salt **208** to an intensely coloured formazan **209** by living cells, as outlined in Scheme 101.[187]

<center>**208**   **209**</center>
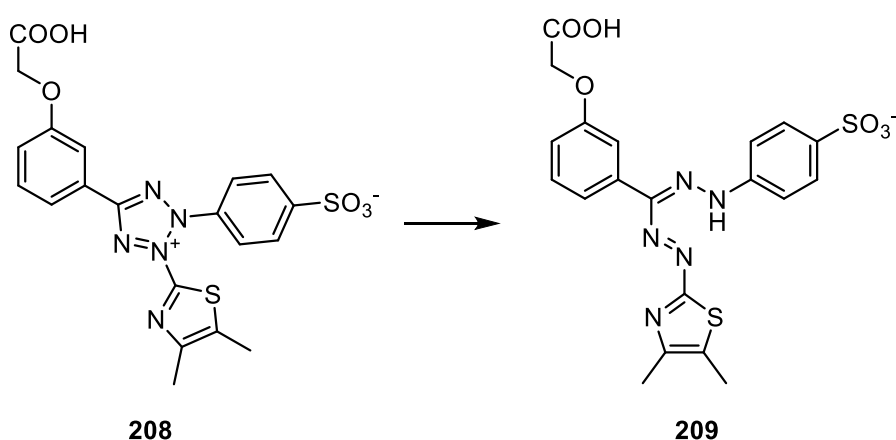
Scheme 101: Structures of MTS tetrazolium **208** and its formazan product **209**.

MTS and XTT assays have the advantage that they produce a water-soluble formazan, bypassing the need for an error-prone solubilisation step required in the MTT assay. Bioreduction of XTT and MTS requires the addition of phenazine methosulfate (PMS). Previous studies have indicated that, unlike MTS, XTT produces an unstable XTT / PMS reagent mixture that can result in poor within-assay precision and assay drift.[187] For the reasons stated, the MTS assay was therefore chosen as the tool to investigate *seco*-nitro-CBIs **197-201** and *seco*-amino-CBIs **202-206**. The amount of formazan **209** produced, and therefore the colour intensity, is directly proportional to the number of viable cells and can be measured at 490 nm.[188,189] Cytotoxic agents cause reduction in the number of viable cells and therefore result in the lowering of formazan levels. This effect should be proportional to the concentration of the cytotoxic agent.

4.2.1 MTS assay procedure

The inhibitory effect of *seco*-nitro-CBIs **197-201** and *seco*-amino-CBIs **202-206** on prostate cancer cell lines was investigated using PC3 cells. PC3 cells are a non-PSA producing human prostate-cancer cell line and are androgen sensitive. A range of concentrations from 0.1 μM to 500 μM was added to PC3 cells in a 96-well plate. Incubation at 37°C in a humidified atmosphere containing 5% CO_2 (v/v) was carried out for 3 d. The number of viable cells was quantified using the MTS reagent and measuring the absorbance of the produced formazan at 490 nm. In reference to the control cell number, the results were expressed as percentage inhibition against the concentration of each compound **197-201**, and **202**-**206**. In addition, the *seco*-nitro-CBIs **197-201** were investigated in a second MTS assay following the same procedure as above but under hypoxic conditions, achieved through incubation of the plates in a hypoxic chamber (< 20 ppm O_2) for four hours. This allowed investigation into hypoxia-induced reduction of the 5-NO_2 group *in-situ* to yield the corresponding amino-CBI.

4.2.3 MTS assay data of the *seco*-amino-CBI compounds 202-206
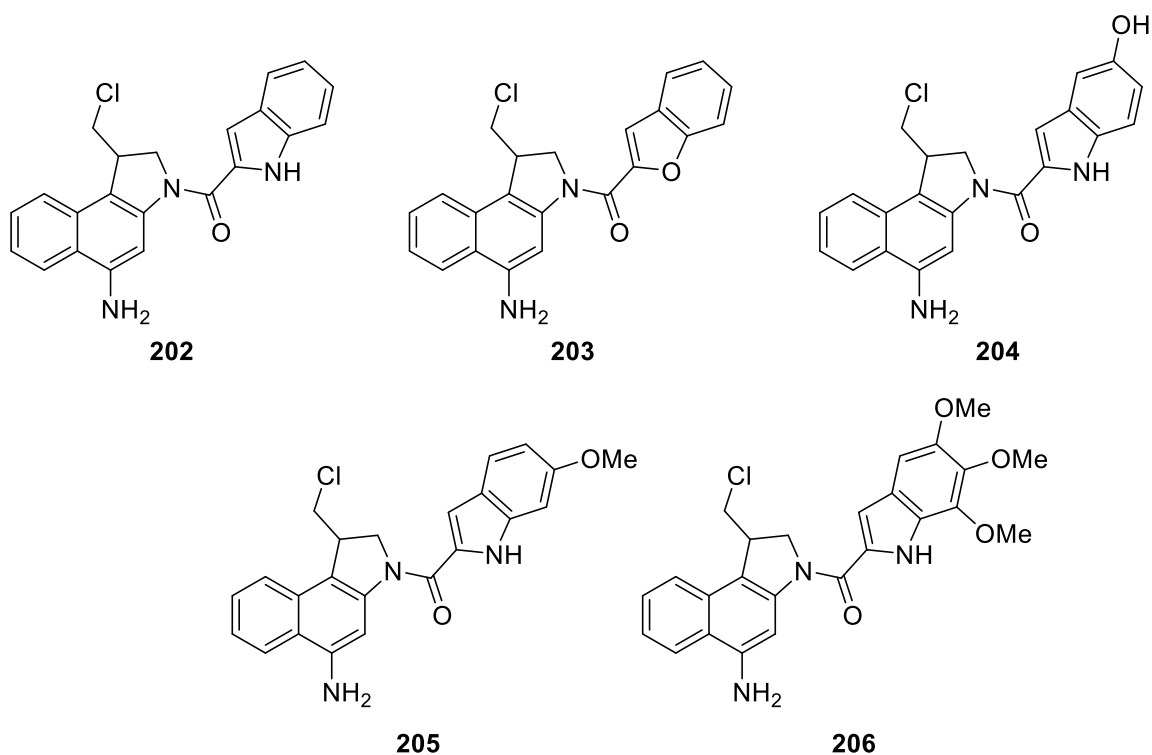
Figure 44: Structures of the *seco*-amino-CBIs **202**-**206**.

Table 6: IC$_{50}$ values for compounds **202-206** against PC3 cells. Comparison IC$_{50}$ values for compound **207** against LnCAP cells* and **9** against L1210 cells**.

Entry	Compound Number	IC$_{50}$ (nM)
1	202	78.9
2	203	13.3
3	204	1.40
4	205	100.0
5	206	2.30
6	207	18*[100]
7	Duocarmycin SA 9	0.01**[190]

The range of *seco*-amino-CBIs **202-206** all showed excellent inhibition of PC3 cells with IC_{50} values ranging from 1.4 to 100 nM as shown in Table 6. It is important to note that these MTS assays have n = 1 and so further investigations are therefore required to verify any preliminary trends identified. *Seco*-amino-CBI **204** showed exquisite cytotoxicity with an IC_{50} of 1.40 nM against PC3 cells. This compound is more than 10-fold more cytotoxic than the *seco*-amino-CBI **207**, with an IC_{50} of 18 nM against LNCaP cells, developed previously by the Threadgill group.[100] Known compound **206** with a trimethoxyindole subunit showed similar potency with an IC_{50} of 2.3 nM. Tercel *et al*.[129] have previously reported that **206** has an IC_{50} of 1.3 nM against the Skov3 cell line. The low IC_{50} of 5-OH **204** is particularly interesting as previous work surrounding structure-activity relationships of minor-groove binding subunits has indicated that the binding affinity of the minor-groove subunits is derived principally from hydrophobic binding and stabilising Van der Waal contacts.[191] Previous work by Boger *et al*.[192] identified the importance of an indole-C5-OCH_3 group, showing that it is deeply embedded in the minor-groove of DNA, providing strong non-covalent binding stabilisation. Furthermore, Boger *et al*.[192] found little difference in activity between the trimethoxy subunit and the mono-methoxy compound. The results reported here indicate that a hydroxy group at the indole-C5 position (**204**) provides strong non-covalent binding stabilisation similar to that of an indole-5-OCH_3. The importance of an indole-C5 substituent can further be observed in the case of indole-6-OCH_3 **205** and indole **202** with IC_{50} values of 100 nM and 78.9 nM respectively. It is clear that a lack of an indole-C-5 substituent in an indole-based minor-groove binding subunit is deleterious to cytotoxicity, most likely through decreased non-covalent binding stabilisation. Benzofuran compound **203** showed a roughly 10-fold increase in cytotoxicity compared to indole **202** with IC_{50} values of 13.3 nM and 100 nM respectively. This observation is attributed to substituting a hydrogen-donating NH for a hydrogen accepting O.

4.2.2 Hypoxic and normoxic MTS assay data of the *seco*-nitro-CBI compounds 197-201
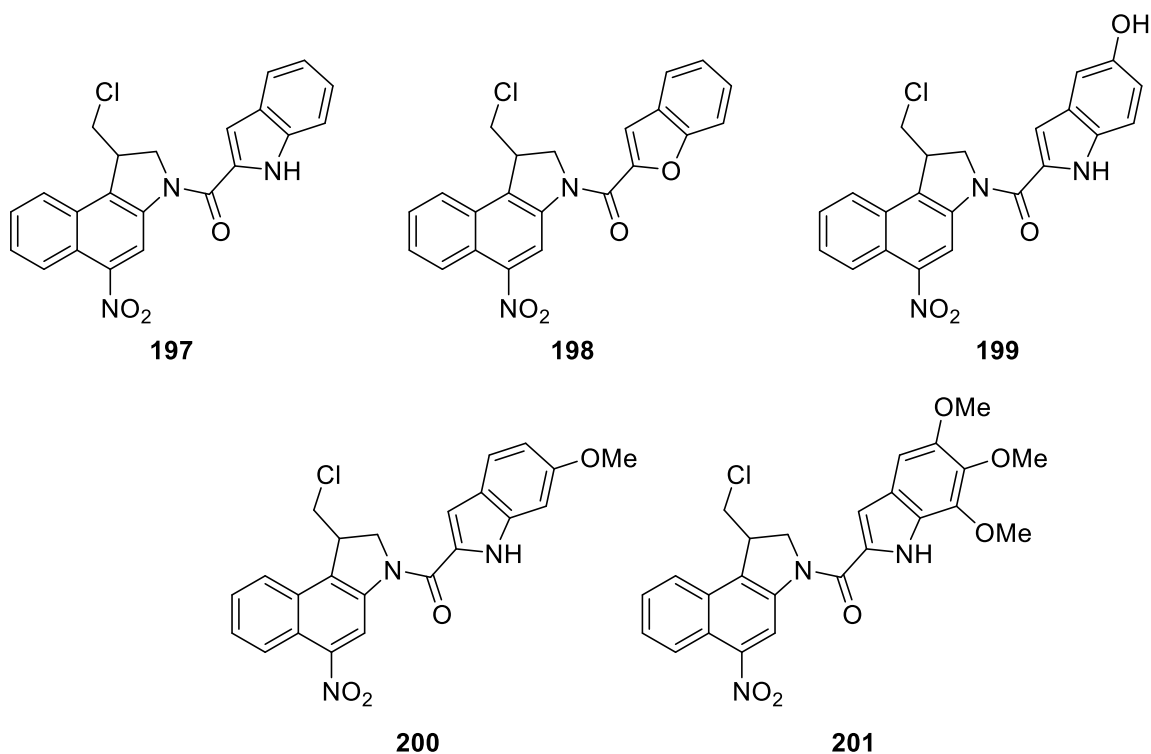
Scheme 102: Structures of the *seco*-nitro-CBIs **197-201**.

Table 7: IC_{50} values for compounds **197-201** against PC3 cells under normoxia and hypoxia. The hypoxia-cytotoxicity ratio (HCR) is calculated as IC_{50}(normoxic)/IC_{50}(hypoxic).

Entry	Compound Number	IC_{50} (µM) under normoxia	IC_{50} (µM) under hypoxia	Hypoxia Cytotoxicity ratio (HCR)
1	197	1.40	0.66	2.12
2	198	1.74	0.79	2.20
3	199	0.75	0.32	2.34
4	200	1.66	1.83	0.91
5	201	1.34	1.10	1.22

The *seco*-nitro-CBIs **197-201** all showed modest cytotoxicity under normoxic conditions ranging between 0.75 μM and 1.74 μM, with a mean IC_{50} of 1.40 μM compared to a mean IC_{50} value of 0.04 μM for the *seco*-amino-CBIs **202-206**. This equates to a roughly 36-fold decrease in mean cytotoxicity for the *seco*-nitro-CBIs compared to the *seco*-amino-CBIs under normoxic conditions. This result was expected as *seco*-nitro-CBIs are unable to undergo the required Winstein cyclisation to yield the corresponding amino-CBI compounds that can then alkylate DNA covalently as shown in Scheme 103.
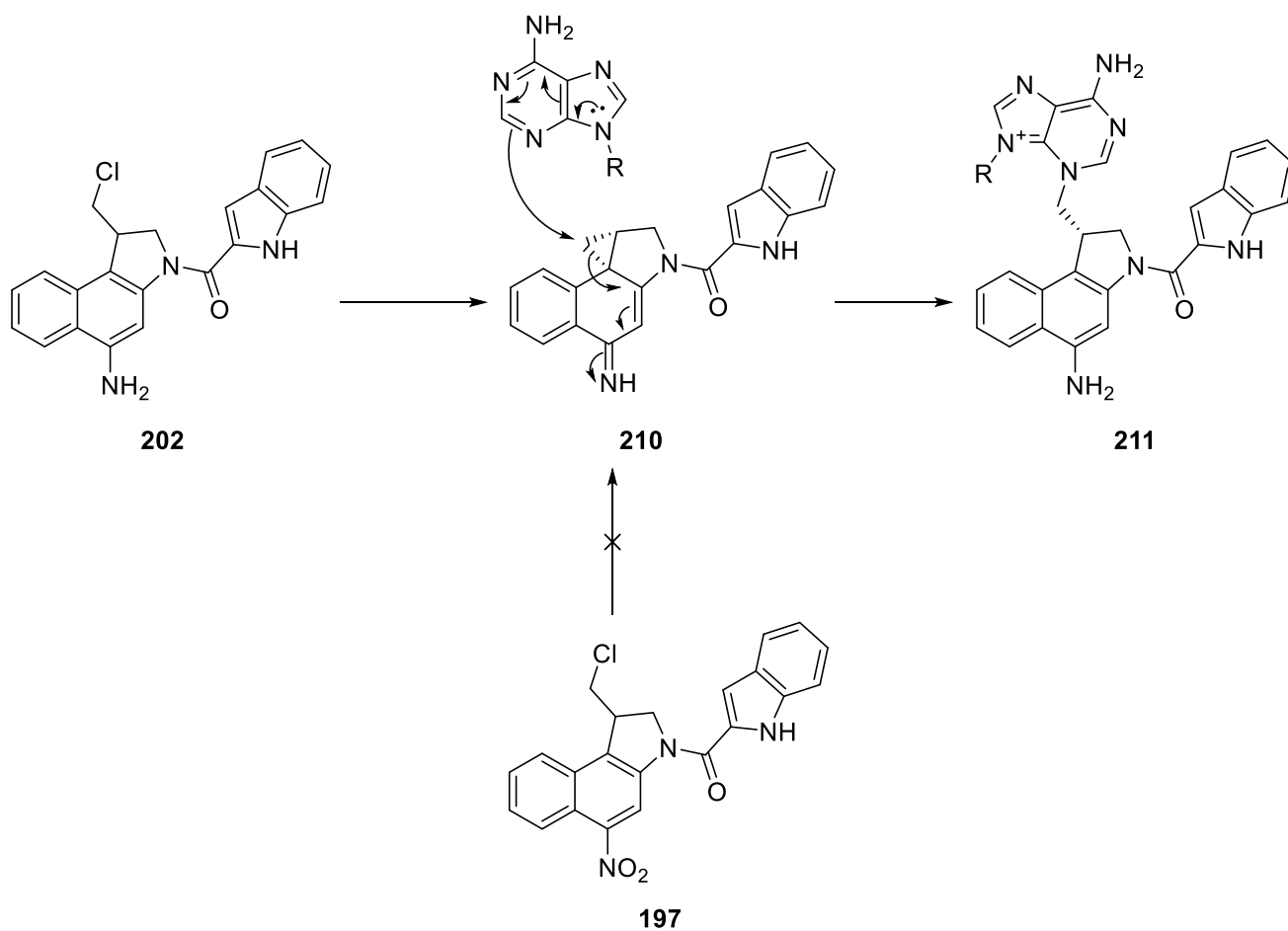
Scheme 103: Winstein cyclisation of **202** followed by DNA alkylation at adenine-N-7. Inability of **197** to undergo Winstein cyclisation.

Comparison of the *seco*-nitro-CBIs **197-201** with the *seco*-amino-CBIs **202-206** under normoxic conditions showed an alignment overall with regard to the substituent effects of the non-alkylating subunits. Analogous **199** and **204** were the most potent compounds in each series, further validating reports in the literature regarding the importance of an indole-C-5 substituent.[186] Trimethoxy indole compounds **201** and **206** were the second most potent compounds in each series, again likely due to the presence of an indole-C-5 substituent.

Benzofuran containing **198** was the least active *seco*-nitro-CBI even though the *seco*-amino-CBI analogue **203** exhibited exquisite potency with an IC$_{50}$ of 13.3 nM. As reduction of the nitro group of **198** is required in order to achieve activity, this result indicates a lack of reduction of **198** under normoxic conditions disproportionally compared to the indole containing *seco*-nitro-CBIs. The lower activities of **197** and **200** compared to **199** and **201** can be attributed to the lack of an indole-C-5 substituent.

Human cells are known to produce nitroreductase enzymes that have been shown to reduce nitro groups.[193] Cytotoxicity under normoxic conditions of compounds **197-201** is to be expected due to the nature in which cells control redox cycling. Under normoxia, cells contain both bio-reductases and bio-oxidases.[126] *Seco*-nitro-CBIs **197-201** will be continually reduced and subsequently re-oxidised under normoxia and therefore, there is the potential for DNA alkylation to occur post-reduction before re-oxidation occurs. This redox cycling can be seen in Scheme 104.
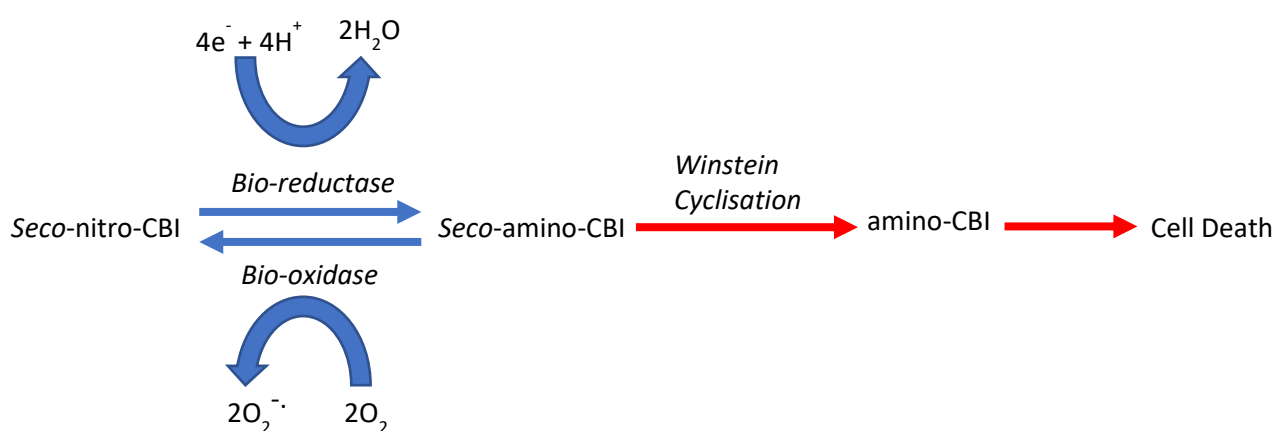
Scheme 104: Overview of redox cycling under normoxia.

Under hypoxia, the lack of oxygen means that once reduced, the newly formed *seco*-amino-CBIs are unable to be re-oxidised to the corresponding *seco*-nitro-CBIs and therefore go on to undergo Winstein cyclisation followed by DNA alkylation. This is the basis for hypoxia targeted bioreductive prodrugs. As can be seen in Table 7, the activity of *seco*-nitro-CBIs **197-201** under hypoxic conditions was increased compared to under normoxia. The mean IC$_{50}$ of **197-201** under hypoxia was 0.94 μM compared to 1.40 μM under normoxia showing a modest increase in activity. As per the MTS assay procedure reported by Tercel *et al.*[129], PC3 cells treated with

compounds **197-201** were incubated in a hypoxic chamber for a period of four hours. It may be that this was in insufficient length of time for sufficient bio-reduction to occur, explaining why the IC_{50} values of **197-201** were closer to that of **197-201** under normoxia compared to **202-206**. Future work would investigate the effect of length of time of incubation under hypoxia against activity.

Compound **199** was the most potent *seco*-nitro-CBI under both normoxia and hypoxia (IC_{50} values of 0.75 µM and 0.32 µM respectively) and also exhibited the greatest HCR of 2.34. The *seco*-amino-CBI analogue **204** was the most potent *seco*-amino-CBI with an IC_{50} value of 1.5 nM. This result validates the findings from the DNA-melting assay where **199** had a ΔT_m value of 2.5°C at 0.25 MEq, the highest value of the *seco*-nitro-CBIs tested. This is in accordance with the literature with regard to importance of an indole-C-5 substituent.[186] Compounds **200** and **201** had disappointing HCR values of 0.91 and 1.22 respectively, indicating that reduction of the nitro group had not readily occurred under hypoxia. This result indicates that electron-donating groups such as methoxy groups are deleterious to bio-reduction which is in agreement with reports in the literature that electron-donating substituents are deleterious to nitro-reduction.[194] Tercel *et al.*[129] successfully attempted to bypass this issue through the incorporation of electron-withdrawing groups on the naphthalene ring such as a 7-nitro group in compound **211**. Compound **211** exhibited an HCR of 70 in Skov3 cells.
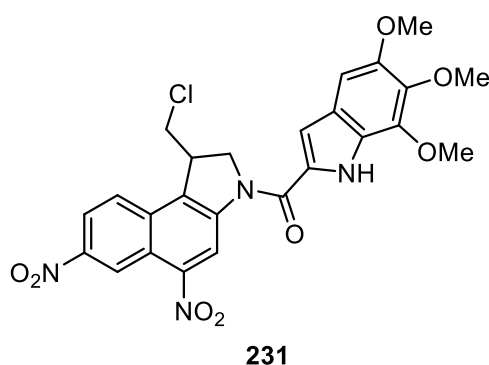
Scheme 105: Structure of **231**.

Future work would investigate the incorporation of electron-withdrawing substituents into the naphthalene ring of the lead *seco*-nitro-CBI compound **199** in order to improve the HCR for development as a hypoxia-activated prodrug. The analogous lead *seco*-amino-CBI

compound **204** would be incorporated into the assembly of the polymeric prodrug system through coupling to a molecular clip-peptide-PEG construct. At this stage, biological evaluation of the polymeric prodrug system can then take place to investigate the effectiveness of PSA-mediated release of **204** to prostate tumours.

5.0 Conclusion

Current chemotherapeutic agents licensed to treat advanced prostate cancer have significant limitations to their effectiveness. These limitations can in part be attributed to a lack of selective targeting of cancerous cells over normal cells. There is currently no curative treatment for advanced prostate cancer.[195] Hypoxia is a fundamental biological phenomena that is associated with the development and aggressiveness of prostate cancer.[196] CBI anti-tumour antibiotics, that have been developed as synthetically accessible analogues to the natural product duocarmycin SA **9**, are highly potent cytotoxins with a novel mode of action.[94,100,105,190] The ability to develop a pro-drug system to deliver these highly efficacious drugs directly to prostate tumours will address the current limitations surrounding chemotherapeutic selectivity of healthy and cancerous tissues. Previous work by the Threadgill group has investigated a pro-drug system that utilises active PSA to selectively release a *seco*-amino-CBI at the prostate tumour site.[100]

Synthesis of the proposed range of *seco*-amino-CBI drugs **202-206** was addressed in two parts, namely, synthesis of the alkylating subunit **55** and synthesis of the range of non-alkylating subunits **75-81**. Synthesis of the alkylating subunit **55** can be split into two parts, synthesis of pre-cyclisation key intermediate **49** and subsequent cyclisation. One of the initial challenges faced in the synthesis of **49** was the unintended reductive de-iodination of 1-iodo-2,4-dinitro naphthalene **45** and subsequent difficulty in chemoselective orthogonal protection of the resulting 2,4-napthalendiamine **46**. To address this issue, a novel route to analogous compound **72** was developed in which the required amine at the 4-position is masked as a nitro group. Starting with 1-hydroxy-2-naphthoic acid **29**, nitration at 4-C yielded **69** which could then be transformed into 1-iodo-4-nitro-2-naphthoic acid **71**. At this stage, the required amine at the 2-position could then be accessed through a Curtius rearrangement to yield the corresponding isocyanate followed by treatment with *tert*-butanol to yield the Boc-protected amine **72**. Reduction of **72** without loss of iodine was achieved in a low yield. Treatment of **72** with *R*-glycidyl nosylate to insert required stereochemistry followed by metal-mediated cyclisation yielded **74** in low yield. Starting with commercially available **29**, synthesis of enantiopure *seco*-nitro-CBI **74** could now be achieved in six steps. Different substituents at

the 4-position such as 4-H **117**, and 4-Br **129**, were investigated with limited success in an attempt to improve the yield of metal-mediated cyclisation as it was hypothesised that the strong electron-withdrawing nitro group was deleterious to the required nucleophilicity of 1-C. Free-radical cyclisation of **72** was achieved in good yield. Boc-deprotection of cyclised **167** followed by coupling to a range of non-alkylating subunits **75-81** provided access to *seco*-nitro-CBIs **197-201** that were then reduced to corresponding *seco*-amino-CBIs **202-206**.

Calf-thymus DNA melting assays of the synthesised *seco*-nitro-CBIs **197-201** and the *seco*-amino-CBIs **202-206** were carried out in order to investigate the structure-activity relationship of the varying non-alkylating. It was confirmed that the *seco*-nitro-CBIs **197-201** are unable to covalently bind and alkylate double stranded DNA due to the inability to undergo Winstein cyclisation to yield the corresponding CBI compounds. On the other hand, *seco*-amino-CBIs **202-206** can undergo Winstein cyclisation and the resulting amino-CBI compounds can alkylate double stranded DNA very efficiently to bring about the cytotoxic effects of **202-206**. This effect was observed as an increase in the melting temperature (T_m) of dsDNA by as much as 14.6 °C, comparable to the T_m of the known cytotoxic agent, doxorubicin (T_m = 18 deg. C). This was despite **202-206** being racemic. The (−)-unnatural enantiomers of the anti-tumour antibiotics tend to have a reduced DNA alkylation efficiency compared to the (+)-natural enantiomers.

Preliminary MTS-assays allowed for further investigation into the structure-activity relationship of the range of non-alkylating subunits in **202-206**. 5-hydroxy **204** showed exquisite potency with an IC_{50} of 1.5 nM against PC3 cells. It has been reported that C-5 substituents groups account for the potency of non-alkylating subunits and this was confirmed as compounds **202** and **205** showed modest potency of 78 nM and 100 nM. The ability of *seco*-nitro-CBIs **197-201** was investigated through performing an MTS-assay under hypoxic conditions. All of the *seco*-nitro-CBIs except **200** showed increased potency under hypoxia compared to under normoxia.

Future work will involve the incorporation of lead compound **204** into the polymeric prodrug system. Once assembly of the prodrug is complete, a range of biological evaluations will be

carried out in order to evaluate the selectivity of drug release toward PSA-expressing prostate tumour cells.

6.0 Experimental

Chemical reagents were purchased from Sigma-Aldrich, Fisher, Alfa and VWR. TLC was carried out on Merck aluminium-backed silica gel 60 TLC plates and viewed under UV light (λ = 254 nm). Column chromatography was carried out on silica gel 60 (35 − 70 micron) from Fisher. NMR data were obtained on either a Varian Mercury VX (400 MHz for ^{1}H and 100 MHz for ^{13}C) or a Bruker Avance III (500 MHz for ^{1}H, 125 MHz for ^{13}C and 470 MHz for ^{19}F). The chemical shifts are recorded in parts per million (ppm). A single mean value of chemical shift is given for multiplets arising from proton(s) in the same chemical environment whilst a range value is given for the chemical shift of multiplets arising from protons of different chemical environments. Mass Spectrometry was carried out on either a micrOTOF from Bruker Daltronics or MAXIS from Bruker Daltronics using an electrospray ionization source (ESI). Melting points were obtained using a Reichert-Jung heated stage microscope. IR spectra were obtained on a Perkin-Elmer 782 infra-red spectrometer. Experiments were carried out at room temperature unless otherwise stated and organic solutions were dried with MgSO$_4$ unless otherwise stated. Solvents were evaporated under reduced pressure. Reactions were heated in DrySyn® blocks.

6.1 1-(Chloromethyl)-5-nitro-1,2-dihydro-3H-benzoindole (42)

Compound **167** (136 mg, 0.377 mmol) was stirred with CF$_3$CO$_2$H (0.10 mL) in CH$_2$Cl$_2$ (15 mL) for 17 h. The reaction mixture was concentrated and filtered through a mixture of K$_2$CO$_3$ and SiO$_2$ (1:9), washing with EtOAc. Evaporation yielded **42** (116 mg, 100%) as a red oil: Rf 0.4 (EtOAc / petroleum ether 3:7); ^{1}H NMR (500 MHz; CDCl$_3$) δ 3.54 (1 H, t, J = 10.8 Hz, 2-H), 3.80 (1 H, dd, J = 11.2, 3.3 Hz, H 2-H), 3.87 (1 H, t, J = 8.7 Hz, C*H*HCl), 3.92 (1 H, dd, J = 10.1 , 2.0 Hz, CH*H*Cl), 4.06 (1 H, br. t, J = 9.5 Hz, 1-H), 7.42 (1 H, t, J = 8.3 Hz, 7-H), 7.52 (1 H, t, J = 8.8 Hz, 8-H), 7.67 (1 H, s, 4-H), 7.71 (1 H, d, J = 8.8 Hz, 9-H), 8.35 (1 H, d, J = 8.3 Hz, 6-H); ^{13}C NMR (125 MHz; CDCl$_3$) δ 44.5 (1-C), 44.6 (2-C), 51.4 (CH$_2$Cl), 110.3 (4-C), 120.6 (5a-C), 122.1 (9-C), 124.3 (6-C), 125.6 (7-C), 126.5 (9b-C), 128.2 (8-C), 131.2 (9a-C), 147.4 (3a-C) 147.9 (5-C); MS (ES+) *m/z* 510.9905 [M + Na]$^+$ (C$_{18}$H$_{18}$^{35}ClIN$_2$NaO$_4$ requires 510.9892).
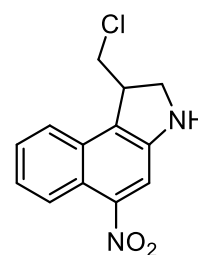
6.2 2,4-Dinitronaphthalen-1-yl trifluoromethanesulfonate (44)

Under N_2, 2,4-dinitronaphthalen-1-ol (5.00 g, 21.4 mmol) and NEt_3 (5.62 g, 55.6 mmol) in anhydrous CH_2Cl_2 (100 mL) were stirred at 0˚C. Trifluoromethanesulfonic anhydride (4.68 mL, 27.8 mmol) was added dropwise and the reaction mixture was allowed to warm to room temperature. After 2 h, aq. HCl (0.5 M, 100 mL) was added and the mixture was stirred for a further 30 min. The organic phase was separated, and the aqueous phase was extracted with CH_2Cl_2 (30 mL). The combined organic phases were washed with sat. aq. $NaHCO_3$ (3×30 mL) and brine (3×30 mL) before drying, evaporation and chromatography (EtOAc / petroleum ether 1:3) yielded **44** (6.9 g, 88%) as an orange crystalline solid: mp 105-106˚C (lit.[197] mp 105-107˚C); Rf 0.5 (EtOAc / petroleum ether 3:7); ^1H NMR (500 MHz; $(CD_3)_2SO$) δ 7.73 (1 H, t, $J =$ 8.3 Hz, 7-H), 7.93 (1 H, t, $J =$ 8.0 Hz, 6-H), 8.55 (1 H, d, $J =$ 8.0 Hz, 8-H), 8.67 (1 H, d, $J =$ 8.3 Hz, 5-H), 8.99 (1 H, s, 3-H); ^{19}F NMR (470MHz; $CDCl_3$) δ -71.84 (s, CF_3); MS (ES +) *m/z* 388.9660 [M + Na]$^+$ ($C_{11}H_5F_3N_2NaO_7S$ requires 388.9667).
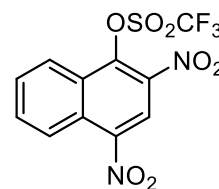
6.3 2,4-Dinitro-1-iodonaphthalene (45)

Compound **44** (5.42 g, 14.9 mmol) was stirred with NaI (7.63 g, 50.9 mmol) in acetone (150 mL) at reflux for 16 h. The evaporation residue, in EtOAc (100 mL), was washed with sat. aq. $Na_2S_2O_3$ (3×30 mL). Drying and evaporation yielded **45** (4.46 g, 87%) as a yellow solid: mp 182-183˚C (lit.[164] mp 183-186˚C); Rf 0.3 (CH_2Cl_2 / petroleum ether 1:4); ^1H NMR δ (400 MHz; $CDCl_3$) 7.82 (1 H, m, 6-H or 7-H), 7.87 (1 H, ddd, $J =$ 8.4, 7.0, 1.4 Hz, 7-H or 6-H), 8.34 (1 H, s, 3-H), 8.47 (1 H, d, $J =$ 7.5 Hz, 5-H), 8.55 (1 H, d, $J =$ 8.4 Hz, 8-H).
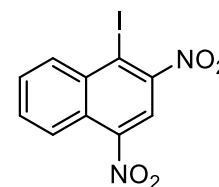
6.4 Naphthalene-1,3-diamine (46)

Compound **45** (335 mg, 0.97 mmol) and $SnCl_2.2H_2O$ (3.30 g, 14.6 mmol) in EtOAc (20 mL) were heated to reflux for 17 h. The cooled mixture was added to ice (30 mL) and the pH was adjusted to 8 by addition of $NaHCO_3$. The mixture was extracted with EtOAc (50 mL). The organic phase was washed with H_2O (3 × 30 mL). Drying and evaporation yielded **46** (124 mg, 81%) as a dark solid: mp 93-94˚C (lit.[198] mp 96˚C); Rf 0.6 (EtOAc / petroleum ether 3:7); ^{1}H NMR (400 MHz; $(CD_3)_2SO$) δ 5.00 (2 H, s, 3-NH_2), 5.43 (2 H, s, 1-NH_2), 6.13-6.14 (2 H, m, 2,4-H_2), 6.93 (1 H, t, J = 7.5 Hz, 7-H), 7.17 (1 H, t, J = 7.5 Hz, 6-H), 7.32 (1 H, d, J = 8.2 Hz, 5-H), 7.78 (1 H, d, J = 8.3 Hz, 8-H).
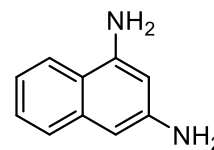
6.5 1-Amino-3-trifluoroacetamidonaphthalene (47)

Trifluoroacetic anhydride (1.74 g, 8.3 mmol) in dry THF (50 mL) was added dropwise during 2 h to **46** (1.31 g, 8.3 mmol) and Pr$^i_2$NEt (3.20 g, 24.8 mmol) in dry THF (150 mL) under N_2 at 0°C. The mixture was allowed to warm to room temperature and was stirred for 16 h. The evaporation residue, in EtOAc (50 mL), was washed with H_2O (3 × 30 mL) and brine (3 × 30 mL). Drying, evaporation and chromatography (EtOAc / petroleum ether 1:4) yielded **47** (326 mg, 15%) as a buff solid: mp 168-169˚C (lit.[164] mp 168-169˚C); Rf 0.5 (EtOAc / petroleum ether 1:3); ^{1}H NMR (400 MHz; $(CD_3)_2SO$) δ 5.97 (2 H, s, NH_2), 6.96 (1 H, s, 2-H), 7.34 (1 H, t, J = 7.6 Hz, 7-H), 7.44-7.41 (2 H, m, 4,6-H), 7.71 (1 H, d, J = 7.7 Hz, 5-H), 8.06 (1 H, d, J = 7.9 Hz, 8-H), 11.16 (1 H, s, NH).
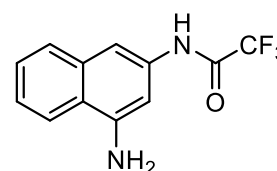
6.6 1,1-Dimethylethyl N-(3-trifluoroacetamidonaphthalen-1-yl)carbamate (48)

Boc$_2$O (1.53 g, 7.0 mmol) was heated under reflux with **47** (357 mg, 1.4 mmol) added in dry THF (10 mL) under N$_2$ for 16 h. The solvent was evaporated and the mixture was purified by column chromatography (EtOAc / petroleum ether 1:4) to yield **48** (393 mg, 79%) as a buff solid: mp 206-207˚C (lit.[164] mp 206-208˚C); Rf 0.6 (EtOAc / petroleum ether 3:7); ^{1}H NMR (400 MHz; (CD$_3$)$_2$SO) δ 1.53 (9 H, s, C(CH$_3$)$_3$), 7.48-7.56 (2 H, m, 6-H & 7-H), 7.91 (1 H, d, J = 7.9 Hz, 5-H), 7.96 (1 H, d, J = 1.8 Hz, 2-H), 8.09 (1 H, d, J = 7.9 Hz, 8-H), 8.17 (1 H, d, J = 1.8 Hz, 4-H), 9.41 (1 H, s, NHBoc), 11.49 (1 H, s, NHCOCF$_3$).
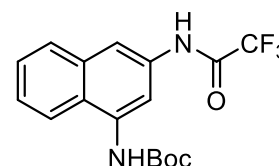
6.7 1,1-Dimethylethyl-N-(1-iodo-2-trifluoroacetamidonaphthalen-4-yl)carbamate (49)

Compound **48** (363 mg, 1.02 mmol) in dry THF (10 mL) was cooled to -78˚C under N$_2$. N-Iodosuccinimide (315 mg, 1.4 mmol) in dry THF (2 mL) was added, followed by TsOH.2H$_2$O (361 mg, 1.9 mmol) in dry THF (2 mL). The mixture was allowed to warm to room temperature slowly. After 16 h, the reaction mixture was quenched with sat. aq. NaHCO$_3$ (30 mL). The mixture was then diluted with H$_2$O (30 mL) and extracted with EtOAc (3 × 30 mL). The organic layer was dried and concentrated, and the resulting crude mixture was purified by column chromatography (EtOAc / petroleum ether 1:9) to yield **49** (151 mg, 32%) as a pale buff solid: mp 198-199˚C (lit.[164] mp 198-199˚C); Rf = 0.5 (EtOAc / petroleum ether 1:9); ^{1}H NMR (400 MHz; CDCl$_3$) δ 1.53 (9 H, s, C(CH$_3$)$_3$), 6.89 (1 H, s, NHBoc), 7.50-7.59 (2 H, m, 6-H & 7-H), 7.79 (1 H, d, J = 8.0 Hz, 5-H), 8.12 (1 H, d, J = 8.0 Hz, 8-H), 8.52 (1 H, s, NHCOCF$_3$), 8.69 (1 H, s, 3-H); MS (ES -) m/z 479.0091 [M - H]$^-$ (C$_{17}$H$_{15}$F$_3$IN$_2$O$_3$ requires 479.0080).
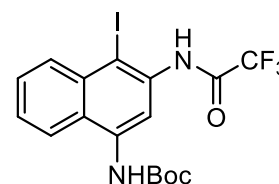
6.8 Attempted synthesis of *tert*-Butyl (*R*)-N-(4-iodo-3-(2,2,2-trifluoro-N-(oxiran-2-ylmethyl)acetamido)naphthalen-1-yl)carbamate (51)

Compound **49** (100 mg, 0.2 mmol), *R*-oxiranylmethyl nosylate (81 mg, 0.3 mmol) and K_2CO_3 (124 mg, 0.9 mmol) in acetone (100 mL) were heated to 50˚C for 3 d under N_2. The mixture was cooled, and 75 mL of the solvent was evaporated. The residue, in EtOAc (50 mL), was washed with sat. aq. $NaHCO_3$ (3 × 30 mL), then brine (1 × 30 mL). Drying, evaporation and chromatography (EtOAc / petroleum ether 3:7) recovered **49** and *R*-oxiranylmethyl nosylate.
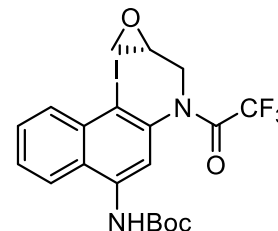
Compound **49** (70 mg, 0.14 mmol), *R*-oxiranylmethyl nosylate (57 mg, 0.21 mmol) and K_2CO_3 (87 mg, 0.63 mmol) in acetone (100 mL) were heated to 50˚C under N_2. After 5 d, K_2CO_3 (100 mg, 0.72 mmol) and acetone (20 mL) were added and the reaction mixture was heated for a further 4 d. After this time, TLC analysis indicated that no reaction had occurred.

Compound **49** (70 mg, 0.14 mmol), *R*-oxiranylmethyl nosylate (57 mg, 0.21 mmol) and Cs_2CO_3 (205 mg, 0.63 mmol) in acetone (50 mL) were heated to 50˚C under N_2. After 5 d, Cs_2CO_3 (205 mg) and acetone (25 mL) were added and the reaction mixture heated for a further 4 d. After this time, TLC confirmed that only starting materials were present. The evaporation residue, in DMF (50 mL), was heated to 120˚C for 5 d. After this time, TLC analysis indicated that no reaction had occurred.

Compound **49** (100 mg, 0.2 mmol), *R*-oxiranylmethyl nosylate (81 mg, 0.3 mmol) and K_2CO_3 (124 mg, 0.9 mmol) in DMF (100 mL) were heated to 120˚C under N_2. After 3 d, TLC analysis indicated that no reaction had occurred.

Compound **49** (100 mg, 0.2 mmol), *R*-oxiranylmethyl nosylate (81 mg, 0.3 mmol) and Cs_2CO_3 (292 mg, 0.9 mmol) in DMF (100 mL) were heated to 120˚C under N_2. After 3 d, TLC analysis indicated that no reaction had occurred.

6.9   *tert*-butyl   (3-(N-allyl-2,2,2-trifluoroacetamido)-4-iodonaphthalen-1-yl)carbamate (54)

KO^{t}Bu (36 mg, 0.32 mmol) was added to a stirred solution of compound **49** (140 mg, 0.29 mmol) in THF (30 mL) under N$_2$. After 0.5 h, allyl bromide (113 mg, 0.93 mmol) was added and the reaction mixture stirred for a further 2 h then heated to 50°C. After 17 h, sat. aq. NaHCO$_3$ (30 mL) was added and the mixture extracted with EtOAc (3 × 20 mL). Drying, evaporating and column chromatography (EtOAc / petroleum ether 1:4) yielded **54** (29 mg, 19%) as a yellow oil: Rf 0.7 (EtOAc / petroleum ether 3:7); ^{1}H NMR (400 MHz; CDCl$_3$) δ 1.55 (9 H, br s, ^{t}Bu), 3.83 (1 H, dd, *J* = 14.6, 7.7 Hz, propenyl 1-H), 4.96 (1 H, dd, *J* = 14.6, 6.0 Hz, propenyl 1-H), 5.17-5.23 (2 H, m, propenyl 3-H$_2$), 5.98 (1 H, m, propenyl 2-H), 6.99 (1 H, s, NH), 7.61-7.67 (2 H, m, 6,7-H$_2$), 7.83-7.87 (1 H, m, 5-H), 7.93 (1 H, s, 3-H), 8.29-8.33 (1 H, m, 8-H).
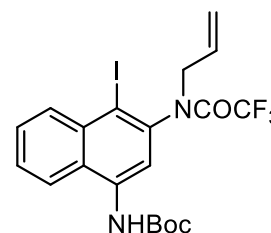
6.10 1-Hydroxy-4-nitronaphthalene-2-carboxylic acid (69)

HNO$_3$ (70%, 1.0 mL) was added to a stirred solution of **29** (1.00 g, 5.3 mmol) in AcOH (20 mL) at 0˚C. After 0.5 h, the reaction mixture was quenched by addition of ice-cold H$_2$O (30 mL). The mixture was extracted with CH$_2$Cl$_2$ (3 × 30 mL). Drying, filtration and evaporation yielded **69** (1.17 g, 95%) as an orange solid: mp 212-213˚C (lit.[199] mp 214˚C) Rf 0.1 (EtOAc / petroleum ether 2:3); ^{1}H NMR (400 MHz; CDCl$_3$) δ 7.79 (1 H, ddd, *J* = 8.3, 7.2 Hz, 1.1 Hz, 7-H), 7.97 (1 H, ddd, *J* = 8.6 Hz, 7.2 Hz, 1.4 Hz, 6-H), 8.67 (1 H, ddd, *J* = 8.5 Hz, 1.4 Hz, 0.6 Hz, 5-H), 8.75 (1 H, ddd, *J* = 8.7 Hz, 1.1 Hz, 0.7 Hz, 8-H), 9.01 (1 H, s, 3-H), 12.53 (1 H, s, OH).
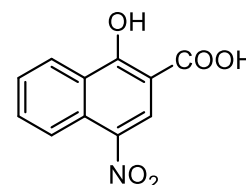
6.11 Attempted synthesis of 4-nitro-1-(((trifluoromethyl)sulfonyl)oxy)-2-naphthoic acid (70)

Under N_2, Compound **69** (550 mg, 2.36 mmol) and NEt_3 (0.85 mL 6.14 mmol) in MeOH (20 mL) were stirred at 0˚C. Trifluoromethanesulfonic anhydride (0.43 mL, 3.00 mmol) was added dropwise and the reaction mixture allowed to warn to room temperature. After 1.5 h, aq. HCl (1 M, 20 mL) was added and the reaction mixture was stirred for a further 17 h. The organic phase was separated, and the aqueous phase was extracted with CH_2Cl_2 (3 × 30 mL). The combined organic phases were washed with HCl (1 M, 3 × 10 mL). Drying and evaporating recovered **69**.
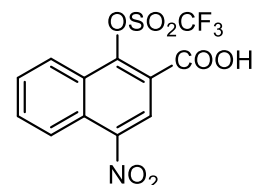
6.12 1-Iodo-4-nitronaphthalene-2-carboxylic acid (71)

Compound **85** (1.0 g, 2.69 mmol) in aq. NaOH (10%, 30 mL) and EtOH (50 mL) was heated to 40˚C for 2 h. The reaction mixture was acidified with aq. HCl (1 M) and extracted with EtOAc (3 × 30 mL). The combined organic phases were washed with brine (3 × 30 mL). Drying and evaporation yielded **71** (818 mg, 89%) as a dark black semi-solid: Rf 0.1 (EtOAc / petroleum ether 1:1); ^{1}H NMR (400 MHz; (CD$_3$)$_2$SO) δ 7.86-7.93 (2 H, m, 6,7-H), 8.29 (1 H, m, 5-H), 8.36 (1 H, s, 3-H), 8.49 (1 H, m, 8-H); ^{13}C NMR (100 MHz; (CD$_3$)$_2$SO) (HSQC / HMBC) δ 108.2 (1-C), 122.2 (3-C), 123.4 (5-C), 124.3 (4a-C), 130.7, 131.6, 134.7 (8-C), 135.4 (8a-C), 138.3 (2-C), 147.2 (4-C), 168.8 (CO); MS (ES +) *m/z* 387.9043 [M + 2 Na − H]$^+$ ($C_{11}H_5INa_2NO_4$ requires 387.9053).
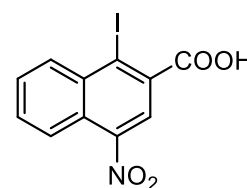
6.13 1,1-Dimethylethyl N-(1-iodo-4-nitronaphthalen-2-yl)carbamate (72)

Aq. NaOH (10%, 30 mL) was added to **85** (1.49 g, 4.01 mmol) in EtOH (50 mL) and the mixture was heated to 40°C. After 45 min, the reaction mixture was acidified with aq. HCl (1 M) and the EtOH was evaporated. The residual aqueous phase was extracted with EtOAc (3 × 30 mL). The extracts were combined and dried and the solvent was evaporated. The residue was treated with $SOCl_2$ (50 mL) and DMF (50 μL). After 17 h, the reagent was evaporated and the residue, in dry toluene (45 mL) was treated with $(CH_3)_3SiN_3$ (1.70 mL, 1.46 g 12.6 mmol) under Ar. After 17 h, the reaction mixture was heated to 120°C under a flow of N_2. After 1.5 h, ^{t}BuOH (4.20 mL, 3.27 g, 44.2 mmol) and NEt_3 (0.75 mL, 540 mg, 5.4 mmol) were added. After 3 h, the reaction mixture was cooled to rt. After 72 h, EtOAc (30 mL) was added and the solution was washed with sat. aq. $NaHCO_3$ (3 × 30 mL). Drying and evaporation yielded **72** as a buff solid (1.25 g, 78%): Rf 0.6 (EtOAc / petroleum ether 3:7); ^{1}H NMR (400 MHz; CDCl$_3$) δ 1.58 (9 H, s, CMe$_3$), 7.34 (1 H, br, N*H*), 7.63 (2 H, m, 6,7-H), 8.24 (1 H, m, 8-H), 8.31 (1 H, m, 5-H), 9.03 (1 H, s, 3-H); ^{13}C NMR (100 MHz; CDCl$_3$) (HSQC, HMBC) δ 28.2 ((CH$_3$)$_3$), 82.3 (O*C*(CH$_3$)$_3$), 97.5 (1-C), 116.3 (3-C), 121.7 (4α-C), 123.4 (5-C), 128.0 (6-C), 129.5 (7-C), 132.6 (8-C), 135.1 (8α-C), 137.3 (2-C), 148.2 (4-C), 152.2 (CO); MS (ES +) *m/z* 436.9998 [M + Na]$^+$ (C$_{15}$H$_{15}$IN$_2$NaO$_2$ requires 436.9974), 415.0173 [M + H]$^+$ (C$_{15}$H$_{16}$IN$_2$O$_2$ requires 415.0155), (ES-) *m/z* 412.9902 [M − H]$^-$ (C$_{15}$H$_{14}$IN$_2$O$_2$ requires 412.9998).
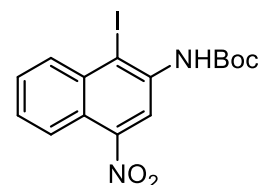
6.14   *tert*-butyl   *(S)*-(1-iodo-4-nitronaphthalen-2-yl)(oxiran-2-ylmethyl)carbamate (73)

Under Ar, a stirred solution of compound **72** (670 mg, 1.43 mmol) and *R*-glycidyl nosylate (570 mg, 2.20 mmol) in an. DMF (15 mL) were cooled to 0˚C followed by addition of NaH (96 mg, 4.00 mmol). After 1.5 h, the reaction mixture was allowed to warm to rt. After 72 h, the reaction mixture was added to ice cold H_2O (20 mL). The mixture was extracted with EtOAc (3 × 20 mL). The combined organic phases were washed with H_2O (3 × 10 mL), then brine (3 × 10 mL). Drying, evaporation and column chromatography (EtOAc / petroleum ether 1:4) yielded **73** (274 mg, 41%) as an orange oil: Rf 0.6 (EtOAc / petroleum ether 3:7); ^{1}H NMR (500 MHz; CDCl$_3$; 55˚C) (HMBC, HSQC) δ 1.38 (9 H, br s, ^{t}Bu), 2.45 (0.5 H, dd, *J* = 4.1, 2.2 Hz, CH$_2$O), 2.52 (0.5 Hz, dd, *J* = 4.9, 2.6 Hz, CH$_2$O), 2.79 (1 H, m, CH$_2$O), 3.08 (0.5 H, br s, NCH), 3.25 (0.5 H, m, CH$_2$C*H*), 3.41 (0.5 H, m, CH$_2$C*H*), 3.67 (0.5 H, br s, NCH), 4.05 (0.5 H, dd, *J* = 14.9, 5.2 Hz, NCH), 4.35 (0.5 H, br s, NCH), 7.67-7.71 (2 H, m, 7,7'-H$_2$), 7.72-7.76 (2 H, m, 6,6'-H$_2$), 8.05 (0.5 H, s, 3-H), 8.18 (0.5 H, s, 3-H), 8.40 (0.5 H, d, *J* = 8.6 Hz, 8-H), 8.42 (0.5 H, d, *J* = 8.6 Hz, 8-H), 8.46 (2 H, d, *J* = 8.6 Hz, 5,5'-H); ^{13}C NMR (125 MHz; CDCl$_3$) (HSQC, HMBC) δ 28.1 (^{t}Bu), 28.4 (^{t}Bu), 45.6 (CH$_2$O), 45.7 (CH$_2$O), 49.6 (CH$_2$*C*H), 50.2 (NCH), 51.1 (CH$_2$*C*H), 52.6 (NCH), 81.7 (^{t}Bu), 82.1 (^{t}Bu), 113.9 (1-C), 114.5 (1-C), 123.4 (5-C), 123.5 (5-C), 123.7 (4a-C), 123.8 (4a-C), 124.1 (3-C), 124.3 (3-C), 125.6, 129.4 (6-C), 129.5 (6-C), 130.1 (7-C), 130.2 (7-C), 134.1 (8-C), 134.2 (8-C), 135.9 (8a-C), 136.0 (8a-C), 142.4 (2-C), 142.6 (2-C), 147.4 (4-C), 147.5 (4-C), 153.3 (CO), 153.4 (CO) ; MS (ES +) *m/z* 963.0685 [2 M + Na]$^+$ ((C$_{18}$H$_{19}$IN$_2$O$_5$)$_2$Na) requires 963.0570, 493.0322 [M + Na]$^+$ C$_{18}$H$_{19}$IN$_2$NaO$_5$ requires 493.0236.
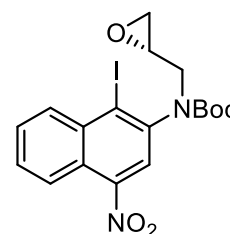
6.15   *tert*-butyl   *(S)*-1-(hydroxymethyl)-5-nitro-1,2-dihydro-3H-benzo[e]indole-3-carboxylate (74)

Under Ar, MeLi (1.6 M in an. Et_2O, 0.82 mL, 1.32 mmol) was added dropwise to a stirred solution of $ZnCl_2$ (0.5 M in an. THF, 0.66 mL) in an. THF (5 mL) at 0˚C. After 0.5 h, the reaction mixture was cooled to -78˚C followed by addition of trimethylsilylisothiocyanate (48 µL, 0.33 mmol). The reaction mixture was allowed to warm to 0˚C for 0.5 h and then cooled to -78˚C followed by dropwise addition of **73** (102 mg, 0.22 mmol) in an. THF (5 mL). After 0.5 h, the reaction mixture was warmed to 0°C. After a further 1 h, the reaction mixture was allowed to warm to rt. After 2.5 h, sat. aq. NH_4Cl (25 mL) was added followed by extraction with CH_2Cl_2 (3 × 20 mL). Drying, evaporating and automated column chromatography (EtOAc / hexane 5:95 -> 1:0) yielded:
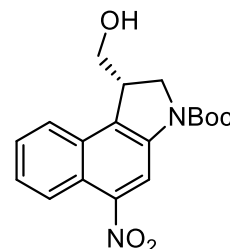
73 (40 mg, 39%).

74 (< 1 mg) as a red oil: Rf 0.7 (EtOAc / petroleum ether 3:7); MS (ES +) *m/z* 367.1284 [M + Na]$^+$ ($C_{18}H_{20}N_2NaO_5$ requires 367.1270).
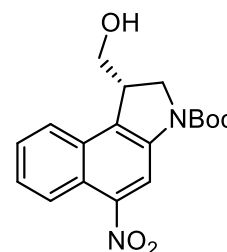
(S)-4-nitro-N-(oxiran-2-ylmethyl)naphthalen-2-amine (112).

(8 mg, 15%) as a red oil: Rf 0.6 (EtOAc / petroleum ether 3:7); ^{1}H NMR (500 MHz; CDCl$_3$) (HMBC, HSQC) δ 3.83 (1 H, d, *J* = 2.9 Hz, CH*H*O), 3.85 (1 H, d, *J* = 1.3 Hz, C*H*HO), 4.11-4.15 (1 H, m, NCH), 4.33 (1 H, t, *J* = 8.7 Hz, NCH), 4.99 (1 H, m, CHO), 7.64 (2 H, m, 6,7-H$_2$), 7.92 (1 H, dd, *J* = 8.0, 1.8 Hz, 8-H), 8.17 (1 H, d, *J* = 2.5 Hz, 1-H), 8.47 (1 H, d, *J* = 8.6 Hz, 5-H), 8.62 (1 H, d, *J* = 2.5 Hz, 3-H); ^{13}C NMR (125 MHz; CDCl$_3$) δ 44.4 (CH$_2$O), 48.1 (CH$_2$N), 71.0 (CHO), 115.6 (3-C), 120.8 (1-C), 121.9 (4a-C), 123.0 (5-C), 128.3 (7 or 8-C), 128.4 (7 or 8-C), 128.6 (6-C), 134.1 (8a-C), 147.1 (4-C), 153.7 (2-C); MS (ES+) *m/z* 267.0751 [M + Na]$^+$ ($C_{13}H_{12}N_2O_3Na$ requires 267.0746), 245.0919 [M + H]$^+$ ($C_{13}H_{13}N_2O_3$ requires 245.0926); MS (ES-) *m/z* 243.0723 [M − H]$^-$ ($C_{13}H_{11}N_2O_3$ requires 243.0770).
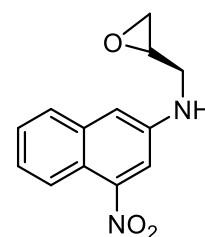
Under N_2 at -78˚C, $Pr^iMgCl·LiCl$ (1.3M in an. THF, 0.32 mmol), was added dropwise to a stirred solution of **73** (97 mg, 0.21 mmol) in an. THF (3 mL). After 45 min. the reaction was allowed to cool to rt. After 1 h, addition of sat. aq. NH_4Cl (15 mL) followed by extraction with CH_2Cl_2 (3 × 10 mL), drying, evaporating and column chromatography (EtOAc / petroleum ether 3:7) yielded trace amounts of **74**: MS (ES +) *m/z* 367.1284 $[M + Na]^+$ ($C_{18}H_{20}N_2NaO_5$ requires 367.1270).

6.16 5,6,7-trimethoxy-1H-indole-2-carboxylic acid (75)

Compound **172** (2.98 g, 11.25 mmol) was added to a stirred solution of EtOH (50 mL) and aq. NaOH ($10\%_{w/w}$, 50 mL). After 17 h, the reaction mixture was concentrated to 50% volume, acidified to pH < 3 *via* dropwise addition of conc. HCl and extracted with EtOAc (3 30 mL). Drying and evaporating yielded **75** (913 mg, 32%) as an off-white solid: Rf 0.1 (EtOAc / petroleum ether 2:3); mp 216-217˚C (Lit.[200] mp 216-217˚C); ^1H NMR (400 MHz; $(CD_3)_2CO$) δ 3.87 (3 H, s, 5-OCH_3), 3.88 (3 H, s, 6-OCH_3), 4.02 (3 H, s, 7-OCH_3), 6.96 (1 H, s, 4-H), 7.11 (1 H, s, 3-H), 10.47 (1 H, br s, OH); MS (ES +) *m/z* 252.0729 $[M + H]^+$ ($C_{12}H_{13}NO_5$ requires 252.0866).
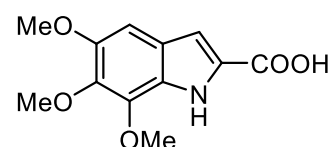
6.17   5-(2-Dimethylaminoethoxy)-1*H*-indole-2-carboxylic   acid hydrochloride (79)

Compound **169** (64 mg, 0.23 mmol) and aq. HCl (1.0 M, 10 mL) in EtOH (10 mL) were heated to reflux for 17 h. Drying and evaporation yielded **79.HCl** (57 mg, 86%) as a pale yellow solid: mp 237-238˚C (lit.[100] mp 238-239˚C); ^1H NMR (400 MHz; D_2O) δ 2.89 (6 H, s, $N(CH_3)_2$), 3.48 (2 H, t *J* = 5.1 Hz, NCH_2), 4.22 (2 H, m, OCH_2), 6.95 (1 H, dd, *J* = 6.4, 2.2 Hz, 4-H), 7.01 (1 H, d, *J* = 1.2 Hz, 3-H), 7.06 (1 H, dd, *J* = 8.2, 1.6 Hz, 6-H), 7.31 (1 H, d, *J* = 9.1 Hz, 7-H).
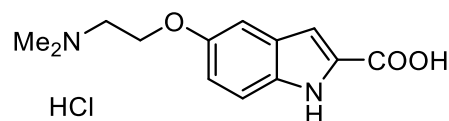
6.18 Ethyl 1-hydroxynaphthalene-2-carboxylate (82)

1-Hydroxynaphthalene-2-carboxylic acid **29** (16.5 g, 87.8 mmol) in EtOH (250 mL) was treated with H_2SO_4 (5 mL) and the mixture was boiled under reflux for 5 d, then allowed to cool. The evaporation residue, in CH_2Cl_2 (200 mL) was washed with sat. aq. $NaHCO_3$ (3 ×40 mL). Drying and evaporation yielded **82** as a buff solid (13.61 g, 72%): Rf 0.9 (EtOAc / petroleum ether 3:7); mp 46-47˚C (lit.[201] mp 46-47˚C); ^{1}H NMR (400 MHz; CDCl$_3$) δ 1.45 (3 H, t, J = 7.2 Hz, CH$_3$), 4.46 (2 H, q, J = 7.2 Hz, CH$_2$), 7.28 (1 H, d, J = 8.8 Hz, 4-H), 7.52 (1 H, ddd, J = 9.6, 7.8, 1.6 Hz, 7-H), 7.60 (1 H, ddd, J = 9.6, 7.4, 1.4 Hz, 6-H), 7.76 (1 H, d, J = 7.4 Hz, 5-H), 7.78 Hz (1 H, d, J = 8.8 Hz, 3-H), 8.42 (1 H, ddt, J = 7.8, 1.4, 0.8 Hz, 8-H), 12.09 (1 H, br, OH); ^{13}C NMR (100 MHz; CDCl$_3$) (HSQC / HMBC) δ 14.2 (CH$_3$), 61.4 (CH$_2$), 105.7 (2-C), 118.4 (4-C), 123.8 (8-C), 124.2 (8a-C), 124.7 (3-C), 125.6 (7-C), 127.4 (5-C), 129.3 (6-C), 137.1 (4a-C), 160.9 (1-C), 171.0 (CO).
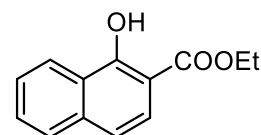
6.19 Ethyl 1-iodo-4-nitronaphthalene-2-carboxylate (85)

Compound **82** (10.19 g, 25.9 mmol) and NaI (13.8 g, 92 mmol) in acetone (200 mL) were heated to reflux for 17 h. The evaporation residue, in EtOAc (100 mL) was washed with sat. aq. Na$_2$S$_2$O$_3$ (4 × 70 mL). Drying and evaporation yielded **85** (9.25 g, 96%) as a dark black solid: Rf 0.8 (EtOAc / petroleum ether 3:7); ^{1}H NMR (400 MHz; CDCl$_3$) δ 1.47 (3 H, t, J = 7.2, CH$_3$), 4.51 (2 H, q, J = 7.2, CH$_2$), 7.76 (1 H, m, 7-H), 7.82 (1 H, m, 6-H), 8.31 (1 H, s, 3-H), 8.45 (1 H, dd, J = 7.2, 0.8 Hz, 5-H), 8.58 (1 H, dd, J = 7.2, 1.2 Hz, 8-H); ^{13}C NMR (100 MHz; CDCl$_3$) (HSQC / HMBC) δ 14.1 (CH$_3$), 62.7 (CH$_2$), 108.2 (1-C) 122.4 (3-C), 123.8 (5-C), 125.6 (4α-C), 130.1 (7-C), 131.3 (6-C), 135.1 (8-C), 147.3 (4-C), 166.3 (CO); MS (ES +) m/z 393.9555 [M + Na]$^+$ (C$_{13}$H$_{10}$INaNO$_4$ requires 393.9552), 371.9732 [M + H]$^+$ (C$_{13}$H$_{11}$INO$_4$ requires 371.9733); (ES -) m/z 369.9546 [M − H]$^-$ (C$_{13}$H$_{19}$INO$_4$ requires 369.9576).
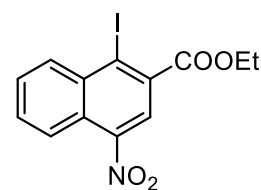
6.20 Methyl 1-hydroxynaphthalene-2-carboxylate (86)

1-Hydroxynaphthalene-2-carboxylic acid **29** (2.00 g, 10.6 mmol) in a mixture of methanol (100 mL) and H_2SO_4 (1 mL) was heated to reflux for 7 d. The evaporation residue, in EtOAc (30 mL), was washed with H_2O (3 × 30 mL) then brine (3 × 30 mL). Drying, evaporation and column chromatography (EtOAc / petroleum ether 3:7) yielded **86** (589 mg, 27%) as a pale buff solid: mp 77-78˚C (lit[202] mp 77-79˚C); ^{1}H NMR (400 MHz; $(CD_3)_2SO$) δ 3.99 (3 H, s, CH_3), 7.27 (1 H, d, J = 8.8 Hz, 3-H), 7.52 (1 H, ddd, J = 9.6, 6.9, 1.3 Hz, 7-H), 7.60 (1 H, ddd, J = 9.5, 6.9, 1.4 Hz, 6-H), 7.76 (2 H, m, 4,5-H_2), 8.42 (1 H, m, 8-H), 11.99 (1 H, s, OH).
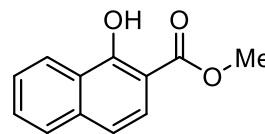
6.21 2-Methoxyethyl 1-hydroxynaphthalene-2-carboxylate (87)

1-Hydroxynaphthalene-2-carboxylic acid **29** (1.02 g, 5.42 mmol) in a mixture of 2-methoxyethanol (50 mL) and H_2SO_4 (1 mL) was heated to reflux for 72 h. The evaporation residue, in EtOAc (30 mL), was washed with sat. aq. $NaHCO_3$ (3 × 30 mL), then H_2O (3 × 30 mL). Drying and evaporation yielded **87** (930 mg, 70%) as a pale white gummy solid: Rf 0.1 (EtOAc / petroleum ether 3:7); ^{1}H NMR (400 MHz; $(CD_3)_2SO$) δ 3.39 (3 H, s, CH_3), 3.77 (2 H, m, CH_2OCH_3), 4.56 (2 H, m, CO_2CH_2), 7.49 (1 H, d, J = 8.6 Hz, 4-H), 7.66 (1 H, ddd, J = 9.4, 6.9, 1.1 Hz, 7-H), 7.75 (1 H, ddd, J = 9.2, 7.0, 1.2 Hz, 6-H), 7.80 (1 H, d, J = 8.8 Hz, 5-H), 7.97 (1 H, d, J = 8.0 Hz, 3-H), 8.36 (1 H, d, J = 8.5 Hz, 8-H), 11.92 (1 H, s, OH).
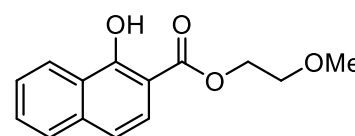
6.22 Ethyl 1-hydroxy-4-nitronaphthalene-2-carboxylate (83)

Compound **82** (47.85g, 0.22 mol) in AcOH (200 mL) was treated with HNO_3 (70%, 35 mL, 0.55 mol). After 2 h, the reaction was quenched by addition of aq. NaOH (1 M) until basic. The mixture was extracted with CH_2Cl_2 (3 × 100 mL). Drying and evaporation yielded **83** as a yellow crystalline solid (54.38 g, 95%): Rf 0.1 (EtOAc / petroleum ether 1:1); mp 87-88˚C (lit.[199] mp 87-88˚C); ^{1}H NMR (400 MHz; $CDCl_3$) δ 1.45 (3 H, t, J = 8.0 Hz, CH_3), 4.48 (2 H, q, J = 8.0 Hz, CH_2),
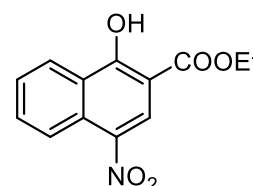
7.62 (1 H, ddd, J = 8.4, 7.1, 1.2 Hz, 7-H), 7.81 (1 H, ddd, J = 8.6, 7.1, 1.4 Hz, 6-H), 8.50 (1 H, ddd, J = 8.4, 1.4, 0.8 Hz, 8-H), 8.71 (1 H, ddd, J = 8.6, 1.2, 0.8 Hz, 5-H), 8.77 (1 H, s, 3-H); MS (ES -) m/z 260.0522 [M – H]$^-$ ($C_{13}H_{10}NO_5$ requires 260.0564).

6.23 Ethyl 4-nitro-1-(((trifluoromethyl)sulfonyl)oxy)-2-naphthoate (84)

Under N$_2$ at 0°C, Trifluoromethanesulfonic anhydride (10.00 g, 35.4 mmol) was added dropwise to a stirred solution of Compound **83** (7.05 g, 27.0 mmol) and NEt$_3$ (9.8 mL 70.3 mmol) in CH$_2$Cl$_2$ (150 mL) and the reaction mixture was then allowed to warm to room temperature. After 2 h, aq. HCl (1 M, 60 mL) was added and the reaction mixture stirred for a further 17 h. The organic phase was separated, and the aqueous phase was extracted with CH$_2$Cl$_2$ (3 × 30 mL). The combined organic phases were washed with sat. aq. NaHCO$_3$ (3 × 100 mL). Drying and evaporating yielded **84** (10.19 g, 96%) as a yellow solid: mp 118-120°C; Rf 0.5 (EtOAc / petroleum ether 1:9); ^{1}H NMR (500 MHz; CDCl$_3$) (HMBC, HSQC) δ 1.47 (3 H, t, J = 6.6 Hz, CH$_3$), 4.53 (2 H, q, J = 7.1 Hz, CH$_2$), 7.84 (1 H, ddd, J = 9.7, 6.9, 1.2 Hz, 7-H), 7.92 (1 H, ddd, J = 9.9, 6.9, 1.3 Hz, 6-H), 8.30 (1 H, d, J = 8.7 Hz, 8-H), 8.58 (1 H, d, J = 8.7 Hz, 5-H), 8.73 (1 H, s, 3-H); ^{13}C NMR (125 MHz; CDCl$_3$) (HSQC, HMBC) δ 14.2 (CH$_3$), 63.2 (CH$_2$), 122.9 (8-C), 123.7 (5-H), 124.6 (3-H), 125.8 (2-C), 127.6 (8a-C), 127.8 (4a-C), 129.5 (7-C), 132.3 (6-C), 145.5 (4-C), 147.3 (1-C), 163.2 (C=O); ^{19}F NMR (470MHz; CDCl$_3$) δ -72.5 (CF$_3$); MS (ES +) m/z 416.0006 [M + Na]$^+$ ($C_{14}H_{10}F_3N_1NaO_7S$ requires 416.0022).
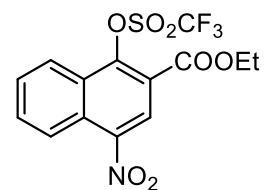
6.24 *tert*-butyl (4-aminonaphthalen-2-yl)carbamate (110)

Compound **72** (47 mg, 0.114 mmol) and Pd/C (10%, 40 mg) in MeOH (10 mL) were stirred vigorously under H$_2$. After 3 h, TLC showed only starting material. Pd/C (10%, 40 mg) was added and the mixture stirred vigorously for 17 h. The reaction mixture was filtered through Celite®. Drying, evaporation and column chromatography (EtOAc / petroleum
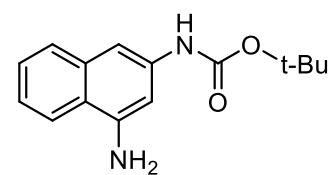
ether 3:7) yielded **110** (19 mg, 65%) as a dark brown oil: Rf 0.2 (EtOAc / petroleum ether 3:7); ^{1}H NMR (400 MHz; CDCl$_3$) δ 1.49 (9 H, s, ^{t}Bu), 6.47 (1 H, br s, NH), 6.86 (1 H, d, *J* = 1.7 Hz, 3-H), 7.21 (1 H, d, *J* = 1.8 Hz, 1-H), 7.27 (1 H, ddd, *J* = 9.6, 6.8, 1.2 Hz, 6-H), 7.35 (1 H, ddd, *J* = 9.3, 6.8, 1.2 Hz, 7-H), 7.63 (1 H, d, *J* = 8.4 Hz, 8-H), 7.66 (1 H, d, *J* = 8.8 Hz, 5-H); MS (ES+) *m/z* 281.1247 [M + Na]$^+$ (C$_{15}$H$_{18}$N$_2$O$_2$Na requires 281.1290).

6.25 Ethyl-1-(trifluoromethanesulfonyloxy)naphthalene-2-carboxylate (113).

Under N$_2$, **82** (1.06 g, 4.90 mmol) and NEt$_3$ (1.3 mL, 9.40 mmol) in CH$_2$Cl$_2$ (15 mL) were stirred for 5 min at 0˚C. Trifluoromethanesulfonic anhydride (1.10 mL, 1.83 g, 6.53 mmol) was added dropwise and the reaction mixture was allowed to warm to room temperature. After 72 h, aq. HCl (1 M, 10 mL) was added. After 0.5 h, the reaction mixture was washed with sat. aq. NaHCO$_3$ (3 × 10 mL), then brine (3 × 10 mL). Drying and evaporation yielded **113** (1.41 g, 83%) as a white solid: Rf 0.3 (EtOAc / petroleum ether 1:4); ^{1}H NMR (500 MHz; CDCl$_3$) δ 1.41 (3 H, t, *J* = 7.2 Hz, CH$_3$), 4.45 (2 H, q, *J* = 7.2 Hz, CH$_2$), 7.58 (1 H, m, 7-H), 7.62 (1 H, m, 6-H), 7.81 (1 H, d, *J* = 8.6 Hz, 4-H), 7.83 (1 H, m, 8-H), 7.92 (1 H, d, *J* = 8.6 Hz, 3-H), 8.12 (1 H, m, 5-H); ^{13}C NMR (125 MHz; CDCl$_3$) (HMBC, HSQC) δ 14.1 (CH$_3$), 62.0 (CH$_2$), 121.9 (2-C), 122.0 (5-C), 126.1 (3,4-C$_2$), 127.9 (8α-C), 128.0 (8-C), 128.1 (6-C), 129.0 (7-C), 136.4 (4α-C), 144.6 (1-C), 164.8 (C=O); ^{19}F NMR (470MHz; CDCl$_3$) δ -73.0 (CF$_3$).
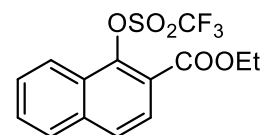
## 6.26 Attempted synthesis of ethyl 1-iodo-2-naphthoate (114)

Compound **113** (1.41 g, 4.05 mmol) and NaI (1.85 g, 12.3 mmol) in acetone (30 mL) were heated to reflux for 17 h. The evaporation residue, in EtOAc (30 mL) was washed with sat. aq. Na$_2$S$_2$O$_3$ (4 × 30 mL). Drying and evaporation yielded starting material **113** (952 mg, 68%).
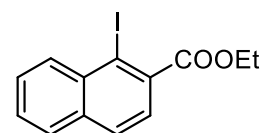
Compound **113** (952 mg, 2.75 mmol) and NaI (9.1 g, 27.5 mmol) in toluene (15 mL) were heated to reflux for 7 d. TLC confirmed starting material. The evaporation residue in DMF (20 mL) was heated to reflux for 5 d. The evaporation residue, in EtOAc (30 mL) was washed with H_2O (4 × 30 mL). Drying and evaporation yielded starting material **113** (711 mg, 75%).

6.27 *tert*-butyl (1-iodonaphthalen-2-yl)carbamate (116)

NIS (101 mg, 0.45 mmol) and **120** (100 mg, 0.41 mmol) in MeCN (5 mL) were heated to reflux for 17 h. The evaporation residue, in CH_2Cl_2 (10 mL), was washed with Na_2SO_3 (3 × 10 mL) and H_2O (3 ×
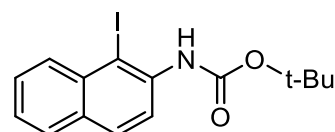
10 mL), Drying and evaporation yielded **116** (81 mg, 54%) as a dark brown oil: ^{1}H NMR (400 MHz; $CDCl_3$) δ 1.53 (9 H, s, [t]Bu), 6.62 (1 H, br s, NH), 7.27-7.33 (2 H, m, 6,7-H_2), 7.49 (1 H, ddd, J = 9.9, 6.9, 1.3 Hz, 5-H), 7.87 (1 H, d, J = 8.4 Hz, 3-H), 8.02 (1 H, d, J = 8.8 Hz, 4-H), 8.21 (1 H, d, J = 8.8 Hz, 8-H); MS (ES +) *m/z* 392.0174 $[M + Na]^+$ ($C_{15}H_{16}NO_2I$ requires 392.0118).

6.28 Attempted synthesis of *tert*-butyl *(S)*-1-(hydroxymethyl)-1,2-dihydro-3H-benzo[e]indole-3-carboxylate (118)

At 0°C, ZnCl$_2$ (0.5 M in THF, 0.69 mL, 0.35 mmol) was added to stirred an. THF (6 mL) followed by dropwise addition of MeLi (1.6 M in THF, 0.86 mL, 4.35 mmol) under Ar. After 0.5 h, the reaction mixture was cooled to -78°C followed by addition of TMS-NCS (50 µL, 0.35 mmol). The reaction mixture was allowed to warm to 0°C and after 0.5 h, was cooled to -78°C followed by dropwise addition of **122** (87 mg, 0.23 mmol in an. THF (4 mL)). After 0.5 h, the reaction mixture was allowed to warm to rt. After 17 h, NH$_4$Cl

118

125
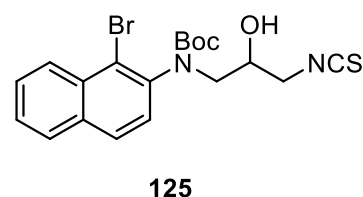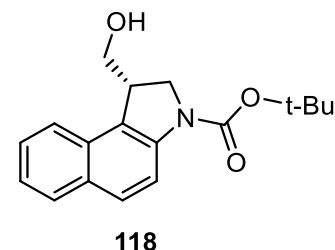
(20 mL) was added and the reaction mixture stirred for a further 0.5 h. Extraction with CH$_2$Cl$_2$ (3 × 20 mL), drying, evaporation and column chromatography (EtOAc / petroleum ether 15:85) yielded **125** (16 mg, 16%) as a yellow oil: Rf 0.8 (EtOAc / petroleum ether 3:7); MS (ES +) *m/z* 436.0380 [M]$^+$ (C$_{19}$H$_{21}$^{79}BrN$_2$O$_3$S requires 436.0456), 438.0360 [M]$^+$ (C$_{19}$H$_{21}$^{79}BrN$_2$O$_3$S requires 438.0436).

6.29 *tert*-Butyl N-(naphthalen-2-yl)carbamate (120)

Naphthalene-2-carboxylic acid (500 mg, 2.90 mmol) and 4Å molecular sieves (1.00 g, powdered) in anhydrous ^{t}BuOH (20 mL) were treated with DPPA (0.62 mL, 800 mg, 2.90 mmol) and NEt$_3$
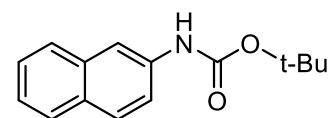
(405 mL, 2.90 mmol). The reaction mixture was heated to 80°C for 16 h. The evaporation residue was purified by column chromatography (EtOAc / petroleum ether (1:4) to yield **120** (544 mg, 77%) as a white powder: mp 92-93°C (lit.[203] mp 92-93°C); Rf 0.8 (EtOAc / petroleum ether 3:7); ^{1}H NMR (400 MHz; CDCl$_3$) δ 1.53 (9 H, s, ^{t}Bu), 6.60 (1 H, br s, NH), 7.28-7.34 (2 H, m, 3,4-H$_2$), 7.39 (1 H, ddd, J = 8.4 Hz, 6.8 Hz, 1.2 Hz, 5-H), 7.70-7.73 (3 H, m, 6,7,8-H$_3$), 7.94 (1 H, br s, 1-H); MS (ES +) *m/z* 267.1231 [M + Na]$^+$ (^{12}C$_{14}$^{13}CH$_{17}$NNaO$_2$ requires 267.1184), 266.1199 [M + Na]$^+$ ^{12}C$_{15}$H$_{17}$NNaO$_2$ (requires 266.1151).

6.30 *tert*-Butyl N-(1-bromonaphthalen-2-yl)carbamate (121)

Compound **120** (190 mg, 0.781 mmol) and *N*-bromosuccinimide (152 mg, 0.854) in MeCN (10 mL) were stirred at rt for 3 h. The evaporation residue, in CH_2Cl_2 (10 mL), was washed with sat. aq. Na_2SO_3 (3 × 10 mL) and H_2O (3 × 10 mL). Drying and evaporation yielded **121** (251 mg, 100%) as a dark red semi-solid: Rf 0.6 (EtOAc / petroleum ether 3:7); ^{1}H NMR (400 MHz; CDCl$_3$) δ 1.54 (9 H, s, ^{t}Bu), 7.28 (1 H, br s, NH), 7.37 (1 H, ddd, *J* = 9.2, 6.9, 1.0 Hz, 6-H) 7.51 (1 H, ddd, *J* = 9.9, 7.0, 1.3 Hz, 7-H), 7.73 (1 H, dd, *J* = 8.2, 0.8, 0.6 Hz, 5-H),7.74 (1 H, d, *J* = 9.0 Hz, 3-H), 8.09 (1 H, dd, *J* = 8.5, 0.8 Hz, 4-H), 8.32 (1 H, d, *J* = 9.0 Hz, 8-H); MS (ES +) *m/z* 346.02 [M + Na]$^+$ (C$_{15}$H$_{16}$^{81}BrNNaO$_2$ requires 346.02), 344.03 [M + Na]$^+$ (C$_{15}$H$_{16}$^{79}BrNNaO$_2$ requires 344.03); MS (ES -) *m/z* 320.0287 [M − H]$^-$ (C$_{15}$H$_{15}$^{79}BrNO$_2$ requires 320.0286).
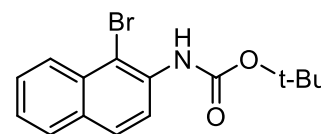
6.31 *tert*-butyl *(S)*-(1-bromonaphthalen-2-yl)(oxiran-2-ylmethyl)carbamate (122)

Under Ar, NaH (20 mg, 0.84 mmol) was added to a stirred solution of compound **121** (95 mg, 0.30 mmol) and *R*-glycidyl nosylate (114 mg, 0.44 mmol) in an. DMF (4 mL) at 0°C. After 1.5 h, the reaction mixture was allowed to warm to rt and stirred for a further 17 h. The mixture was extracted with EtOAc (3 × 5 mL) and the combined organic phase washed with H_2O (3 × 5 mL) and brine (3 × 5 mL). Drying, evaporating and column chromatography (EtOAc / petroleum ether 3:7) yielded **122** (98 mg, 89%) as a yellow oil and as a pair of inseparable rotamers about the Ar-C-N bond: Rf 0.5 (EtOAc / petroleum ether 3:7); ^{1}H NMR (500 MHz; CDCl$_3$) (HSQC, HMBC) δ 1.28 (4.5 H, s, ^{t}Bu), 1.29 (4.5 H, s, ^{t}Bu), 2.36 (0.5 H, dd, *J* = 4.7, 2.6 Hz, CH$_2$O), 2.44 (0.5 H, dd, *J* = 4.7, 2.6 Hz, CH$_2$O), 2.70 (1 H, q, *J* = 4.2 Hz, CH$_2$O), 3.16 (0.5 H, m, CHO), 3.22 (0.5 H, dd *J* = 14.7, 7.4 Hz, NCH), 3.34 (0.5 H, m, CHO), 3.59 (0.5 H, dd, *J* = 14.5, 5.0 Hz, NCH), 3.99 (0.5 H, dd, *J* = 14.7, 5.0 Hz, NCH), 4.14 (0.5 H, dd, *J* = 14.5, 3.7 Hz, NCH), 7.30 (0.5 H, d, *J* = 8.1 Hz, 3-H), 7.39 (0.5 H, d, *J* = 8.6 Hz, 3-H), 7.50 (1 H, m, 6-H), 7.56 (1 H, m, 7-H), 7.74-7.81 (2 H, m, 4,5-H$_2$), 8.27 (1 H, br t, *J* = 7.7 Hz, 8-H); ^{13}C NMR (125 MHz; CDCl$_3$) δ 28.1 (^{t}Bu), 28.3 (^{t}Bu), 45.8 (CH$_2$O), 46.1 (CH$_2$O), 49.9 (CHO), 50.4 (CHO), 51.0 (NCH), 52.5 (NCH), 80.6 (^{t}Bu), 80.7 (^{t}Bu),
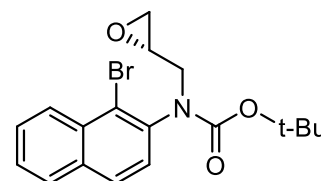
123.6 (4a-C), 123.7 (4a-C), 126.7 (6-C), 126.8 (6-C), 127.4 (7-C), 127.5 (7-C), 127.6 (3-C), 127.7 (3-C), 128.0 (4 or 5-C), 128.1 (4 or 5-C), 128.3 (4 or 5-C), 128.4 (4 or 5-C), 132.7 (8a-C), 132.8 (8a-C), 133.4 (1-C), 133.5 (1-C), 139.5 (2-C), 139.6 (2-C), 154.9 (CO), 155.0 (CO); MS (ES +) *m/z* 378.0487 [M + H]$^+$ (C$_{18}$H$_{20}$^{79}BrNO$_3$ requires 378.0699).

6.32 4-Bromo-1-hydroxynaphthalene-2-carboxylic acid (126)

Compound **29** (670 mg, 3.56 mmol) and *N*-bromosuccinimide (760 mg, 4.28 mmol) in CH$_2$Cl$_2$ (50 mL) were stirred at rt. After 3 h, *N*-bromosuccinimide (178 mg, 1.00 mmol) was added. After 24 h, the evaporation residue, in EtOAc (30 mL), was washed with aq. NaOH (1.0 M, 3 × 20 mL). Drying and evaporation yielded **126** (452 mg, 47%) as a white solid: mp >230˚C (lit.[204] mp 238˚C); Rf 0.7 (EtOAc / petroleum ether 3:7); ^{1}H NMR (400 MHz; (CD$_3$)$_2$CO) δ 7.71 (1 H, ddd, *J* = 8.4 Hz, 6.8 Hz, 1.2 Hz, 7-H), 7.79 (1 H, ddd, *J* = 8.0 Hz, 6.8 Hz, 1.2 Hz, 6-H), 7.96 (1 H, s, 3-H), 8.18-8.21 (1 H, m, 5-H), 8.40 (1 H, m, 8-H) 8.88 (1 H, br s, OH); ^{13}C NMR (100 MHz; (CD$_3$)$_2$CO) (HSQC, HMBC) δ 103.3 (2-C), 112.2 (4-C), 123.7 (8-C), 127.3 (8a-C), 127.7 (5-C), 127.9 (7-C) 129.1 (6-C), 132.6 (4a-C), 133.0 (3-C), 135.3 (1-C), 149.7 (C=O), MS (ES -) *m/z* 266.9478 [M − H]$^-$ (C$_{11}$H$_6$^{81}BrO$_3$ requires 266.9485), 264.9503 [M − H]$^-$ (C$_{11}$H$_6$^{79}BrO$_3$ requires 264.9500).
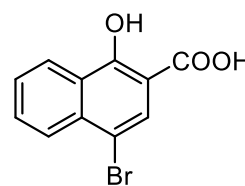
6.33 4-bromo-1-(((trifluoromethyl)sulfonyl)oxy)-2-naphthoic acid (127)

Under N$_2$, Compound **126** (115 mg, 0.43 mmol) and NEt$_3$ (2.00 mL, 14.35 mmol) in CH$_2$Cl$_2$ (8 mL) were stirred at 0˚C. Trifluoromethanesulfonic anhydride (94 µL, 0.56 mmol) was added dropwise and the reaction mixture was allowed to warn to room temperature. After 4 h, aq. HCl (1 M, 20 mL) was added and the reaction mixture was stirred for a further 17 h. The organic phase was separated, and the aqueous phase was extracted with CH$_2$Cl$_2$ (3 × 20 mL). The combined organic phases were washed with sat. aq. NaHCO$_3$ (3 × 20 mL). Drying and evaporating yielded **127** (85 mg, 50%)
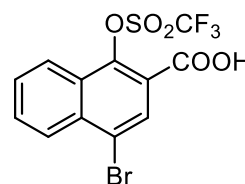
as an off-white semi-solid: Rf 0.2 (EtOAc / petroleum ether 3:7); ^{1}H NMR (400 MHz; CDCl$_3$) (HSQC, HMBC) δ 7.56 (1 H, ddd, *J* = 9.5, 7.0, 1.4 Hz, 7-H), 7.62 (1 H, ddd, *J* = 9.7, 6.9, 1.4 Hz, 6-H), 7.79 (1 H, s, 3-H), 8.13 (1 H, ddd, *J* = 8.5, 1.0, 0.6 Hz, 5-H), 8.25 (1 H, ddd, *J* = 8.2, 1.4, 0.6 Hz, 8-H); ^{13}C NMR (100 MHz; CDCl$_3$) (HSQC, HMBC) δ 103.3 (2-C), 113.6 (4-C), 122.8 (8-C), 125.2 (8a-C), 126.9 (7-C), 127.1 (5-C), 128.1 (6-C), 131.1 (3-C), 132.0 (4a-C), 148.4 (1-C), 162.8 (C=O).

6.34 Attempted synthesis of 4-bromo-1-iodonaphthalene-2-carboxylic acid (128)

Synthesis of 4-bromonaphthalen-1-ol (137)

Compound **127** (62 mg, 0.16 mmol) was stirred with NaI (75 mg, 0.50 mmol) in acetone (10 mL) at reflux for 72 h. The evaporation residue, in EtOAc (15 mL), was washed with sat. aq. Na$_2$S$_2$O$_3$ (3 × 10 mL). Drying and evaporation yielded crude **137** as a dark brown solid: mp 125-126˚C (Lit.[205] mp 126-127˚C) Rf 0.2 (EtOAc / petroleum ether 3:7); ^{1}H NMR (500 MHz; CDCl$_3$) δ 5.80 (1 H, br s, OH), 6.70 (1 H, d, *J* = 8.4 Hz), 7.50-7.65 (3 H, m), 8.15 (1 H, d, *J* = 8.5 Hz), 8.18 (1 H, d, *J* = 8.5 Hz); ^{19}F NMR (470 MHz; CDCl$_3$) showed no peaks; MS (ES -) *m/z* 222.9537 [M − H]$^-$ (C$_{10}$H$_6$^{81}BrO requires 222.9582), 20.9558 [M − H]$^-$ (C$_{10}$H$_6$^{79}BrO requires 220.9602).
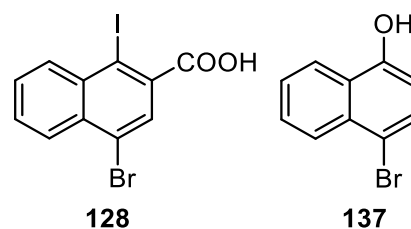
6.35 Ethyl 4-bromo-1-hydroxynaphthalene-2-carboxylate (138)

Compound **82** (400 mg, 2.14 mmol) and *N*-bromosuccinimide (533 mg, 3.00 mmol) in CH$_2$Cl$_2$ (25 mL) were stirred at rt. After 17 h, the evaporation residue in EtOAc (30 mL) was washed with aq. NaOH (1 M, 3 × 10 mL). Drying and evaporation yielded **138** (438 mg, 69%) as an off-white solid: mp 88-89˚C (lit.[206] mp 86-87˚C); ^{1}H NMR (400 MHz; CDCl$_3$) δ 1.42 (3 H, t, *J* = 7.2 Hz, CH$_3$), 4.42 (2 H, q, *J* = 7.2 Hz, CH$_2$), 7.54 (1 H, ddd, *J* = 8.4 Hz, 7.2 Hz, 1.2 Hz, 7-H), 7.68 (1 H, ddd, *J* = 8.0 Hz, 6.8
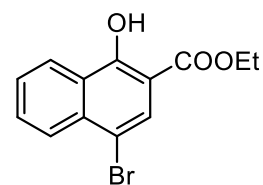
Hz, 1.2 Hz, 6-H), 8.04 (1 H, s, 3-H), 8.11 (1 H, d, J = 7.6 Hz, 5-H), 8.40 (1 H, d, J = 8.0 Hz, 8-H), 11.98 (1 H, s, OH).

6.36 Attempted synthesis of ethyl 4-amino-1-iodo-2-naphthoate (139)

Under N_2, compound **85** (500 mg, 1.35 mmol) and DIPEA (1.17 mL, 6.74 mmol) in an. MeCN (10 mL) were cooled to 0°C. $HSiCl_3$ (0.68 mL, 4.72 mmol) in an. MeCN (4mL) was added dropwise over 10 min. The stirred reaction mixture was allowed to warm to rt. After 17 h, sat. aq. $NaHCO_3$ (12 mL) was added and the mixture stirred for a further 2 h. Extraction with EtOAc (3 × 20 mL) followed by washing with brine (3 × 20 mL), drying and evaporating yielded **145** as a buff solid (227 mg, 78%).
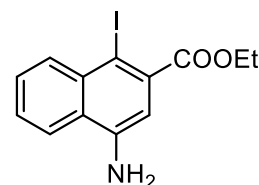
6.37 Synthesis of *tert*-butyl (4-amino-1-iodonaphthalen-2-yl)carbamate (140)

Under N_2, **72** (144 mg, 0.35 mmol) and Pr^i_2NEt (0.30 mL, 1.70 mmol) in an. MeCN (2.5 mL) were cooled to 0°C. $HSiCl_3$ (127 μL, 1.26 mmol) in an. MeCN (1 mL) was added dropwise during 10 min. The stirred reaction mixture was allowed to warm to rt. After 17 h, sat. aq. $NaHCO_3$ (3 mL) was added and the mixture was stirred for a further 0.5 h. Extraction with EtOAc (3 × 10 mL), drying (Na_2SO_4) and column chromatography (EtOAc / petroleum ether 1:9) yielded only trace amounts of **140**: MS (ES +) m/z 385.0474 [M + H]$^+$ ($C_{15}H_{17}IN_2O_2$ requires 385.0408).
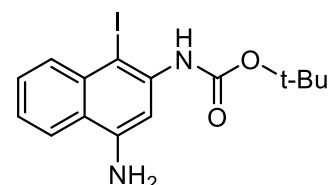
6.38 Ethyl 1-aminonaphthalene-3-carboxylate (143)[207]

$SnCl_2 \cdot 2H_2O$ (8.46 g, 37.5 mmol) was added to **85** (913 mg, 2.5 mmol) in EtOAc (60 mL) and the mixture was boiled under reflux for 17 h. The mixture was cooled, ice was added and aq. NaOH (1 M) was added until
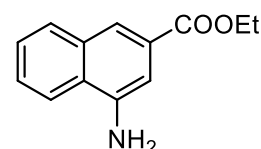
the mixture became basic. The mixture was extracted with EtOAc (3×30 mL) and the organic layers were combined and washed with H_2O (3×30 mL) and brine (30 mL). Drying and evaporating yielded **143** (289 mg, 54%) as a buff solid: ^1H NMR (400 MHz; $CDCl_3$) δ 1.39 (3 H, t, J = 7.1 Hz, CH_3), 4.21 (2 H, s, NH_2), 4.37 (2 H, q, J = 7.1 Hz, CH_2), 7.32 (1 H, d, J = 1.6 Hz, 2-H), 7.51 (1 H, ddd, J = 8.0, 6.8, 1.4 Hz, 6-H) 7.55 (1 H, ddd, J = 8.4, 6.9, 1.8 Hz, 7-H), 7.79 (1 H, m, 8-H), 7.85-7.87 (1 H, m, 5-H), 8.02 (s, 4-H); ^{13}C NMR (100 MHz; $CDCl_3$) (DEPT135, HMBC) δ 14.4 (CH_3), 61.0 (CH_2), 108.5 (2-C), 120.8 (8-C), 121.8 (4-C), 125.7 (8α-C), 126.5 (6-C), 127.1 (7-C), 128.1 (3-C), 130.0 (5-C), 133.5 (4α-C), 142.3 (1-C), 167.0 (C=O); MS (ES +) *m/z* 218.1100 [M + H]$^+$ ($^{12}C_{11}^{13}C_2H_{13}NO_2$ requires 218.1077), 217.1076 [M + H]$^+$ ($^{12}C_{12}^{13}C_1H_{13}NO_2$ requires 217.1051), 216.1046 [M + H]$^+$ ($^{12}C_{13}H_{13}NO_2$ requires 216.1019).

6.39 Ethyl 4-(*tert*-butoxycarbonylamino)naphthalene-2-carboxylate (144)

Boc$_2$O (854 μL, 3.72 mmol) was added to **143** (400 mg, 1.86 mmol) in THF (50 mL) and the mixture was heated to reflux for 17 h. Evaporation and column chromatography (EtOAc / petroleum ether 3:7) yielded **144** (995 mg, 85%) as an off-white semi-solid: Rf 0.5 (EtOAc / petroleum ether 3:7); ^1H NMR (400 MHz; $CDCl_3$) (HMBC, HSQC) δ 1.44 (3 H, t, J = 7.2 Hz, CH_3), 1.56 (9 H, s, ^tBu), 4.44 (2 H, q, J = 7.2 Hz, CH_2), 6.83 (1 H, br s, NH), 7.55 (1 H, ddd, J = 9.2, 6.9, 1.0, 7-H), 7.62 (1 H, ddd, J = 9.9, 6.9, 1.5, 6-H), 7.91 (1 H, d, J = 8.6 Hz, 5-H), 7.96 (1 H, d, J = 8.1 Hz, 8-H), 8.40 (2 H, br s, 1,3-H); ^{13}C NMR (100 MHz; $CDCl_3$) (HMBC, HSQC) δ 14.6 (CH_3), 28.6 (C(CH_3)$_3$), 61.4 (CH_2), 80.9 (*C*(CH_3)$_3$), 118.2 (1-C or 3-C), 126.6 (7-C), 127.5 (1-C or 3-C), 127.8 (2-C or 4-C), 128.3 (6-C), 128.8 (4α-C), 130.2 (8-C), 133.2 (8α-C), 133.3 (2-C or 4-C), 153.3 (*C*OO^{t}Bu), 166.6 (*C*OOEt); MS (ES -) *m/z* 316.1385 [M − H]$^-$ ($^{13}C_2^{12}C_{16}H_{21}NO_4$ requires 316.1446), 315.1365 [M − H]$^-$ ($^{13}C_1^{12}C_{17}H_{21}NO_4$ requires 315.1420), 314.1333 [M − H]$^-$ ($^{12}C_{18}H_{21}NO_4$ requires 314.1387).
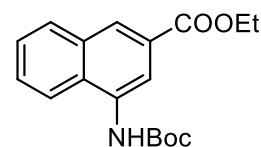
6.40 Attempted synthesis of *tert*-butyl (3-((2-oxo-2-phenyl-1γ^2-ethyl)amino)naphthalen-1-yl)carbamate (145)

Under N$_2$, DPPA (176 μL, 0.80 mmol) was added to a stirred solution of compound **147** (236 mg, 0.80 mmol) and NEt$_3$ (75 μL, 0.54 mmol) in anhydrous 1,4-dioxane (10 mL). After 0.5 h, the reaction mixture was poured into H$_2$O (20 mL) and extracted with Et$_2$O (3 × 10 mL). The combined organic phases were washed with H$_2$O (10 mL) and brine (10 mL), Drying over Na$_2$SO$_4$ and evaporating yielded the acid azide intermediate which was used without purification. The acid azide intermediate in xylene (10 mL) was heated to rf for 17 h and then cooled to 0°C. Benzyl alcohol (128 μL, 1.23 mmol) and NEt$_3$ (100 μL, 0.72 mmol) were added to the reaction mixture and stirred for a further 2 h. The reaction mixture was quenched *via* addition of H$_2$O (30 mL) and extracted with EtOAc (3 × 30 mL). Drying and evaporating failed to yield the desired product.
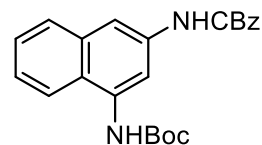
6.41 4-((*tert*-butoxycarbonyl)amino)-2-naphthoic acid (147)

NaOH (10%, 20 mL) was added to a stirred solution of compound **144** (467 mg, 1.48 mmol) in EtOH (30 mL). After 17 h, the solution pH was adjusted to 1 with HCl (1 M) and extracted with EtOAc (3 × 30 mL). Drying and evaporating yielded **147** (380 mg, 89%) as an off white semi-solid: Rf 0.1 (EtOAc / petroleum ether 3:7); ^{1}H NMR (400 MHz; CDCl$_3$) δ 2.10 (9 H, s, ^{t}Bu), 7.74-7.85 (3 H, m, 1,6,7-H$_3$), 8.44 (1 H, d, *J* = , 5 or 8-H), 8.46 (1 H, s, 3-H), 8.62 (1 H, d, *J* = , 5 or 8-H), 10.01 (1 H, br s, OH); ^{1}H NMR ((CD$_3$)$_2$SO) (HMBC, HSQC) δ 1.57 (9 H, s, ^{t}Bu), 7.66 (1 H, ddd, *J* = 8.9, 6.8. 1.0 Hz, 7-H), 7.71 (1 H, ddd, *J* = 10.0, 7.1, 1.4 Hz, 6-H), 8.15-8.19 (3 H, m, 1,5,8-H), 8.43 (1 H, s, 3-H), 9.45 (1 H, s, NH); ^{13}C NMR (100 MHz; (CD$_3$)$_2$SO) (HMBC, HSQC) δ 28.7 (^{t}Bu), 80.2 (^{t}Bu), 119.9 (1-C), 123.4 (5-C), 127.3 (3-C), 127.4 (7-C), 128.5 (6-C), 129.9 (4a-C), 130.1 (8-C), 133.3 (8a-C), 153.9 (COO^{t}Bu), 167.9 (COOH); MS (ES +) *m/z* 310.1040 [M + Na]$^+$ (C$_{16}$H$_{17}$NNaO$_4$ requires 310.1055); MS (ES -) *m/z* 286.1075 [M − H]$^-$ (C$_{16}$H$_{16}$NO$_4$ requires 286.1079).
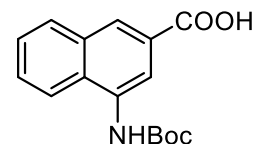
6.42 *tert*-Butyl N-(1-iodo-4-nitronaphthalen-2-yl)-N-(prop-2-enyl)carbamate (148)
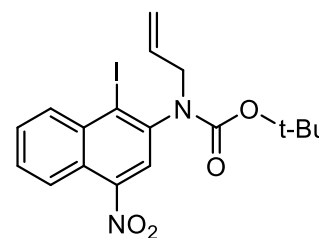
Allyl bromide (59 µL, 0.69 mmol) was added to **72** (85 mg, 0.21 mmol) and K$_2$CO$_3$ (116 mg, 0.84 mmol) in acetone (15 mL). The reaction mixture was heated to 50˚C for 48 h. The evaporation residue was purified by column chromatography (EtOAc / petroleum ether 1:9) to yield two inseparable rotamers about the 2-C-N bond of **148** (77 mg, 81%) as an orange semi-solid: Rf 0.6 (EtOAc / petroleum ether 3:7); ^{1}H NMR (500 MHz; CDCl$_3$) (HSQC) δ 1.27 (4.5 H, s, ^{t}Bu), 1.47 (4.5 H, s, ^{t}Bu'), 3.81 (0.5 H, dd, J = 14.3, 7.1 Hz, NCH), 4.57 (0.5 H, dd, J = 13.7, 4.3 Hz, NCH), 5.02 (0.5 H, d, J = 16.7 Hz, *trans*-3'-H), 5.07 (0.5 H, d, J = 10.4 Hz, *cis*-3'-H), 5.92 (0.5 H, m, 2'-H), 7.65 (1 H, t, J = 6.9 Hz, 7-H), 7.70 (1 H, t, J = 6.9 Hz, 6-H), 7.90 (0.5 H, br s, r-3-H), 7.97 (0.5 H, br s, r'-3-H), 8.37 (1 H, d, J = 8.1 Hz, 8-H), 8.42 (1 H, d, J = 8.1 Hz, 5-H); ^{13}C NMR (125 MHz; CDCl$_3$) (HSQC) δ 28.4 (^{t}Bu), 52.2 (1'-C), 119.5 (3'-C), 123.7 (5-C), 124.6 (3-C), 129.3 (7-C), 130.0 (6-C), 133.1 (2'-C), 134.5 (8-C), 145.7 (4-C), 157.2 (C=O); MS (ES +) *m/z* 931.0670 [2M + Na]$^+$ (C$_{36}$H$_{38}$I$_2$N$_4$NaO$_8$ requires 931.0677), 477.0253 [M + Na]$^+$ (C$_{18}$H$_{19}$IN$_2$NaO$_4$ requires 477.0297).

6.43 *tert*-Butyl-5-nitro-1-(((2,2,6,6-tetramethylpiperidin-1-yl)oxy)methyl)-1,2-dihydro-3*H*-benzo[*e*]indole-3-carboxylate (149)

Bu$_3$SnH (420 mL, 454 mg, 1.57 mmol) was added to **148** (750 mg, 1.65 mmol) and TEMPO (820 mg, 5.23 mmol) in benzene (40 mL). The reaction mixture was heated to 60˚C and additional Bu$_3$SnH (420 µL, 454 mg, 1.57 mmol) was added after 0.75 h and 1.5h. After 2 h, the reaction mixture was allowed to cool to rt. After a further 17 h, the evaporation residue was purified by column chromatography (EtOAc / petroleum ether 1:20 -> 1:0) to yield **149** (398 mg, 50%) as an orange crystalline solid: Rf 0.6 (EtOAc / petroleum ether 3:7); ^{1}H NMR (500 MHz; CDCl$_3$) (135DEPT, HSQC, HMBC) δ 0.80-1.08 (12 H, m, 2,2,6,6-tetramethyl), 1.18-1.35 (6 H, m, C*H$_2$*C*H$_2$*C*H$_2$*), 1.55 (9 H, br s, ^{t}Bu), 3.82-3.93 (2 H,
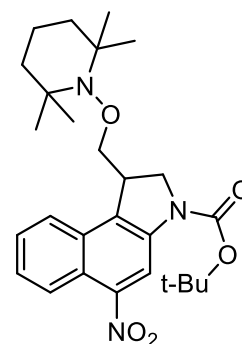
m, 1,2-H$_2$), 3.96-4.02 (1 H, m, 2-H), 4.03-4.11 (1 H, m, 1a-H), 4.27 (1 H, br d, 10.8 Hz, 1a-H), 7.45-7.53 (2 H, m, 7,8-H$_2$), 7.82 (1 H, br d, J = 7.2 Hz, 9-H), 8.38 (1 H, br s, 6-H), 8.83 (1 H, br s, 4-H); ^{13}C NMR (125 MHz; CDCl$_3$) (135DEPT, HSQC, HMBC) δ 16.9 (piperidin-1-yl 3,5-C), 20.0 (4 × piperidin-1-yl CH$_3$), 28.3 (^{t}Bu), 39.5 (piperidin-1-yl 4-C), 52.3 (1a-C), 59.9 (2 × piperidin-1-yl CCH$_3$), 77.4 (2-C), 77.6 (5-C), 82.1 (C(CH$_3$)$_3$), 121.8 (5a-C), 123.6 (9-C), 123.9 (6-C), 126.9 (7-C), 127.6 (8-C), 130.9 (9a-C), 139.4 (3-C), 152.1 (C=O); MS (ES +) m/z 486.2878 [M + H]$^+$ (^{12}C$_{25}$^{13}C$_2$H$_{37}$N$_3$O$_5$ requires 486.2866), 485.2851 [M + H]$^+$ (^{12}C$_{26}$^{13}CH$_{37}$N$_3$O$_5$ requires 485.2838), 484.2819 [M + H]$^+$ (^{12}C$_{27}$H$_{37}$N$_3$O$_5$ requires 484.2819).

6.44 2,6-Dimethyl-2,3,4,5-tetrahydropyridine-1-oxide (153)

MeReO$_3$ (44 mg, 0.18 mmol) in MeOH (20 mL) was treated with urea.H$_2$O$_2$ (2.49 g, 26.5 mmol) under N$_2$. After 20 min, cis-2,6-dimethylpiperidine **152** (1.00 g, 8.8 mmol) was added at 0˚C and the reaction mixture was allowed to warm to rt and stirred for 24 h. The evaporation residue in CH$_2$Cl$_2$ (20 mL), was filtered. Evaporation yielded **153** (1.12 g, 100%) as a dark viscous oil: Rf 0.1 (EtOAc / petroleum ether 1:1); ^{1}H NMR (400 MHz; CDCl$_3$) δ 1.42 (3 H, d, J = 6.8 Hz, 6-CH$_3$), 1.68-1.76 (3 H, m, 4-H2, 5-H), 1.96-2.02 (1 H, m, 5-H), 2.02 (3 H, dd, J = 2.3, 1.0 Hz, 2-CH$_3$), 2.36-2.40 (2 H, m, 3-H$_2$), 3.81-3.86 (1 H, m, 6-H$_2$).
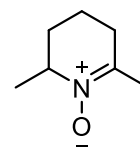
6.45 2,6-dimethyl-2-phenylpiperidin-1-ol (154)

PhMgBr (1 M in THF, 26.5 mL) was added dropwise to **153** (1.12 g, 8.83 mmol) in dry THF (80 mL) under N$_2$. After 1 h, the reaction was quenched with sat. aq. NaHCO$_3$ (60 mL) and concentrated to half volume. The aqueous solution was filtered and then extracted with Et$_2$O (3 × 30 mL). Drying and evaporating yielded **154** (1.25 g, 69%) as a dark viscous oil: ^{1}H NMR (400 MHz; CDCl$_3$) δ 1.10 (3 H, d, J = 6.5 Hz, 6-CH$_3$), 1.20-1.29 (2 H, m, piperidinyl-H$_2$), 1.38 (3 H, s, 2-CH$_3$), 1.83-1.93 (2 H, m, piperidinyl-H$_2$), 1.99-2.14 (2 H, m, piperidinyl-H$_2$), 3.76 (1 H, m, 6-H), 7.20 (1 H, t, J = 6.0 Hz, Ar-H), 7.30-7.37 (2 H, m, Ar-H$_2$), 7.45 (1 H, t, J = 7.9 Hz, Ar-H), 7.60 (1 H, dd, J = 8.2 Hz, 1.8 Hz, $ortho$-Ar-H).
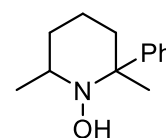
6.46 2,6-Dimethyl-2-phenyl-2,3,4,5-tetrahydropyridine 1-oxide (158)

Compound **157** (380 mg, 1.85 mmol) was dissolved in CH_2Cl_2 (25 mL) at 0˚C. MnO_2 (258 mg, 2.96 mmol) was added portion-wise and the reaction mixture stirred for 17 h. The reaction mixture was filtered through Na_2SO_4. Drying and evaporating yielded **158** (376 mg, 100%) as a dark viscous oil: MS (ES+) *m/z* 204.1327 $[M + H]^+$ ($C_{13}H_{18}NO$ requires 204.1388).
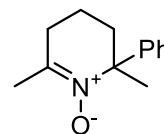
6.47 2,6-Dimethyl-2,6-diphenylpiperidin-1-ol (159)

PhMgBr (1 M, 2.78 mL) was added dropwise to compound **158** (376 mg, 1.85 mmol) in dry THF (16 mL) under N_2. After 1 h, the reaction mixture was quenched with Sat. aq. $NaHCO_3$ (5 mL) and the solvent evaporated. The mixture was filtered and extracted with Et_2O (3 × 30 mL). Drying and evaporating yielded compound **159** (290 mg, 56%) as a dark viscous oil that was taken forward to the next step without further purification.
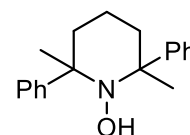
6.48 2,6-Dimethyl-2,6-diphenylpiperidine (160)

Compound **159** (290 mg, 1.00 mmol) and Zn (327 mg, 5.00 mmol) in HCl (1 M, 15 mL) was heated at 80˚C for 1 h. The reaction mixture was quenched with NaOH (1 M, 30 mL) and extracted with Et_2O (3 × 30 mL). Drying and evaporating yielded compound **160** (171 mg, 64%) as a dark viscous oil: MS (ES+) *m/z* 266.1833 $[M + H]^+$ ($C_{19}H_{24}N$ requires 266.1903).
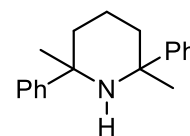
6.49 5-nitro-1-(((2,2,6,6-tetramethylpiperidin-1-yl)oxy)methyl)-2,3-dihydro-1H-benzo[e]indole (161)

HCl was bubbled through a solution of compound **149** (367 mg, 0.47 mmol) in an. Et_2O (20 mL) for 4 h. Evaporating yielded **161** (379 mg, 0.71 mmol) as a yellow solid: Rf: 0.5 (EtOAc / petroleum ether 3:7); ^{1}H NMR (500 MHz; $CDCl_3$) (HSQC, HMBC, COSY) δ 1.15 (4 H, t, J = 7.2 Hz, 2 × piperidinyl-3,5-CH_2), 1.55 (12 H, br s, 4 × piperidinyl-CH_3), 2.37 (2 H, m, piperidinyl-4-CH_2), 4.07 (1 H, m, 1-H), 4.18 (2 H, m, 2-H_2), 4.85-5.02 (2 H, br s, 1a-H_2), 7.54 (2 H, m, 7,8-H_2), 7.83 (1 H, d, J = 7.2 Hz, 9-H), 8.39 (1 H, d, J = 7.8 Hz, 6-H), 8.54-8.56 (1 H, m, 4-H); MS (ES-) m/z 417.2192 [M − H + Cl]$^-$ ($C_{22}H_{28}N_3O_3{}^{35}Cl$ requires 417.1819).
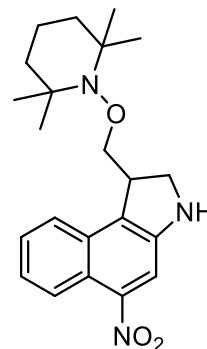
6.50 6-nitrobenzo[f]quinoline (162)

Bu_3SnH (0.4 mL, 1.57 mmol) was added to a stirred solution of **148** (710 mg, 1.57 mmol) and TEMPO (777 mg, 5.00 mmol) in benzene (40 mL). The reaction mixture was heated to 40°C and Bu_3SnH (0.4 mL, 1.57 mmol) was added after 0.75 h and 1.5 h. The reaction mixture was cooled to rt. After 17 h, TFA (5 mL) was added to the evaporation residue in CH_2Cl_2 (20 mL). After 17 h, the evaporation residue in EtOAc (20 mL) was washed with H_2O (3 × 10 mL), aq. NaOH (1 M, 2 × 10 mL) and H_2O (1 × 10 mL). Drying, concentrating and column chromatography (1:9 EtOAc / petroleum ether) yielded compound **162** (40 mg, 11%) as a red oil: ^{1}H NMR (500 MHz; $CDCl_3$) δ ; 7.65 (1 H, dd, J = 8.4, 4.2 Hz, 2-H), 7.76 (2 H, m, 8,9-H_2), 8.35-8.38 (1 H, m, 7-H), 8.53 (1 H, s, 5-H), 8.65 (1 H, dd, J = 7.0, 1.8 Hz, 10-H), 8.92 (1 H, ddd, J = 8.5, 1.4, 0.7 Hz, 1-H), 9.01 (1 H, dd, J = 4.3, 1.5 Hz, 3-H); ^{13}C NMR (125 MHz; $CDCl_3$) (HMBC, HSQC) δ 122.9 (6a-C), 123.0 (10-C), 123.8 (2-C), 124.0 (7-C), 125.4 (5-C), 127.6 (1a-C), 128.6 (8-C), 129.0 (9-C), 130.6 (10a-C), 130.7 (1-C), 145.5 (4a-C), 148.9 (6-C), 151.3 (3-C); MS (ES +) m/z 225.0754 [M + H]$^+$ ($C_{13}H_9N_2O_2$ requires 225.0664).
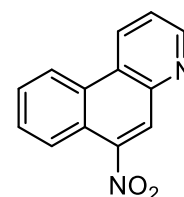
6.51 *tert*-butyl (3-chloroallyl)(1-iodo-4-nitronaphthalen-2-yl)carbamate (166)

Compound **72** (1.00 g, 2.40 mmol) and NaH (72 mg, 3.00 mmol) in DMF (6.00 mL) were stirred for 1 h followed by addition of 1,3-dichloropropene (0.72 mL, 7.80 mmol). After 17 h, the reaction mixture was quenched by addition of aq. NaCl (10%, 10 mL) followed by extraction with EtOAc (3 × 10 mL). Drying, evaporating and column chromatography (EtOAc / hexane 1:9) yielded a pair of rotamers around the C-N bond of **166** (548 mg, 47%) as a yellow oil; Rf 0.3 (EtOAc / hexane 1:9); ^{1}H NMR (500 MHz; (CD$_3$)$_2$SO) (105˚C) δ 1.40 (9 H, s, ^{t}Bu), 4.11 (1 H, dd, *J* = 15.5, 7.3, 0.5'-H), 4.33 (0.5 H, dd, *J* = 15.5, 7.3, 1'-H'), 4.44 (0.5 H, dd, *J* = 15.0, 7.3 Hz, 1'-H), 4.61 (0.5 H, dd, *J* = 16.0, 6.3 Hz, 1'-H'), 6.20 (1 H, m, 2'-H), 6.34-6.37 (1 H, m, 3'-H), 7.84 (2 H, m, 6,7-H), 8.14 (0.5 H, s, 3-H'), 8.18 (0.5 H, s, 3-H), 8.29 (1 H, d, *J* = 8.1 Hz, 8-H), 8.44 (1 H, dd, *J* = 7.4, 1.9 Hz, 5-H); MS (ES +) *m/z* 512.9891 [M + Na]$^+$ (C$_{18}$H$_{18}$^{37}ClIN$_2$O$_4$ requires 512.9868), 510.9879 [M + Na]$^+$ (C$_{18}$H$_{18}$^{35}ClIN$_2$O$_4$ requires 510.9898).
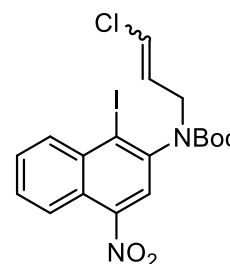
6.52 *tert*-Butyl 1-(chloromethyl)-5-nitro-1,2-dihydro-3*H*-benzo[*e*]indole-3-carboxylate (167)

Bu$_3$SnH (325 μL, 1.21 mmol) was added to a stirred solution of AIBN (24 mg, 0.15 mmol) and **166** (589 mg, 1.2 mmol) in dry benzene (7 mL) under N$_2$ and the reaction mixture was heated to reflux. After 17 h, K$_2$CO$_3$ (100 mg of K$_2$CO$_3$, 10%$_{w/w}$ on SiO$_2$) was added to the evaporation residue in EtOAc (15 mL). After 17 h, the evaporation residue was purified by column chromatography (EtOAc / hexane 0:1 -> 1:0) to yield **167** (200 mg, 46%) as a red oil: Rf (EtOAc / hexane 3:7); ^{1}H NMR (500 MHz; CDCl$_3$) (HMBC, HSQC) δ 1.57 (9 H, s, ^{t}Bu), 3.49 (1 H, t, *J* = 10.6 Hz, CHCl), 3.87 (1 H, dd, *J* = 10.8, 2.4 Hz, CHCl), 4.07 (1 H, t, *J* = 9.2 Hz, 1-H), 4.15 (1 H, t, *J* = 9.0 Hz, 2-H), 4.26-4.33 (1 H, m, 2-H), 7.51 (1 H, t, *J* = 6.9 Hz, 7-H), 7.57 (1 H, t, *J* = 8.0 Hz, 8-H), 7.75 (1 H, d, *J* = 8.0 Hz, 9-H), 8.37 (1 H, d, *J* = 7.8 Hz, 6-H), 8.55-8.80 (1 H, m, 4-H); ^{13}C NMR (125 MHz; CDCl$_3$) (HMBC, HSQC) δ 28.6 (C(*CH$_3$*)$_3$), 41.9 (1-C), 44.0
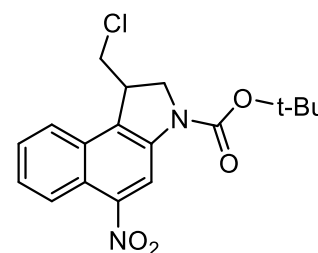
(2-C), 46.0 (CHCl), 82.6 (C(CH$_3$)$_3$), 113.6 (4-C), 122.7 (9-C), 124.3 (6-C), 127.1 (7-C), 128.4 (8-C), 130.2 (9α-C); MS (ES +) m/z 387.0883 [M + Na]$^+$ (C$_{18}$H$_{19}$^{37}ClN$_2$NaO$_4$ requires 387.0918), 385.0915 [M + Na]$^+$ (C$_{18}$H$_{19}$^{35}ClN$_2$NaO$_4$ requires 385.0926).

6.53 Ethyl 5-hydroxy-1*H*-indole-2-carboxylate (168)
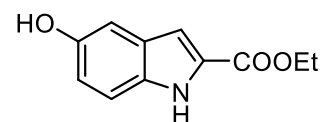
Compound **76** (982 mg, 5.54 mmol) and aq. conc. H$_2$SO$_4$ (40 μL) in EtOH (50 mL) were heated to 78°C for 17 h. The evaporation residue in EtOAc (20 mL) was washed with sat. aq. NaHCO$_3$ (3 × 10 mL). Drying and evaporation yielded **168** (932 mg, 82%) as a white solid: mp 151-153°C (lit.[100] mp 152-154°C); ^{1}H NMR (400 MHz; (CD$_3$)$_2$SO) (COSY) δ 1.38 (3 H, t, J = 7.0 Hz, CH$_3$) , 4.36 (2 H, q, J = 7.6 Hz, CH$_2$), 6.86 (1 H, dd, J = 8.8, 2.4 Hz, 6-H), 6.98 (1 H, d, J = 2.4 Hz, 4-H), 7.00 (1 H, d, J = 2.4 Hz, 3-H), 7.31 (1 H, d, J = 8.8 Hz, 7-H), 8.93 (1 H, s, OH), 11.60 (1 H, s, NH).

6.54 Ethyl 5-(2-dimethylaminoethoxy)-1*H*-indole-2-carboxylate (169)
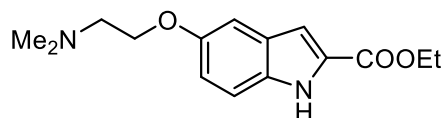
2-Chloro-N,N-dimethylethylamine HCl (922 mg, 6.4 mmol) and K$_2$CO$_3$ (2.35 g, 6.4 mmol) were added to a solution of **168** (870 mg, 4.26 mmol) in CHCl$_3$ (35 mL) and H$_2$O (7 mL). The mixture was heated to 80°C for 17 h. CHCl$_3$ was then removed under vacuum and H$_2$O (20 mL) was added. The aqueous solution was extracted with toluene (3 × 10 mL). The combined organic layers were then extracted with aq. HCl (1 M, 2 × 15 mL). The combined acidic aqueous phases were adjusted to pH 14 with aq. NaOH (10%) and extracted with toluene (3 × 10 mL). Drying and evaporation of the solvent from the combined organic phases yielded **169** (534 mg, 45%) as a white solid: mp 108-109°C (lit.[100] mp 108-109°C); ^{1}H NMR (400 MHz; CDCl$_3$) δ 1.40 (3 H, t, J = 7.2 Hz, CH$_2$CH_3), 2.34 (6 H, s, NMe$_2$), 2.75 (2 H, t, J = 5.7 Hz, ((CH$_3$)$_2$NCH_2CH$_2$), 4.10 (2 H, t, J = 5.6 Hz, (CH$_3$)$_2$CH$_2$CH_2), 4.39 (2 H, q, J = 7.2 Hz, CH_2CH$_3$), 7.02 (1 H, dd, J = 9.2 Hz, 2.8 Hz, 6-H), 7.08 (1 H, d, J = 2.4 Hz, 4-H), 7.12 (1 H, dd, J = 2 Hz, 0.8 Hz, 3-H), 7.29 (1 H, d, J = 9.2 Hz, 7-H), 8.86 (1 H, br s, NH); ^{13}C NMR (100 MHz; CDCl$_3$) (HMBC / HSQC) δ 14.3 (OCH$_2$$CH_3$), 45.9

(N(CH$_3$)$_2$), 58.4 ((CH$_3$)$_2$NCH$_2$CH$_2$), 60.8 (OCH$_2$CH$_3$), 66.6 ((CH$_3$)$_2$NCH$_2$CH$_2$), 103.7 (4-C), 108.1 (3-C), 112.6 (7-C), 117.5 (6-C), 127.8 (2-C), 127.9 (3α-C), 132.2 (7α-C), 153.9 (5-C), 161.8 (C=O).

6.55 *Z*-Ethyl 2-azido-3-(3,4,5-trimethoxyphenyl)acrylate (171)

3,4,5-Trimethoxybenzaldehyde **170** (852 mg, 4.35 mmol) was added NaOMe (470 mg, 8.70 mmol) in EtOH (7.5 mL) at -10˚C followed by addition of methyl azidoacetate (1.00 g, 8.70 mmol) in EtOH (2.5 mL). The reaction mixture was allowed to warm to 0°C. After 4 h, the reaction mixture was poured into ice-water (20 mL) and the precipitate was collected by filtration and dried to yield **171** (613 mg, 46%) as a yellow solid: mp 59-60˚C (lit.[200] mp 60-61˚C); ^{1}H NMR (400 MHz; CDCl$_3$) δ 1.40 (3 H, t, *J* = 7.6 Hz, CH$_2$C*H*$_3$), 3.84 (3 H, s, OCH$_3$), 3.85 (6 H, s, 2 × OCH$_3$), 4.37 (2 H, q, *J* = 7.6 Hz, C*H*$_2$CH$_3$), 6.83 (1 H, s, alkene-C*H*), 7.09 (2 H, s, Ar 2,6-H$_2$). ^{13}C NMR (100 MHz; CDCl$_3$) (DEPT135, HSQC, HMBC) δ 14.2 (CH$_2$CH$_3$), 56.2 (2 × OCH$_3$), 60.9 (OCH$_3$), 62.2 (*C*H$_2$CH$_3$), 108.1 (2 × Ar-CH), 124.7 (2-C), 125.3 (3-C), 128.6 (Ar 1-C), 139.4 (Ar 4-C), 152.9 (Ar 3,5-C), 163.5 (C=O).
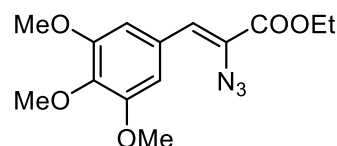
6.56 Ethyl 5,6,7-trimethoxy-1H-indole-2-carboxylate (172)

Compound **171** (580 mg, 1.89 mmol) in xylene (15 mL) was heated to reflux for 17 h. The evaporation residue was dissolved in toluene (20 mL) and the solvent was evaporated yield **172** (327 mg, 62%) as a yellow oil: ^{1}H NMR (400 MHz; CDCl$_3$) δ 1.36 (3 H, t, *J* = 6.4 Hz, CH$_3$), 3.84 (3 H, s, OCH$_3$), 3.87 (3 H, s, OCH$_3$), 4.02 (3 H, s, OCH$_3$), 4.34 (2 H, q, *J* = 7. 2 Hz, CH$_2$), 6.76 (1 H, s, 7-H), 7.05 (1 H, d, *J* = 2.4 Hz, 3-H), 8.85 (1 H, br s, NH); MS (ES -) *m/z* 278 [M − H]$^-$ C$_{14}$H$_{16}$N$_1$O$_5$ requires 278.
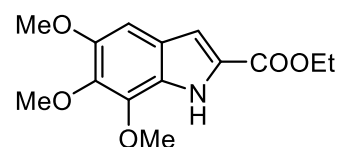
6.57 Attempted synthesis of *tert*-butyl *(S)*-(4-amino-1-iodonaphthalen-2-yl)(oxiran-2-ylmethyl)carbamate (173)

Aq. NaBH$_4$ (2 M, 300 μL) was added portion-wise to a stirred solution of **73** (145 mg, 0.31 mmol) in MeOH (10 mL) and Pt/C (10%, 1 mg). The reaction yielded starting material **73**.
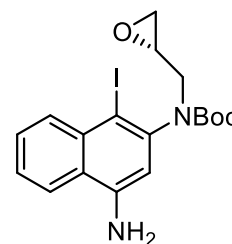
6.58 *(S)*-2,2-Dimethyltetrahydrothiazole-4-carboxylic acid hydrochloride (186)

Under N$_2$, D-cysteine (1.00 g, 8.25 mmol) was stirred in 2,2-dimethoxypropane (15 mL) and acetone (75 mL) at reflux for 17 h. The solid was collected by filtration to yield **186** (594 mg, 3.00 mmol) as a white crystalline solid: mp 167-168˚C (lit.[177] mp 166-170˚C); ^{1}H NMR (500 MHz; D$_2$O) δ 1.84 (3 H, s, CH$_3$), 1.88 (3 H, s, CH$_3$), 3.53 (1 H, dd, *J* = 11.8, 7.6 Hz, 3-H), 3.66 (1 H, t, *J* = 9.5 Hz, 3-H), 4.75 (1-H, br. s, 4-H); MS (ES +) *m/z* 184.0431 [M + Na]$^+$ (C$_6$H$_{11}$N$_1$O$_2$S$_1$ requires 184.0403), 162.0610 [M + H]$^+$ (C$_6$H$_{12}$N$_1$O$_2$S$_1$ requires 162.0583).
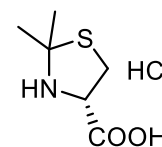
6.59 *(S)*-2,2-Dimethyl-3-(N-(1,1-dimethylethoxycarbonyl)-L-leucyl)tetrahydrothiazole-4-carboxylic acid (187)

Pr$^i_2$NEt (1.18 mL, 872 mg, 6.76 mmol) was added to a stirred solution of **186** (493 mg, 2.25 mmol) and **193** (850 mg, 2.04 mmol) in anhydrous DMF (20 mL). The evaporation residue, in EtOAc (20 mL), was washed with aq. citric acid (5%, 3 × 10 mL), H$_2$O (3 × 10 mL) and brine (3 × 10 mL). Drying and evaporation yielded **187** (764 mg, 100%) as a colourless gummy solid: ^{1}H NMR (500 MHz; CDCl$_3$) δ 0.78-0.86 (6 H, m, 2 × Leu-CH$_3$), 1.38
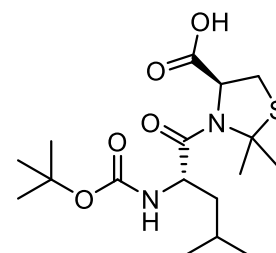
(9 H, s, ^{t}Bu), 1.50–1.60 (2 H, m, Leu β-H$_2$, Leu γ-H), 1.79 (3 H, s, 2-CH$_3$), 1.82 (3 H, s, 2-CH$_3$), 3.28-3.34 (2 H, m, 2 × 5-H), 4.07-4.14 (1 H, m, Leu α-H), 5.01 (1 H, d, J = 9.2 Hz, NH), 5.69 (1 H, m, 4-H); MS (ES -) m/z 375.1692 [M − H]$^-$ (^{12}C$_{15}$^{13}C$_2$H$_{30}$N$_2$O$_2$S requires 375.1788), 374.1743 [M − H]$^-$ (^{12}C$_{16}$^{13}CH$_{30}$N$_2$O$_2$S requires 374.1822) 373.1717 [M − H]$^-$ (^{12}C$_{17}$H$_{30}$N$_2$O$_2$S requires 373.1792).

6.60 perfluorophenyl (S)-3-((tert-butoxycarbonyl)-L-leucyl)-2,2-dimethylthiazolidine-4-carboxylate (188)

Under N$_2$ and at 0˚C, compound **187** (764 mg, 2.04 mg) was added to a stirred solution of DCC (558 mg, 2.70 mmol) and pentafluorophenol (499 mg, 2.70 mmol) in EtOAc (10 mL). After 3 h, the reaction mixture was filtered through celite® and concentrated to yield **188** (1.10 g, 100%) as a yellow oil: ^{1}H NMR (500 MHz; CDCl$_3$) δ 0.75 (3 H, d, J = 6.4 Hz, Leu-CH$_3$), 0.82 (3 H, d, J = 6.4 Hz, Leu-CH$_3$), 1.37 (9 H, s, ^{t}Bu), 1.48-1.53 (2 H, m, Leu-β,γ-H$_2$), 1.80 (3 H, s, 2-CH$_3$), 1.81 (3 H, s, 2-CH$_3$), 3.40 (1 H, dd, J = 12.9, 5.6 Hz, 5-H), 3.45 (1 H, d, J = 12.1 Hz, 5-H), 4.10 (1 H, m, Leu-α-H), 4.82 (1 H, d, J = 8.9 Hz, 4-H), 6.10 (1 H, d, J = 5.1 Hz, NH); MS (ES+) m/z 563.1709 [M + Na]$^+$ (C$_{23}$H$_{29}$F$_5$N$_2$O$_5$SNa requires 563.1610), 541.1879 [M + H]$^+$ (C$_{23}$H$_{30}$F$_5$N$_2$O$_5$S requires 541.1790).
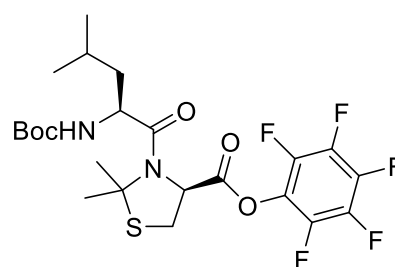
6.61 pentafluorophenyl (tert-butoxycarbonyl)-L-leucinate (193)

Under N$_2$, DCC (454 mg, 2.2 mmol) was added to a stirred solution of Boc-L-Leu-OH **192** (500 mg, 2 mmol) and pentafluorophenol (406 mg, 2.2 mmol) in EtOAc (5 mL) at 0°C. After 3 h, the mixture was filtered through celite® and the precipitate washed with cold EtOAc (15 mL). The dried precipitate in hexane (10 mL) was stored at 4˚C for 16. Concentration yielded **193** (794 mg, 100%) as a colourless oil (Lit.[131] oil); ^{1}H NMR (500 MHz; CDCl$_3$) δ 0.94 (6 H, d, J = 6.3 Hz, 2 ×
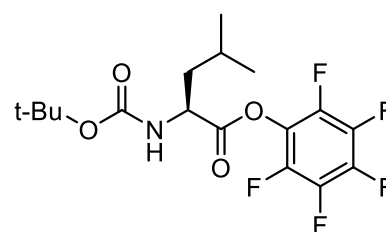
Leu-CH$_3$), 1.40 (9 H, s, ^{t}Bu), 1.58-1.64 (2 H, m, Leu-β-H), 1.69-1.78 (2 H, Leu-β-H, Leu-γ-H), 4.56 (1 H, m, Leu-α-H), 4.82 (1 H, br s, NH); ^{19}F NMR (470MHz; CDCl$_3$) δ -162.1, -157.6, -152.2.

6.62 Attempted synthesis of (5-(2-(dimethylamino)ethoxy)-1H-indol-2-yl)(5-nitro-1-(((2,2,6,6-tetramethylpiperidin-1-yl)oxy)methyl)-1,2-dihydro-3H-benzo[e]indol-3-yl)methanone (194)

Under N$_2$, compound **79** (60 mg, 0.23 mmol) was added to a stirred solution of **161.HCl** (62 mg, 0.16 mmol) and DIPEA (0.15 mL, 0.86 mmol) in an. CH$_2$Cl$_2$ (5.00 mL). After 17 h, the reaction was heated to 50˚C. After 7 h, no reaction progress was observed by TLC and **161** and **79** were recovered.
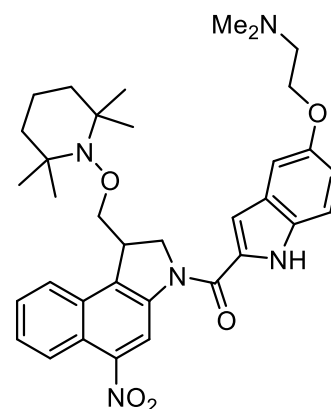
Under N$_2$ at 0˚C, DIPEA (174 µL, 1.00 mmol) and DCC (218 mg, 1.06 mmol) were added sequentially to a stirred solution of **79** (150 mg, 0.53 mmol) and HOBt (164 mg, 1.06 mmol) in an. DMF (15 mL). After 1 h, **161.HCl** (275 mg, 0.71 mmol) was added and the reaction mixture allowed to warm to rt. After 17 h, the reaction mixture was washed with sat. aq. NaHCO$_3$ (3 × 10 mL) and extracted with EtOAc (3 × 10 mL). Drying, evaporating and column chromatography (EtOAc / petroleum ether 1:4) failed to yield product.

6.63 Attempted Synthesis of (5-nitro-1-(((2,2,6,6-tetramethylpiperidin-1-yl)oxy)methyl)-1,2-dihydro-3H-benzo[e]indol-3-yl)(5,6,7-trimethoxy-1H-indol-2-yl)methanone (195)

Under Ar, compound **75** (113 mg, 0.45 mmol), DIC (70 μL, 0.45 mmol) and DIPEA (131 μL, 0.75 mmol) in DMF (10 mL) were stirred for 1 h followed by addition of compound **161.HCl** (126 mg, 0.30 mmol). The reaction mixture was warmed to 30°C for 3 h and then warmed to 50°C followed by addition of DIPEA (131 μL, 0.75 mmol). After 17 h, TLC indicated that no reaction had occurred.
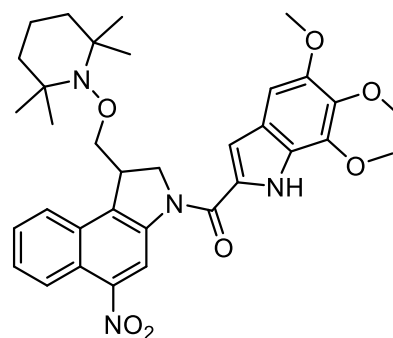
Under Ar, compound **75** (113 mg, 0.45 mmol), EDC·HCl (86 mg, 0.45 mmol) and DIPEA (131 μL, 0.75 mmol) in DMF (10 mL) were stirred for 1 h followed by addition of compound **161.HCl** (126 mg, 0.30 mmol). The reaction mixture was warmed to 30°C for 3 h and then warmed to 50°C followed by addition of DIPEA (131 μL, 0.75 mmol). After 17 h, TLC indicated that no reaction had occurred.

Under Ar, compound **75** (113 mg, 0.45 mmol), EDC·HCl (86 mg, 0.45 mmol), DMAP (1 mg, 0.01 mmol) and DIPEA (131 μL, 0.75 mmol) in DMF (10 mL) were stirred for 1 h followed by addition of compound **161.HCl** (126 mg, 0.30 mmol). The reaction mixture was warmed to 30°C for 3 h and then warmed to 50°C followed by addition of DIPEA (131 μL, 0.75 mmol). After 17 h, TLC indicated that no reaction had occurred.

Under Ar, compound **75** (30 mg, 0.12 mmol), EDC·HCl (23 mg, 0.12 mmol), DMAP (1 mg, 0.01 mmol) and DIPEA (68 μL, 0.39 mmol) in DMF (0.2 mL) were stirred for 0.5 h followed by addition of compound **161.HCl** (50 mg, 0.12 mmol). After 17 h, TLC indicated that no reaction had occurred.

Under Ar, compound **75** (30 mg, 0.12 mmol), DIC (19 μL, 0.12 mmol), and DIPEA (68 μL, 0.39 mmol) in DMF (0.2 mL) were stirred for 0.5 h followed by addition of compound **161.HCl** (50 mg, 0.12 mmol). After 17 h, TLC indicated that no reaction had occurred, and mass spec confirmed only starting material **161** was present.

Under Ar, compound **75** (30 mg, 0.12 mmol), DIC (19 μL, 0.12 mmol), and DIPEA (68 μL, 0.39 mmol) in THF (0.3 mL) were stirred for 0.5 h followed by addition of compound **176** (50 mg, 0.12 mmol). After 17 h, TLC indicated that no reaction had occurred, and mass spec confirmed only starting material **161** was present.

Under Ar, compound **75** (30 mg, 0.12 mmol), EDC·HCl (23 mg, 0.12 mmol), DMAP (1 mg, 0.01 mmol) and DIPEA (68 μL, 0.39 mmol) in THF (0.3 mL) were stirred for 0.5 h followed by addition of compound **161** (50 mg, 0.12 mmol). After 17 h, TLC indicated that no reaction had occurred.

6.64 Attempted synthesis of (3-methoxyphenyl)(5-nitro-1-(((2,2,6,6-tetramethylpiperidin-1-yl)oxy)methyl)-1,2-dihydro-3H-benzo[e]indol-3-yl)methanone (196)

Under N_2, 3-methoxy-benzoyl chloride (10.7 μL, 0.079 mmol) was added to a stirred solution of **161.HCl** (30 mg, 0.072 mmol) and NEt_3 (20.0 μL, 0.143 mmol) in an. CH_2Cl_2 (0.5 mL). After 4 h, NEt_3 (100 μL, 0.715 mmol) was added. After 17 h, 3-methoxy-benzoyl chloride (30.0 μL, 0.216 mmol) was added. After 48 h, the evaporation residue yielded starting material.
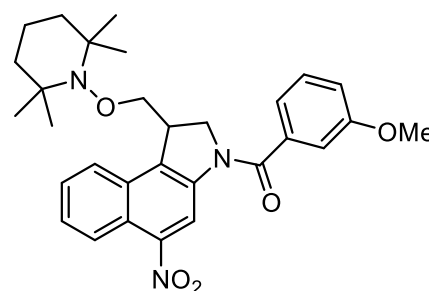
6.65 General Procedure for *seco*-Nitro-CBIs 197-201

EDCI (32 mg, 0.168 mmol) was added to a stirred solution of amine **42** (20 mg, 0.0762 mmol) and acid **75-81** (0.0838 mmol) in anhydrous DMA (0.3 mL). After 17 h, the evaporation residue was purified by column chromatography (EtOAc / hexane 1:9) to yield **197-201**:

(±)-1-Chloromethyl-3-(indole-2-ylcarbonyl)-5-nitro-1,2-dihydro-3H-benzo[e]indole (197)

According to the general procedure described above, indole-2-carboxylic acid **78** (13.5 mg, 83.8 µmol) was used to synthesise **197** (13 mg, 42%) as a dark red solid: Rf 0.4 (EtOAc / petroleum ether 3:7); ^{1}H NMR (500 MHz; CDCl$_3$) (HSQC, HMBC) δ 3.63 (1 H, dd, J = 9.2, 8.0 Hz, 2-H), 4.02 (1 H, dd, J = 9.2, 2.4 Hz, 2-H), 4.35 (1 H, tt, J = 7.6, 1.6 Hz, 1-H), 4.83 (1 H, t, J = 8.4 Hz, CHCl), 4.96 (1 H, dd, J = 8.8, 1.6 Hz, CHCl), 7.18 (1 H, d, J = 1.2 Hz, indole-4-H), 7.23 (1 H, m, indole-5-H), 7.40 (1 H, td, J = 7.0, 0.8 Hz, indole-6-H), 7.52 (1 H, dd, J = 8.3, 0.8 Hz, indole-7-H), 7.67 (1 H, ddd, J = 9.7, 7.1, 1.2 Hz, 7-H), 7.71 (1 H, td, J = 9.2, 7.1, 0.8 Hz, 8-H), 7.78 (1 H, dd, J = 8.0, 0.8 Hz, indole-3-H), 7.91 (1 H, dd, J = 8.3, 0.8 Hz, 9-H), 8.48 (1 H, d, J = 8.1 Hz, 6-H), 9.28 (1 H, s, 4-H), 9.47 (1 H, br s, NH); ^{13}C NMR (125 MHz; CDCl$_3$) (HSQC, HMBC) δ 43.6 (1-C), 45.6 (2-C), 54.7 (CCl), 106.9 (indole-4-C), 111.9 (indole-7-C), 115.5 (4-C), 121.1 (indole-5-C), 122.6 (indole-3-C), 122.9 (5α,9-C$_2$), 124.4 (6-C), 125.8 (indole-6-C), 127.9 (7,8-C$_2$), 128.2 (indole-3a-C), 129.0 (indole-2-C), 129.8 (9a-C), 130.1 (9b-C), 136.0 (indole-7a-C), 140.4 (3-C), 147.9 (5-C), 160.7 (C=O); MS (ES -) *m/z* 407.0725 [M − H]$^-$ (^{13}C$_1$^{12}C$_{21}$H$_{16}$^{37}ClN$_3$O$_3$ requires 407.0803), 406.0666 [M − H]$^-$ (^{12}C$_{22}$H$_{16}$^{37}ClN$_3$O$_3$ requires 406.0769), 405.0758 [M − H]$^-$ (^{13}C$_1$^{12}C$_{21}$H$_{16}$^{35}ClN$_3$O$_3$ requires 405.0830), 404.0730 [M − H]$^-$ (^{12}C$_{22}$H$_{16}$^{35}ClN$_3$O$_3$ requires 404.0796).
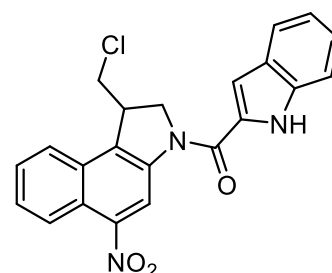
benzofuran-2-yl(1-(chloromethyl)-5-nitro-1,2-dihydro-3*H*-benzo[*e*]indol-3-yl)methanone (198)

According to the general procedure described above, benzofuran-2-carboxylic **81** acid (14 mg, 0.0838) was used to synthesise **198** (14 mg, 45%) as a red solid: ^{1}H NMR (500 MHz;
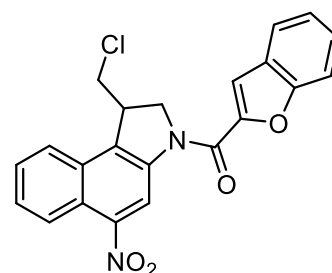
CDCl$_3$) δ 3.57 (1 H, dd, J = 11.7 Hz, 9.6 Hz, 2-H), 3.92 (1 H, ddd, J = 11.5 Hz, 4.2 Hz, 0.7 Hz, 2-H), 4.24 (1 H, dddd, J = 9.6 Hz, 9.26 Hz, 4.2 Hz, 3.2 Hz, 1-H), 4.78 (1 H, dd, J = 11.7 Hz, 8.6 Hz, 1a-H), 4.96 (1 H, dd, J = 11.8 Hz, 2 Hz, 1a-H), 7.31 (1 H, td, J = 7.0 Hz, 1.0 Hz, indole-7-H), 7.44 (1 H, td, J = 7.2 Hz, 1.3 Hz, indole-6-H), 7.56-7.57 (1 H, m, indole-5-H), 7.58-7.59 (1 H, m, 7-H), 7.60-7.64 (1 H, m, 8-H, indole-3-H), 7.68 (1 H, ddd, J = 7.9 Hz, 1.2 Hz, 0.8 Hz, indole-4-H), 7.84 (1 H, d, J = 8.9 Hz, 9-H), 8.38 (1 H, d, J = 8.9 Hz, 6-H), 9.14 (1 H, br. s, 4-H); ^{13}C NMR (125 MHz; CDCl$_3$) (HSQC, HMBC) δ 43.2 (1-C), 45.5 (2-C), 54.2 (1α-C), 112.1 (indole-5-C), 114.6 (indole-2-C), 115.4 (4-C), 122.7 (indole-4-C), 122.9 (9-C), 123.0 (indole-3a-C), 124.0 (indole-3-C), 124.3 (6-C), 126.8 (indole-2-C), 127.5 (indole-6-C), 127.9 (5a-C), 128.0 (7-C), 128.5 (8-C), 129.7 (9a-C), 130.4 (9b-C), 140.1 (3-C), 147.8 (5-C), 155.2 (indole-7a-C), 158.2 (C=O); MS (ES +) m/z 410.0799 [M + H]$^+$ (^{13}C$_1$^{12}C $_{22}$H$_{15}$^{37}ClN$_2$O$_4$ requires 410.0769), 409.0773 [M + H]$^+$ (C$_{22}$H$_{15}$^{37}ClN$_2$O$_4$ requires 409.0769), 408.0830 [M + H]$^+$ (^{13}C$_1$^{12}C$_{21}$H$_{15}$^{35}ClN$_2$O$_4$ requires 408.0799), 407.0798 [M + H]$^+$ (C$_{22}$H$_{15}$^{35}ClN$_2$O$_4$ requires 407.0799).

(1-(chloromethyl)-5-nitro-1,2-dihydro-3H-benzo[e]indol-3-yl)(5-hydroxy-1H-indol-2-yl)methanone (199)

According to the general procedure described above, **76** (14.8 mg, 0.0838 mmol) was used to synthesise **199** (24.0 mg, 75%) as a red semi-solid: Rf 0.3 (EtOAc / hexane 1:4); ^{1}H NMR (500 MHz; (CD$_3$)$_2$CO) (HMBC, HSQC, COSY) 3.97 (1 H, ddd, J = 9.5, 7.1, 2.5 Hz, 2-H), 4.06 (1 H, ddd, J = 11.4, 3.4, 1.9 Hz, 2-H), 4.52 (1 H, m, 1-H), 4.78 (1-H, dt, J = 10.9, 2.4 Hz, 1a-H), 4.87 (1 H, td, J = 9.9, 4.3 Hz, 1a-H), 6.81 (1 H, dd, J = 8.9, 2.3 Hz, indole-6-H), 6.98 (1 H, d, J = 2.3 Hz, indole-4-H), 7.04 (1 H, m, indole-3-H), 7.32 (1 H, d, J = 9.2, indole-7-H), 7.61 (2 H, m, 7,8-H), 7.84 (1 H, br s, NH), 8.09 (1 H, d, J = 7.9 Hz, 9-H), 8.25 (1 H, d, J = 8.6 Hz, 6-H), 9.13 (1 H, s, 4-H), 10.64 (1 H, br s, OH); ^{13}C NMR (125 MHz; (CD$_3$)$_2$CO) (HMBC, HSQC, COSY) 42.8 (1-C), 47.0 (2-C), 54.9 (1a-C), 104.9 (indole-4-C), 105.4 (indole-7a-C), 105.8 (indole-3-C), 113.0 (indole-7-H), 115.0 (4-C), 116.2 (indole-6-C), 122.3 (5a-C), 123.6 (6-C), 123.9 (9-C), 127.9 (7-C), 128.5 (8-C), 128.8 (indole-3a-C), 130.1 (9a-C), 131.5 (9b-C), 141.4 (3-C), 147.4 (5-C), 152.1 (indole-5-C), 161.8 (C=O); MS (ES -) m/z 422.0736 [M − H]$^-$ (C$_{22}$H$_{15}$^{37}ClN$_3$O$_4$ requires 422.0716), 420.0775 [M − H]$^-$ (C$_{22}$H$_{15}$^{35}ClN$_3$O$_4$ requires 420.0746).
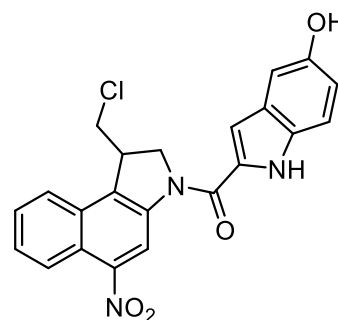
(1-(chloromethyl)-5-nitro-1,2-dihydro-3*H*-benzo[*e*]indol-3-yl)(6-methoxy-1*H*-indol-2-yl)methanone (200)

According to the general procedure described above, 6-methoxyindole-2-carboxylic acid **77** (16 mg, 0.0838 mmol) was used to synthesise **200** (18 mg, 54%) as a red oil: ^{1}H NMR (500 MHz; CDCl$_3$) δ 3.52 (1 H, t, *J* = 10.5 Hz, 2-H), 3.78 (3 H, s, OCH$_3$), 3.91 (1 H, dd, *J* = 11.6 Hz, 2.6 Hz, 2-H), 4.24 (1 H, t, *J* = 8 Hz, 1-H), 4.68 (1 H, t, *J* = 9.8 Hz, ClC*H*H), 4.80 (1 H, d, *J* = 10.7 Hz, ClCH*H*), 6.76-6.81 (2 H, m, indole-5,7-H), 7.01 (1 H, s, indole-3-H), 7.52 (1 H, d, *J* = 8.9 Hz, indole-4-H), 7.55 (1 H, d, *J* = 8 Hz, 9-H), 7.59 (1 H, t, *J* = 7.9 Hz, 8-H), 7.79 (1 H, d, *J* = 7.9 Hz, 7-H), 8.34 (1 H, d, *J* = 8.6 Hz, 6-H), 9.16 (1 H, s, 4-H), 9.35 (1 H, s, NH); ^{13}C NMR (125 MHz; CDCl$_3$) (DEPT135, HSQC, HMBC) δ 43.6 (1-C), 45.6 (2-C), 54.7 (CH$_2$Cl), 55.5 (OCH$_3$), 93.4 (indole-7-C), 107.4 (indole-3-C), 112.9 (indole-5-C), 115.5 (4-C), 122.2 (indole-3a-C), 122.8 (9b-C), 122.9 (7-C), 123.4 (indole-4-C), 124.4 (6-C), 127.8 (9-C), 128.1 (indole-2-C), 128.5 (8-C), 129.8 (9a-C), 130.0 (5a-C), 137.3 (indole-7a-C), 140.6 (3-C), 147.8 (5-C), 159.2 (indole-6-C), 160.7 (C=O); MS (ES -) *m/z* 437.0814 [M − H]$^-$ (^{13}C$_1$^{12}C$_{22}$H$_{17}$^{37}ClN$_3$O$_4$ requires 437.0878), 436.0780 [M − H]$^-$ (C$_{23}$H$_{17}$^{37}ClN$_3$O$_4$ requires 436.0878), 435.0840 [M − H]$^-$ (^{13}C$_1$^{12}C$_{22}$H$_{17}$^{35}ClN$_3$O$_4$ requires 435.0907), 434.0908 [M − H]$^-$ (C$_{23}$H$_{17}$^{35}ClN$_3$O$_4$ requires 434.0907).

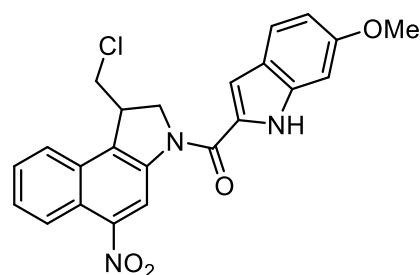**(1-(chloromethyl)-5-nitro-1,2-dihydro-3H-benzo[e]indol-3-yl)(5,6,7-trimethoxy-1H-indol-2-yl)methanone (201)**

According to the general procedure described above, **75** (21 mg, 0.0838 mmol) was used to synthesise **201** (12 mg, 32%) as a dark red oil: Rf 0.3 (EtOAc / hexane 1:4); ^{1}H NMR (500 MHz; CDCl$_3$) δ 3.51 (1 H, t, *J* = 11.0 Hz, 2-H), 3.80-3.89 (7 H, m, 2 × OCH$_3$, 2-H), 4.03 (3 H, s, OCH$_3$), 4.24 (1 H, m, 1-H), 4.69 (1 H, t, *J* = 10.0 Hz, CHCl), 4.82 (1 H, dd, *J* = 10.8, 2.0 Hz), 6.81 (1 H, s, indole-3-H), 6.97 (1 H, d, *J* = 2.2 Hz, indole-4-H), 7.59 (2 H, m, 8,7-H$_2$), 7.81 (1 H, d, *J* = 7.5 Hz, 9-H), 8.39 (1 H, d, *J* = 8.4 Hz, 6-H), 9.18 (1 H, s, 4-H), 9.33 (1 H, s, NH); MS (ES+) *m/z* 520.1100 [M + Na]$^+$ (C$_{25}$H$_{22}$^{37}ClN$_3$O$_6$Na requires 520.1066), 518.1136 [M + Na]$^+$ (C$_{25}$H$_{22}$^{37}ClN$_3$O$_6$Na requires 518.1095).
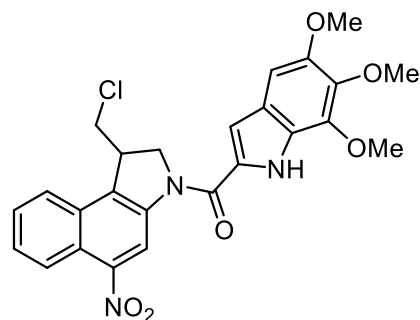
Attempted synthesis of (1-(chloromethyl)-5-nitro-1,2-dihydro-3H-benzo[e]indol-3-yl)(5-(2-(dimethylamino)ethoxy)-1H-indol-2-yl)methanone

(201)

Compound **42** (20 mg, 76.1 µmol), was added to a stirred solution containing **79** (21 mg, 80.6 µmol), EDCI (32 mg, 206.0 µmol) and an. TsOH (8 mg, 46.5 µmol) in dry DMA (0.3 mL). After 17 h, the evaporation residue was purified *via* column chromatography (EtOAc / hexane 1:9) to recover **42**.
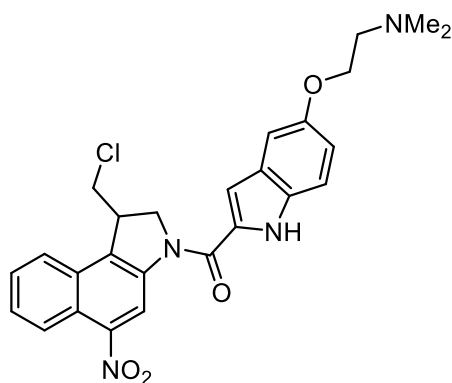
Compound **42** (20 mg, 76.1 µmol), was added to a stirred solution containing compound **79** (21 mg, 80.6 µmol), EDCI (32 mg, 206.0 µmol) in an. DMA (0.3 mL). After 72 h, the evaporation residue was purified by column chromatography (EtOAc / hexane 1:9) to recover **42**.

Compound **42** (20 mg, 76.1 µmol), was added to a stirred solution containing compound **79** (21 mg, 80.6 µmol), EDCI (32 mg, 206.0 µmol) and DIPEA (16 µL, 91.9 µmol) in an. DMA (0.3 mL). After 7 d, no reaction was observed by TLC to have taken place.

6.66 General procedure for the synthesis of *seco*-amino-CBIs 202-206

In an NMR tubes, *Seco*-nitro-CBI **197** (1.745 mg, 4.30 μmol) in deuterated-DMSO was treated with $SnCl_2 \cdot 2H_2O$ (9.70 mg). Yields were determined by quantitative NMR and the reaction was monitored by ^1H NMR experiments every 10 minutes.

(5-amino-1-(chloromethyl)-1,2-dihydro-3H-benzo[e]indol-3-yl)(1H-indol-2-yl)methanone (202)

According to the general procedure described above, **197** (1.745 mg, 4.30 μmol) was used to synthesise **202** (1.491 mg, 92%) as a red oil: ^1H NMR (500 MHz; $(CD_3)_2SO$) δ 3.86 (1 H, dd, *J* = 10.7, 7.6 Hz, 2-H), 4.03 (1 H, dd, *J* = 10.7, 3.1 Hz, 2-H), 4.23 (1 H, m, 1-H), 4.57 (1 H, d, *J* = 9.9 Hz, CHCl), 4.81 (1 H, dd, *J* = 10.7, 9.9 Hz, CHCl), 7.10 (1 H, t, *J* = 7.4 Hz), 7.21 (1 H, d, *J* = 1.2 Hz), 7.26 (1 H, t, *J* = 7.7 Hz), 7.34 (1 H, t, *J* = 7.4 Hz), 7.50-7.52 (2 H, m), 7.71 (1 H, d, *J* = 8.3 Hz), 7.86 (1 H, d, *J* = 8.9 Hz), 7.95 (1 H, d, *J* = 8.3 Hz), 8.18 (1 H, s, 3-H), 9.12 (1 H, br s, NH), 11.73 (1 H, br s, NH).
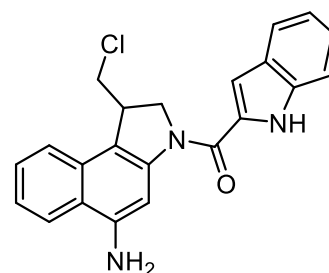
**(5-amino-1-(chloromethyl)-1,2-dihydro-3H-benzo[e]indol-3-yl)(benzofuran-2-yl)methanone (203)**

According to the general procedure described above, **198** (0.38 mg, 0.934 μmol) was used to synthesise **203** (0.28 mg, 80%) as a dark red oil: ^1H NMR (500 MHz; $(CD_3)_2SO$) (HSQC, HMBC) δ 3.87 (1 H, dd, *J* = 11.0, 7.4 Hz, CHCl), 4.01 (1 H, dd, *J* = 11.0, 3.2 Hz, CHCl), 4.23 (1 H, m, 1-H), 4.58 (1 H, dd, *J* = 11.0, 1.6 Hz, 2-H), 4.78 (1 H, m, 2-H), 7.36 (1 H, ddd, *J* = 9.5, 6.9, 1.1 Hz, 7-H), 7.40 (1 H, ddd, *J* = 8.9, 7.2, 0.9 Hz, 8-H), 7.53 (2 H, tt, *J* = 8.4, 1.2 Hz, benzofuran-4,5-H_2), 7.75 (1 H, s, benzofuran-3-H), 7.76 (1 H, dd, *J* = 8.4, 0.7 Hz, benzofuran-7-H), 7.86 (2 H, t, *J* = 7.5 Hz, 9-H, benzofuran-6-H), 7.95 (1 H, d, *J* = 8.5 Hz, 6-H), 8.10 (1 H, br s, 4-H), 8.54 (1 H, s, NH), 9.14 (1 H, br s, NH); ^{13}C NMR ($(CD_3)_2SO$) (HSQC, HMBC) δ 41.9 (1-C), 48.2 (CHCl), 55.2 (2-C), 98.5 (4-C), 112.6 (benzofuran-3,7-C_2), 122.9 (6-C), 123.6 (9-C, benzofuran-6-C), 124.0 (7-C), 124.7 (8-C), 127.5 (benzofuran-4,5-C_2).

(5-amino-1-(chloromethyl)-1,2-dihydro-3H-benzo[e]indol-3-yl)(5-hydroxy-1H-indol-2-yl)methanone (204)

According to the general procedure described above, **199** (0.256 mg, 0.653 µM) was used to synthesise **204** as a dark red oil: ^{1}H NMR (500 MHz; ((CD$_3$)$_2$SO)) (HSQC) δ 3.84 (1 H, dd, *J* = 11.2, 7.8 Hz, CHCl), 4.02 (1 H, dd, *J* = 10.9, 2.9 Hz, CHCl), 4.21 (1 H, m, 1-H), 4.55 (1 H, dd, *J* = 10.6, 1.7 Hz, 2-H), 4.77 (1 H, dd, *J* = 10.9, 9.2 Hz, 2-H), 6.80 (1 H, dd, *J* = 9.0, 2.4 Hz, indole-6-H), 6.98 (1 H, d, *J* = 2.4 Hz, indole-4-H), 7.01 (1 H, d, *J* = 1.9 Hz, indole-3-H), 7.31 (1 H, d, *J* = 8.5 Hz, indole-7-H), 7.34 (1 H, t *J* = 8.1 Hz, 7-H), 7.51 (1 H, t, *J* = 7.1 Hz, 8-H), 7.85 (1 H, d, *J* = 8.1 Hz, 9-H), 7.94 (1 H, d, *J* = 8.5 Hz, 6-H), 8.16 (1 H, s, 4-H), 8.52 (1 H, br s, NH or OH), 8.89 (1 H, br s, NH or OH), 9.10 (1 H, br s, NH or OH), 11.40 (1 H, br s, indole-NH); ^{13}C NMR ((CD$_3$)$_2$SO) (HSQC) δ 41.9 (1-C), 48.1 (CHCl), 55.5 (2-C), 98.9 (4-C), 105.0 (indole-4-C), 105.3 (indole-3-C), 113.3 (indole-7-C), 115.9 (indole-6-C), 123.1 (6-C), 123.2 (7-C), 123.7 (9-C), 127.2 (8-C).

5-amino-(1-(chloromethyl)-1,2-dihydro-3H-benzo[e]indol-3-yl)(6-methoxy-1H-indol-2-yl)methanone (205)

According to the general procedure described above, **200** (0.7 mg, 1.61 µmol) was used to synthesise **205** as a red oil: ^{1}H NMR (500 MHz; (CD$_3$)$_2$SO) (HSQC) δ 3.80 (3 H, s, OCH$_3$), 3.85 (1 H, dd, *J* = 11.0, 7.6 Hz, CHCl), 4.02 (1 H, dd, *J* = 10.5, 2.3 Hz, CHCl), 4.22 (1 H, m, 1-H), 4.55 (1 H, d, *J* = 10.5 Hz, 2-H), 4.78 (1 H, t, *J* = 9.3 Hz, 1-H), 6.76 (1 H, dd, *J* = 8.2, 1.8 Hz, indole-5-H), 6.96 (1 H, s, indole-3-H), 7.15 (1 H, s, indole-7-H), 7.33 (1 H, t, *J* = 7.6 Hz, 7-H), 7.50 (1 H, t, *J* = 7.0 Hz, 8-H), 7.58 (1 H, d, *J* = 8.8 Hz, indole-4-H), 7.84 (1 H, d, *J* = 8.2 Hz, 9-H), 7.93 (1 H, d, *J* = 8.2 Hz, 6-H), 8.18 (1 H, s, 4-H), 8.52 (1 H, br s, NH), 9.10 (1 H, br s, NH), 11.53 (1 H, br s, NH).

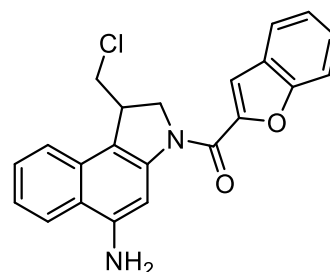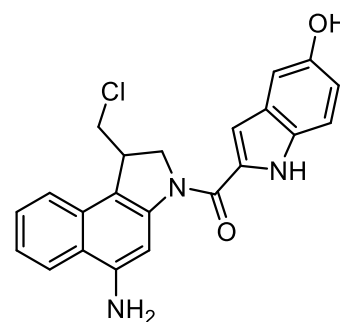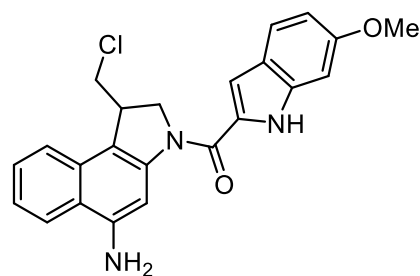**(5-amino-1-(chloromethyl)-1,2-dihydro-3H-benzo[e]indol-3-yl)(5,6,7-trimethoxy-1H-indol-2-yl)methanone (206)**

According to the general procedure described above, **201** (2.59 mg, 5.22 μmol) was used to synthesise **206** (1.78 mg, 73%) as a dark red oil: ^{1}H NMR (500 MHz; (CD$_3$)$_2$SO) (HSQC, HMBC) δ 3.74 (1 H, m, CHCl), 3.75 (3 H, s, OCH$_3$), 3.77 (3 H, s, OCH$_3$), 3.88 (3 H, s, OCH$_3$), 3.95 (1 H, dd, J = 10.3, 3.2 Hz, CHCl), 4.12 (1 H, m, 1-H), 4.41 (1 H, d, J = 10.9 Hz, 2-H), 4.67 (1 H, t, J = 9.6 Hz, 2-H), 6.91 (1 H, br s, indole-3-H), 7.01 (1 H, d, J = 1.7 Hz, indole-4-H), 7.28 (1 H, t, J = 7.8 Hz, 7-H), 7.44 (1 H, t, J = 7.2 Hz, 8-H), 7.78 (1 H, d, J = 8.1 Hz, 9-H), 7.88 (1 H, d J = 8.3 Hz, 6-H), 8.04 (1 H, br s, 4-H), 8.45 (1 H, br s, NH), 9.04 (1 H, br s, NH), 11.41 (1 H, s, NH); ^{13}C NMR (125 MHz; (CD$_3$)$_2$SO) (HSQC, HMBC) δ 41.7 (1-C), 48.0 (CHCl), 55.6 (2-C), 56.6 (OCH$_3$), 61.5 (OCH$_3$), 61.8 (OCH$_3$), 98.4 (indole-3-C), 98.7 (4-C), 106.5 (indole-4-C), 123.0 (6-C), 123.5 (7-C), 123.7 (9-C), 127.4 (8-C), 130.1 (9a-C), 149.0 (5-C).
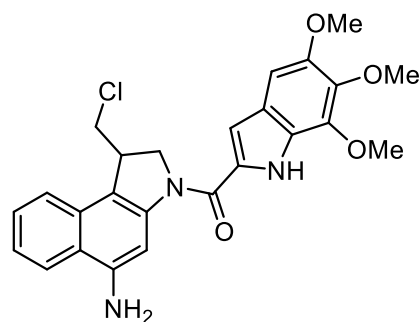
6.67 *In vitro* cellular cytotoxicity assays.

The human prostate cancer cell line PC3 (ATCC catalogue # CRL-1435) was cultured in RPMI 1460 cell culture media (ThermoFisher Scientific UK, gibco, catalogue # A1049101), which was supplemented with foetal bovine serum (FBS, 10% (v/v) ThermoFisher Scientific UK, gibco, catalogue # 10500-064), penicillin G sodium salt (100 U/mL) and streptomycin sulphate (100 μg/mL) solution (5%, ThermoFisher Scientific UK, gibco, catalogue # 15140-122) at 37°C in a humidified atmosphere containing 5% (v/v) CO2. Cells were maintained in T75 (Nunc; 75 cm2) tissue culture flasks and passaged once weekly with new T75 flasks being seeded with the required cell numbers to reach 80-90% confluence in preparation for subsequent experiments. Seed density experiments were performed to determine the amount of cells required to give an acceptable optical density value after a 72-hour incubation period. The seed density of PC3 cells required for the MTS assay was 2000 cells/50 μL. The MTS assay is based on the reagent: Promega 'Cell Titer 96® Aq. One Solution Cell Proliferation Assay' and was used as recommended by the manufacturer (Promega, U.S.A) followed by incubation at 37°C, in humidified atmosphere containing 5% (v/v) CO2 for 4 hours after which, the

absorbance of each well was measured at 490 nm using a BMG labtech FLUOstar Omega microplate reader. Centrifugation of cell suspensions was performed using a Jouan CR412 centrifuge at 1400 rpm.

6.67.1 Procedure

Preparation of cell suspensions

Using aseptic techniques, growth media was removed from the T75 flask and the cells washed with DPBS (5 mL, ThermoFisher Scientific UK, gibco, catalogue # 14190-086). After removal of DPBS, cells were treated with trypsin/EDTA solution (2 mL; 0.25% ThermoFisher Scientific UK, gibco, catalogue # 25200-056) at 37°C until the detachment of cells were confirmed under light microscope (5-8 minutes). Fresh medium (8 mL) was added to neutralise the Trypsin/ EDTA solution and to suspend the cells. The suspension was transferred to a sterile 50mL centrifuge tube and centrifuged at ~1400 rpm for 10 min. The supernatant was removed, and the cell pellet was re-suspended in fresh medium (10 mL). A volume of 100 μL of cell suspension was used to perform a 1 in 2 dilution using trypan blue stain in order to count viability using a haemocytometer. Further dilutions were made to the original cell suspension to provide the required number of cells per well for the experiment (see above). Finally, 50 μL of cells at the required cell density were plated into the appropriate wells of a sterile 96 well cell culture microtiter plate (ThermoFisher Scientific UK, Nunc, catalogue # 167008). The cells were allowed to attach for 6 hours at 37°C, in humidified atmosphere containing 5% (v/v) CO_2 before treating with inhibitor.

Preparation of test compounds

Test agents were prepared at 100x final concentration in DMSO (Sigma Aldrich). A stock solution of inhibitor solution was prepared initially and then serially diluted to provide the required 100x concentrations in DMSO. The 100x DMSO stock solutions were then diluted into tissue culture medium (1 in 50) to provide 2x final compound concentration. Finally, 50

μL of the 2x concentration solutions were added to wells containing 50 μL of cell suspension to provide a final 1x concentration of compound.

Triplicate samples were run by adding the following reagents to the appropriate wells:

Culture medium only (negative control) → 100 μL medium per well; cells suspension only (positive control) → 50 μL medium to 50 μL cell suspension; cells + 1% DMSO(v/v) vehicle → 50 μL of 2% (v/v) DMSO in medium added to 50 μL cell suspension; cells + test compound in 1% DMSO (v/v) vehicle → 50 μL of drug at 2 × concentration with 2% (v/v) DMSO in medium added to 50 μL cell suspension. Each well contained a final volume of 100 μL medium containing final vehicle concentration of 1% DMSO (v/v) and was incubated at 37°C, in a humidified atmosphere containing 5% CO_2 (v/v) for 72 h. Cell viability was measured by chemical treatment with MTS reagent as recommended by the manufacturer (Promega, U.S.A), followed by incubation at 37°C in humidified atmosphere containing 5% CO_2 (v/v) for 4 hours after which, the absorbance of each well was measured at 490 nm using a BMG labtech FLUOstar Omega microplate reader.

The determination of IC_{50} data was calculated using a four-parameter logistic curve and SigmaPlot 13.0 software (SPSS Inc.) for windows. Means and standard deviations were calculated from background corrected absorbance.

7.0 Appendix
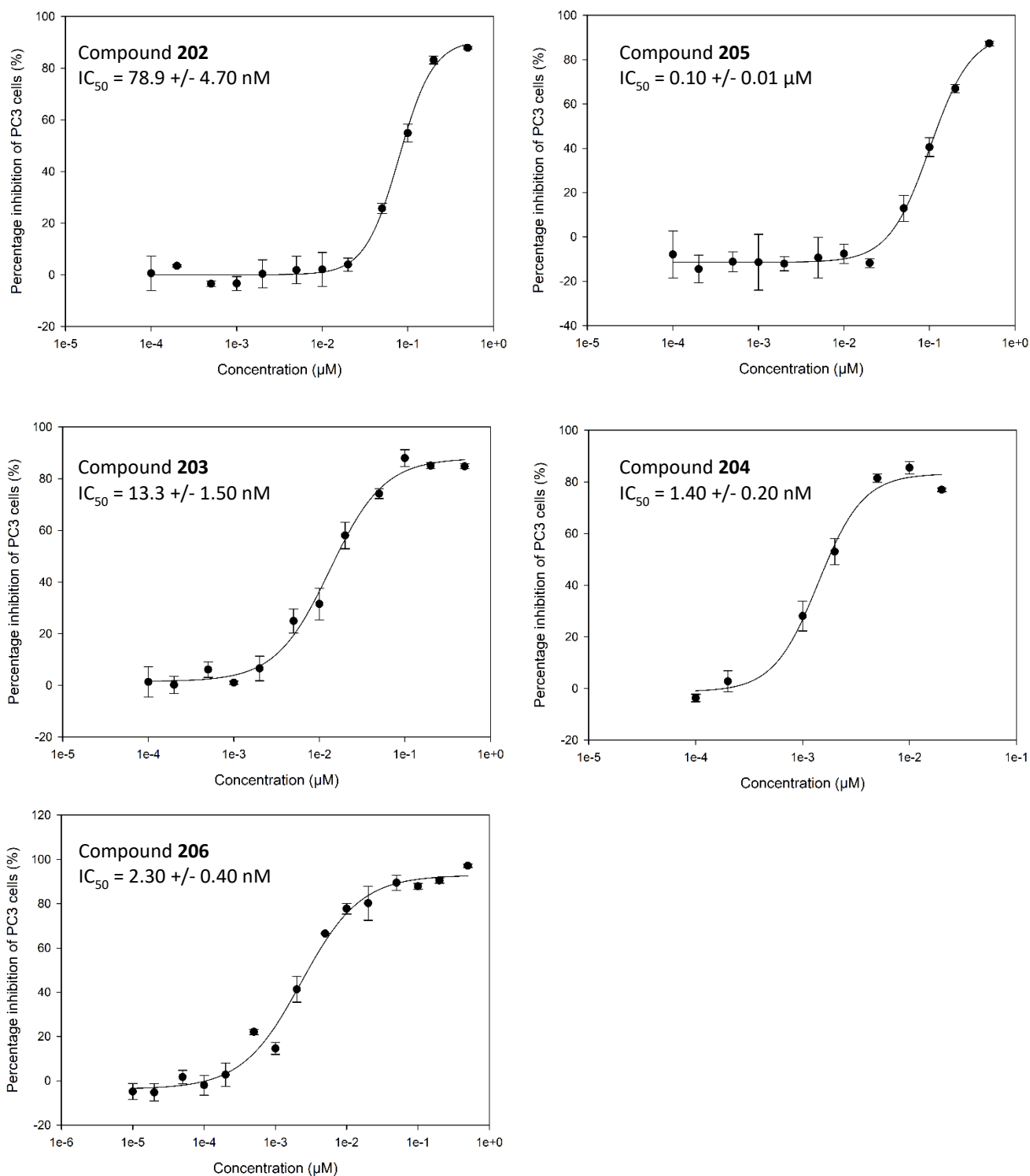
Figure 45: Inhibitory effect of compounds **202-206** on PC3 cells under normoxic conditions.
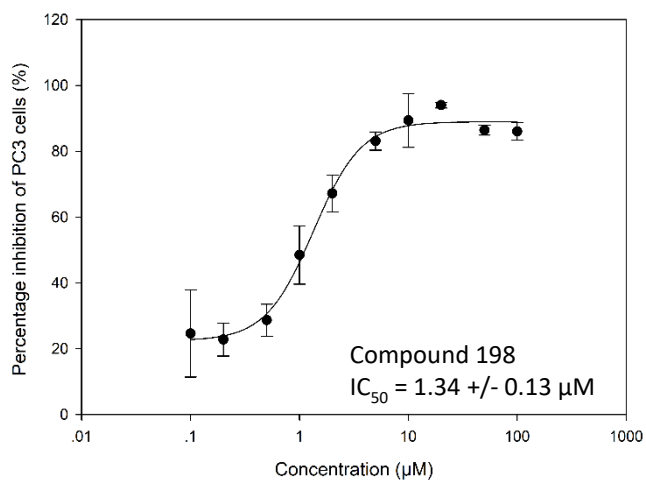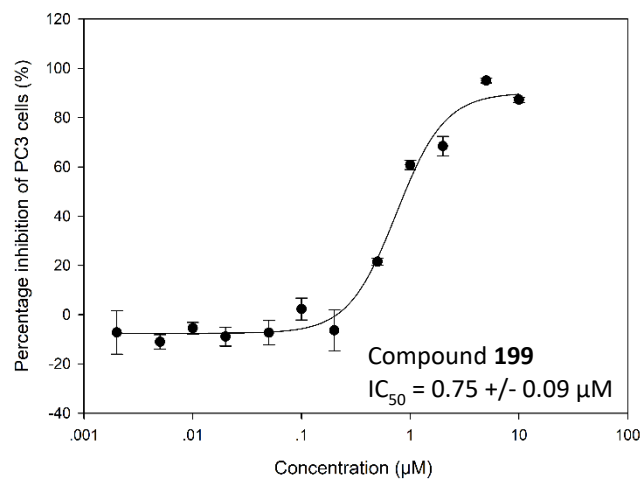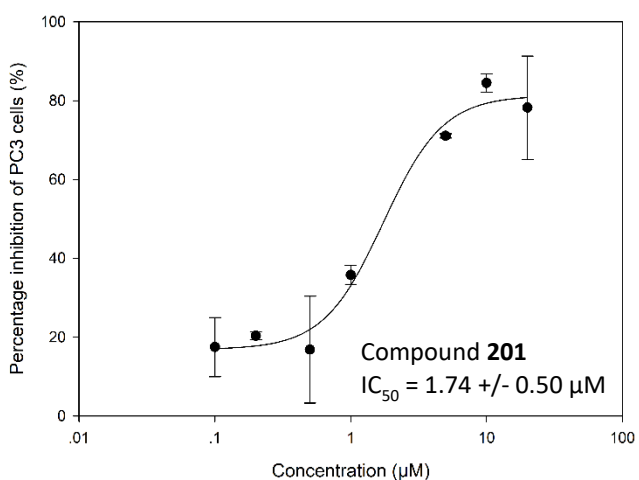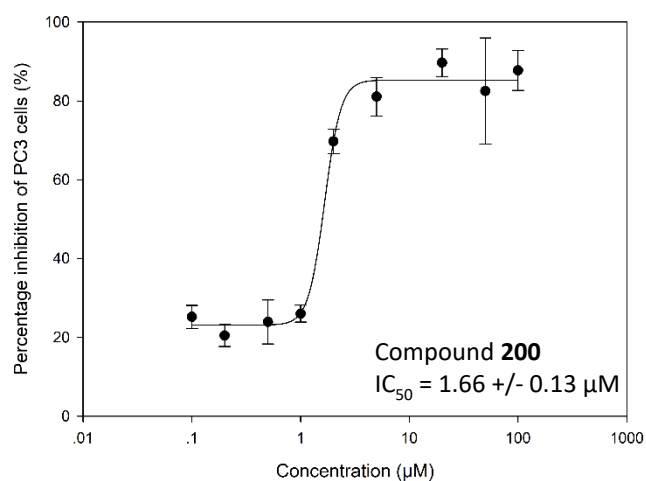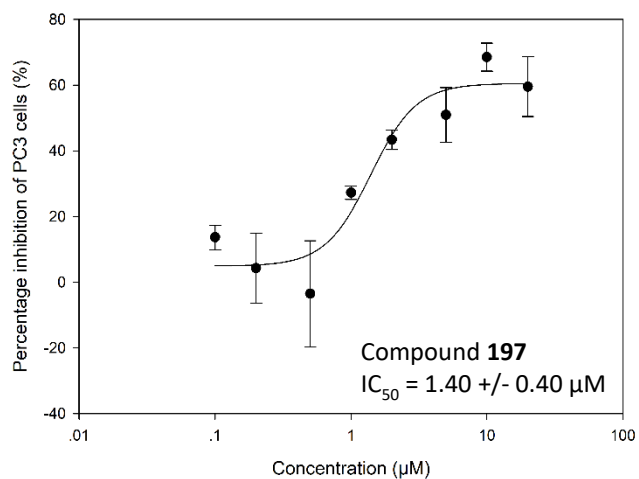
Figure 46: Inhibitory effect of compounds **216-220** on PC3 cells under normoxic conditions.
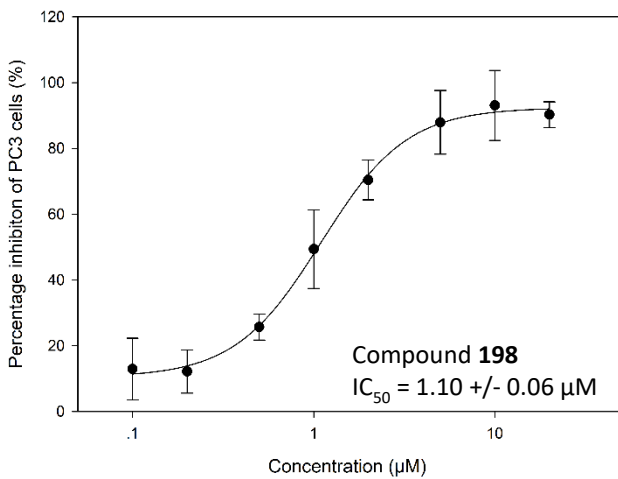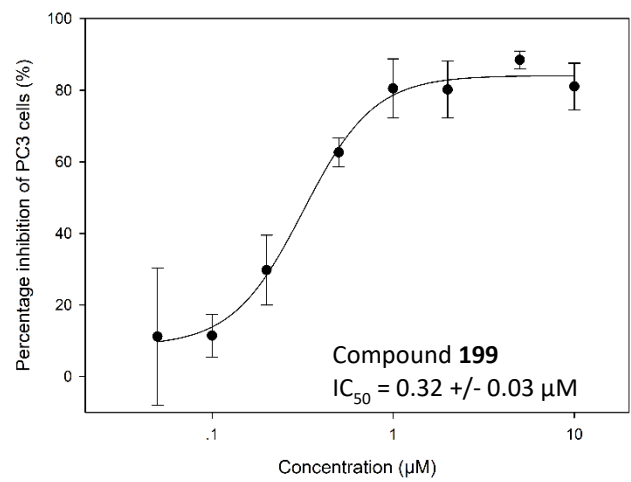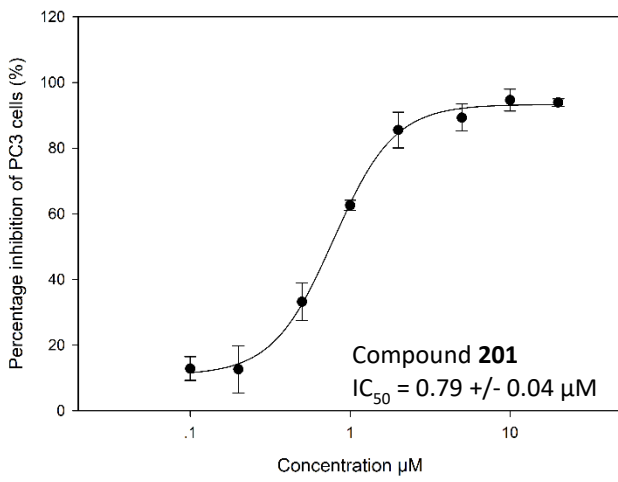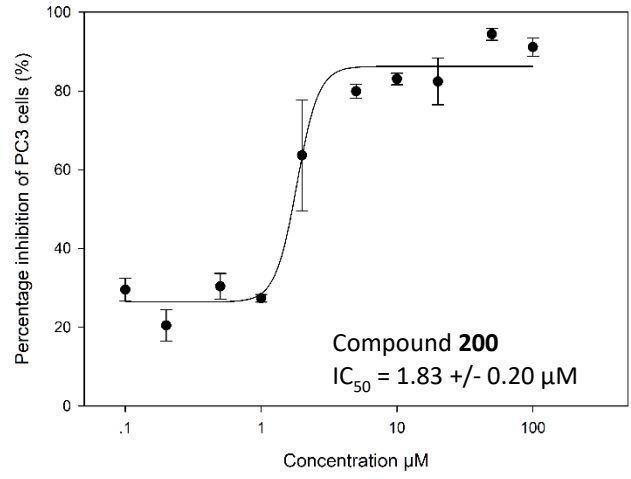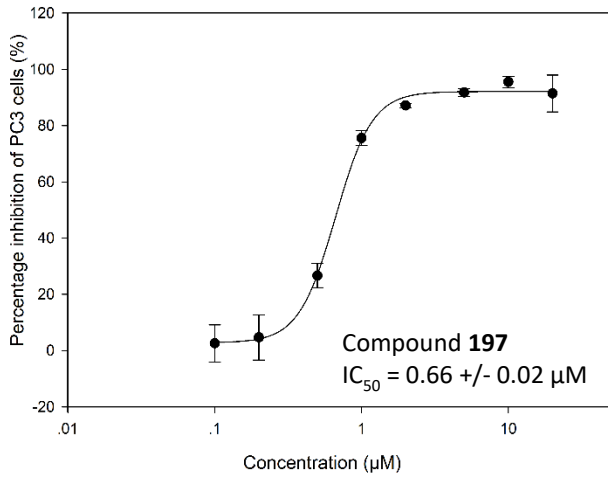
Figure 47: Inhibitory effect of compounds **216-220** on PC3 cells under hypoxic conditions.

8.0 References

1   A. Griffiths, S. R. Wessler, S. B. Carroll and J. Doebly, *Introduction To Genetic Analysis*, 2012.

2   K. Vermeulen, D. R. Van Bockstaele and Z. N. Berneman, *Cell Prolif.*, 2003, **36**, 165–175.

3   K. Vermeulen, D. R. Van Bockstaele and Z. N. Berneman, *Cell Prolif.*, 2003, **36**, 131–149.

4   B. Alberts, A. Johnson, J. Lewis, D. Morgan, M. Raff, K. Roberts and P. Walter, *Molecular Biology of the Cell*, Garland Science, New York, 6th edn., 2015.

5   I. Vivanco and C. L. Sawyers, *Nat. Rev. Cancer*, 2002, **2**, 489–501.

6   K. D. Courtney, R. B. Corcoran and J. A. Engelman, *J. Clin. Oncol.*, 2010, **28**, 1075–1083.

7   M. P. Myers, I. Pass, I. H. Batty, J. Van der Kaay, J. P. Stolarov, B. A. Hemmings, M. H. Wigler, C. P. Downes and N. K. Tonks, *Proc. Natl. Acad. Sci. U. S. A.*, 1998, **95**, 13513–13518.

8   M. Andjelkovic, D. R. Alessi, R. Meier, A. Fernandez, N. J. C. Lamb, M. Frech, P. Cron, P. Cohen, J. M. Lucocq and B. A. Hemmings, *J. Biol. Chem.*, 1997, **272**, 31515–31524.

9   A. Bellacosa, T. O. Chan, N. N. Ahmed, K. Datta, S. Malstrom, D. Stokoe, F. McCormick, J. Feng and P. Tsichlis, *Oncogene*, 1998, **17**, 313–325.

10   J. a Romashkova and S. S. Makarov, *Nature*, 1999, **401**, 86–90.

11   L. D. Mayo and D. B. Donner, *Proc. Natl. Acad. Sci.*, 2001, **98**, 11598–11603.

12   S. R. Datta, H. Dudek, T. Xu, S. Masters, F. Haian, Y. Gotoh and M. E. Greenberg, *Cell*, 1997, **91**, 231–241.

13   A. Brunet, A. Bonni, M. J. Zigmond, M. Z. Lin, P. Juo, L. S. Hu, M. J. Anderson, K. C. Arden, J. Blenis and M. E. Greenberg, *Cell*, 1999, **96**, 857–868.

14   D. Hanahan and R. A. Weinberg, *Cell*, 2000, **100**, 57–70.

15   C. Sherr, *Science*, 1996, **274**, 1672–1677.

16   T. Hunter and J. Pines, *Cell*, 1994, **79**, 573–582.

17   NHS England, Stages of Cancer, http://www.cancerresearchuk.org/about-cancer/what-is-cancer/stages-of-cancer, (accessed 23 April 2018).

18   J. Malm and H. Lilja, *Scand. J. Clin. Lab. Invest.*, 1995, **55**, 15–22.

19   S. W. Hayward and G. R. Cunha, *Radiol. Clin. North Am.*, 2000, **38**, 1–14.

20   G. R. Cunha, A. A. Donjacour, P. S. Cooke, H. Mee, R. M. Bigsby, S. J. Higgins and Y. Sugimura, *Endocr. Rev.*, 1987, **8**, 338–362.

21   G. R. Cunha, L. W. K. Chung, J. M. Shannon and B. A. Reese, *Biol. Reprod.*, 1980, **22**, 19–42.

22   C. A. Bondy, H. Werner, C. T. Roberts and D. LeRoith, *Mol. Endocrinol.*, 1990, **4**, 1386–98.

23   G. Aumüller and J. Seitz, *Int. Rev. Cytol.*, 1990, **121**, 127–231.

24   H. Lilja, P. A. Abrahamsson and A. Lundwall, *J. Biol. Chem.*, 1989, **264**, 1894–1900.

25   A. Peter, H. Lilja, Å. Lundwall and J. Malm, *Eur. J. Biochem.*, 1998, **252**, 216–221.

26   H. Lilja, J. Oldbring, G. Rannevik and C. B. Laurell, *J. Clin. Invest.*, 1987, **80**, 281–5.

27   H. Lilja and C.-B. Laurell, *Scand. J. Clin. Lab. Invest.*, 1984, **44**, 447–452.

28   A. Christensson, C. -B Laurell and H. Lilja, *Eur. J. Biochem.*, 1990, **194**, 755–763.

29   M. C. Wang, L. D. Papsidero, M. Kuriyama, L. A. Valenzuela, G. P. Murphy and T. M. Chu, *Prostate*, 1981, **2**, 89–96.

30   Å. Lundwall and H. Lilja, *FEBS Lett.*, 1987, **214**, 317–322.

31   K. W. Watt, P. J. Lee, T. M'Timkulu, W. P. Chan and R. Loor, *Proc. Natl. Acad. Sci. U. S. A.*, 1986, **83**, 3166–70.

32   J. M. Atkinson, C. S. Siller and J. H. Gill, *Br. J. Pharmacol.*, 2009, **153**, 1344–1352.

33   L. H. Cazares, R. R. Drake, a Esquela-Kirscher, R. S. Lance, O. J. Semmes and D. a Troyer, *Cancer Biomark.*, 2010, **9**, 441–59.

34   A. Mhaka, S. R. Denmeade, W. Yao, J. T. Isaacs and S. R. Khan, *Bioorg. Med. Chem. Lett.*, 2002, **12**, 2459–2461.

35   B. G. Timms and L. E. Hofkamp, *Differentiation*, 2011, **82**, 173–183.

36   NHS England, NHS conditions - Prostatitis, https://www.nhs.uk/conditions/Prostatitis/, (accessed 2 April 2018).

37   R. M. Pluta, C. Lynm and R. M. Golub, *JAMA*, 2012, **307**, 527.

38   PCUK, Infographic, http://prostatecanceruk.org/prostate-information/what-is-my-risk/infographic-what-is-my-risk, (accessed 2 September 2015).

39   J.-E. Damber and G. Aus, *Lancet*, 2008, **371**, 1710–1721.

40   IACR, Prostate Cancer Estimated Incidence, Mortality and Prevalence Worldwide in

2012, http://globocan.iarc.fr/old/FactSheets/cancers/prostate-new.asp, (accessed 7 April 2018).

41   CRUK, Prostate cancer incidence statistics, http://www.cancerresearchuk.org/health-professional/cancer-statistics/statistics-by-cancer-type/prostate-cancer/incidence, (accessed 7 April 2018).

42   A. Heidenreich, P. J. Bastian, J. Bellmunt, M. Bolla, S. Joniau, T. van der Kwast, M. Mason, V. Matveev, T. Wiegel, F. Zattoni, N. Mottet and European Association of Urology, *Eur. Urol.*, 2014, **65**, 124–37.

43   S. R. J. Bott, A. J. Birtle, C. J. Taylor and R. S. Kirby, *Postgrad. Med. J.*, 2003, **79**, 643–5.

44   S. R. J. Bott, A. J. Birtle, C. J. Taylor and R. S. Kirby, *Postgrad. Med. J.*, 2003, **79**, 575–80.

45   E. D. Crawford, *Urology*, 2003, **62**, 3–12.

46   A. W. Hsing, *Front. Biosci.*, 2006, **11**, 1388.

47   NICE, *Prostate cancer: diagnosis and treatment. Clinical guideline 175*, 2014.

48   M. E. Taplin, G. J. Bubley, T. D. Shuster, M. E. Frantz, A. E. Spooner, G. K. Ogata, H. N. Keer and S. P. Balk, *N. Engl. J. Med.*, 1995, **332**, 1393–1398.

49   PCUK, Hormone Therapy, http://prostatecanceruk.org/prostate-information/c, (accessed 6 September 2015).

50   N. Yadav and H. V. Heemers, *Minerva Urol. e Nefrol.*, 2012, 64, 35–49.

51   C. Tran, S. Ouk, N. J. Clegg, Y. Chen, P. a Watson, V. Arora, J. Wongvipat, P. M. Smith-Jones, D. Yoo, A. Kwon, T. Wasielewska, D. Welsbie, C. D. Chen, C. S. Higano, T. M. Beer, D. T. Hung, H. I. Scher, M. E. Jung and C. L. Sawyers, *Science (80-.).*, 2009, **324**, 787–790.

52   Q. Wang, W. Li, Y. Zhang, X. Yuan, K. Xu, J. Yu, Z. Chen, R. Beroukhim, H. Wang, M. Lupien, T. Wu, M. M. Regan, C. A. Meyer, J. S. Carroll, A. K. Manrai, O. A. Jänne, S. P. Balk, R. Mehra, B. Han, A. M. Chinnaiyan, M. A. Rubin, L. True, M. Fiorentino, C. Fiore, M. Loda, P. W. Kantoff, X. S. Liu and M. Brown, *Cell*, 2009, **138**, 245–256.

53   M. Shiota, A. Yokomizo, T. Adachi, H. Koga, A. Yamaguchi, K. Imada, A. Takeuchi, K. Kiyoshima, J. Inokuchi, K. Tatsugami and S. Naito, *Jpn. J. Clin. Oncol.*, 2014, **44**, 860–867.

54   C. L. Morais, M. Herawi, A. Toubaji, R. Albadine, J. Hicks, G. J. Netto, A. M. De Marzo, J. I. Epstein and T. L. Lotan, *Prostate*, 2015, **75**, 1610–1619.

55   F. Demichelis, K. Fall, S. Perner, O. Andrén, F. Schmidt, S. R. Setlur, Y. Hoshida, J.-M. Mosquera, Y. Pawitan, C. Lee, H.-O. Adami, L. a Mucci, P. W. Kantoff, S.-O. Andersson, a M. Chinnaiyan, J.-E. Johansson and M. a Rubin, *Oncogene*, 2007, **26**, 4596–4599.

56   S. H. Lee, D. Johnson, R. Luong and Z. Sun, *J. Biol. Chem.*, 2014, **290**, 2759–2768.

57   Tests for Prostate Cancer, https://www.cancer.org/cancer/prostate-cancer/detection-diagnosis-staging/how-diagnosed.html, (accessed 2 February 2017).

58   S. Jain, A. G. Bhojwani and J. K. Mellon, *Postgrad. Med. J.*, 2002, **78**, 646–50.

59   Prostate Cancer UK, Prostate biopsy, https://prostatecanceruk.org/prostate-information/prostate-tests/prostate-biopsy, (accessed 7 April 2018).

60   Prostate Cancer UK, mpMRI before biopsy can radically improve diagnosis, https://prostatecanceruk.org/about-us/what-we-think-and-do/mpmri, (accessed 7 April 2018).

61   PCEC, Gleason Score, https://www.prostateconditions.org/about-prostate-conditions/prostate-cancer/newly-diagnosed/gleason-score, (accessed 8 April 2018).

62   Prostate Cancer UK, *Surgery: radical prostatectomy*, 2017.

63   D. E. Spratt, J. Y. Lee, R. T. Dess, V. Narayana, C. Evans, A. Liss, R. Winfield, M. J. Schipper, T. S. Lawrence and P. W. McLaughlin, *Eur. Urol.*, 2017, **72**, 617–624.

64   Prostate Cancer UK, Advanced prostate cancer, https://prostatecanceruk.org/prostate-information/advanced-prostate-cancer, (accessed 8 April 2018).

65   Y. Tolkach, S. Joniau and H. Van Poppel, *BJU Int.*, 2013, **111**, 1021–1030.

66   W. D. Figg, C. H. Chau and E. J. Small, *Drug management of prostate cancer*, Springer, 2010.

67   I. S. Shergill, M. Arya, P. Grange and A. R. Mundy, *Medical therapy in urology*, Springer-Verlag, 2010.

68   T.-H. Lin, S. O. Lee, Y. Niu, D. Xu, L. Liang, L. Li, S.-D. Yeh, N. Fujimoto, S. Yeh and C. Chang, *J. Biol. Chem.*, 2013, **288**, 19359–69.

69   R. Hu, C. Lu, E. A. Mostaghel, S. Yegnasubramanian, M. Gurel, C. Tannahill, J. Edwards, W. B. Isaacs, P. S. Nelson, E. Bluemn, S. R. Plymate and J. Luo, *Cancer Res.*, 2012, **72**, 3457–62.

70   K. A. Lyseng-Williamson and C. Fenton, *Drugs*, 2005, **65**, 2513–2531.

71   A. Heidenreich, P. J. Bastian, J. Bellmunt, M. Bolla, S. Joniau, T. van der Kwast, M.

Mason, V. Matveev, T. Wiegel, F. Zattoni, N. Mottet and European Association of Urology, *Eur. Urol.*, 2014, **65**, 467–79.

72   N. D. James, J. S. de Bono, M. R. Spears, N. W. Clarke, M. D. Mason, D. P. Dearnaley, A. W. S. Ritchie, C. L. Amos, C. Gilson, R. J. Jones, D. Matheson, R. Millman, G. Attard, S. Chowdhury, W. R. Cross, S. Gillessen, C. C. Parker, J. M. Russell, D. R. Berthold, C. Brawley, F. Adab, S. Aung, A. J. Birtle, J. Bowen, S. Brock, P. Chakraborti, C. Ferguson, J. Gale, E. Gray, M. Hingorani, P. J. Hoskin, J. F. Lester, Z. I. Malik, F. McKinna, N. McPhail, J. Money-Kyrle, J. O'Sullivan, O. Parikh, A. Protheroe, A. Robinson, N. N. Srihari, C. Thomas, J. Wagstaff, J. Wylie, A. Zarkar, M. K. B. Parmar and M. R. Sydes, *N. Engl. J. Med.*, 2017, **377**, 338–351.

73   D. L. Boger and D. S. Johnson, *Proc. Natl. Acad. Sci. U. S. A.*, 1995, **92**, 3642–9.

74   M. Ichimura, H. Ogawa, K. Takahashi, E. Kobayashi, I. Kawamoto, T. Yasuzawa, I. Takahashi and H. Nakano, *J. Antibiot. (Tokyo).*, 1990, **43**, 1037–1038.

75   W. Wrasidlo, D. S. Johnson and D. L. Boger, *Bioorganic Med. Chem. Lett.*, 1994, **4**, 631–636.

76   J. P. McGovren, G. L. Clarke, E. A. Pratt and T. F. DeKoning, *J. Antibiot. (Tokyo).*, 1984, **37**, 63–70.

77   W. C. Krueger and M. D. Prairie, *Chem. Biol. Interact.*, 1992, **82**, 31–46.

78   N. Ghosh, H. M. Sheldrake, M. Searcey and K. Pors, *Curr. Top. Med. Chem.*, 2009, **9**, 1494–524.

79   D. L. Boger, *Acc. Chem. Res.*, 1995, **28**, 20–29.

80   D. L. Boger, *Pure Appl. Chem.*, 1994, **65**, 837–844.

81   D. L. Boger and W. Yun, *J. Am. Chem. Soc.*, 1994, **116**, 5523–5524.

82   P. G. Baraldi, G. Balboni, M. G. Pavani, G. Spalluto, M. A. Tabrizi, E. De Clercq, J. Balzarini, T. Bando, H. Sugiyama and R. Romagnoli, *J. Med. Chem.*, 2001, **44**, 2536–2543.

83   D. L. Boger, H. Zarrinmayeh, S. A. Munk, P. A. Kitos and O. Suntornwat, *Proc. Natl. Acad. Sci. U. S. A.*, 1991, **88**, 1431–1435.

84   L. F. Tietze, B. Krewer, H. Frauendorf, F. Major and I. Schuberth, *Angew. Chemie Int. Ed.*, 2006, **45**, 6570–6574.

85   L. Díaz, M. Chiong, A. Quest, S. Lavandero and A. Stutzin, *Cell Death Differ.*, 2005, **12**, 1449–1456.

86 S. W. G. Tait, G. Ichim and D. R. Green, *J. Cell Sci.*, 2014, **127**, 2135–2144.

87 S. Elmore, *Toxicol. Pathol.*, 2007, **35**, 495–516.

88 D. L. Boger, P. Mesini and C. M. Tarby, *J. Am. Chem. Soc.*, 1994, **116**, 6461–6462.

89 D. L. Boger and P. Turnbull, *J. Org. Chem.*, 1997, **62**, 5849–5863.

90 D. L. Boger, A. Santillán, M. Searcey and Q. Jin, *J. Am. Chem. Soc.*, 1998, **120**, 11554–11557.

91 D. L. Boger, T. Ishizaki, H. Zarrinmayeh, S. A. Munk, P. A. Kitos and O. Suntornwat, *J. Am. Chem. Soc.*, 1990, **112**, 8961–8971.

92 R. J. Sundberg and T. Nishiguchi, *Tetrahedron Lett.*, 1983, **24**, 4773–4776.

93 K. S. MacMillan and D. L. Boger, *J. Med. Chem.*, 2009, **52**, 5771–5780.

94 D. L. Boger, R. M. Garbaccio and Q. Jin, *J. Org. Chem.*, 1997, **62**, 8875–8891.

95 B. Cacciari, R. Romagnoli, P. G. Baraldi, T. Da Ros and G. Spalluto, *Expert Opin. Ther. Pat.*, 2000, **10**, 1853–1871.

96 J. P. Parrish, D. B. Kastrinsky, F. Stauffer, M. P. Hedrick, I. Hwang and D. L. Boger, *Bioorg. Med. Chem.*, 2003, **11**, 3815–3838.

97 † Jared B. J. Milbank, † Moana Tercel, † Graham J. Atwell, ‡ William R. Wilson, ‡ and Alison Hogg, † William A. Denny*, J. B. J. Milbank, M. Tercel, G. J. Atwell, W. R. Wilson, A. Hogg and W. A. Denny, *J. Med. Chem.*, 1999, **42**, 649–658.

98 S. Winstein and R. Baird, *J. Am. Chem. Soc.*, 1957, **79**, 756–757.

99 W. S. Murphy and S. Wattanasin, *Chem. Soc. Rev.*, 1983, **12**, 213.

100 E. A. Twum, A. Nathubhai, P. J. Wood, M. D. Lloyd, A. S. Thompson and M. D. Threadgill, *Bioorg. Med. Chem.*, 2015, **23**, 3481–3489.

101 G. J. Atwell, M. Tercel, M. Boyd, W. R. Wilson and W. A. Denny, *J. Org. Chem.*, 1998, **63**, 9414–9420.

102 M. Tercel, F. B. Pruijn, P. D. O'Connor, H. D. S. Liyanage, G. J. Atwell and S. M. Alix, *ChemBioChem*, 2014, 1998–2006.

103 D. L. Boger, W. Yun and B. R. Teegarden, *J. Org. Chem.*, 1992, **57**, 2873–2876.

104 L. F. Tietze, J. M. Von Hof, B. Krewer, M. Müller, F. Major, H. J. Schuster, I. Schuberth and F. Alves, *ChemMedChem*, 2008, **3**, 1946–1955.

105 G. J. Atwell, W. R. Wilson and W. A. Denny, *Bioorg. Med. Chem. Lett.*, 1997, **7**, 1493–1496.

106 A. L. Williams, S. R. Dandepally and S. V. Kotturi, *Mol. Divers.*, 2010, **14**, 697–707.

107   K. T. Howard and J. D. Chisholm, *Org. Prep. Proced. Int.*, 2016, **48**, 1–36.

108   L. F. Tietze, H. J. Schuster, S. M. Hampel, S. Rühl and R. Pfoh, *Chem. - A Eur. J.*, 2008, **14**, 895–901.

109   L. Shi, Y. Chu, P. Knochel and H. Mayr, *Org. Lett.*, 2012, **14**, 2602–2605.

110   L. Shi, Y. Chu, P. Knochel and H. Mayr, *J. Org. Chem.*, 2009, **74**, 2760–2764.

111   L. Shi, Y. Chu, P. Knochel and H. Mayr, *Angew. Chemie Int. Ed.*, 2008, **47**, 202–204.

112   J. P. Lajiness and D. L. Boger, *J. Org. Chem.*, 2011, **76**, 583–587.

113   A. Omlin, O. Sartor, C. Rothermundt, R. Cathomas, J. S. De Bono, L. Shen, Z. Su and S. Gillessen, *Clin. Genitourin. Cancer*, 2015, **13**, 205–208.

114   K. C. Chen, K. Schmuck, L. F. Tietze and S. R. Roffler, *Mol. Pharm.*, 2013, **10**, 1773–1782.

115   A. L. Wolfe, K. K. Duncan, N. K. Parelkar, S. J. Weir, G. a. Vielhauer and D. L. Boger, *J. Med. Chem.*, 2012, **55**, 5878–5886.

116   M. Uematsu and D. L. Boger, *J. Org. Chem.*, 2014, 9699–9703.

117   A. Kamal, V. Tekumalla, P. Raju, V. G. M. Naidu, P. V. Diwan and R. Sistla, *Bioorg. Med. Chem. Lett.*, 2008, **18**, 3769–3773.

118   K. D. Bagshawe, *Clin. Pharmacokinet.*, 1994, **27**, 368–376.

119   L. N. Jungheim and T. A. Shepherd, *Chem. Rev.*, 1994, **94**, 1553–1566.

120   F. M. Huennekens, *Trends Biotechnol.*, 1994, **12**, 234–239.

121   B. R. S. Dipaola, J. Rinehart, J. Nemunaitis, S. Ebbinghaus, E. Rubin, T. Capanna, M. Ciardella, S. Doyle-lindrud, S. Goodwin, M. Fontaine, N. Adams, A. Williams, M. Schwartz, G. Winchell, K. Wickersham, P. Deutsch and S. Yao, *J. Clin. Oncol.*, 2002, **20**, 1874–1879.

122   D. DeFeo-Jones, V. M. Garsky, B. K. Wong, D. M. Feng, T. Bolyar, K. Haskell, D. M. Kiefer, K. Leander, E. McAvoy, P. Lumma, J. Wai, E. T. Senderak, S. L. Motzel, K. Keenan, M. Van Zwieten, J. H. Lin, R. Freidinger, J. Huff, A. Oliff and R. E. Jones, *Nat. Med.*, 2000, **6**, 1248–1252.

123   P. Vaupel, P. Okunieff, F. Kallinowski and L. J. Neuringer, *Radiat. Res.*, 1989, **120**, 477.

124   P. Okunieff, M. Hoeckel, E. P. Dunphy, K. Schlenger, C. Knoop and P. Vaupel, *Int. J. Radiat. Oncol.*, 1993, **26**, 631–636.

125   T. L. Clanton, *J. Appl. Physiol.*, 2007, **102**, 2379–2388.

126   W. R. Wilson and M. P. Hay, *Nat. Rev. Cancer*, 2011, 11, 393–410.

127 I. Parveen, D. P. Naughton, W. J. . Whish and M. D. Threadgill, *Bioorg. Med. Chem. Lett.*, 1999, **9**, 2031–2036.

128 M. Tercel, W. A. Denny and W. R. Wilson, *Bioorg. Med. Chem. Lett.*, 1996, **6**, 2741–2744.

129 M. Tercel, G. J. Atwell, S. Yang, R. J. Stevenson, K. J. Botting, M. Boyd, E. Smith, R. F. Anderson, W. A. Denny, W. R. Wilson and F. B. Pruijn, *J. Med. Chem.*, 2009, **52**, 7258–7272.

130 R. S. DiPaola, *J. Clin. Oncol.*, 2002, **20**, 1874–1879.

131 G. A. R. Y. Suaifan, M. F. Mahon, T. Arafat and M. D. Threadgill, *Tetrahedron*, 2006, **62**, 11245–11266.

132 G. A. R. Y. Suaifan, T. Arafat and M. D. Threadgill, *Bioorganic Med. Chem.*, 2007, **15**, 3474–3488.

133 H. Maeda, J. Wu, T. Sawa, Y. Matsumura and K. Hori, *J. Control. Release*, 2000, **65**, 271–284.

134 S. Dumitriu and V. Popa, *Polymeric Biomaterials: Medicinal and Pharmaceutical Applications, Volume 2*, CRC Press, 2013.

135 H. Maeda, *J. Drug Target.*, 2017, **25**, 781–785.

136 C. L. Waite and C. M. Roth, *Crit. Rev. Biomed. Eng.*, 2012, **40**, 21–41.

137 J. W. Nichols and Y. H. Bae, *J. Control. Release*, 2014, **190**, 451–464.

138 N. Cao and S.-S. Feng, *Biomaterials*, 2008, **29**, 3856–3865.

139 T. Yin, Q. Wu, L. Wang, L. Yin, J. Zhou and M. Huo, *Mol. Pharm.*, 2015, **12**, 3020–3031.

140 L. Seymour, K. Ulbrich, P. Steyger, M. Brereton, V. Subr, J. Strohalm and R. Duncan, *Br. J. Cancer*, 1994, **70**, 636–641.

141 P. A. Vasey, R. Duncan, S. B. Kaye and J. Cassidy, *Eur. J. Cancer*, 1995, **31**, S193.

142 Y. Wang, J. Jiang, X. Jiang, S. Cai, H. Han, L. Li, Z. Tian, W. Jiang, Z. Zhang, Y. Xiao, S. C. Wright and J. W. Larrick, *Bioorganic Med. Chem.*, 2008, **16**, 6552–6559.

143 Y. Ben-David, M. Gozin, M. Portnoy and D. Milstein, *J. Mol. Catal.*, 1992, **73**, 173–180.

144 X. Yan, J. Sun, Y. Xu and J. Yang, *Chinese J. Catal.*, 2006, **27**, 119–123.

145 N. M. N. Barl, E. Sansiaume-Dagousset, G. Monzón, A. J. Wagner and P. Knochel, *Org. Lett.*, 2014, **16**, 2422–2425.

146 E. A. Twum, 2013.

147 J. Aubé, C. Fehl, R. Liu, M. C. McLeod and H. F. Motiwala, *Compr. Org. Synth. II*, 2014,

598–635.

148   L. I. Zakharkin, V. N. Kalinin and V. V. Gedymin, *Tetrahedron*, 1971, **27**, 1317–1322.

149   E. S. Wallis and J. F. Lane, in *Organic Reactions*, John Wiley & Sons, Inc., Hoboken, NJ, USA, 2011, pp. 267–306.

150   E. C. Franklin, *Chem. Rev.*, 1934, **14**, 219–250.

151   R. F. Stockel and D. M. Hall, *Nature*, 1963, **197**, 787–788.

152   J. Clayden, S. Warren and N. Greeves, *Organic Chemistry*, Oxford, 2nd edn., 2012.

153   A. Jarrahpour and M. Zarei, *Tetrahedron*, 2009, **65**, 2927–2934.

154   W. Treibs, H.-J. Neupert and J. Hiebsch, *Chem. Ber.*, 1959, **92**, 141–154.

155   P. T. Kaye, M. J. Mphahlele and M. E. Brown, *J. Chem. Soc. Perkin Trans. 2*, 1995, **31**, 835.

156   M. Orlandi, F. Tosi, M. Bonsignore and M. Benaglia, *Org. Lett.*, 2015, **17**, 3941–3943.

157   S. Roy, P. Stollberg, R. Herbst-Irmer, D. Stalke, D. M. Andrada, G. Frenking and H. W. Roesky, *J. Am. Chem. Soc.*, 2015, **137**, 150–153.

158   A. Krasovskiy, V. Malakhov, A. Gavryushin and P. Knochel, *Angew. Chemie - Int. Ed.*, 2006, **45**, 6040–6044.

159   M. Uchiyama, M. Kameda, O. Mishima, N. Yokoyama, M. Koike, Y. Kondo and T. Sakamoto, *J. Am. Chem. Soc.*, 1998, **120**, 4934–4946.

160   M. Uchiyama, M. Koike, M. Kameda, Y. Kondo and T. Sakamoto, *J. Am. Chem. Soc.*, 1996, **118**, 8733–8734.

161   A. S. Guram and S. L. Buchwald, *J. Am. Chem. Soc.*, 1994, **116**, 7901–7902.

162   R. a. Green and J. F. Hartwig, *Org. Lett.*, 2014, 140818123645002.

163   G. D. Vo and J. F. Hartwig, *J. Am. Chem. Soc.*, 2009, **131**, 11049–11061.

164   E. a Twum, T. J. Woodman, W. Wang and M. D. Threadgill, *Org. Biomol. Chem.*, 2013, **11**, 6208–14.

165   C. Peebles, P. M. Alvey, V. Lynch and B. L. Iverson, *Cryst. Growth Des.*, 2014, **14**, 290–299.

166   A. Goti and L. Nannelli, *Tetrahedron Lett.*, 1996, **37**, 6025–6028.

167   W. A. Herrmann, R. W. Fischer, W. Scherer and M. U. Rauch, *Angew. Chemie Int. Ed. English*, 1993, **32**, 1157–1160.

168   J. Einhorn, C. Einhorn, F. Ratajczak, A. Durif, M.-T. Averbuch and J.-L. Pierre, *Tetrahedron Lett.*, 1998, **39**, 2565–2568.

169   T. W. Greene and P. G. M. Wuts, *Protective Groups in Organic Synthesis*, John Wiley & Sons, Inc., New York, USA, 1999.

170   J. P. McGovren, G. L. CLARKE, E. A. PRATT and T. F. DeKoning, *J. Antibiot. (Tokyo).*, 1984, **37**, 63–70.

171   W. L. Heaner IV, C. S. Gelbaum, L. Gelbaum, P. Pollet, K. W. Richman, W. DuBay, J. D. Butler, G. Wells and C. L. Liotta, *RSC Adv.*, 2013, **3**, 13232.

172   Z. Wang, in *Comprehensive Organic Name Reactions and Reagents*, John Wiley & Sons, Inc., Hoboken, NJ, USA, 2010, pp. 1375–1378.

173   H. Hemetsberger, D. Knittel and H. Weidmann, *Monatshefte fur Chemie*, 1970, **101**, 161–165.

174   P. Chauhan, *Synthesis of DNA Minor Groove Binders for Attachment to Prodrug System for Treatment of Prostate Cancer*, 2017.

175   a. Sudhakara, H. Jayadevappa, K. M. Mahadevan and V. Hulikal, *Synth. Commun.*, 2009, **39**, 2506–2515.

176   G. A. R. Y. Suaifan, T. Arafat and M. D. Threadgill, 2007, **15**, 3474–3488.

177   G. A. R. Y. Suaifan, M. F. Mahon and M. D. Threadgill, 2006, **62**, 11245–11266.

178   L. Kisfaludy and I. Schön, *Synthesis (Stuttg).*, 1983, **1983**, 325–327.

179   J. C. Sheehan and G. P. Hess, *J. Am. Chem. Soc.*, 1955, **77**, 1067–1068.

180   F. Albericio, J. M. Bofill, A. El-Faham and S. A. Kates, *J. Org. Chem.*, 1998, **63**, 9678–9683.

181   E. Fischer and E. Fourneau, *Berichte der Dtsch. Chem. Gesellschaft*, 1901, **34**, 2868–2877.

182   B. G. Wouters, L.-H. Wang and J. M. Brown, *Ann. Oncol.*, 1999, **10**, S29–S33.

183   M. Ahmadi, Z. Ahmadihosseini, S. J. Allison, S. Begum, K. Rockley, M. Sadiq, S. Chintamaneni, R. Lokwani, N. Hughes and R. M. Phillips, *Br. J. Pharmacol.*, 2014, **171**, 224–36.

184   J. M. French, J. R. Griffiths and S. T. Diver, *Adv. Synth. Catal.*, 2015, **357**, 361–365.

185   C. E. Garrett and K. Prasad, *Adv. Synth. Catal.*, 2004, **346**, 889–900.

186   D. L. Boger, B. Bollinger and D. S. Johnson, *Bioorg. Med. Chem. Lett.*, 1996, **6**, 2207–2210.

187   C. J. Goodwin, S. J. Holt, S. Downes and N. J. Marshall, *J. Immunol. Methods*, 1995, **179**, 95–103.

188   J. A. Barltrop, T. C. Owen, A. H. Cory and J. G. Cory, *Bioorg. Med. Chem. Lett.*, 1991, **1**, 611–614.

189   G. Malich, B. Markovic and C. Winder, *Toxicology*, 1997, **124**, 179–192.

190   D. L. Boger, A. Santillán, M. Searcey and Q. Jin, *J. Org. Chem.*, 1999, **64**, 5241–5244.

191   D. L. Boger, B. J. Invergo, R. S. Coleman, H. Zarrinmayeh, P. A. Kitos, S. C. Thompson, T. Leong and L. W. McLaughlin, *Chem. Biol. Interact.*, 1990, **73**, 29–52.

192   D. L. Boger, Donald L. Hertzog, Bernd Bollinger, Douglas S. Johnson, Hui Cai, and Joel Goldberg and P. Turnbull, , DOI:10.1021/JA9637208.

193   M. N. Green, J. B. Josimovich, K.-C. Tsou and A. M. Seligman, *Cancer*, 1956, **9**, 176–182.

194   M. Takamatsu, K. Fukase, R. Oka, S. Kitazume, N. Taniguchi and K. Tanaka, *Sci. Rep.*, 2016, **6**, 35872.

195   G. Pirtskhalaishvili, R. L. Hrebinko and J. B. Nelson, *Cancer Pract. ()(pp 295-306), 2001.Date Publ. 2001.*, 2001, **9**, 295–306.

196   B. Bao, A. Ahmad, D. Kong, S. Ali, A. S. Azmi, Y. Li, S. Banerjee, S. Padhye and F. H. Sarkar, *PLoS One*, , DOI:10.1371/journal.pone.0043726.

197   S. Yang and W. A. Denny, *J. Org. Chem.*, 2002, **67**, 8958–8961.

198   E. F. J. Atkinson and J. F. Thorpe, *J. Chem. Soc., Trans.*, 1906, **89**, 1906–1935.

199   H. C. Barany, M. Pianka, W. A. Waters, A. Schönberg, R. Moubasher and A. Mostafa, *J. Chem. Soc.*, 1946, 965–967.

200   F. Zhang, Y. Zhao, L. Sun, L. Ding, Y. Gu and P. Gong, *Eur. J. Med. Chem.*, 2011, **46**, 3149–3157.

201   A. R. Katritzky, S. K. Singh, C. Cai and S. Bobrov, *J. Org. Chem.*, 2006, **71**, 3364–3374.

202   M. N. Hoque, A. Basu and G. Das, *J. Fluoresc.*, 2014, **24**, 411–416.

203   M. Nowak, Z. Malinowski, E. Fornal, A. Jóźwiak, E. Parfieniuk, G. Gajek and R. Kontek, *Tetrahedron*, 2015, **71**, 9463–9473.

204   H. Tripathy, D. G. Pradhan, B. C. Dash and G. N. Mahapatra, *Agric. Biol. Chem.*, 1973, **37**, 1375–1383.

205   Z. Ding, S. Xue and W. D. Wulff, *Chem. - An Asian J.*, 2011, **6**, 2130–2146.

206   G. Jadhav, S. Rao and N. Hirwe, *J. Indian Chem. Soc.*, 1936, **13**, 609–612.

207   M. E. Garst, D. D. Cox, R. W. Harper and D. S. Kemp, *J. Org. Chem.*, 1975, **40**, 1169–1170.